DEPARTMENT OF MARINE AND FISHERIES SCIENCES

UNIVERSITY OF GHANA

GEOCHEMISTRY OF ESTUARINE SEDIMENTS OF GHANA: PROVENANCE, TRACE METAL ACCUMULATION TRENDS AND ECOTOXICOLOGICAL RISKS

EDEM MAHU

SID: 10328600

This thesis is submitted to the University of Ghana, Legon in partial fulfillment of the requirement for the award of PhD Oceanography degree.

DECEMBER, 2014

DECLARATION

This thesis is the result of original research work undertaken solely by Ms. Edem Mahu in the Department of Marine and Fisheries Sciences (DMFS) of the University of Ghana under the supervision of Professors Elvis Nyarko, Kenneth H. Coale and Daniel K. Asiedu. No part of this thesis may be reproduced in any from without prior authorization from the author. All references cited in the study have been dully acknowledged.

Sign ……... **Date** ……...

Edem Mahu
(Student)
(SID: 10328600)

Sign: …… **Date**…….

Professor Elvis Nyarko
(Principal Supervisor)
(Department of Marine and Fisheries Sciences, University of Ghana)

Sign:..... **Date** May 14, 2015

Professor Kenneth Coale
(Supervisor)
(Moss Landing Marine Laboratories-California State University)

Sign:…….. **Date**……

Professor Daniel K. Asiedu
(Supervisor)
(Department of Earth Science-University of Ghana)

ABSTRACT

The sedimentary record, as revealed in sediment cores, can be used to reconstruct the past history of contaminant input into the aquatic environment. This is because contaminant inputs equilibrate rapidly with sediment supply, and the sediment column represents a continuous sequence of sediments that are associated with contaminant accumulation. With radiometric techniques, it is possible to date recent sediments over a period corresponding to about five half-lives (approximately 100-200 years using ^{210}Pb). To understand the geochemistry of estuarine sediments in relation to their provenance, trace metal accumulation trends and potential ecotoxicological risks, this study investigated sediment cores and surficial sediments from the Ankobra, Pra, Amisa, Densu, Sakumo II and Volta estuaries of Ghana. Geochemical and petrographical techniques were used to reveal the source of sediment supply into the estuarine environments. In addition, Gamma Spectroscopy and Inductively Coupled Plasma Mass Spectrometric (ICP-MS) techniques were used for deriving geochronologies, sedimentation rates, spatial and temporal accumulation of Mo, Cd, Pb, V, Cr, Cu, Zn, As and Hg in the study sites. The pollution status of the estuarine sediments was investigated using Aluminum-normalized enrichment factors (EFs). Cluster and correlation analysis differentiated natural from anthropogenic sources of trace metal in the estuaries. The excess fluxes of trace metals, estimated using sedimentation rates helped in quantifying the extent of anthropogenic contamination of metals in each estuary. AQUARISK software was used to assess any potential ecotoxicological risks associated with trace metal enrichments. Results showed that sediments from the Ankobra, Pra, Densu and Volta estuaries comprised quartzose sedimentary provenance while those of Amisa and Sakumo II estuaries comprised mafic igneous provenance. The sedimentation rates estimated from the constant rate of supply model were 0.24±0.10 $gcm^{-2}y^{-1}$, 0.47±0.20 $gcm^{-2}y^{-1}$, 0.43±0.02 $gcm^{-2}y^{-1}$, 0.31±0.13

$gcm^{-2}y^{-1}$, 0.20±0.01$gcm^{-2}y^{-1}$ and 0.54±03 $gcm^{-2}y^{-1}$ for the Ankobra, Pra, Amisa, Densu, Sakumo II and Volta estuaries respectively. The sediment core from the Ankobra estuary was significantly enriched with Hg ($5.0<EF\leq8.4$) and extremely enriched with As ($69.3<EF\leq114.3$) over time. Similarly, the sediment core from the Pra estuary showed significant enrichment with Hg ($5.0<EF\leq10.2$) between 1980 AD and 1995 AD and very high enrichment with As (EFs around 20.5) since 1875 AD to present. Likewise, the sediment core from the Amisa estuary showed significant enrichment with Hg (EF=6.3) around 1940 AD and a significant enrichment with As ($5.0<EF\leq6.5$) from 1960 AD to present. On the contrary, the sediment core from the Densu estuary was not enrichment with trace metals although a sharp peak correlating to a moderate EF of 4 was observed around 1965 AD for Hg. The sediment core from the Sakumo II estuary was significantly enriched with Hg ($5.0<EF\leq6.3$) since 2005 AD to present, with other trace metals showing potentials for enrichment over the last 20 years. Extremely high enrichments of Hg (EF=375.2, 16.01 and 111.3) were observed around 2003 AD, 1977 AD and 1965 AD respectively in the Volta estuary. In addition, significant enrichments of As were seen around 1995 AD and 1965 AD in this estuary. Results of ecotoxicological risk assessment showed that As and Hg posed potential ecotoxicological risks to the biota in the Ankobra estuary while Cd, Cu, Pb and Hg posed potential risk to the biota in the Sakumo II estuary. None of the metals analyzed posed ecotoxicological risks to the biota in the Volta estuary. To achieve at least 75% species protection in the Ankobra estuary, a substantial percent reduction of about 97.8% and 12.7% in the current levels of As and Hg are required respectively. In the same way, a substantial percent reduction of about 99.8%, 99.9%, 73.8% and 100% in the current levels of Cd, Pb, Hg and Cu respectively are currently required to achieve at least a 75% species protection in the Sakumo II estuary.

ACKNOWLEDGMENTS

This work was carried out through collaboration between the Department of Marine and Fisheries Sciences of the University of Ghana and Moss Landing Marine Laboratories of the California State University, San Jose, USA. Special thanks go to my supervisors, Professors Elvis Nyarko, Kenneth Hamilton Coale and Daniel K. Asiedu for their assistance, criticisms and contributions towards this research work. I am particularly indebted to the International Atomic Energy Agency's (I.A.E.A) RAF/7/009 Project, the Ghana Education Trust Fund (GETFund), the Ministry of Environment Science and Technology's Mathematics Science and Technology Scholarship Scheme (MASTESS) of Ghana, the International Students Exchange Program (ISEP) of the University of Ghana, the International Programs Office of the University of Ghana, the California State University's Council on Ocean Affairs, Science and Technology (CSU-COAST), the Department of Biology, San Jose State University and the International Foundation for Science (IFS) for awarding me the various scholarships, fellowships and financial support to carry out this research. I am also grateful to Professor Ivano Aiello (MLML), Dr Peter Swazeinski of the United States Geological Survey (USGS), Dr Samuel Hulme (MLML) and Dr. Wesley Heim (MLML) for their kind supports and for granting me access to their instruments. My sincere gratitude also goes to the Crew onboard the R/V Fridjoff Nansen especially Mr. Lloyd Allotey and Mr. Benjamin Botwe for making shelf sediment samples available for this work. Thanks to all the technicians in the Department of Marine and Fisheries Sciences especially Mr. Emmanuel Klubi, Mr. Mario Boateng and Mr. James Akomea for assisting me with sediment sampling. Special thanks go to my intern, Ms. Jessica Hanaway for assisting me in some of my analysis. I am greatly indebted to my dear husband Mr. Eric Kyere-Yeboah for his indulgence and immeasurable supports. Special thanks go to my family and my dear brother Mr. Seth Mahu for their numerous supports. To my precious mum, I say God

richly bless you for being the best nanny to my son while I worked on this thesis. Finally, I am grateful to the Coale, the Mazariegos and the Awity families for receiving me into homes while in California. Thank you all for the company, several rides and great foods.

DEDICATION

To God be the glory for the great things He has done. I dedicate this work to my dear husband, Mr. Eric Kyere-Yeboah and our son Nana Kwesi Kyere-Yeboah Jnr.

"When I started counting my blessings, my whole life turned around."

TABLE OF CONTENTS

Content **Page**

LIST OF FIGURES

LIST OF TABLES

LIST OF PLATES

LIST OF ABBREVIATIONS AND ACRONYMS

ANSTO: Australian Nuclear Science and Technology Organization

CASM: Comprehensive Aquatic Systems Model

CF: Contamination Factor

CF-CS: Constant Flux Constant Sedimentation

CHSA: Communities and Habitats Status Assessment

CIA: Chemical Index of Alteration

CIC: Constant Initial Concentration

COPC: Contaminants of Potential Concern

CRS: Constant Rate of Supply

CSUCOAST: California State University Council on Ocean Affairs, Science and Technology

DDTs: Dichloro-Diphenyl-Trichloroethanes

DLRA: Detailed Level Risk Assessment

DMFS: Department of Marine and Fisheries Sciences

EF: Enrichment Factor

EHC: Environmental Health Criteria

ENA: Ecological Network Analysis

EPA: Environmental Protection Agency

ERA: Ecotoxicological Risk Assessment

EtHg: Ethyl Mercury

FFWM: Fugacity-Based Food Web Model

GETFund: Ghana Education Trust Fund

HQ: Hazard Quotient

IAEA: International Atomic Energy Agency's

ICP-MS: Inductively Coupled Plasma Mass Spectrometer

ISEP: International Students Exchange Program

MBM: Multimedia Box Model

Me_2Hg: Dimethyl Mercury

MeHg: Methyl Mercury

MLML: Moss Landing Marine Laboratories

ReVA: Regional Vulnerability Assessment

ROC: Receptors of Concern

SLRA: Screening Level Risk Assessment

SOPC: Stressors of Potential Concern

SPM: Suspended Particulate Matter

SQG: Sediment Quality Guideline

TOC: Total Organic Carbon

UNEP: United Nations Environmental Programme

USGS: United States Geological Survey

WIP: Weathering Index of Parker

WQG: Water Quality Guidelines

CHAPTER ONE

INTRODUCTION

1.1 Background Information

Estuaries act as transition zones in which continental materials are trapped, and through which some of the trapped materials are transported to the open sea (Hatje *et al.*, 2001). By virtue of their nature and position between terrestrial and marine environments, they have become the focal point for a wide variety of human activities including the siting of major ports, industries, residential and other recreational developments (Ridgeway and Shimmield, 2002). As a result, estuaries have evolved to become the ultimate repositories for anthropogenic contaminants discharged through industrial activities and by residents living along them (Mil-Homens *et al.*, 2009). Toxic contaminants such as metals and other organic pollutants have placed increasing pressures on the ecological health of coastal and estuarine ecosystems over the past decades, and the sediment accumulative potential of estuaries further exacerbates this problem.

Naturally, sediments act as the main sink for trace metals that are introduced into estuaries due to characteristics such as grain-size distribution, total organic carbon content as well as the redox state and pH of pore waters (Szava-Kovats, 2008). Trace metals adsorb onto fine-grained sediments more readily than coarse-grained sediment (Blanton, 1995). This trend is predominantly attributed to sorption, co-precipitation and complexity of metals to particle surfaces and coatings as well as surface-area to grain-size/weight ratio (Parizanganeh, 2008). These sediment accumulative potentials of estuaries enable them to store evidence of past environmental changes such as metal accumulation, thereby enabling the study of interactions between humans and their alteration of these ecosystems over time (Cohen *et al*., 2005).

Although trace metals may get accumulated in deep-sea sediments without being released back into the water column, the opposite is the case in the estuarine environment

because of their dynamic nature. Under complex biological (such as bioturbation and bioirrigation), geochemical (such as changes in sediment redox states and pH), and hydrodynamic conditions (effects of currents and tides), sediment-bound trace metals may be remobilized and enter the water or food chain (Eggleston, 2012). In addition to entering the food chain, remobilized sediment-bound trace metals may disperse over hundreds of kilometers into adjacent shelf and deep-sea areas (Salomons, 1995).

The flux of trace metals into estuarine and coastal areas are geochemically coupled to sediment flux. For instance according to Schafer *et al.* (2002), an increase or decrease in the anthropogenic flux of trace metals into the continental shelves are said to be a direct function of the sediment discharge rate. Thus apart from the direct discharge of metal-rich effluents into estuaries, other anthropogenic activities along estuaries such as clearing of land, may accelerate sediment supply into estuaries to altering the natural geochemical cycles of trace metals (Schafer *et al.*, 2002).

The export of metal-bound terrigenous sediment from estuaries into nearshore and deep-sea areas is made possible through the interplay of hydrodynamic processes occurring in the estuarine and the coastal environment (Anderson, 1988). Metal-bound sediment transported by rivers into estuaries mostly end up deposited on the continental margin to form loose piles which may get overly steep and become re-suspended by earthquakes, storms or wave events (Anderson, 1988). Tidal currents are particularly known to be effective in re-suspending sediment from continental slopes, and creating mid-depth nephloid layers or dirty waters that can be advected horizontally offshore (Anderson, 1988). This re-suspension of sediment into bottom waters causes them to be denser than overlying waters, thus generating downslope hyperpycnal flows in the form of

underwater slides and slumps into the deep ocean basins (Libes, 2009). Studies conducted by Syvitski *et al.* (2003) and Chakrapani (2005) suggested that about 90% of the terrigenous sediment transported to the oceans annually is via estuaries (Table 1.1).

Table 1.1 Global estimate of terrigenous sediment flux from land to ocean (Chakrapani, 2005)

Transport Mechanism	Global Flux (Gt/year)
Rivers via estuaries	23
glaciers, sea ice, icebergs	2
Wind	0.7
Coastal erosion	0.2

Aluminosilicates (clay minerals), notably smectites, illites, kaolinites, montmorillonite, and chlorites are the most abundant (about 84%) of all the mineral types in intensively weathered terrigenous sediment transported into the ocean (Libes, 2009). They are important to the crustal-ocean-atmosphere interfaces, not only due to their abundance, but also for the fact that they participate in several geochemical processes. Aluminosilicates carry net negative surface charges that enable them to adsorb a wide array of cations (dominant among which are metals) while in suspension before settling on the seafloor (Libes, 2009).

Although metals play important metabolic and physiological roles in processes such as photosynthesis, respiration and absorption of major nutrients of aquatic organisms when in trace amounts (Morel *et al.*, 1991), elevations in their concentrations may be toxic and pose ecotoxicological risks. Elevated levels of metals in the aquatic environment are of critical concern because they are not biodegradable and can get accumulated in

biological systems (Siddiquee *et al.*, 2009). The accumulation and magnification of trace metals in the food chain is of public health concern because humans are vulnerable to the toxic effects of these metals as well (Erdogan, 2009). Toxic trace metals may cause genetic alteration of cells (mutation), neurophysiological disturbances, morphological abnormalities teratogenesis and carcinogenesis in both marine organisms and humans (Erdogan, 2009). Toxicity experiments have shown negative effects of elevated trace metal concentrations on hormonal and enzymatic activities, growth rate and, increase mortality in aquatic organisms (Bubb and Lester, 1991).

1.2 Scope of Study

The focus of this study revolved around understanding the geochemistry of estuarine sediments of Ghana in relation to their origin, trace metal accumulation trends and ecotoxicological risks. As the fluxes of trace metals into nearshore and deep-sea environments are strongly coupled with sediment flux, mineralogy and anthropogenic activities in the watershed, a preliminary provenance study was conducted on the estuarine sediment to determine their source and mineralogical compositions. The study also addressed trace metal accumulation trends and fluxes in the estuarine sediment over time and compared nearshore concentrations to those of the deepsea to see if their accumulation patterns are similar. Finally an ecotoxicological risk assessment was carried out to determine if current metal levels pose any threat to the biota.

1.3 Study Area

The study was conducted in the Ankobra, Pra, Amisa, Densu, Sakumo II, and Volta estuaries along the Coast of Ghana. The Ankobra and Pra estuaries are located on the western part of the coastline while the Amisa and Densu are located along the central

part of coastline. The Sakumo II and Volta are located on the Eastern part of the coastline. The study was designed taking into consideration the anthropogenic activities within the watersheds of each estuary that are likely to alter the natural geochemical cycling of trace metals into each estuary. The watersheds of the Ankobra, Pra and to some extent the Amisa are known to be dominated by alluvial mining (legal and illegal) operations through which mining effluents are discharged into the rivers that feed these estuaries. The Densu estuary was also selected due to the increasing rates of urbanization and automobile usage within it's watershed over the last 30 years. Similarly, the watershed of the Sakumo II estuary in addition to being heavily urbanized is the most industrialized of all the estuaries. The Volta estuary was chosen as a control site because comparatively its watershed is the least urbanized and industrialized.

1.4 General Aim

The study assessed provenance and trace metal accumulation trends in estuarine sediments of Ghana and evaluated their ecotoxicological risks to the biota

1.4.1 General Objectives

Specifically, the study aimed to:

1. Investigate the geochemical and mineralogical composition of the estuarine sediments and trace them to their origin (provenance)
2. Reconstruct historical trace metal accumulation trends in the estuaries over time;
3. Determine if trace metal accumulation patterns in estuarine sediments are reflected in nearshore and deep-sea sediments;
4. Examine any potential ecotoxicological risks the metals may pose to biota.

1.5 General Hypotheses (Alternate)

1. Trace metal accumulation has been occurring in Ghana's estuarine environments over the past 100 years.

2. There is an anthropogenic historical contribution of trace metals into the estuarine sediments that may be reflected in trace metal accumulation patterns in nearshore and deep-sea sediments.

3. Trace metal enrichment in sediment pose ecotoxicological risks to estuarine organisms.

CHAPTER TWO

LITERATURE REVIEW

2.1 Introduction

A number of published literature exist on the study of estuarine sediment geochemistry in relation to their origin, trace metal accumulation and ecotoxicological potentials. Although literature pertaining to the main study sites in investigation is limited, a great deal of effort has been made in using investigations of similar environments worldwide to explain the concepts to be used in this study. An objective of this study is to investigate the geochemical and mineralogical composition of nearshore bottom sediment and trace them to their parent material (provenance). A review of literature on nearshore sediment composition, geochemical processes shaping it, as well as geochemical and mineralogical approaches used in determining the origin of sediments is of utmost importance to this study. As this thesis also focuses on the occurrence and distribution (spatial and temporal) of trace metals in bottom sediment, it is crucial to review existing literature on the geochemistry of each metal of interest and their potential ecotoxicological threats. Related to this objective will be a review of radiometric techniques that are used in dating the sediments in the estuaries studied. Finally, a detailed review on ecotoxicological risk assessment and methodologies is also presented.

The literature review has been split into three broad sections (2.2, 2.3 and 2.4 with a general summary of the three sections at the end of the review). Section 2.2 reviewed existing literature on the general approach to provenance analysis of sediment citing specific examples where literature exists. Section 2.3 presents recent approaches to studying the accumulation trends of metals in estuaries, with respect to sediment dating, while section 2.4 stresses the need for ecotoxicological risk assessment of metals in nearshore-coastal environments and presents some recent advances in the area of risk

assessment. This section also reviewed the AQUARISK model that was used in this study.

2.2 Geochemical and Mineralogical Assessment of Provenance using Estuarine Sediments

2.2.1 A Source to Sink Summary of Sediment Supply to the Estuarine Environment

Igneous and metamorphic rocks are formed where temperature and pressure conditions are relatively high within the earth. Once formed, these rocks maybe exposed by erosion or tectonic uplifting where temperature and pressure conditions are entirely different from those within the earth (Bekele, 2011). Changes in these conditions may result in the physical/mechanical weathering of the parent rocks without altering the original mineral constituents (Nesbitt and Young, 1996). In addition to physical weathering, the mineralogical constituents of rocks at the earth's surface are further exposed to weak carbonic acid through precipitation resulting in the chemical breakdown of original materials and reorganization of the original constituent elements that recombine to form new mineral constituents (Cox *et al.,* 1995). These weathered materials are transported in either an aquatic or air media over varying length scales, and are deposited as sediment in rivers, estuaries and oceans, where they undergo further post-depositional transformations (Bekele, 2011). Human activities in watersheds can either speed up the supply of the weathered sediment to estuaries either due to urban or agricultural developments; or decrease sediment yield due to reservoir development (Syvistski *et al.,* 2003).

2.2.2 Provenance Analysis of Estuarine Sediments

The chemical composition of estuarine sediment is determined by the composition of river-derived material that is dependent on the catchment petrology as well as the biogenic contribution (Cho *et al.,* 1999). Variations in mineral composition, lithogenic components, organic material, and major and trace elements abundance are a tool for unraveling possible sediment sources, and for discriminating physico-chemical processes affecting the geological record. The characteristics of sediment deposited in estuarine environments largely reflect the prevailing geology of the continental source area, in addition to oceanographic, climatic and hydrographic conditions (Weltje and von Eynatten, 2004). Provenance analyses of sediment are not only useful for revealing their source but also could be applied in pollution studies to trace the possible source of pollutants transported along with sediment into coastal environments. Provenance assessment of sediment can be achieved through the use of petrographical (mineralogical) techniques (Schwab, 1975) or geochemical approaches (Roser and Korsch, 1988).

2.2.2.1 Mineralogical Provenance Analysis of Estuarine Sediment.

The relationships between the ternary compositions of sediment and provenance of depositional basins were first explored by Crook (1974) and Schwab (1975) and presented formally by Dickinson and colleagues (Dickinson *et al.,* 1983; Dickinson, 1985) in what became known as the ‘Dickinson Model’. The 'Dickinson model' used ternary diagrams subdivided into different provenance fields to plot the mineralogical compositions of sediment for the discrimination of their origin as well as the tectonic settings of their parent-rocks. Discrimination fields using the ratios of the major detrital components quartz (Q), feldspar (F) and lithoclasts (L) have been built from well-known

geodynamical settings to interpret clastic deposits of any depositional system (See Table 2.1 for detailed description detrital components). Ternary systems based on these grain categories were developed as follows: the Quartz-Feldspar-Lithic (QFL) framework which emphasizes on maturity of the sediment or geologic material; the Monocrystalline Quartz-Feldspar-Total Unstable Lithic Fragments (QmFLt) framework emphasizing on the parent rock; the Monocrystalline Quartz-Plagioclase Feldspar Grain-Alkali Feldspar (QmPK) subcomposition which emphasizes on monomineralic grains and the Polycrystalline Quartz-Volcanic Lithic Fragments-Sedimentary Lithic Fragments (QpLvLs) subcomposition which emphasizes on the lithic fragments (Fig. 2.1).

All four ternary systems/diagrams are subdivided into different provenance fields namely continental block provenance (A), magmatic arc provenance (B), recycled provenance (C) and mixed provenance (M) as shown in Fig. 2.1.

Table 2.1. Detrital components used in discriminating sediment source (Adapted from Dickinson and Suczek, 1979)

Main Parameter	Components
Quartz (Q)	Monocrystalline Quartz (Qm) + Polycrystalline Quartz (Qp)
Total Feldspar (F)	Plagiclase Feldspar Grains (P) + Alkali Feldspar Grains (K)
Total Unstable Lithic Fragments (Lt)	Volcanic Lithic Fragments (Lv) +Sedimentary Lithic Fragments (Ls)
Total Lithic Fragment (L)	Total Unstable Lithic Fragments +Qp

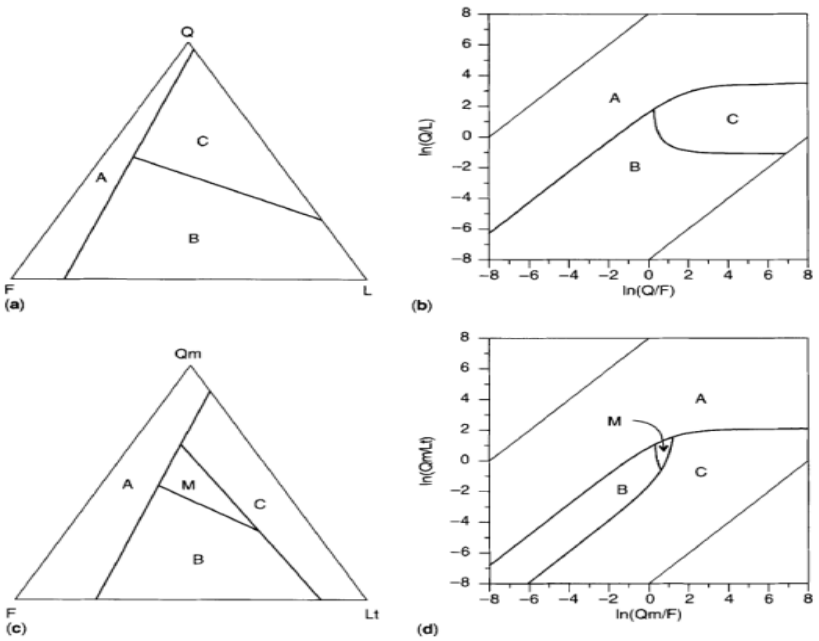

Figure 2.1 Subdivision of ternary spaces into provenance fields according to Dickinson (1985). (a,b) QFL system anFigure 0.2d (c, d) QmFLt system).

Based on this model, Kasper-Zubillaga and Dickinson (2001) used petrography to discriminate provenance and tectonic settings of modern beach, dune and fluvial sediment of the Gulf of Mexico, and the Kapitti and Foxton Coasts of New Zealand. Their study reiterated the effectiveness of the QFL, and QmKP system in discriminating source terranes of beach and fluvial sediment from different regions. Based on their findings, they concluded that, provenance discrimination is even more effective and better achieved when sediment came from quartz-rich source overlapped by volcanogenic andesitic source as was seen in the sediment from the Gulf of Mexico.

In addition, Yen and Lundberg (2006) carried out modal analysis on sediment from nearshore and offshore and related them to the source rocks in the modern arc-continent collision zone in southern Taiwan. Their study concluded that sediment deposited south

of the island of Taiwan were lithic-rich, reflecting the ongoing arc-continent collision that has built Taiwan. The compositions of these sediments also distinguished petrogenetic provinces in three distinct morpho-tectonic domains: the frontal (western) slope of an submarine accretionary prism, plus the nearby seafloor of the incoming South China Sea; the complex region north of the forearc basin, in which a suture zone is developing; and the forearc basin and its immediate western slope, the rear slope of an accretionary prism.

2.2.2.2 Geochemical Provenance Analysis of Estuarine Sediment

The geochemical approach to provenance analysis of sediment is based on the effect of chemical weathering on their source materials. The chemical weathering process results in the dissolution of primary minerals (particularly feldspars), that leads to the selective leaching of cations based on their chemical reactivity (Nesbitt and Young, 1996). The result of this is the concentration of immobile elements and depletion of mobile elements in fluvially-deposited sediment (Nesbitt and Young, 1996). Consequently, ratios between mobile and immobile elements change during chemical weathering, as cations have different mobility's in aqueous fluids (Roy *et al.*, 2008). Also, mobile major cations such as, sodium (Na), potassium (K), calcium (Ca) and manganese (Mg) ions are leached from source rock while immobile ones such as aluminum (Al) and titanium (Ti) ions are concentrated in the sediment (Roy *et al.*, 2008).

In most soft-bottom estuarine sediment, it is possible to recognize two other types of source components in addition to those derived from the weathering of continental rocks. There is a biogenic component consisting of skeletal remains, and a hydrogenous or authigenic component (clays, ferromanganese oxyhydroxides), directly precipitated from

the water column or produced by the reaction of sediment particles with seawater or through microbial activity (Schulz and Zabel, 2006).

The relative contribution of these inputs to nearshore and shelf sediment is the principal factor controlling their bulk chemical composition, which can provide valuable insights into the mechanisms involved in sediment formation, transport, dispersal, deposition, hydrodynamic regimes and lithology of the adjacent land areas (Condie, 1993). An in-depth understanding of the chemical composition of bottom sediment in estuaries and oceans is therefore of paramount importance to provenance identification (Condie, 1993; McLennan *et al*., 1993; Nesbitt *et al*., 1997).

Based on the geochemical composition of some major sedimentary environments in New Zealand and their behavior from initial weathering of source rock materials to their final deposition and burial, Roser and Korsch (1988) used discriminant function analysis to discriminate provenances of their sediment. Standardized discriminant function coefficients and associated statistics showed large eigenvalues and canonical correlations for the first two functions (F1 and F2), suggesting they are potentially good discriminators as they collectively accounted for 98.6% of the variability in the data (Table 2.2).

Table 2.2. Standardized discriminant function coefficients (Roser and Korsch, 1988)

	F1	F2	F3
TiO_2	-0.286	0.072	1.703
Al_2O_3	1.464	0.168	-0.987
Fe_2O_{3T}	1.027	-0.338	-1.229
MgO	-1.085	0.827	0.483
CaO	0.643	0.457	0.331
Na_2O	0.392	1.136	0.381
K_2O	-1.142	1.331	0.808
Eigen Value	7.48	3.94	0.16
Percent of Variance	64.57	34.01	1.42
Cumulative percent	64.57	98.58	100
Canonical correlation	0.94	0.89	0.38

These major element discriminant functions discriminate four sedimentary provenances namely; the mafic provenance which plots in a P1 region, intermediate igneous provenance which plots in a P2 region, felsic provenance which plots in a P3 region and quartzose recycled provenance which plots in the P4 region (Fig. 2.2).

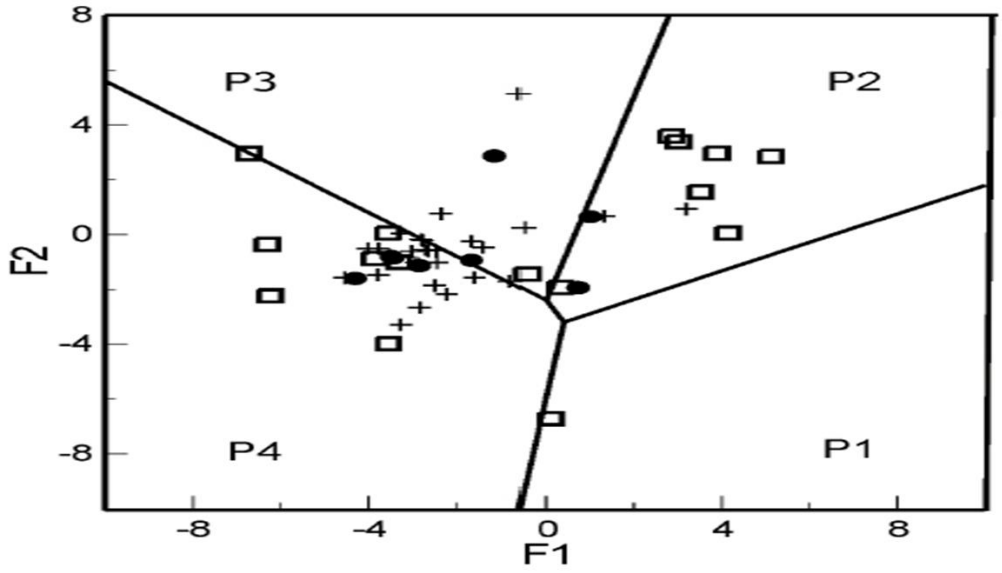

Figure 2.2. Classification plot function (F1) and function 2 (F2) for New Zealand Sediment (n=248). (Roser and Korsch, 1988).

Roser and Korsch (1988) identified volcanogenic sediment of the Maitai terrane and the Kays Creek Formation of Caples terrane in the P1 region of the classification plot to reflect a source from primarily mafic and lesser intermediate rocks. Earlier petrography studies had reported that sediment from some parts of Maitai terrane showed average composition of $Q_2F_{26}L_{72}$ (Aitchison, 1985). These sediments were depleted in detrital quartz and feldspar and abundant in volcanogenic detritus which consisted of basaltic-intermediate volcanic lithic fragments, plagioclase and mafic minerals indicating a mafic source (Landis 1980).

Lithic volcanogenic greywacke sediment from the Waipapa and Prelorus group of the Caples terrane originated primarily from an intermediate igneous source and plotted in the P2 region of the discriminant function diagram. The fragments were predominantly andesitic, although other evolved volcanic lithic fragments (dacites, rhyolites and trachytes) were also present in the sandstone. Earlier petrography studies reported QFL

ranges of $Q_{10-35}F_{15-29}L_{50-75}$ (Turnball, 1979). Obviously, detrital quartz and plagioclase were relatively higher in the P2 than in the P1.

Sediment from the Permian-Cretaceous Torlesse terrane originated primarily from a felsic igneous source and plotted in the P3 region of the discriminant function plot. The sediment consisted of quartzo-feldspathic sandstone (greywacke) and interbedded argillites. Earlier mineralogy studies had reported that the Torlesse sediment represent a source from a silicic crystalline (plutonic-metamorphic) terrane with a lesser intermediate-acid volcanic component (Mackinnon, 1983; Korsch, 1984). Korsch (1984) and Mackinnon (1983) reported average QFL compositions of $Q_{40}L_{43}L_{17}$ and $Q_{24}F_{50}L_{26}$ respectively. The sediment obviously had more quartz and depleted in lithics than those in P1 and P2.

The sediment that plotted in the P4 region of the discriminant function plot originated from quartzose sediment of matured continents and were represented by sandstone and argillites of the Ordovician Greenland group. These sediments were rich in quartz and depleted in feldspars and lithics with average QFL of about $Q_{80}F_{8}L_{12}$ (Laird, 1972). Most of the rocks from the Ordovician Greenland Group are quartzites or intransformational sediment that would plot in the craton interior or recycled orogen tectonic setting fields (Dickinson *et al.*, 1983). The sediment could be derived from deeply weathered granitic-gneissic terrane or from pre-existing sedimentary terrane (Laird, 1972).

These two discriminant functions have been used widely on both present and previous geochemical data for the discrimination of sedimentary provenances in aquatic and terrestrial terrains. A few studies in Ghana have used the approach for studying the

provenance of mudstone and sandstone suites of some major outcrops but not on estuarine sediments.

For instance Anani *et al.,* (2013) used the discriminant functions of Roser and Korsch, (1988) to study the provenances of sandstones from the Middle Voltaian Oti-Pendjari Group in the Anyaboni and surrounding areas. Their study concluded that the sediments were derived from recycled sedimentary rocks.

Similarly, Osae *et al., (*2006) used the discriminant functions of Roser and Korsch (1988) to study the provenances of 10 sandstone samples from the Late Proterozoic Buem Structural Unit of southeastern Ghana. In their study, the Buem sandstones plotted in the P4 region of the discriminant function diagram suggesting they were derived from granitic-gneissic or sedimentary source area.

Hofer *et al.,* (2013) studied the geochemistry of fine-grained sediment of shallow marine deposits of the Paleogene Gosau Group in Australia and related it to source rock using the discriminant functions of Roser and Korsch (1988) in addition to other geochemical proxies. Results of the analysis concluded a generally a mixed provenance. Different sample groups plotted in all end-member sources (mafic, intermediate, felsic and quartzose), and clustered mainly around the intersections.

In a related study, Armstong-Altrin *et al.,* (2012) looked at the geochemical composition of beach sands of different grain sizes from three locations along the western Gulf of Mexico and their implications for provenance using the discriminant functions of Roser and Korsch (1988). For their results, the medium-grained sands of Playa Azul plotted in

the quartzose recycled sedimentary and felsic igneous provenance fields while all the very fine-grained sands of Playa Azul occupied the intermediate igneous provenance field. Similarly, most of the sands from Tecolutla plotted in the intermediate igneous provenance field while very fine-grained sands of Nautla plotted in the mafic provenance field. They concluded that, the compositional differences identified in the three beach areas implied that the composition of sediment in the different rivers delivering sands to the beach is the most important factor controlling the geochemical composition of beach sands.

2.2.3 The Weathering Profile and Provenance Discrimination of Estuarine Sediment

Estuarine sediments are predominantly composed of river-transported debris resulting from continental weathering (Schropp and Windom, 1988). The intensity of chemical weathering on source materials can also be deduced from bottom sediments based on the geochemical fractionation of mobile and immobile cations during weathering (Nesbitt and Young, 1982). In line with this principle, several geochemical indices have been recommended for studying the intensity of chemical weathering on continental, lacustrine, estuarine or marine sediment based on the variable geochemical behavior of specific elements and isotopes in the different depositional environment.

The Silica-Alumina Ratio for example equated silica loss to total element loss (Ruxton, 1968). The ratio of SiO_2 to Al_2O_3 was considered indicative of the degree of weathering and applicable to free draining, acidic weathering environments in humid climates on acidic rocks. The weathering Index of Parker (WIP) was also derived based on the proportions of the major alkaline metals and their bond strength with oxygen (Parker, 1970). The WIP is applicable to acid, intermediate and basic rocks where hydrolysis is

the main process of silicate weathering (Parker, 1970). The Chemical Index of Alteration (CIA) was proposed based on the fact that feldspars are the most abundant reactive minerals in the earth's upper crust and that, calcium, sodium and potassium are generally removed from the feldspars during weathering, (Nesbitt and Young, 1982). The CIA is based on the assumption that during weathering the proportion of alumina to alkalis would typically increase in the weathered product. Amongst all the weathering indices however, the Chemical Index of Alteration (CIA) and the Weathering Index of Parker (WIP) are the most widely applied indices.

Parker (1970) and Hamdan and Burnham (1996) used the WIP (defined as, WIP= $\{100\times[(2Na_2O/0.35)+(MgO/0.9)+(2K_2O/0.25)+(CaO/0.7)]\}$) for evaluating the intensity of weathering on silicate rocks based on the proportions of alkali and alkaline earth elements in the weathered products. The stronger the intensity of chemical weathering on parent rocks, the smaller the WIP index and vice versa. The WIP has been suggested by many authors to be most appropriate for weathering profiles on heterogeneous parent rocks and most likely not applicable to highly weathered materials such as sediment because its formula includes only highly mobile alkali and alkaline elements (Hamdan and Burnham, 1996; Duzgoren-Aydin *et al*., 2002; Price and Velbel, 2003).

Nesbitt and Young (1982) used the Chemical Index of Alteration (CIA) (defined as, CIA= $\{[Al_2O_3/ (Al_2O_3+CaO^*+Na_2O+K_2O)]^*100\}$) in molecular proportion as a measure of the extent of chemical weathering in the production of sediment. The CIA is based on the assumption that the dominant process during chemical weathering is the degradation of feldspars and the formation of shales rich in clay minerals like illite and kaolinite, and Fe-oxyhydrates like goethite. High CIA values depict the considerable removal of mobile

cations (Ca^{2+}, Na^{+}, K^{+}) relative to stable residual constituents (Al^{3+}, Ti^{4+}) through intensive chemical weathering likely to occur under warm and humid conditions. Consequently, low CIA values indicate the near absence of chemical weathering, thereby reflecting cool and/or arid conditions (Yan *et al*., 2010).

In both indices, the CaO represent the calcium content of silicates minerals only (Nesbitt and Young, 1989). It is therefore necessary to make a correction to the measured CaO content for the presence of carbonates (calcite, dolomite) and apatite. A correction can be made by correcting for phosphate using available P_2O_5 data (CaO* = mole CaO − mole P_2O_5 × 10/3). Where the remaining number of moles is less than that of the measured Na_2O, the CaO value was adopted as the CaO*. Otherwise, the CaO* was assumed to be equivalent to Na_2O (McLennan, 1993).

Values of CIA plotted in an Al_2O_3-(CaO* + Na_2O)-K_2O (A-CN-K) ternary diagrams aids the analysis of sediment mineralogy particularly clay minerals in relation to weathering of fluvial sediment as well as their provenance. Sediment produced under intense chemical weathering would usually plot in regions commensurate with high CIA values 80−100, whereas incipiently weathered sediment would plot near the feldspar and CIA junction of 50−70 (Yan *et al*., 2010).

Additionally, provenance pathways and the distribution of rocks in source regions exert a first order control on the composition of siliciclastic deposits (Johnsson, 1993). Therefore differences in provenance are also reflected in the weathering indices (Fedo *et al.*, 1995). Weathering trends for silicate rocks are parallel to the CN-A join of the A-CN-K diagram (Nesbitt and Young, 1984). The weathering of average granodiorite or

upper continental crust (UCC) will result in the transformation of labile components including feldspars first to illite thus causing the sample's composition to plot ever closer to the A-K join and the illite composition (Nesbitt and Young, 1984).

This study combines the approaches discussed above to explain the transformations in the geochemical and mineralogical compositions of the estuarine sediment from production to deposition as well as the geogenic origin of sediment.

2.3 Trace Metal Accumulation in Estuarine Environments

Trace metals are natural constituents of all environments and traces of all heavy metals are found in estuarine waters, organisms and sediment (Abdul and Subrahmanyam, 1998). Metals such as zinc (Zn), iron (Fe), copper (Cu), cobalt (Co), molybdenum (Mo) and manganese (Mn) are known to play important physiological roles in coastal and other aquatic environments. These metals serve as cofactors of metalloenzymes and proteins where they are involved in the general metabolic processes of phytoplankton and other marine organisms (Morel *et al*., 1991; Hunter *et al*., 1997). In addition, they serve a variety of essential biochemical functions such as helping to maintain conformation and tertiary structures in some proteins (Morel *et al*., 1991), or acting as redox centers in others. Despite the physiological roles of some trace metals, their background concentrations in the coastal environment may be enriched due to inputs from anthropogenic sources to produce toxic effects. Metals such as cadmium (Cd), arsenic (As), mercury (Hg), lead (Pb), and zinc (Zn) have particularly received much attention because of their toxic effects on marine organisms at high concentrations (Valavanidis and Vlachogianni, 2010). Chromium (Cr^{6+}) is generally not required for metabolic activity and is toxic to living organisms even at very low concentrations

(Merian, 1991). Enrichment of trace metals as a result of anthropogenic inputs into nearshore and deep-sea ecosystems is of uttermost concern. Once introduced into the water column, they may get accumulated in the sediment where they undergo physical, biological and chemical transformations that could have implications for living organisms (Erdogan, 2009).

Metals in seawater, porewater and sediment occur in three major forms namely the free hydrated metal ion, inorganic complexes (ion pairs) and organic complexes (Kozelka and Bruland, 1998). The free hydrated metal ion is known to be the most bioavailable and toxic component of the metal (Kozelka and Bruland, 1998). Although some organic forms are generally considered not biologically available, nutrient-metals such as Fe, for which there are specific uptake mechanisms involving complexation with organic ligands such as siderophores and the organic forms of others such as Hg are considered bioavailable to organisms (Kozelka and Bruland, 1998).

The transport of trace metals to and fro estuaries is influenced by hydrodynamic processes operating within the estuarine environment which in turn affects metal sorption processes. Advective transport for instance influences movement of metals from bottom sediment pore waters (Delfino and Otto, 1986) while coagulation of riverine particles may remove trace metals from solution. Particulate scavenging (adsorption onto suspended particulate matter (SPM) and bottom sediments) is an important mechanism controlling the fate and transport of trace metals (Comber *et al.*, 1996).

To understand the general geochemical behavior of metals with respect to their sources, speciation and potential threats to nearshore coastal environments, a brief geochemical

review on each trace metal of interest to this study; that is As, Cd, Cr, Hg, Mo, V, Cu and Zn has been given below. Arsenic (As), Cd, Hg, and Pb were chosen in this study because, they are not required for any biological functions (Valavanidis and Vlachogianni, 2010). Their enrichment in sediment provides no nutritional value and may present a toxic or inhibitory limitation to benthic organisms as well as other nekton (Valavanidis and Vlachogianni, 2010). Although Zn and Cu play important biological roles in the aquatic environment, their enrichment in sediment, above biologically required levels, pose a threat to the biota and food chain (Morel *et al*., 1991; Hunter *et al*., 1997). In addition, the chemistry of Cr in the aquatic environment allows it toxic form (Cr^{6+}) to dominate the non-toxic form making it a potential threat to organisms (Chung *et al*., 1994; Fendorf *et al.*, 1997) at high levels. Finally, Mo and V have been considered in this study because of their ability to help explain metal enrichments due to authigenesis rather than discharges from anthropogenic sources (Hope, 1997; Zheng *et al.*, 2000).

2.3.1 Arsenic in Estuarine Environments

Arsenic is a metalloid widely distributed in the earth's crust that can be found in trace quantities in all rocks, soils, waters and air and is mobilized through a combination of natural processes such as weathering reactions, biological activity and volcanic emissions (Smedley and Kinniburgh, 2002). Smelter operations, fossil-fuel combustion, mine wastes and mill tailings are the most important anthropogenic inputs into the nearshore-coastal environments (Azcue and Nriagu, 1995; Smedley and Kinniburgh, 2002; Melamed, 2005).

Studies have shown Arsenic to exhibit unique sensitivity to mobilization at pH values typically found in groundwaters (pH 6.5–8.5) and under both oxidizing and reducing conditions (Azcue and Nriagu, 1995). Although As in the coastal and deepsea environment has been found to exist in several oxidation states (-3, 0, +3 and +5), the As (III) and As (V) are most stable, hence the main forms present in marine and estuarine environments (Ehrlich, 1996). The concentration of both As (III) and As (V) in free and pore water is solely a function of redox potential as As (III) may dominate in more anoxic sediment while As (V) may dominate under oxic conditions. A study by (Rajeeva *et al.*, 2012) reiterated the importance of water depth in the precipitation of both As (III) and As (V). Their study showed that the more toxic form As (III) significantly dominated over the less toxic As (V) as water depth increases towards the bottom and they attributed this trend to increasing microbial activities that cause greater reduction of As (V). The implication of this could be that As (III) may be an important addition to increasing total As concentration in bottom waters. Both forms of As are toxic and carcinogenic to marine organisms, though, As (III) species are much more toxic (Duester *et al*., 2008).

Ghana is no exception to the story of natural pollution of groundwater resources in Africa with As. In addition to the natural occurrence of As in the reducing groundwaters of fluvial deposits, other anthropogenically enhanced levels have been found. Being an important gold mining country, studies have revealed high levels of As in soils that are in close proximity to major gold mining towns and nearby rivers (Bowell, 1992, 1993). Intense amalgamation of underground ores consisting predominantly of sulphides – pyrites (FeS_2) and arsenopyrites (FeAsS) to liberate gold could however be the main cause of As enrichment into Ghanaian estuaries and coast via rivers.

2.3.2 Cadmium in Estuarine Environments

Cadmium is a rare, non-essential, toxic transition element that is released into estuarine and marine environments via a number of natural and anthropogenic processes. Natural release of Cd from the crust and mantle into aquatic environments occurs via volcanic eruptions, weathering, burning of vegetation, sea salt spray, and the production of marine biogenic aerosols (Nriagu, 1990; Pacyna and Pacyna, 2001). The perturbation of the natural biogeochemical cycle of Cd by man is very pronounced and cannot be overemphasized.

Cadmium (Cd) has been artificially released into nearshore environments through a number of man-made processes, prominent among which are the processing of non-ferrous ores, combustion of fossil fuels, anti-corrosion plating, use in paints, incineration of refuse and disposal of Cd-containing products (Pacyna and Pacyna, 2001). Cadmium is also produced as a by-product of mining, smelting and refining of zinc and, to a lesser degree, as a by-product of lead and copper production, hence a function of zinc production rather than cadmium demand (UNEP, 2008).

Although Cd is not thought to have a biological function or algal requirement (Bruland, 1992), recent studies suggested that it can fulfill the biochemical role of Zn in phytoplankton growth in marine and estuarine waters containing biolimiting concentrations of Zn (Rice and Morel, 1990). In addition, the oceanic distribution of Cd does not reflect a true biochemical demand for it by marine plants or animals, but rather, the efficiency of Cd scavenging onto organic-rich biogenic particles (Bruland, 1992).

Unlike sediment, organic content of water generally decreases the uptake and toxic effect by binding cadmium and reducing its availability to organisms although some organic matter may have opposite effect (Environmental Health Criteria 135, 1992). Environmental factors also affect the uptake and, therefore, the toxic impact of cadmium on aquatic organisms. Increasing temperature for instance increases the uptake and toxic impact, whereas increasing salinity or water hardness decreases them (Rosenberg and Costlow, 1979). Available data on the toxicity of cadmium to aquatic organisms indicates that tropical and freshwater organisms are even more sensitive to cadmium than their estuarine and marine counterparts (Rosenberg and Costlow, 1979).

2.3.3 Chromium in Estuarine Environments

Chromium is a naturally occurring element present in water, sediment, rocks, soils, biota, and volcanic emissions (Burbridge *et al*., 2012). It is a major component of the minerals chromite ($FeCr_2O_4$) and the rare crocoite ($PbCrO_4$), and present as an accessory element in others such as spinel, amphibole, mica, pyroxene and garnet. High levels of chromium in estuarine sediment are however as a result of industrial discharge of effluents associated with tanning, smelting, and plating facilities although enrichment may sometimes be due to the high presence of ultramafic minerals (Burbridge *et al*., 2012).

Although Cr in water and sediment occurs in a number different oxidation states, the Cr^{3+} (non-toxic) and Cr^{6+} (toxic) oxidation states are the most reported in literature because they are thermodynamically stable in the presence of oxygen. Chromium III (Cr^{3+}) is stable at pH < 2 while Cr^{6+} is stable at higher pH either as hydro-chromate, dichromate or chromate under oxidizing conditions (Cutter, 1992). Chromium VI (Cr^{6+}) also exists as water-soluble complex anions and may persist in seawater, but may exhibit a shorter

lifetime in water rich in organic contents (Callahan, *et al.*, 1979) and when in sediment, it may be reduced to Cr^{3+} in the presence of organic matter. Chromium VI Cr^{6+} is strong oxidant that can be quickly reduced to Cr^{5+}, which is a known carcinogen that can assimilate in living tissues to form cancerous growths (Fendorf *et al.*, 1997).

Erin Brockovich and her attorney's lawsuit against Pacific Gas and Electric in a case of alleged contamination of Hinkely's drinking water with hexavalent chromium which was settled for USD 33million in 1996 is a true story of the destructive nature of Cr^{6+} to both aquatic organisms and man. The Pacific Gas and Electric Company used water containing hexavalent chromium to cool towers to prevent rust in the machinery and afterwards stored the effluent water in unlined ponds which percolated into the ground and contaminated groundwater resources in Hinkley, California. A 2010 report, released by the California Cancer Registry, showed that cancer rates in Hinkley still remained high from 1988 to 2008.

2.3.4 Mercury in Estuarine Environments

Mercury is a natural element, known to be present in every major compartment of the planet at low concentrations (Sonke *et al.*, 2013). Naturally, Hg is released into the marine environment via aerial and sub-aerial volcanism, and gradual degassing of soil systems, while man-made emissions are by intentional and unintentional use of it. Intentional uses include Hg use in gold mining and the use of Hg in industrial processes, notably chlor-alkali plants and other chemical industries (Sonke *et al.*, 2013). Hg is unintentionally emitted into the environment predominantly by coal-fired power plants, cement production, and pyrometallurgy (Sonke *et al.*, 2013).

The mobility and availability of Hg in aquatic environments is influenced by various processes including the thermodynamic solubility of Hg and Hg compounds (Randall and Chattopadhyay, 2013). In the aquatic environment, Hg exists in an elemental volatile form, Hg^{o}, which is relatively non-reactive and a number of toxic mercuric species, Hg^{2+}, and organic Hg, mainly monomethyl mercury (MeHg), dimethylmercury (Me_2Hg) and some ethyl (EtHg) mercury (Ullrich *et al*., 2001). The formation of MeHg is influenced by a number of environmental factors including temperature, pH, redox potential, activity and structure of bacterial community, speciation, age, and the presence of inorganic and organic complexing agents (Ullrich *et al*., 2001). Wetland and estuarine sediment commonly have a lower oxidation–reduction potential (ORP), one of the key pathways to Hg speciation. Decreasing ORP promotes microbial- mediated sulfur-reduction, which promotes the methylation of Hg (Randall and Chattopadhyay, 2013).

The accumulation of reduced sulfur, primarily as dissolved sulfide, precipitates inorganic Hg as a highly insoluble HgS mineral, cinnabar which is red in coloration or meta-cinnabar which is black in color and slightly more soluble (Randall and Chattopadhyay, 2013). Increases in dissolved sulfide concentrations result in decreases in Hg methylation rates because inorganic Hg is removed as a sparingly soluble solid (Gilmour *et al*., 1992).

There is no biological requirement for Hg and it has been listed as a high priority pollutant due to its persistence in the environment and high toxicity to organisms (Jiang *et al*., 2006). The, conversion of inorganic Hg to MeHg is an important link in the bioaccumulation of Hg in fish and ultimately its toxicity to humans and wildlife (Randall and Chattopadhyay, 2013). Marine organisms exposed to different Hg concentrations in laboratory experiments have shown several effects. Effects range from hormonal and

reproduction alterations at larval stage (WHO, 1990), changes in hematological parameters (Olson *et al.,* 1973; Berntssen *et al.,* 2004) histopathological alterations in liver and kidney (Who, 1990), decreasing of enzymatic activities (Gill *et al.,* 1990), problems during gonad development (Wiener and Spry, 1996), reduction of eggs incubation success and survival during embryo-larval stages (Mc kim *et al.,* 1976; Friedmann *et al.,* 1996), decreased locomotor activity, reduction of escape capacity, brain lesions (Wiener *et al.,* 2003) and genotoxic effects (Nepomuceno, 1997).

2.3.5 Lead in Estuarine Environments

Lead is a trace constituent in rocks, soils, water, plants, animals, and air that is toxic at very low exposure levels and has acute and chronic effects on human health (UNEP, 2008). It is a common anthropogenic pollutant with numerous sources to nearshore and coastal environments including automobile exhaust emissions, coal-fired power stations, waste from runoff and incineration, batteries, paints and other chemicals (such as those used in photography), and other industrial effluents (Ritson *et al*., 1999; Hansmann and Köppel, 2000).

The widespread distribution of Pb through anthropogenic activities, especially during the past 40 years, has resulted in an increase in Pb residues throughout the environment that has significantly perturbed the equilibrium of its biogeochemical cycle (Eisler, 1988).

Studies have shown that Pb is neither essential nor beneficial to aquatic organisms with all existing data showing that its metabolic effects are rather adverse (Storelli *et al*., 2005; Lahaye, 2006; Julshamn *et al*., 2008). It is a metabolic poison that affects behavior, as well as the hematopoietic, vascular, nervous, renal, and reproductive systems of

aquatic organisms (Eisler, 1988). Elevated Pb levels in humans are believed to be related to Pb contaminated water and sediment in urban areas (Mielke *et al*., 2007; Kampa and Castanas, 2008; Huang *et al*., 2011).

2.3.6 Molybdenum in Estuarine Environments

Molybdenum, the most abundant transition element in the ocean, is a redox-sensitive trace metal that has an almost conservative behavior under oxygenated conditions (Morris, 1975; Collier, 1985). It is naturally present in the lithosphere and released into the environment via weathering with rivers serving as the dominant route to estuaries and oceans; whereas oxic and anoxic marine sedimentary systems are believed to be the primary sinks (Crusius *et al.*, 1996). Anthropogenically, Mo is distributed in the marine environment as a result of fossil-fuel burning, leaching from fly ash, mobilization from mine and quarry wastes, and fertilizer applications (Zhang and Reardon, 2003).

In oxygenated waters, Mo is present as the soluble chemical species molybdate (Mo (VI) O_4^{2-}) where it is adsorbed on Fe-Mn oxyhydroxides and accumulates in surface sediment (Morford *et al.*, 2007). Under anoxic conditions, MoO_4^{2-} reacts with H_2S to form thiomolybdates, (Mo VI) $O_4^{2-}{}_{-x}S_x^{2-}$ (Erickson and Helz, 2000) which is either scavenged by iron sulfides (Helz *et al*., 2011), sulfurized organic matter (Tribovillard *et al*., 2004) or reduced Mo(VI)-S compounds (Dahl *et al*., 2013) in the sediment.

Correlating sediment trace metal concentrations to Mo can thus help in explaining whether or not their enrichment is dependent on redox changes in the water column rather than anthropogenic inputs. Although an excess of it pose threat to benthic and

other organisms in the aquatic environment, Mo is essential to all aquatic organisms as a cofactor in enzymatic redox reactions (Helz *et al*., 1996).

2.3.7 Vanadium in Estuarine Environments

Vanadium (V) is a naturally occurring crustal element that is released naturally into estuaries and oceans mainly from the weathering of bedrocks (Schwertmann and Pfab, 1994). Known anthropogenic sources are products of coal combustion, leachates, oil refineries and effluents from the mining and milling of uranium and titanium (Nriagu and Pacyna, 1988; Hope, 1997).

The speciation of vanadium in the aquatic environment is predominantly a function of the redox conditions prevailing in the system (Pettersson *et al*., 2003). In natural waters, dissolved V generally exists as V (IV) and V (V) oxidation states (Wang and Sañudo-Wilhelmy, 2008) with V (V) being the thermodynamically stable form in oxygenated seawater and V (IV) is even more stable under moderately reducing conditions (Siddiq, 1988). Ions of V (IV), such as VO^{2+}, are the most biologically available forms generally internalized into the cytoplasm through passive diffusion (Yang *et al*., 2003).

The solubility of vanadium decreases with decreasing valency, thus V (IV) increases proportionally with decreasing total dissolved vanadium as the environment becomes more reducing (Sadiq, 1988). Compared to the Atlantic Ocean for instance, dissolved V concentrations are depleted by approximately 60% in reducing deep waters of the Black Sea and the Cariaco Basin, suggesting that reducing sediment may serve as a major sink for V (Emerson and Huested, 1991; Nameroff *et al*., 2002).

When in trace amounts, vanadium represents an essential element for normal cell growth for marine organisms, although elevated levels may produce adverse effects (Hope, 1997). It is an essential element for many marine phytoplankton species macroalgae and many other organisms (Taylor *et al*., 1997). Enzymes such as haloperoxidases (Butler and Carter-Franklin, 2004), nitrate reductases (Antipov *et al*., 1999), and nitrogenases (Rehder, 2000) contain vanadium as their metal center in the active site.

2.3.8 Copper in Estuarine Environments

Copper (Cu) is a ubiquitous natural element found in many industrial and nonpoint source effluents that enter the marine environment (Blake *et al*., 2004). Natural sources of copper to marine environment include windblown dust and weathering while anthropogenic releases come from copper mines, leaching antifouling hull coatings on ships, agricultural use, smelters, iron foundries, power stations and combustion sources such as municipal incinerators (Blake *et al*., 2004).

The concentration and bioavailability of copper in the aquatic environment depends on factors such as water hardness and alkalinity, ionic strength, pH and redox potential, complexing ligands, suspended particulate matter and organic carbon, and the interaction between sediment and water (Environmental Health Criteria, 1998). In seawater, Cu exists as a number of chemical species, including the free hydrated ion Cu^{2+}, dissolved organic and inorganic complexes, colloidal complexes, and particulate copper (Santschi *et al*., 1997).

While water/sediment quality criteria for copper are typically based on the total or dissolved concentration, a large body of scientific data indicates that it is the free or

aqueous cupric ion, Cu^{2+}, that relates best to copper toxicity in marine and estuarine organisms (Campbell, 1995) although the dissolved organic and inorganic complexes may also be of concern when pH increases above 7.5 (De Schamphelaere *et al*., 2002; Arnold *et al*., 2005; Martins and Bianchini, 2008).

Copper is a required constituent in many enzyme systems, the most notable of which are perhaps the enzyme cytochrome oxidase, and the electron carrier, plastocyanin so that very low levels of it can limit the growth of higher plants and some phytoplankton (Shkolnik, 1984). Free Cu^{2+} concentrations found in aquatic environments (in the picomolar to nanomolar range) have been shown to reduce cell division rates of phytoplankton in culture (Brand *et al*., 1986). Elevated free Cu^{2+} has also been shown to decrease photosynthetic rates and interfere with the uptake of other essential trace metals such as manganese (Sunda 1989; Sunda and Huntsman, 1998), and disrupt enzyme function by both producing hydroxyl radicals and binding to -SH groups (Brown *et al*., 1994).

2.3.9 Zinc in Estuarine Environments

Zinc is a naturally occurring element that is released into the marine environment naturally through the weathering of parent rocks (Liu *et al*., 2013). Anthropogenic activities account for about 96% of the total zinc discharged into estuaries and coastal environments (Leonard and Gerber, 1989). Major anthropogenic sources of zinc to the marine environment include electroplaters, smelting and ore processors, drainage from active and inactive mining operations, domestic and industrial sewage, combustion of fossil fuels and solid wastes, corrosion of zinc alloys and galvanized surfaces, and erosion of agricultural soils (Weatherley *et al*., 1980; Buhl and Hamilton, 1990). Due to

the application of Zn in several agro-processes such as in fertilizers, liming materials or manures, fungicides and pesticides, the concentration of Zn in farmlands is usually higher than adjacent lands (Sensi *et al*., 1999). This elevated farmland levels result in increase in concentration in surrounding aquatic ecosystems (Liu *et al*., 2013).

Marine and estuarine sediment act as a major reservoir for a larger percentage of zinc released into the world's oceans and other aquatic ecosystems. During periods of high dissolved oxygen, low salinity and low pH, zinc is released from sediment into the water column (Eisler, 1993). Dissolved zinc usually consists of the toxic aquo ion Zn $(H_2O)_6)^{2+}$ and various organic and inorganic complexes. The aquo ion and other toxic species have their greatest effects on aquatic organisms with depreciating environmental conditions such as comparatively low pH, low alkalinity, low dissolved oxygen, and high temperatures (Eisler, 1993).

Effects of excess zinc on estuarine and marine organisms are modified by numerous variables, especially by interactions with other chemicals or elements such as Cd, Ni, Cu, Pb as well as organic and inorganic substances. These interactions generate radically altered patterns of accumulation, metabolism, and toxicity some of which are beneficial to the organism whereas others are harmful (Eisler, 1993). For instance, Pb-Zn mixtures were found more-than-additive in toxicity to marine copepods and significantly delayed development of mud crab (*Rithropanopeus harrisii*) larvae (Environmental Protection Agency, 1987). Lead is accumulated up to 10 times more rapidly by marine fish at elevated zinc concentrations in seawater (Eisler 1981; Eisler 1993).

2.3.10 Estuarine Sediments as Trace Metal pollution Monitoring Tools

The natural tendency with which organic and inorganic contaminants adsorb to sediment makes sediment analysis an indispensable tool with which to assess, monitor and track contaminant migration in the marine environments (Szava-Kovats, 2008). Enrichment of trace metals in sediment aside, heavy anthropogenic input depends largely on characteristics such as the grain-size distribution and total organic carbon content of the sediment (Schiff and Gossett 1998; Szava-Kovats, 2008) as well as the redox state and pH of the sediment pore waters. Fine-grained sediment will adsorb onto metals more readily than coarse-grained sediment (Horowitz, 1991; Blanton 1995); a trend that is predominantly attributed to sorption, co-precipitation and complexity of metals to particle surfaces and coatings as well as surface-area to grain-size/weight ratio (Sinex and Helz, 1981; Blanton, 1995; Parizanganeh, 2008).

Studies have also shown that aluminosilicates and organic matter that have chemical affinity for metals and organic pollutants are concentrated in the clay and fine silt fraction of sediment (Herut and Sandler, 2006). In addition to these, the concentration of trace metals and organic pollutants in the marine environment to some extent depend on the origin and source of sediment. Although coarse grains may not have natural affinity towards contaminants as discussed, their close proximity to adjacent agricultural and industrial settings may result in higher loads of trace metal pollutants (Parizanganeh, 2008).

To understand and quantify the extent to which anthropogenic enrichment has occurred in marine and estuarine sediment, the contamination factor (CF), enrichment factor (EF),

and the geochemical accumulation indices (Igeo) have been proposed. The CF is calculated as;

$$CF = Cn/Bn \quad (2\text{-}1)$$

Where Cn is the measured concentration of the examined metal (n) in the sediment, Bn is the pre-industrial concentration of the metal (n). Where CF < 1 implies low contamination factor; 1≤CF < 3 implies moderate contamination factor; 3≤ CF < 6 implies considerable contamination factor and finally C ≥ 6 implies very high contamination factor (Hakanson, 1980).

The enrichment factor (EF), is used in explaining the origin of elements in sediment of estuaries and other aquatic ecosystems (Reimann and de Caritat, 2005). It is estimated from the formula:

$$EF = [(C_n/C_{ne})_S / (C_n/C_{ne})_{RS}] \quad (2\text{-}2)$$

Where Cn is the concentration of element n in the sample of interest and C_{ne} is concentration of the immobile element in the sample or the selected reference sample. Thus $(C_n/C_{ne})_S$ is the heavy metal to immobile element ratio in the samples of interest, and $(C_n/C_{ne})_{RS}$ is the heavy metal to immobile element ratio in the selected reference sample (Zhang *et al.*, 2007). According to Sutherland (2000), five contamination categories can be recognized on the basis of the enrichment factor: $EF<2$ imply depletion to mineral enrichment; $2\leq EF<5$ imply moderate enrichment; $5\leq EF<20$ imply significant enrichment; $20\leq EF<40$ imply very high enrichment; and $EF>40$ imply extremely high enrichment.

The immobile/reference element is usually taken to be Al although other relatively immobile elements such as Li, Sc, Zr, Fe and Mn may be used (Sutherland, 2000). The geochemical justification for selecting Al as normalizer to natural versus anthropogenic enrichment of trace metals is due to its properties during weathering. Most of the naturally occurring metals transported by rivers are tightly bound in an aluminosilicates (clay) solid phases because there is very little geochemical fractionation between the metals and aluminum during weathering (Schropp and Windom, 1988). Although metals coming from both natural and anthropogenic sources are ultimately concentrated in estuarine sediments, adsorbed anthropogenic metals is more loosely bound while natural component of metals in estuarine sediments are non-labile because they are chemically bound in the aluminosilicate structure (Schropp and Windom, 1988).

2.3.11 Use of Estuarine Sediments for Paleoenvironmental Studies

Sediment accumulation in estuaries enables them to store evidence of past environmental changes. These sediment accumulative potentials enable the study of interactions between humans and their alteration of estuarine ecosystems over time (Cohen *et al.*, 2013). As already mentioned, the bed composition of estuaries is mostly muds and silts with greater surface areas for adsorption of metals, pesticides, nutrients and organic carbon, which get accumulated over time (Lotze and Worm, 2009). Estuarine sediment are therefore becoming more useful tools for studying past eutrophication, contamination histories, and carbon sequestration rates, in addition to establishing baseline conditions and other watershed changes over time.

Recent advancements have made it possible for researchers to reconstruct historical environmental changes in estuarine and marine ecosystems. The use of estuarine

sediment to provide information on changing ecosystem health, particularly trace metal pollution over time has been studied thoroughly (Ruiz-Fernandez *et al*., 2003; Ruiz-Fernandez *et al*., 2009; Diaz-Asencio *et al*., 2009; Covelli *et al*., 2012). In addition the examination of ^{210}Pb profiles in sediment cores has proven to be one of the most widely accepted and validated methods for dating surface sediment cores.

2.3.11.1 Sediment Dating with ^{210}Pb

Dating sediment with ^{210}Pb is based on the principle that the naturally occurring isotope has been constantly delivered to the earth's surface, and is undergoing a continuous radioactive decay following incorporation into progressively accumulating sediment. The ^{210}Pb sediment dating method provides a very consistent dating estimate over the past 100-200 years (Smith, 2001). This period covers the start of the industrial age at the end of the 19th century for developed countries and the pre and post-industrial age for most developing countries.

Lead-210 (22.26 year half-life), is a naturally occurring isotope in sediment forming through the intermediate decay of ^{226}Ra (1622 year half-life) to the noble gas ^{222}Rn (3.85 day half-life). This ^{222}Rn diffuses into the atmosphere at a constant flux where it decays to ^{210}Pb. The atmospheric ^{210}Pb then adheres to aerosols that return to the surface of the earth as precipitation or dry deposition (Cheevaporn and Mokkongpai, 1996). The precipitation of atmospheric ^{210}Pb results in the addition of ^{210}Pb to sediment which is in excess of the amount supplied from the in situ decay of ^{226}Ra which forms the basis of the ^{210}Pb dating method (Cheevaporn and Mokkongpai, 1996).

To date sediment using the ^{210}Pb method, a number of models have been proposed. The original model, the Constant Flux-Constant Sedimentation (CFCS) model was the first to be developed (Robbins, 1978). Assumptions underlying this model are that:

I. There has been a constant atmospheric flux of excess ^{210}Pb to the surface of the earth.

II. The ^{210}Pb in water is quickly removed from solution onto particulate matter so that the excess ^{210}Pb activity in sediment is essentially from overhead fallout from the atmosphere,

III. The initial excess ^{210}Pb activity in sediment laid down on the bed of the lake is not redistributed by post-depositional processes and it decays exponentially with time in accordance with the radioactive decay law.

Based on these assumptions, a logarithmic plot of excess ^{210}Pb per unit mass of sediment against depth should generate a linear relationship, and the sediment accumulation rate can be determined from its slope (Robbins, 1978). The overall success of CF-CS model however requires an environment that meets all the listed assumptions. However, often times one or more of the assumption may be violated as such environment are rare to come by (Carroll and Lerche, 1995). Preliminary use of the CF-CS focused on sites where sedimentation rates were more or less constant though short-term environmental fluctuations combined with longer-term changes in accretion rates are common features of many sedimentary environments. In the midst of the dramatic environmental changes that have occurred over the past 150 years, the rates at which sedimentary environments have been eroding and accumulating are expected to have changed significantly during this period (Carroll and Lerche, 1995).

To address these environmental changes and to enable ^{210}Pb dating at sites where the sedimentation rate has changed, Robbins (1978) proposed another model known as the Constant Flux (CF) model or the Constant Rate of Supply (CRS) model (Appleby and Oldfield, 1978). The CRS which is the most commonly used model in ^{210}Pb dating assumes that ^{210}Pb flux has remained constant over time, but sediment accumulation rates have changed. Appleby and Oldfield (1983) proposed that, knowing the excess ^{210}Pb activity within sediment of depth *z* (g cm^{-2}) and age *t*, then it is shown in the CRS model that the age *t* of sediment of depth *m* satisfies the equation;

$$A(z) = A(0)\, e^{-\lambda t} \qquad 2\text{-}3$$

Where A (0) is the total excess ^{210}Pb activity of the entire core, λ is the ^{210}Pb decay constant (0.03114 year^{-1}). Both A (z) and A (0) are determined by an integration of the ^{210}Pb profile, leaving the sediment age t as a function of depth *z as;*

$$t = \frac{1}{\lambda} Ln \frac{(Ao)}{(Az)} \qquad 2\text{-}4$$

Based on this model, the changing sedimentation rate can be estimated from the equation;

$$r = \frac{\lambda A}{C} \qquad 2\text{-}5$$

Where A is inventory of ^{210}Pb and C is the excess ^{210}Pb activity. For a more accurate use of the model, particularly the first few levels above the equilibrium, a reliable estimates of the ^{210}Pb inventory is critical as an under estimation of A (0) will cause the ^{210}Pb dates of these levels to be too old.

A third model known as the Constant Initial Concentration, CIC (Appleby, 2001), is an alternative to the CRS model. The CIC model was developed to suit environments where

the excess ^{210}Pb flux is not delivered directly by local atmospheric fallout (Appleby, 2001). The CIC model is intended to work where the local ^{210}Pb flux is responding to remote changes in larger sedimentary systems such as abyssal environments in deep ocean basins or large lakes (Roux and Marshall, 2010). The model allows the sedimentation rate to change over time, but assumes that the initial excess ^{210}Pb activity has changed in proportion to the sediment supply (Appleby, 2001). According to this model, the excess ^{210}Pb activity in a layer z (cm) of sediment A (z) is given as;

$$A(z) = A(0) \times e^{-\lambda \times (z/w)\, t} \qquad 2\text{-}5$$

Where A (0) is the excess ^{210}Pb activity in the top layer of the sediment core, λ is the ^{210}Pb decay constant (0.03114 year^{-1}), and w is the sedimentation rate (cmyear^{-1}).

Model validation using independently determined dates from the stratigraphic records of artificial fallout of radionuclides such as ^{137}Cs proposed by Pennington *et al.* (1973) or ^{241}Am proposed by Appleby *et al.* (1991) is mandatory when using any of the above models. Assuming little, if any, surface mixing of sediment, the maximum depth of ^{137}Cs has been traced to the year 1954 where detectable levels of ^{137}Cs was first introduced into the environment as a result of atmospheric nuclear weapon testing by the United States of America (Watson, 2008). Thus, if ^{137}Cs is detected at a given depth, the date is interpreted to be 1954 onward.

The testing of nuclear weapons increased greatly in between the late 1950s and the early 1960s and actually peaked in the year 1963. Therefore if ^{137}Cs analysis is out at various depths in a sediment core, another ^{137}Cs marker is often found in the form of a concentration maximum at the year 1963 or even 1986 for the more recent Northern Hemisphere Chernobyl incident (Roux and Marshall, 2010). Cesium-137 has a half-life

of 30.2 years and retains specific properties, making it a very important and viable sediment tracer. Most importantly is the fact there are no natural sources of ^{137}Cs and fallout is highly related to local precipitation patterns with total fallout varying linearly with rainfall within different latitudes. In addition, ^{137}Cs is known to be strongly adsorbed onto clay and organic particles and is non-exchangeable (Ritchie and McHenry, 1990).

2.3.11.2 Reconstruction of Metal Pollution History in Estuaries using ^{210}Pb dating

The use of sediment in the reconstruction of metal pollution in different depositional environments has been thoroughly researched using radiometric and geochemical approaches. Using sediment cores dated with ^{210}Pb, Ruiz-Fernandez *et al*., (2003) examined historical trends of metal pollutions in the Culiacan River Estuary, Northwestern Mexico. They observed an increase in the flux Cu, Co, Cd and Zn metals beginning in 1948 and attributed this increase to the intensive clearing of the catchment for agriculture and the rapid demographic development of Culiacan City and other neighboring villages.

A similar study by Ruiz-Fernandez *et al*., (2009) in the Gulf of California also developed ^{210}Pb geochronologies of Cd, Cu, Hg, and Pb fluxes taken from the intertidal mudflat sediment cores of the coastal lagoons Chiricahueto, Estero de Urías, and Ohuira in the Mexican Pacific. Their results showed that sediment from Chiricahueto were significantly contaminated with enrichment factors as high as 7, 10, 12, and 18 for Cu, Hg, Cd, and Pb, respectively while the cores from the other two (relatively pristine) lagoons did not show any enrichment for Cu or Pb (EF<2). They also observed some significant enrichment for Cd at Ohuira lagoon (EF= 8 and 27) and extremely high

enrichment of Hg at Estero de Urías lagoon (EF=80). The historical increases of metal fluxes obtained from the sediment records in this study were also related to the release of agricultural wastes into the lagoons.

Diaz-Asencio *et al*., (2009) also reconstructed a one century sedimentary record of Hg and Pb pollution in the Sagua estuary (Cuba) using ^{210}Pb and ^{137}Cs chronology. Their study concluded that the depth profiles of Hg (concentrations up to 2.7 mg/kg) and Pb (concentrations up to 22 mg/kg) showed important anthropogenic inputs to the coastal environment which was attributed to the incomplete treatment of the chlor-alkali plant residuals and the increase of the Sagua la Grande City population.

Similarly, Covelli *et al*., (2012) studied the historical flux of mercury associated with mining and industrial sources in the Marano and Grado Lagoon (northern Adriatic Sea) using thirteen 1-m deep sediment cores collected from the subtidal, intertidal and saltmarsh zones. For most of the analyzed cores the study found natural background levels of Hg from depths 50-100 cm. The eastern area, showed Hg contamination to be at its maximum level at the core top (up to 12 mg/kg) as a consequence of the long-term Hg mining activity. The vertical distribution of mercury was related to the influence of the single-point contamination sources, whereas the grain-size variability or organic matter content seemed not to affect it. Hg concentration at western area did not to exceed 7mg/kg and contamination was recorded only in the first 20-30 cm. Result of the geochronological measurements showed that the depositional flux of Hg was influenced by anthropogenic inputs from mining operations after 1800, and after 1950, increase in Hg concentration was attributed to discharges from the Aussa River, which delivers Hg from the chlor-alkali plant.

Cundy *et al.*, (2001) studied historical trends in metal input from heavily-disturbed and contaminated Bilbao (Spain), Hamble (Southampton Water, UK) and Mulinello (Sicily) estuaries using ^{210}Pb and ^{137}Cs chronologies. Only the core from the Mulinello estuary provided a high-resolution record of recent heavy metal inputs in their study. A partial record of changing metal inputs over time was retained due to land-claim and possible early-diagenetic remobilization in Southampton water, while at Bilbao the vertical distribution of heavy metals in intertidal flats were said to be controlled mainly by input on reworked sediment particles and variations in sediment composition.

Garcia-Orellana, *et al*. (2011), also reconstructed a historical record of metals from a sediment core from the Port of Maó (Minorca, Spain), the second natural largest harbor in Europe. Their study showed that; the anthropogenic input of Pb and Sn inputs started during the second half of the 19th century and increased progressively until mid-20th century, while the accumulation Ag, Cd, Ni, Zn, Cu and Cr began in the 1940s, peaking in the late 1970s. The commissioning of a submarine outfall in 1978 was reported to have reduced metal concentrations in subsequently deposited sediment in the estuary.

An assessment of the present state and historical changes of trace metal pollution was carried out in Kaoping coastal sediment, southwestern Taiwan by Hung and Hsu (2004). Their study evaluated temporal metal concentrations and enrichment factors in sediment and related them to geomorphological and compositional parameters of the sediment. The concentrations of trace metals correlated closely with distributions of mud (<63 micron grain size) and organic carbon which accumulated largely around river mouths and within the Kaoping Canyon. Also with the exception of Cd, Cr and Ni in certain

areas with coarse sediment, metals were generally elevated above the baseline levels over the studied area.

Although the ^{210}Pb dating method has been widely recognized, and proven powerful in assessing temporal changes in metal concentrations in estuarine sediment, to date there have been no such studies in many places that are experiencing rapid industrialization including Ghana. This study therefore uses the ^{210}Pb dating method for the first time to assess temporal changes in metal concentrations in sediment from some Ghanaian estuaries.

2.3.12 Export of Trace Metals from Estuaries to Nearshore and Deep-sea Areas

Geochemical processes occurring in terrestrial environment may be directly or indirectly coupled to those occurring in the oceanic environment (Yue *et al.*, 2003). Metals enter the sea via several major routes, most notably through river input, atmospheric deposition, and industrial waste disposal (Kennish, 1997). Terrestrial runoff is however one of the most important routes for metals entering the coastal environment (Morton and Blackmore, 2001). Estuaries serve as the main channels linking activities on land to the ocean hence playing major geochemical roles in the biogeochemical cycling of materials between rivers and the oceanic environments (Morton and Blackmore, 2001). Agricultural, mining, industrial and municipal discharges are the main sources for metals released into rivers. As discussed earlier, metals in estuarine sediments may get remobilized through biological, geochemical and hydrodynamic process, where they enter the water column to be transported to offshore areas (Yue *et al.*, 2003).

2.4 Ecotoxicological Risk Assessment of trace Metals in Estuarine Environments using the AQUARISK Model

2.4.1 Ecotoxicological Risk Assessment (ERA) of Estuarine Ecosystems

The aim of ERA is to estimate the probability of the occurrence of adverse effects to communities of species in locations that are potentially exposed to pollutants and other substances (Solomon and Sibley, 2002). The process involves problem formulation, exposure and effects analyses, and risk characterization (Garnier-Laplace *et al*., 2009).

The problem formulation stage involves systematic planning and gathering of information that is geared towards determining the overall scope and objectives of the ERA. Effects analysis on the other hand deals with the gathering and analysis of data focused on the determination of exposure concentrations or rates not associated with adverse ecological effects (Hill *et al*., 2000). The exposure assessment process also involves gathering and analysis of data to determine the relevant exposure concentrations for ecological resources of concern at the site of interest. Finally, the risk characterization stage integrates the results of the effects and exposure assessments to characterize risks to the receptors in the aquatic environment such as phytoplankton, macrofauna, meiofauna and microfauna (Hill *et al*., 2000).

The tiered approach used in ERA is widely recognized as the effective way to conduct ecotoxicological risk assessments (CCME, 1996; European Commission, 1996; US ACOE, 1996; US EPA, 1998) on aquatic ecosystems. Although there are a variety of terms used to classify various ERA tiers, the screening-level risk assessment (SLRA) or tier 1 and the detailed-level risk assessment (DLRA), which is the second and other subsequent tiers, are the most widely reported in literature (Hill *et al.*, 2000).

SLRA is the first iteration process in an ERA and it is intended to identify which stressors or contaminants may pose potentially unacceptable risks and which ones can be ruled out from further tiers. The SLRA is a very conservative approach used in developing a good conceptual site model that identifies stressor sources, pathways and fate of stressors of potential concern (SOPC). In addition, the process identifies receptors of concern (ROC) using available information to focus the ERA on those SOPC/ROC combinations having the potential for unacceptable risks (Hill, *et al*., 2000).

Once the problem formulation is completed, both the exposure and effect analysis (which involve the estimation of hazard quotients (HQ) = estimated exposure/effects benchmark) are carried out effectively to screen SOPC/ROC combinations (Chapman and Mann, 1999). At this final stage of the SLRA, SOPC/ROC combinations with HQ<1 are considered risk-free and are 'screened out' of the ERA while SOPC/ROC combinations with HQ>1 are 'screened in' for evaluation in a DLRA (Chapman and Mann, 1999). The exposure estimates are based on data collected from the site of interest, while effects benchmarks are usually derived from literature. SLRA is a very conservative process hence the fact that a substance is "screened in" the SLRA does not necessitate a real risk or conversely the manner in which a substance is "screened out" should convincingly indicate the lack of risk (Chapman and Mann, 1999; Hill *et al*, 2000).

The goal of a DLRA is to reduce residual uncertainty from the SLRA. During the SLRA stage, data for effects benchmarks are derived from literature sources or data collected from other sites which typically necessitates that a conservative assumption is made in the effects assessment to ensure that site-specific risks are not underestimated. An HQ>1

indicates either there are truly unacceptable risks, or conservative assumptions and uncertainties prevented an assessor from concluding that there are not unacceptable risks (Burmaster and Harris, 1993).

In DLRA and subsequent tiers, If the HQ>1 from the SLRA was based on ambient concentrations, more site-specific information is gathered to characterize either exposure or effects (Chapman and Mann, 1999). For effects analysis an alternative approach to the use of environmental quality values would be to derive receptor-specific values which specify an exposure level corresponding to an acceptable effect level (Hill *et al*., 2000). Such receptor-specific values could be the ambient concentration of a contaminant that will results in a 20% effect level for a particular receptor.

The exposure values could be estimated specifically from either intake rate or a daily dose or the nature of the exposure pathway, by measuring tissue concentrations (Hill *et al*., 2000). In cases where bioaccumulation is important, it may be possible to estimate bioaccumulation factors (BAFs) to estimate the uptake of a contaminant by a receptor of concern (Hill *et al*., 2000).

2.4.2 Risk Assessment Models

Ecological risk assessment models can be grouped into three broad categories; namely food web-based models, ecosystem- based models and socio-ecological models (Chen *et al.*, 2013).

In food web models, information derived from the analyses of complex relations among species and variation over time and space within a given ecological food web, are used in

modeling cumulative effects of toxic chemicals and other stressors in the environment (Preziosia and Pastorok, 2008). The multimedia box models (MBMs) (Mackay, 1991), AQUATOX (USEPA, 2004), and the fugacity-based food web model (FFWM) (Wang *et al.*, 2010) are a few of the known food web-based models used in the assessment of risk to aquatic ecosystems.

The MBM model was originally developed for assessing the effects of agricultural practices on soil structure from the system's perspective. In this model, a collective pattern about how agricultural practices change food web structure and function is established based on a comparison of five long-term system level studies of soil food webs on native and agricultural soils (Mackay, 1991 in Chen *et al.*, 2013). The basic assumptions underlying the MBM model have been complemented with bioaccumulation modules to address contaminant fluxes in basic food web structures (Gobas, 1993).

AQUATOX was developed based on considerations on ecological effects and environmental fate, to predict the fate of nutrients and organic contaminants in water bodies in addition to their effects on the organisms (USEPA, 2004; Park *et al.*, 2008; Zhang *et al.*, 2013). AQUATOX simulates multiple environmental stressors, such as toxic chemicals, nutrients, organic loadings, and temperature, and evaluates their adverse effects on algal, macrophyte, invertebrate, and fish communities in aquatic ecosystems (Preziosia and Pastorok, 2008).

The FFWM model was developed to assess exposure to specific pollutants (Wang *et al.*, 2010) in an ERA. It was developed to specifically simulate the bioaccumulation of dichloro-diphenyl-trichloroethanes (DDTs) within aquatic ecosystems based on the

formulations of internal exposure distributions and internal species sensitivity distributions in the ecosystem (Chen *et al*., 2013). Initial result of this model showed that the bioaccumulation factors increased with increasing trophic level in the food web (Wang *et al*., 2010). The FFWM model is therefore capable of predicting the degree of cumulative effects of hydrophobic organic pollutants obtained through the food web on organisms to evaluate the risk they pose to aquatic ecosystems (Wang *et al*., 2010).

In addition to assessing changes of predator–prey relationships within organisms, ecosystem-based risk assessment models incorporate the altered interactions among organisms and environmental factors such as sunlight, temperature, soil and water that are associated with a certain hazard (Dale *et al*., 2008). These models have demonstrated their potential to evaluate structural and functional response within a variety of ecosystems in the context of ecosystem-based risk management (Chen *et al*., 2011). The comprehensive aquatic systems model (CASM) (De Angelis *et al*., 1989; Bartell *et al*., 1999), the regional vulnerability assessment (ReVA) (Boughton *et al*., 1999), the ecological network analysis (ENA) (Fath and Patten, 1999; Fath, 2004; Chen and Chen, 2012b), the communities and habitats status assessment (CHSA) (Robinson *et al*., 2010), and the aquatic ecological risk assessment (AQUARISK) (Twinning *et al.,* 2005), are a few of the ecosystem-based models used in ERA.

The CASM model was developed to simulate the daily production dynamics of the populations inhabiting a water column, a littoral zone, and a benthic zone (De Angelis *et al*., 1989). Upon a few modifications however, the model is now capable of estimating the probability of changes in the biomass of multiple populations as a direct or indirect

result of toxic effects of the dissolved chemical contaminant, which has caused changes in the competitive or predator–prey relations in complex food webs (Bartell *et al*., 1999).

The ReVA model is an integrated assessment which involves the identification and locating of both environmental resources and the conditions that are stressing these resources on ecosystem scale (Boughton *et al*., 1999). The model uses four interactive functions (landscape, research gaps, real world, and data and analytical tool) to develop regional assessments that address current and future risk of ecosystems (Chen *et al*., 2013). One application of this model was the development of an early-warning system to identify ecosystems which are most vulnerable to being lost or permanently harmed in the coming years and determine which stressors are likely to cause the greatest risk (Boughton *et al*., 1999).

2.4.2.1 The AQUARISK model

AQUARISK is an ecosystem-based ERA software package developed by the Australian Nuclear Science and Technology Organization (ANSTO). AQUARISK utilizes a 3-tier approach to provide a convenient means by which site-specific ecological risks can be assessed in a scientifically defensible manner (Twinning *et al*., 2005).

Tier 1 initially determines chemicals of potential concern (COPCs) by comparing measured or modeled concentrations of metal pollutants in water and sediment with water and sediment quality guidelines (WQG AND SQG), whileTiers 2 and 3 analyses involves more detailed probabilistic modeling using site-specific data (Twinning *et al*., 2005). Based on the assumption that the data are representative of a more extensive distribution of real concentrations, the analyzed water or sediment quality data for each metal are fitted to both lognormal and Burr Type III distributions which are tested using

goodness of fit tests. This is done to assess whether the measured concentrations fit the fitted distributions and the cumulative probability distribution functions of the observed data and the fitted distributions are plotted to "screen in" any COPCs (Twinning *et al*., 2008).

Where COPCs are identified in the Tier 1 analysis, dose-response-data (DRD) are accessed for the metals that exceed the guideline values. For the water and sediment quality data, log-normal and Burr Type III distributions are fitted to the data for each metal and their goodness of fit analyzed for the measured biological-effect concentrations to be observed graphically against the fitted distributions and the guideline value (Twinning *et al*., 2005; Twinning *et al*., 2008). At this stage, the organisms in the dose-response database would have been assigned to arbitrary trophic level categories as plant, herbivore, carnivore etc. for the graphical representation to indicate the trophic levels most at risk from the hazard (Twinning *et al.*, 2005). Once the distribution parameters and their uncertainties have been determined, critical values namely the median Hazardous Concentration (*HC)* affecting 5% of species (HC_5) and its 95% lower confidence limit ($HC_{5,95}$), based on the selected dose response data, can be determined (Twinning *et al*., 2005).

In sum, AQUARISK estimates the degree to which the water and sediment quality are likely to exceed the guideline values (Tier 1) and the critical values (HC_5, $_{95}$, or user defined $HC_{x,y}$ values) determined from the DRD (Tiers 2 and 3) (Twinning *et al*., 2005). It further reports the average percentage of species likely to be affected by the measured or modeled water or sediment quality parameter through an estimate of the extent to which the two probability distributions overlap, so that water or sediment quality data

exceeds DRD (Twinning *et al*., 2008). The total risk to an aquatic community from all chemicals present is also calculated (Twinning *et al*., 2005). Lastly, the AQUARISK software package is also able to estimate the required reduction in the water/sediment quality metal concentrations (either in the form of exceedence probability of the various criteria or an agreed tolerable degree of harm, as measured by the percentage of biotic species likely to be affected) needed to achieve acceptable risk (Twinnig *et al*., 2005).

Since its inception, AQUARISK has been adopted by ANSTO and nearby regions as a quantitative and probabilistic metal and radio-ecological risk assessment tool mostly for water (Twinning *et al*., 2008: Hoffmann *et al*., 2003). Slight modifications of sediment quality data allows for the use of the software package in performing ERA in the benthic environment (Twinning *et al*., 2008).

2.4.3 Summary of Review

Estuarine environments provide record of rich sediment deposition that serves as sinks for trace metals and other substances. A comprehensive review of available literature shows that sediments from these environments contain vital information that are useful to the understanding of geochemical processes occurring within their drainage basins. Provenance analysis of coastal sediment using their bulk geochemistry and mineralogy are very useful in tracing the origin of sediments in depositional basins. These studies are even more useful in the sense that they could help in explaining the source of materials transported with sediment into the estuarine environment. Also the use of estuarine and marine sediment for paleoenvironmental analysis such as metal pollution reconstruction are very useful in setting baselines and explaining trace metal accumulations due to urbanization and industrialization. Knowledge on the accumulation trends of metals,

their current levels and potential of posing threats (risks) to estuarine ecosystems is therefore of paramount importance to aquatic researchers and environmental managers. Although the assessment of provenance, trace metal accumulation trends and ecotoxicological risk of estuarine sediment are very crucial and widely applied, no data to date exists on the use of any of these approaches on estuarine sediments from Ghana. This current study will therefore incorporate the three approaches in explaining geochemical processes occurring in estuarine sediments from Ghana.

CHAPTER THREE

GEOCHEMICAL AND PETROGRAPHICAL ASSESSMENT OF ESTUARINE SEDIMENTS FROM GHANA: IMPLICATIONS FOR PROVENANCE AND WEATHERING PROCESSES

3.1 Introduction

The geochemical composition of nearshore sediment is controlled primarily by its source rocks as well as modifications that occurred during transport from source regions. Thus sequences of sediment within the estuarine environments provide valuable forensic information for determining aspects of formation as well as provenance (Nesbitt and Young, 1982). Provenance, is a term adopted by sedimentary petrographers to encompass all factors relating to the production of sediment, with specific reference to the composition of the parent rocks as well as the physiography and climate of the source area from which the sediment are derived (Weltje, 2004). Provenance studies are necessary in nearshore geochemical studies because information gathered from such studies are useful for understanding the main source of sediment supply and to some extent contaminants that are carried with the sediment into depositional basins (Singh and Rajamani, 2001).

The compositions of major elements such as SiO_2, Al_2O_3, Na_2O, MgO, P_2O_5, K_2O, CaO, TiO_2, and Fe_2O_3 in coastal sediment are useful indicators of their source, tectonic setting and paleo-weathering conditions (Roser and Korsch, 1986). The discriminant functions of Roser and Korsh (1988) have proven very useful in the discrimination of sedimentary provenances from different depositional basins (Singh and Rajamani, 2001; Tripathi and Rajamani, 2003).

In addition to the bulk geochemical analysis of major elements, petrographical approaches particularly the Quartz-Feldspar-Lithic (QFL) mineralogical framework of sediment have also been adopted for the discrimination of provenance in depositional basins (Bekele, 2011). Identification of these mineralogical frameworks is typically

achieved through the preparation of thin sections and smear slides for analysis under petrographic microscopes and percent values of these main compositions are input into simple QFL ternary plots for provenance study.

This study incorporated modal mineralogy and chemical composition of sediment deposited in major Ghanaian estuaries within the last 100-200 years to disclose their origin. The fine-grained nature of the sediment necessitated the use of both petrographic and chemical analysis for provenance assessment because the chemical analyses helped to elucidate compositional details not resolvable with the petrographic microscope, especially in the very fine-grained matrix.

3.1.1 Justification of study

The geochemistry of trace metals in estuarine environments is strongly coupled to sediment supply and flux into depositional basins. Sediment are often the ultimate sink for trace metals in the aquatic environment and provenance studies are useful for understanding geochemical transformations of the sediment from their source to sink. Although petrological and geochemical studies have been carried out on some super group outcrops and formations in Ghana for discriminating provenance (Asiedu *et al.*, 2004; Osae *et al.*, 2006), provenance information on sediment from marine and estuarine environments do not exist. This study therefore reconstructed provenance of the parent-rock assemblages of estuarine sediment cores from Ghana and explained any modifications in elemental compositions of sediments. The results of this study would help in explaining the possible source of sediment and trace metal supply to the estuaries.

3.1.2 Aim and Objectives

The study used petrographical and geochemical methods to reveal the composition of the estuarine sediment cores and reconstructed the parent-rock assemblages of the sediment in each estuary. Specifically to:

I. Assess grain size compositions and general characteristics of each core;

II. Determine the mineralogical composition of each core using petrological and geochemical approaches;

III. Elucidate the source of sediment supply to each estuary.

3.2 Materials and Methods

3.2.1 Environmental and Geological setting of study sites

3.2.1.1 Ankobra Estuary

The Ankobra estuary is located between latitudes $4^{o}53^{1}$N and $4^{o}54^{1}$N and longitudes $2^{o}16^{1}$W and $2^{o}17^{1}$W at the mouth of the Ankobra River which begins south of Sefwi-Bekwai, and runs about 190 km to Axim where it discharges into the Gulf of Guinea (Plate 1). The estuary forms part of the Ankobra basin which is about 8400 km^2 going through the townships of Dompem, Prestea, Bogoso, Asankragua, Awaso, Tarkwa, Egyembra, Esiama and Axim (Dickson and Benneh, 1980).

The geology of the basin consists mainly of the lower proterozoic rocks divided into the lower and upper Birimian systems, and unconformity overlain by the Tarkwaian system (Fig. 3.1). Igneous rocks ranging from meta-dolerite to felsite and quartz porphyry, gabbro and norite intrude into both the Birimian and the Tarkwaian systems at several places (Junner *et al.* 1942). The Lower Birimian rocks make about 60% of basin and

comprising the townships of Prestea, Awaso, Asankragua, Bogoso and Esiama (Junner *et al.* 1942; Kesse, 1985). The rock compositions of the lower Birimian basements are mainly quartzites, phyllites, grits and conglomerates, and schists (Junner *et al.* 1942).

The Upper Birimian system covers the Axim and Domprem townships and constitutes about 8% of the basin. The basin is dominated by rocks of volcanic and pyroclastic rocks, metamorphosed lavas, hypabyssal basic intrusive, phyllites and greywackes (Junner *et al.* 1942; Kesse, 1985). The Tarkwaian system, which underlies the Tanoso Township and its surroundings, forms nearly 15% of the basin and consist mainly of basic intrusive rocks. Gold mining both legal and illegal, cash crop farming and fishing are major economic activities dominating the entire drainage basin.

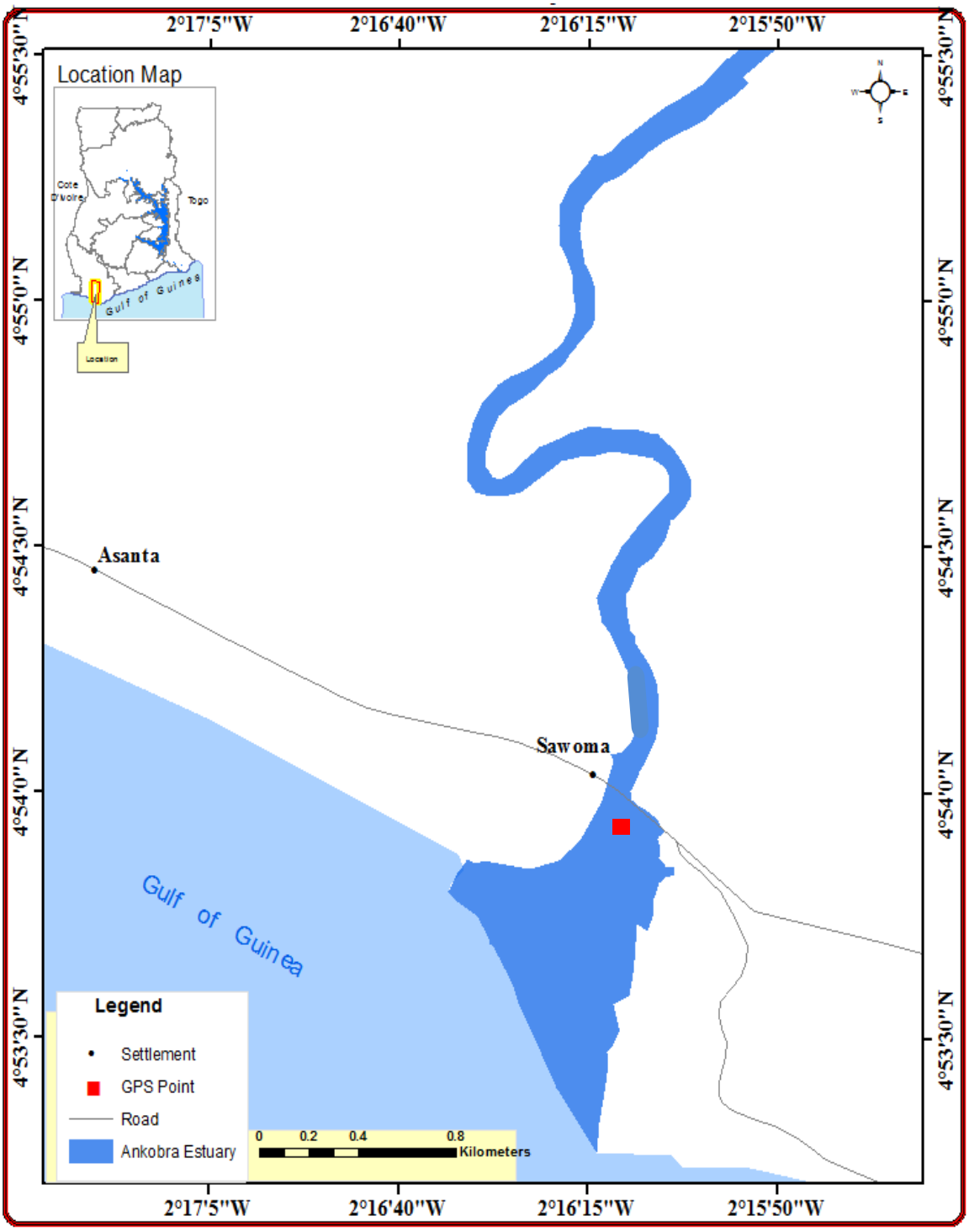

Figure 3.1 Map of the Ankobra estuary showing sediment coring site and watershed areas.

3.2.1.2 Pra Estuary

The estuary of the Pra River is located between latitudes $5^{o}00^{1}$N and $5^{o}01^{1}$N and longitudes $1^{o}36^{1}$W and $1^{o}3^{7}$W (Fig. 3.2). The Pra River takes it source from the Kwahu Plateau before connecting with rivers Offin and Birim to enter the Gulf of Guinea at Shama in the Western Region of Ghana (Donkor *et al.*, 2005). The Pra is known to be one of the largest rivers in the country with an estimated mean annual discharge of about $214m^3s^{-1}$, draining a total area of $29,000km^2$ (WRC, 2012). It runs through the townships of Obuasi, Dunkwa, Bogoso, Fosu, Twifo Praso, Tarkwa in the upper to middle reaches and Sekondi Takoradi, Aboadze, Nsuta, Inchaban, Aboso and Shama in its lower reaches (WRC, 2012).

The rocks underlying the region are pre-Cambrian and classified mostly into crystalline basement granitoid complex (Tarwaian) although a few are Birimian (Fig. 3.3). The rock compositions of the Obuasi, Dunkwa, Bogoso, Fosu, Twifo Praso, Elmina, Tarkwa Takoradi, Sekondi and Inchaban areas are mostly quartzites, phyllites, grits, conglomerates while those of Shama and Aboadze are metamorphosed lavas, pyroclastic rocks, hypabyssal basic intrusives, phyllites and greywackes (Dickson, and Benneh, 1988). Major economic activities in the basin include mining (legal and illegal), crop farming and wood processing.

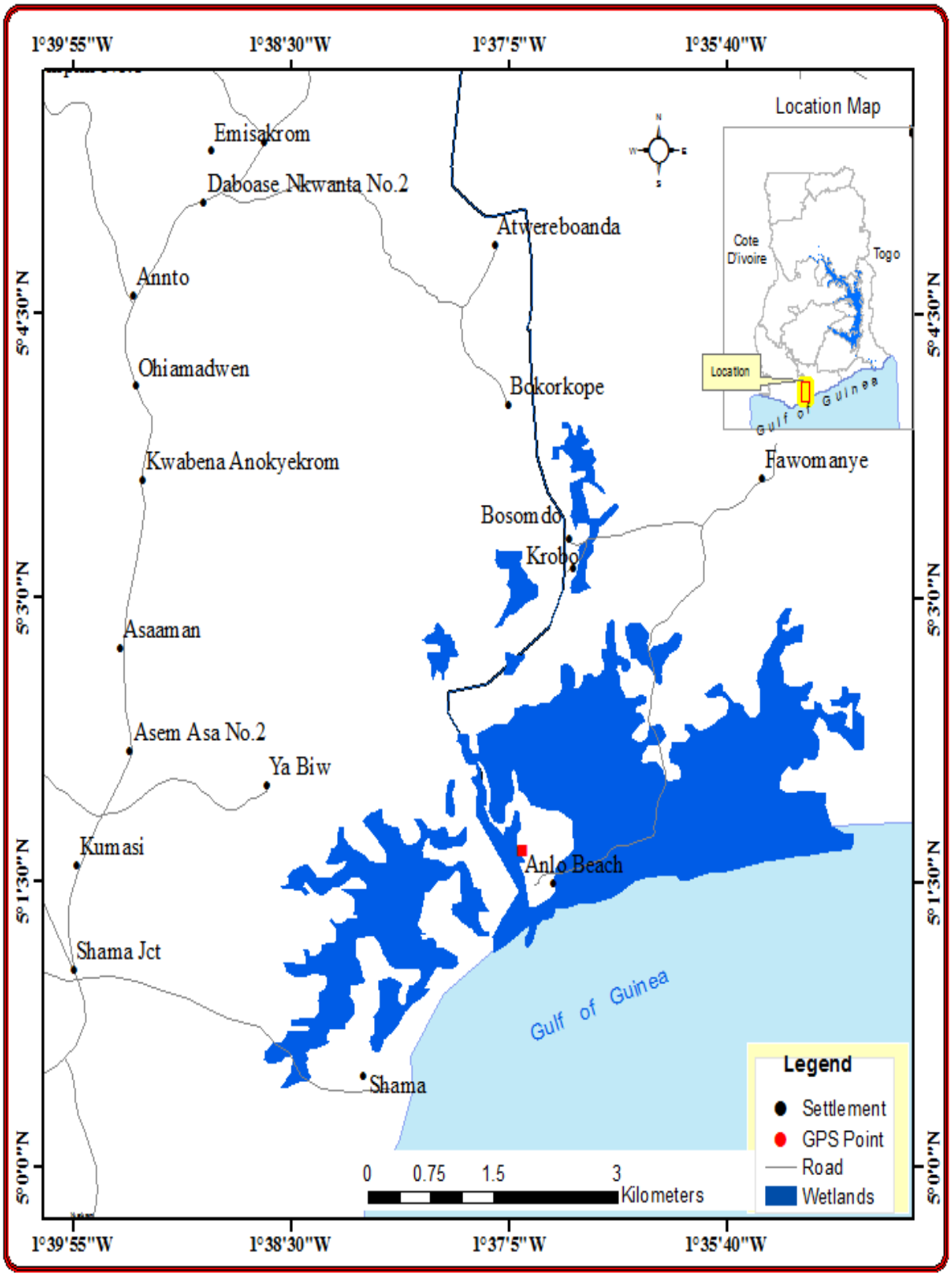

Figure 3.2. Map of the Pra estuary showing sediment coring site and watershed areas

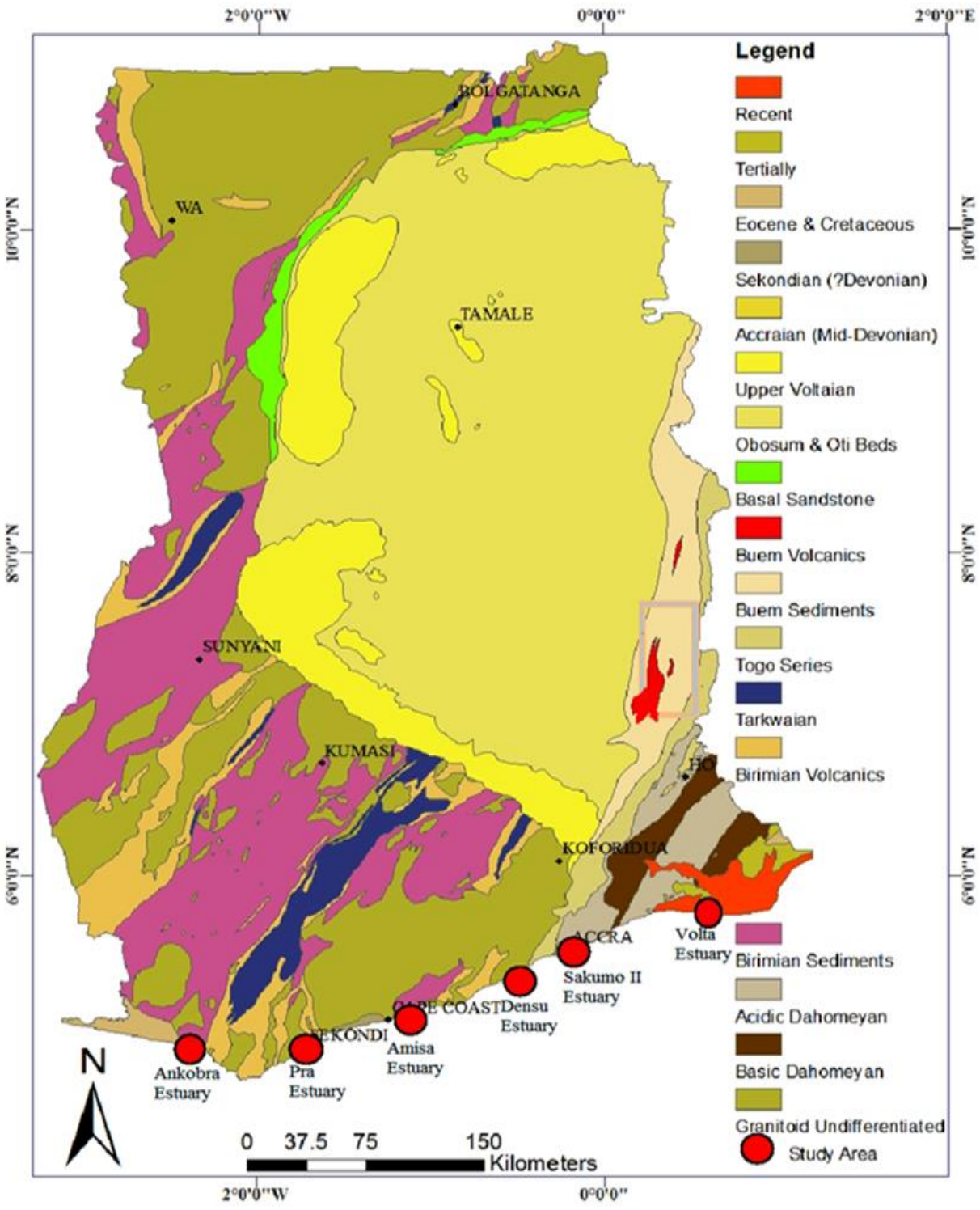

Figure 3.3 Generalized Geological map of Ghana showing study Areas

3.2.1.3 Amisa Estuary

The Amisa estuary is located between latitudes $5^{o}12^{1}$N and $5^{o}13^{1}$N and longitudes $0^{o}59^{1}$W and $0^{o}100^{1}$W (Fig. 3.4). It is a small estuary (about 3km long and 1km wide) with a peripheral floodplain of about 7500 ha that formed at the mouth of the Amisa river in Amisano at Saltpond in the Central region. The Amisa drains Abakrampa, Asebu, Biriwa, Mankesim, Dunkwa, Enyan Denkyira, and Asaafa in the Mfantseman District.

Most areas in the Mantseman district are characterized by elevations lower than 60m above sea level and underlain by upper and lower Birrimian and intrusive Tarkwaian rocks (Fig. 3.3). The rock composition of the basin varies from Granite, biotites, muscovites, granodiorites, pegmatites and aplites with biotite schist pendants for the Asebu, Abakrampa, Enyan Denkyira townships; phyllites, schsits, tuffs and greywackes for the Mankesim, Biriwa, Abandze and Abaasa townships; while the township of Saltpond consist mostly of upper Voltaian sandstones (Dickson and Benneh, 1980).

The main economic activities of the basin include, farming in the upper reaches, fishing and salt production in the lower reaches.

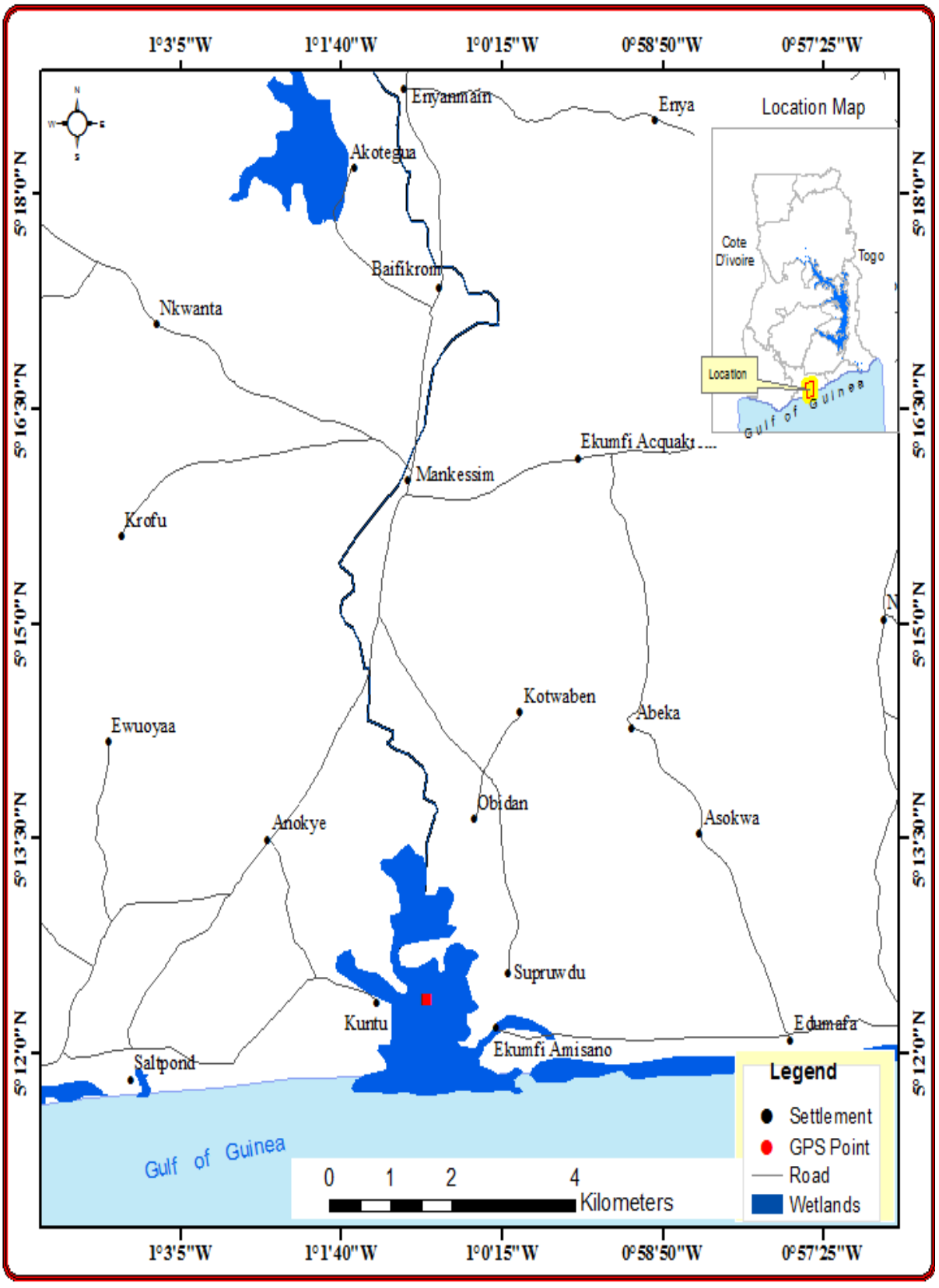

Figure 3.4. Map of the Amisa estuary showing sediment coring site and watershed areas

3.2.1.4 Densu Estuary

The Densu estuary is located between latitudes $5^{o}30^{1}$N and $5^{o}31^{1}$N and longitudes $0^{o}17^{1}$W and $0^{o}18^{1}$W (Fig 3.5). It formed at the mouth of the River Densu which takes its source from the Atewa-Atwiredu mountain range near Kibi in the East Akyem District of the Eastern Region of Ghana (Hagan *et al.,* 2011). The river, whose main tributaries include rivers Adeiso, Nsakyi, Dobro, and Kuia is about 116 km long with a catchment area of 2564 km^2 covering nine administrative districts (Debrah, 1999). The river drains through the Old Tafo, New Tafo, Akwadum, Koforidua, Suhum, Nsawam, Adaiso, Asuhoe, Mangoase, Bepowase townships which are underlain by Birimiam and Dahomeyan basement rocks; and Pokuase, Weija, Bortianor, Kokrobite and Nyanyanu townships which are underlain by the Togo series rocks (Fig. 3.3). Granites, biotite and muscovite granites, granodiorites, pegmatites, aplites with biotite schist pendants are the main composition of rocks in the Birimiam and Dahomeyan basement rocks (Amuzu, 1975).

Marine series of shales, sandstones, limestones, glauconite sandstones and oil, basaltic, andesitic and trachytic lavas, agglomerates, tuffs and jaspers form the main geology of the Togo series basement rocks of the Bortianor, Kokrobite and Nyanyanu areas (Amuzu, 1975). The Densu River which serves as a wide link among the villages and towns from Tafo to Accra is one of the largest terrestrial fresh water reservoir supplying Accra, the capital of Ghana with drinking water thus playing an important role in the ecology, history and economy of the industrialized northeastern part of Ghana. The estuary is a designated Ramsar site as well as an important fishery source to the townships surrounding the lower reaches of the river and some other parts of Accra. Cultivation of crops such as cocoa, maize, cassava, vegetables, pineapples and cocoyam

as well as the raising of livestock and fishing form the main economic activities in the upper catchment.

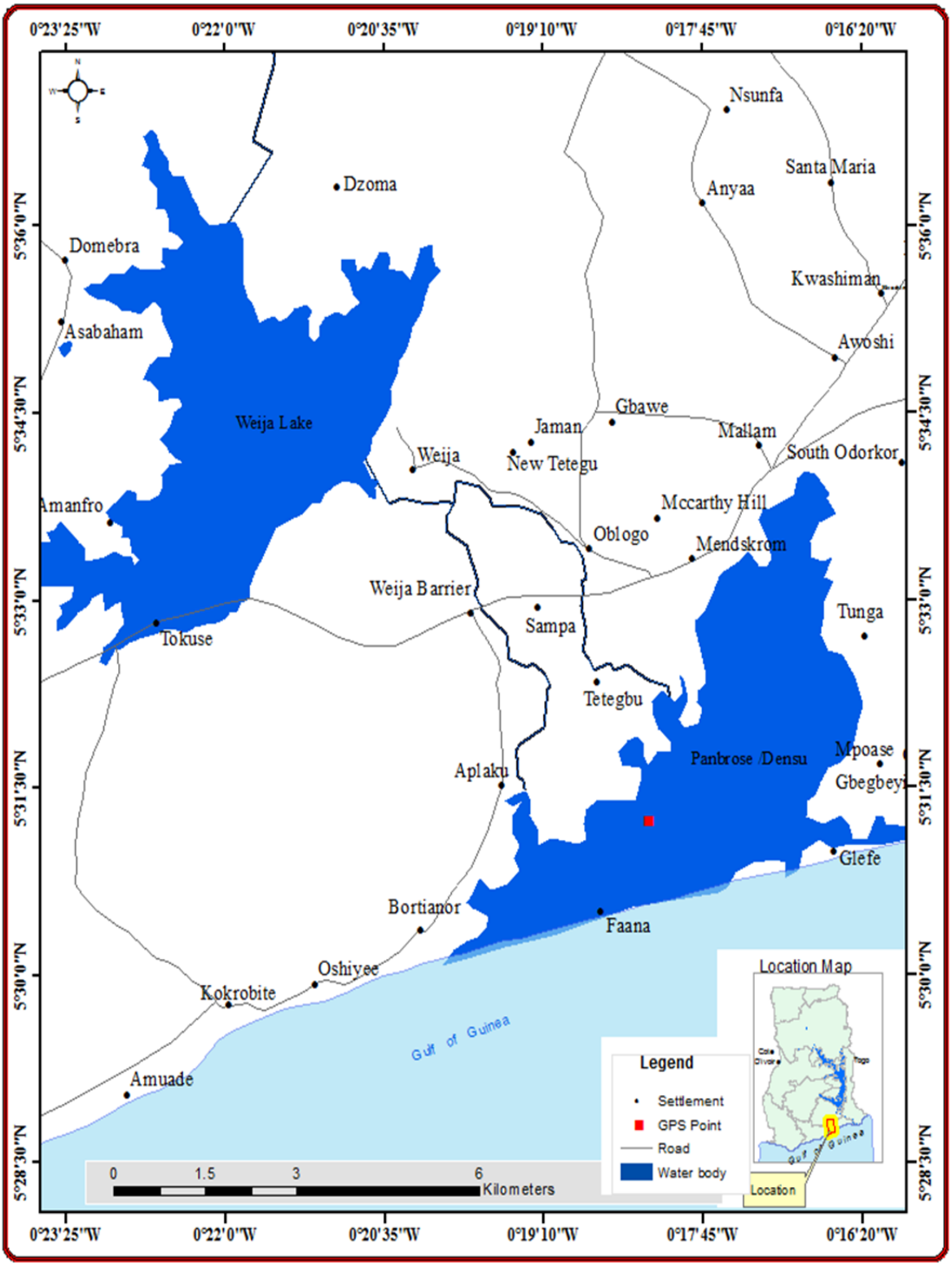

Figure 3.5. Map of the Densu estuary showing coring site and watershed areas

3.2.1.5 Sakumo II Estuary

The Sakumo II lagoon (Fig. 3.6) occupies an area of about 3.5 km^2 and lies between latitude 5^o 36^I N and 5^o 41^I N and longitude 0^o 01^I W and 0^o 04^I W, about 3 km west of Tema. The lagoon was naturally closed to seawater exchange (Kwei, 1974) until the construction of two artificial culverts which now allow constant exchange of water and materials between the lagoon and the adjacent sea. Although the lagoon has an effective catchment area of about 27,634ha, the area liable to flooding by water bodies including the lagoon and other smaller pools is about 812ha (Laar *et al*., 2011). The lagoon is a habitat to about thirteen (13) fish species belonging to thirteen (13) genera and eight (8) families with *Sarotherodon melanotheron* being the most represented fish species consisting of about 97% of the entire fish population (Koranteng, 1995). The Tema, Sakumono, Afienya, Lashiba townships form the main lower drainage basins of the dworwulu and mamahuma, the main rivers feeding the lagoon while the upper drainage goes through the Dododowa townships and environs. Acidic ortho and para gneisses, schists and migmatites rich in garnets, hornblendes and biotites form the rock composition of the Tema and Sakumono areas (Fig. 3.2).

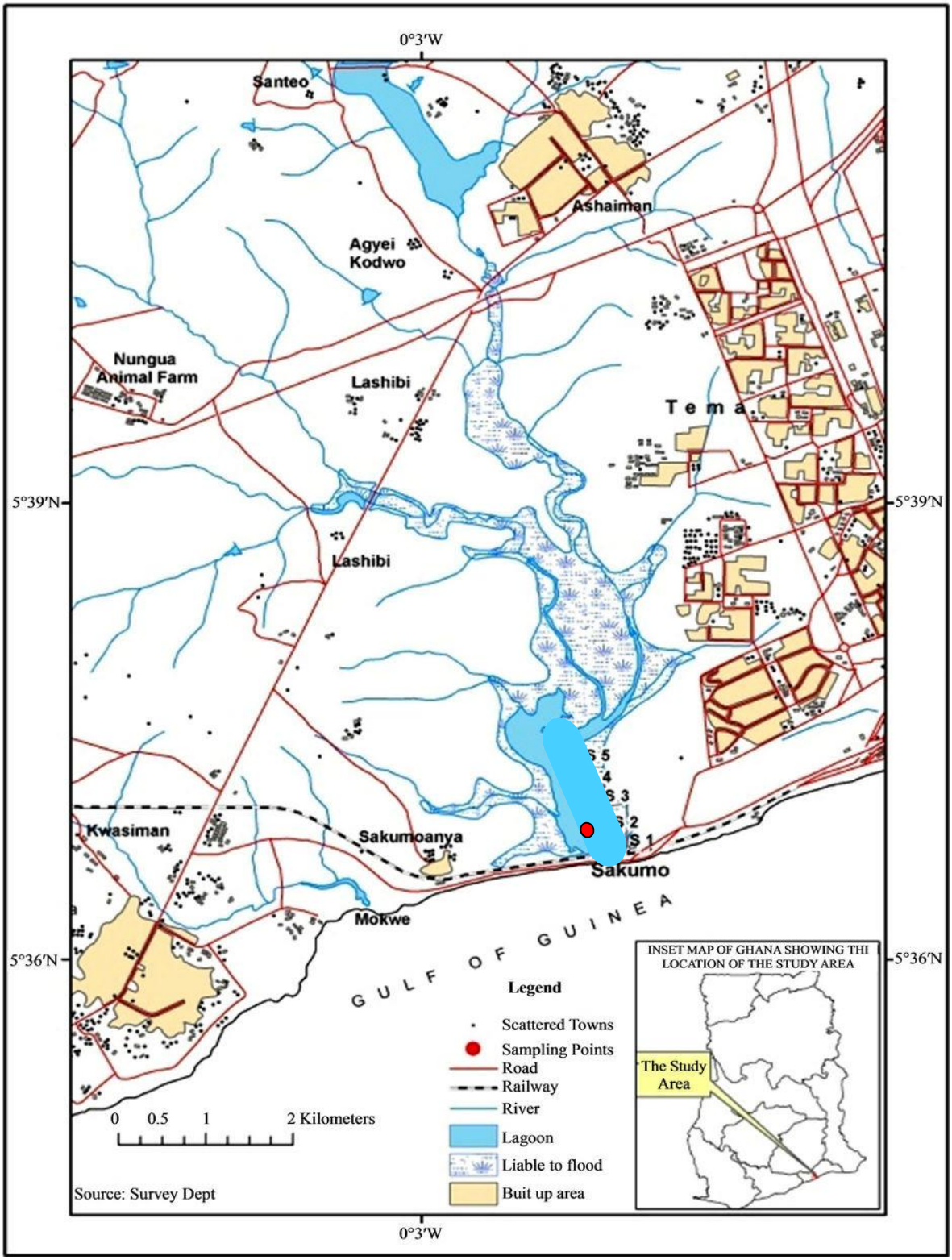

Figure 3.6 Map of the Sakumo II estuary showing sediment coring site and watershed areas

3.2.1.6 Volta Estuary

The Volta estuary formed at the mouth of the Volta River and can be located between latitudes $5^{o}46^{1}$N and $5^{o}48^{o}$N and longitudes $0^{o}37^{1}$E and $0^{o}41^{1}$E (Fig. 3.7). The entire basin of the Volta river stretches from about latitude 5^{o} 30^{1}N in Ghana to 14^{o} 30^{1}N in Mali spreading across six West African countries (43% in Burkina Faso, 42% in Ghana, and 15% in Togo, Benin, Cote d'Ivoire and Mali (Barry *et al.,* 2005). The Akosombo dam which generates about 80% of power produced in the country is by far the most significant structure built in the basin. Draining about 70.1 of the total landarea of Ghana, the volta river runs through the main townships of: Daboya, Tolon, Bimbila, Zabzugu, Salaga,Yeji, Kwame Danso, and Atebubu in the Northern and Brong Ahafo regions; Tafo, Kpong and Akosombo in Eastern region; Kete Krachi, Kpando, Kpeme, Ho and Sogakope in the Volta region; and finally joins the Gulf of Guinea in Ada. The geology of most of basin (Daboya, Tolon, Bimbila, Zabzugu, Salaga,Yeji Kwame Danso, and Atebubu in the Northern and Brong and Ahafo regions; Tafo, Kpong and Akosombo in Eastern region; Kete Krachi) consist of the Voltaian Supergroup or province while the the eastern part (Akosombo, Akuse, Kpong, Osudoku, Fute, lolonya, Akplabanya, Anyanui, Kpando, Kpeme, Ho, Big Ada) of the basin falls mostly within the Togo series or Pan African Province (Fig. 3.3). The Voltaian Supergroup which consists mainly of sanstones has been sub-divided into three groups based on stratigraphic succession namely; the Obosum, Pendjari and kwahu groups (Kesse, 1985). The Obosum group which comprise of the Densubon and Dukro sandstone formations younger (of cambrian in age) is about 400-500m deep. It consist mainly of continental detrital sequence characterised by red and green coloration and frequenly coarse grained. It considered as the molasse deposits of the dahomeyan group (Kesse, 1985). The Pendjari group which comprise the Tease sandstone formation and Bimbila formation is about 2000m deep and

green in coloration. It has a flysch-like sequence which is composed of siltstones and sandstones that are more or less argilliceous, shales, and greywackes with rare intercalations of limestone containing stomatolites and sponge remains (Kesse, 1985). The Kwahu group which comprises the Anyaboni, Obocha, Abetifi and Mpreaso sandstone formations is about 0-700m deep consisting of sandstones, siltstones and shales with a few interlayers of limestones sandwiched two sandy formations (Kesse, 1985).

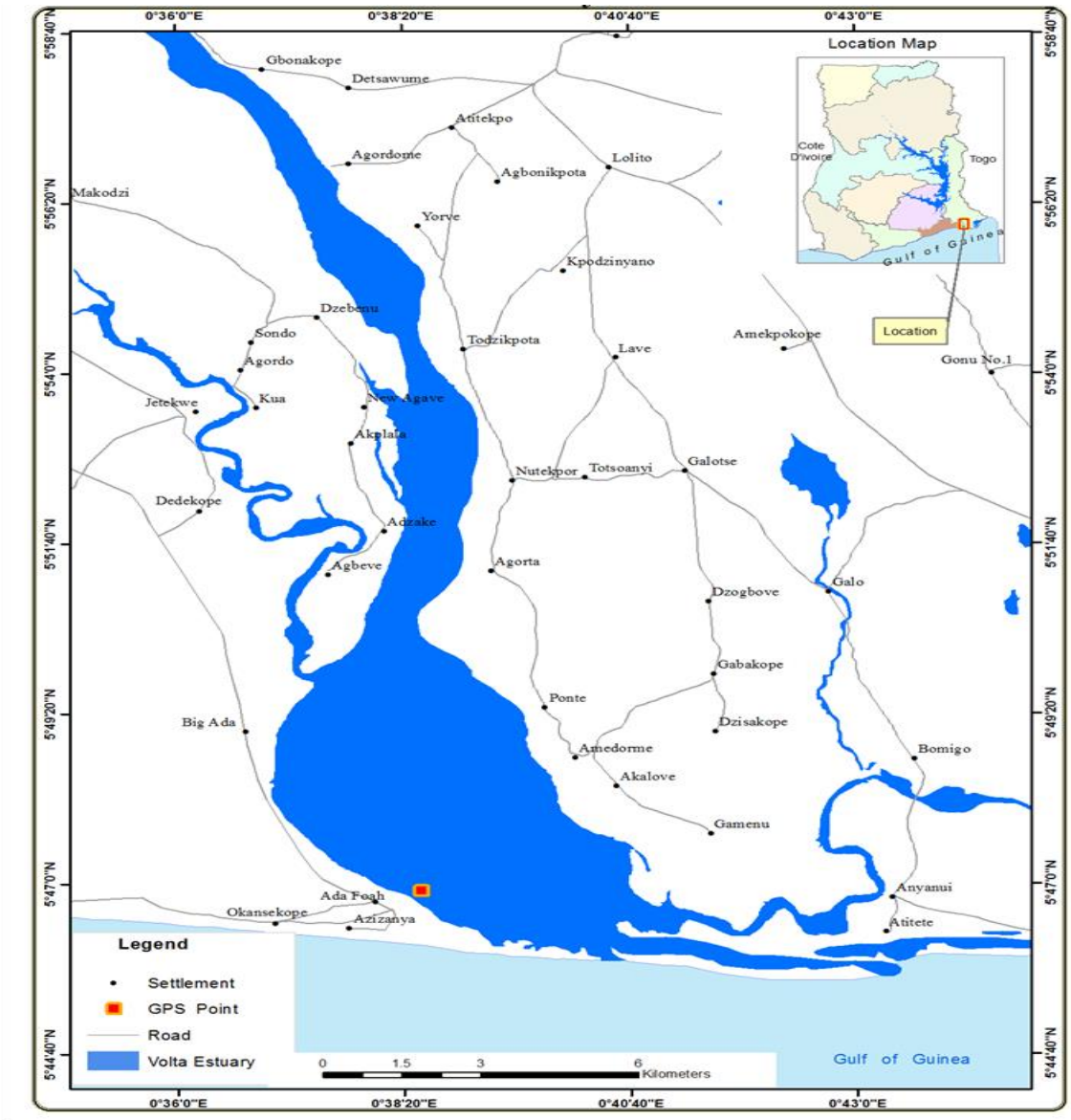

Figure 3.7. Map of the Volta Estuary showing coring site and watershed areas

3.2.2 Sampling Procedure

A total of 6 hand sediment cores were taken close to the mouths of the Ankobra, Pra, Amisa, Densu, Sakumo II and Volta river estuaries in 2012 using PVC Uwitec corers (60 cm in height and 8 cm in diameter). Specific details of cores and their locations are given in Table 3.1.

Table 3.1. Sampling Information and Core Descriptions

Estuary	Latitude	Longitude	Depth (m)	Length (cm)	Date
Ankobra (ANK)	4.903389	-2.2695278	0.9	50	04/05/12
Pra (PRA)	5.027778	-1.6166389	0.9	52	04/05/12
Amisa (AMI)	5.206361	-1.0152556	1.6	55	04/06/12
Densu (DEN)	5.520556	-0.3038056	0.9	55	06/30/12
Sakumo II (SAK)	5.614861	-0.3263889	1.4	56	06/30/12
Volta (VOL)	5.7818611	0.64183333	0.9	56	07/1/12

Cores were transported in upright positions to the laboratory where their overlying waters were gently syphoned. Each core was sub-sectioned at 0-2cm intervals to a total length of 40cm, oven-dried at 60^{o}C to constant weight (see plates showing section preparations in Appendix A1). The dried sediment samples were analyzed for grain size (laser particle sizer), mineral characteristics (petrographic microscopy), and trace metals (inductively coupled plasma mass spectrometry) at Moss Landing Marine Laboratories (MLML), California. Radiometric analyses were performed using a high purity germanium detector at the United States Geological Survey facility in Santa Cruz, California. Details of these procedures are described below.

3.2.3 Lithology

3.2.3.1 Grain Size Analysis

Grain size analysis was performed on every 2cm section of oven dried sediment using a pre-calibrated Beckman Coulter LS-1320 laser particle sizer at MLML. The LS-1320 Laser particle sizer incorporates Beckman Coulter's patented polarization intensity differential scattering (PIDS) technology to provide a dynamic range that spans from 0.04 to 2000 μm. In this technique, a parallel beam of monochromatic light is passed through a suspension of sediment and the diffracted light is focused onto a multi-element ring detector which senses the angular distribution of the scattered light. Size distributions of particles are acquired by measuring the pattern of light scattered by the particles based on the principle that particles of a given size will diffract light at a given angle which increases with decreasing particle size (Syvitski, 1991). As particle size decreases, the observed scattering angle increases logarithmically. Scattering intensity is also dependent on particle size, diminishing with particle volume. Large particles therefore scatter light at narrow angles with high intensity whereas small particles scatter at wider angles but with low intensity. Ultra sonication was used to disaggregate sediment where necessary prior to analysis. Particle size analysis was carried out on the fraction below 2mm for each section, in accordance with standard procedure relating to the use of the laser particle analyzer.

3.2.3.2 Sediment Characterization

Smeared slides were made on every section of each core for a detailed look at sediment composition. The slides were prepared by first applying a small amount of sediment onto a clean glass slide followed by the addition of a small drop of water and smearing with

pin to disperse the particles. The smeared slides were placed on a hotplate (heated to about 25^{o}C) to accelerate drying. Once the slides were dry, a drop of Norland optical adhesive (Fisher Scientific) was used to mount a cover slip on the samples on each slide and allowed to air dry. Slides were analyzed using a LEICA DM75O P double polarized petrographical microscope to make a qualitative estimate of biogenic materials (diatoms, forams, sponge spicules, and others) in plane polarized light, and non-biogenic materials (quartz, feldspar, accessory minerals, silts, lithic fragments and organic materials) in both plane and cross polarized lights. Identification of minerals and fossils was done using textbook (Haq and Boersma, 1998), online portals and with the help of experts at MLML.

3.2.4 Magnetic Susceptibility

Volume magnetic susceptibility (k) was measured directly on sediment at 2cm intervals using a Bartington MS2 magnetic susceptibility meter with a surface scanning sensor (MS2K). Three repeated measurements were made on each section, averaged and drift corrected. The magnetic susceptibility meter records raw data that does not account for density changes down the core. As the data may reflect changes in density rather than volume susceptibility, the data was mass corrected using the following equation:

$$X = K/\rho \qquad 3\text{-}1$$

Where X is the mass specific susceptibility, K is the volume susceptibility, and ρ is the dry bulk density of the sediment.

3.2.5 Major Elemental Analysis

Sediment digestion and preparation was carried out in a Class 100 trace metal laboratory at MLML under a laminar air-flow clean fume hood. In order to avoid the loss of some key temperature sensitive elements during the digestion process and also to develop a quick method for digesting the large numbers of samples in this study, four method development tests (Appendix A2) were carried out on selected samples and standard reference material (SRM) BCSS-1 prepared by the National Research Council of Canada in 1995. The digestates from samples were analyzed in an element 2 high resolution inductively coupled plasma-mass spectrometer (ICP-MS).

A comparison of results was made between samples while SRM results were compared with certified known values. Results showed that all four digestion methods produced reliable results leading to selection of method 1 as an efficient, fast and convenient method for digesting the large numbers of sediment samples in this study.

In this method, 2 mL of OPTIMA grade hydrogen peroxide (H_2O_2) purchased from Fisher Scientific was added to about 500-1000 mg sediment in acid-clean Teflon beakers and left to sit under a fume hood for 24 hrs to remove any organic materials present in the sediment. Beakers were placed on hot plates at 50^{o}C to allow complete dryness and removal of any residual organic materials. Two (2) mL each of quartz distilled 6N hydrochloric acid (HCL) and 14N nitric acid (HNO_3) and 1mL 26N hydrofluoric acid (HF) were added to the dried samples in one step. Beakers were covered with Teflon watch glasses and placed back on the hot plate (calibrated to 85^{o}C) for 24 hrs ensuring that temperatures inside the Teflon beakers do not rise above 60^{o}C. After 24 hrs, watch

glasses were removed carefully and the temperature of hot plates was raised to 100^{o}C to ensure complete dryness of beaker contents.

Any brown residues left were further treated with 200-400 µL of the nitric acid depending on the intensity of the brownness and placed back on the hot plate for final drying. A final solution of 10 mL was made by adding 1 mL of 14N nitric acid to the digestate and pipetted into low density polyethylene bottles followed by rinsing and subsequent addition of Milli-Q (18 megaohm Milli-Q, Millipore Systems ®). The BCSS-1 certified standard reference material and method blanks were prepared using the same procedure as above. All major elements were quantified using a Perkin-Elmer Element 2 high resolution Inductively Coupled Plasma Mass Spectrometer (ICP-MS). Multi and single element standards, method blanks and SRM were analyzed for quality control purposes.

3.2.6 Statistical Analysis and Graphical Display of Data

Graphical displays (ternary, line and discrimination plots) of data were carried out using the microcal origin 6.0 statistical software. Correlation analysis was performed on the magnetic susceptibility data and major elements to reveal any possible associations using SPSS software (version 13 for Windows).

3.3 Results

3.3.1 Grain Size Analysis

3.3.1.1 Ankobra Estuary

Mean grain size ranging from 27.5-37.8 µm was observed in the entire core while modal values varied between 55.1-105 µm. The core showed close to homogenous

mean/median ratios. Grains were poorly sorted with sorting values varying between 2.9-3. 7 µm. Grains were negatively skewed throughout the entire core. Kurtosis varied between 0.7 and 8.1 µm throughout the core (Appendix A3). Line and ternary classification (Fig. 3.8) of sediment into clay, silt and sand fractions revealed a disturbed profile for the sand and silt fractions with depth (Fig. 3.8A). About 40% of the samples fell within the sand fraction while 40% fell within the silt fraction with clay forming the least fraction (Fig. 3.8B).

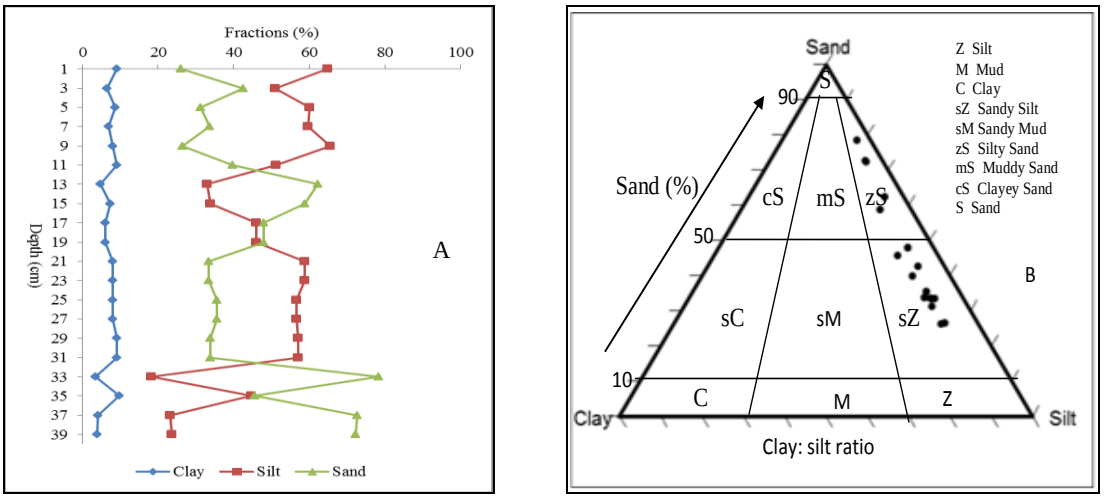

Figure 3.8. Composition of size fractions of the sediment core from the Ankobra estuary: (a) depth profiles of fractions; and (b) ternary plot of fractions

3.3.1.2 Pra Estuary

Mean grain size varied between 15.9 and 41.2 µm while modal values varied between 38.0-66.5 µm. The core showed close to homogenous mean/median ratios. Also grains were poorly sorted with sorting values varying between 3.4 and 3.9 µm. Grains were negatively skewed throughout the entire core. Kurtosis varied between 0.9 and 4.7 µm in entire the core (Appendix A4). The line and ternary classifications of the core showed the first 32 cm of the core to be dominated with silt while sandy grains dominated from depth of 32 cm to the bottom (Fig. 3.9A). Between 30-40% of the sediments fell within

the sand fraction, while 45-50% fell within the silt fraction with clay constituting less than 10% of the sediment (Fig. 3.9B).

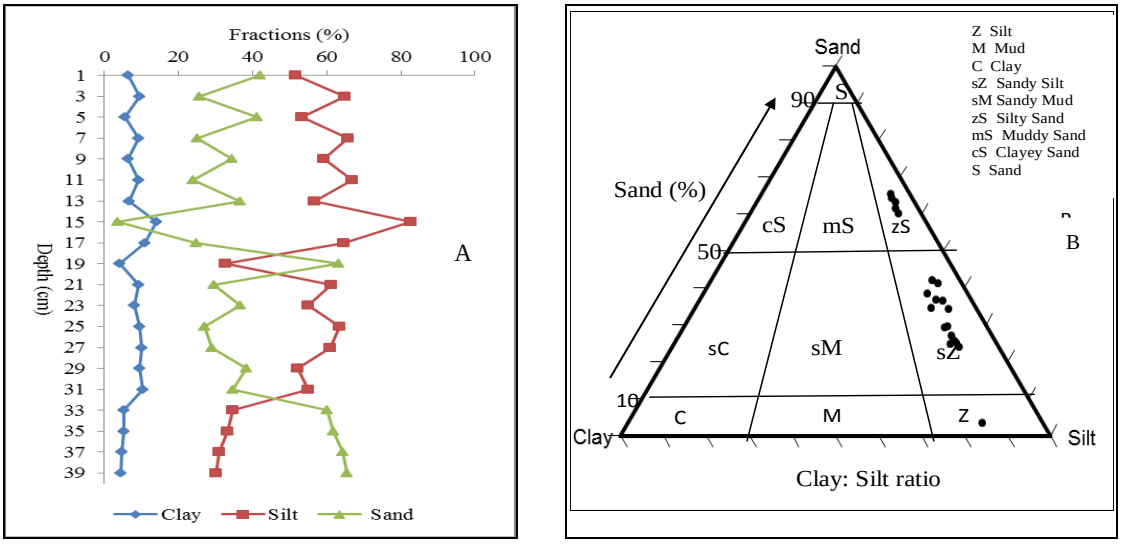

Figure 3.9. Composition of size fractions of the sediment core from the Pra estuary: (a) Depth profiles of fractions; and (b) ternary plot of fractions.

3.3.1.3 Amisa Estuary

Mean grain size varied between 17.3 and 25.3 µm, while modal values varied between 66.4-185.4 µm. The core showed close to homogenous mean/median ratios. Grains were poorly sorted with sorting values varying between 3.3 and 4.5 µm. Grains were negatively skewed throughout the entire core with kurtosis varying between 0.4 and 1.0 µm (Appendix A5). The line and ternary classifications of the core showed silts dominated the entire core from the top (youngest) section to the bottom (oldest) (Fig. 3.10A). Close to 80% of the sediment fell within the silt fraction while clay and sand constituted about 20% of the sediment (Fig. 3.10B).

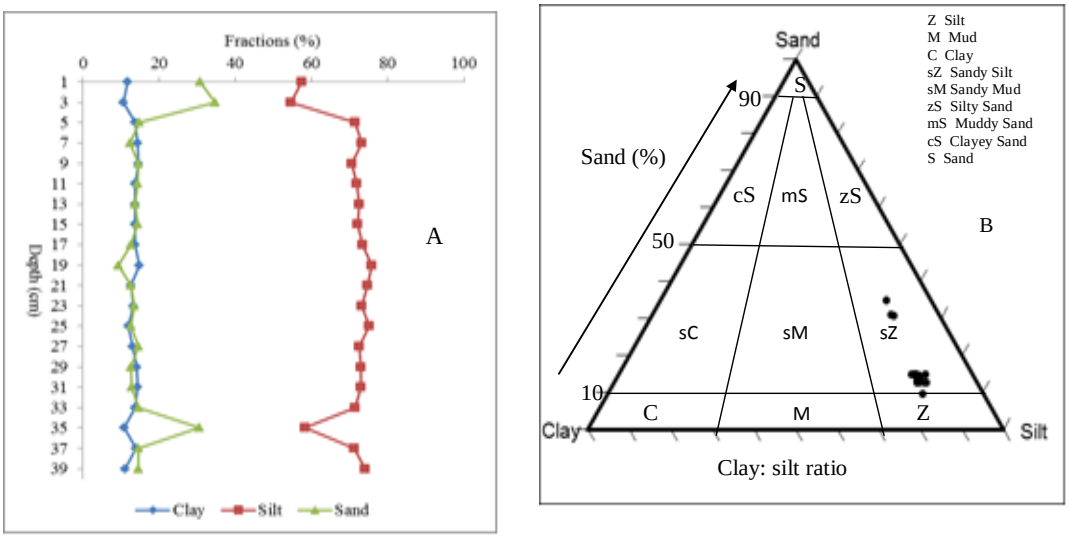

Figure 3.10. Composition of size fractions of the sediment core from the Amisa estuary: (a) Depth profiles of fractions; and (b) ternary plot of fractions

3.3.1.4 Densu Estuary

Mean grain size varied between 49.3 and 88.3 µm, while modal values varied between 127.6-185.4 µm. The core showed close to homogenous mean/median ratios. Grains were poorly sorted with sorting values varying between 3.0 and 3.9 µm. Grains were negatively skewed throughout the core while kurtosis varied between 2.8 and 7.2 µm in entire the core (Appendix A6). The line graph and ternary diagrams showed that the core was dominated with sand grains from the youngest to the oldest section (Fig. 3.11A). Close to 70% of the sediment fell within the sand fraction, silt constituted about 20-25% of the sediment while clay forming the least fraction made less 5% (Fig. 3.11B).

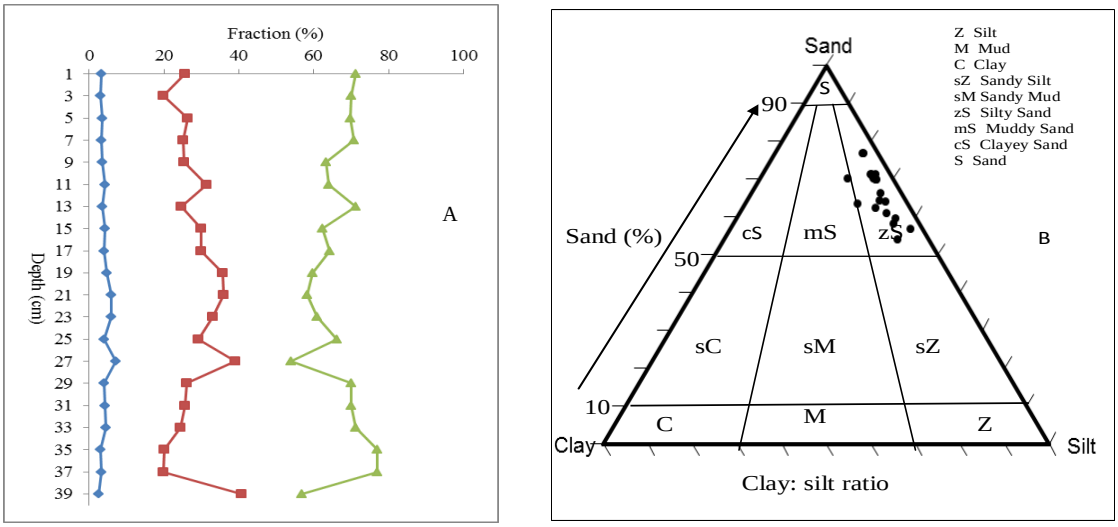

Figure 3.11. Composition of size fractions of the sediment core from Densu estuary: (a) Depth profiles of fractions; and (b) ternary plot of fractions.

3.3.1.5 Sakumo II Estuary

Mean grain size varied between 5.6 and 23.6 µm while modal values ranged from 5.4-105.9 µm. The core showed close to homogenous mean/median ratios. Grains were poorly sorted with sorting values varying between 2.9 and 3.7 µm. Grains were negatively skewed throughout the core. Positive kurtosis values were observed from the youngest interval through to 28 cm, while negative kurtosis values were observed from depth 28 cm downwards (Appendix A7). The line graph and ternary diagrams showed an interesting depth profile for the core from this estuary (Fig. 3.12). Silt dominated the entire core from the youngest section to the oldest with clay showing an increasing trend down the core. Sand showed a decreasing trend with depth from 27% at the youngest section to 0% at the oldest (Fig. 3.12A). About 70% of the sediment fell within the silt fraction while clay constituted about 10% at topmost section and about 30% at the bottom (Fig. 3.12B).

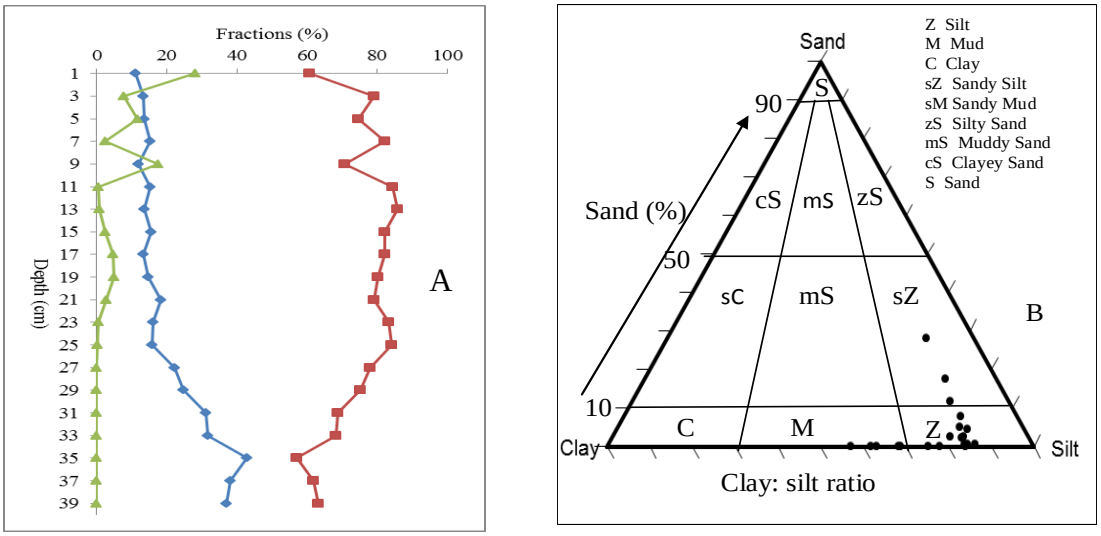

Figure 3.12. Composition of size fractions of the core from the Sakumo II estuary; (a) Depth profiles of fractions and (b) ternary plot of fractions

3.3.1.6 Volta Estuary

Mean grain size varied between 20.1 and 64.9 µm, while modal values ranged from 55.1-153.8 µm. The core showed a close to homogenous mean/median ratios. Grains were poorly sorted with sorting values varying between 3.1 and 4.3 µm. Grains were negatively skewed throughout the core. Kurtosis varied between 0.1 and 7.2 µm in the entire core (Appendix A8). The line and ternary diagram also showed a disturbed depth profile; with sand dominating from the youngest to middle section, silt dominating from the middle to about 30 cm, and sand dominating again from 30 cm to the bottom (Fig. 3.13A). About 60% of the sediment fell within the sand fraction while about 30% fell within the silt fraction and clay constituted less than 10% (Fig. 3.13B).

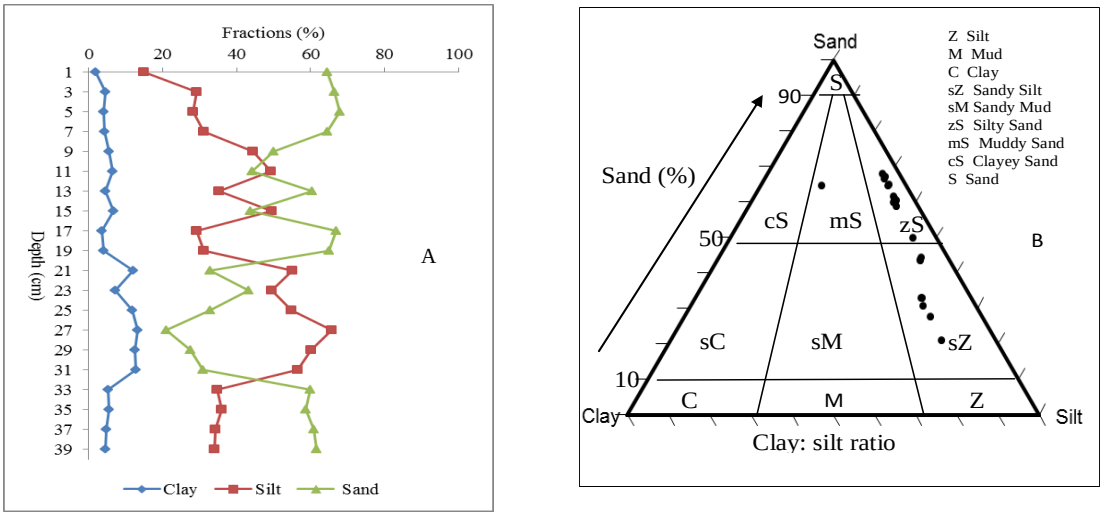

Figure 3.13. Composition of size fractions of the sediment core from the Volta estuary: (a) Depth profiles of fractions; and (b) ternary plot of fractions

3.3.2 Magnetic Susceptibility (MS) of Cores

MS values for the core from the Ankobra estuary varied between $0.5x10^{-8}$-$1.0x10^{-8}$ m^3/kg down the core (Fig. 3.14). MS showed strongly positive correlations with Al (r=0.83; p=0.00; n=20), P (r=0.77; p=0.00, n=20), K (r=0.81; p=0.00, n=20), and Fe (r=0.82; p=0.00, n=20 and no correlations (r= -0.02; p=0.47; n=20) with Ca (Appendix A9). MS values for the core from the Pra estuary showed an increasing profile towards the bottom from about $0.5x10^{-8}$ m^3/kg at the youngest section to about $1.8x10^{-8}$ m^3/kg at the oldest section with sharp peaks at 13 cm and 25 cm (Fig. 3.14). MS values of the Pra core correlated strongly with Li (r=0.71, p=0.00, n=20), Mg (r=0.69; p=0.00; n=20), Al (r=0.65; p=0.00; n=20), K (r=0.61; p=0.00, n=20), Ti (r=0.68; p=0.00; n=20) and Fe (r=0.71; p=0.00; n=20) and very weakly with Ca (r=0.16; p=0.45; n=20) (Appendix A10). MS values varied between $1.0x10^{-8}$ m^3/kg and $2.5x10^{-8}$ m^3/kg (Fig. 3.14) for the Amisa core with no distinct trend and no correlation with any of the major elements (Appendix A11). The core from Densu had the least MS values decreasing towards the bottom from $0.6x10^{-8}$ m^3/kg at the youngest section to $0.1x10^{-8}$ m^3/kg at the bottom (Fig. 3.14). MS correlated positively with Na (r=0.75; p=0.00; n=20), Mg (r=0.88; p=0.00;

n=20), Al (0.85; p=0.00; n=20), P (r=0.69; p=0.00; n=20), Ti (r=0.74; p=0.00; n=20), and Fe (r=0.87; p=0.00; n=20) and very weakly with Ca (r=0.22; p=0.19; n=20) (Appendix A12). The MS values of the Sakumo II core was round $3.0x10^{-8}$ m^3/kg for entire core with a peak of $5.0x10^{-8}$ m^3/kg at 15 cm. The MS values showed no correlation with any of the major element analyzed for this core (Appendix A13). MS values of the core from the Volta estuary did not show any distinct pattern and varied between $0.7x10^{-8}$ m^3/kg and $3.0x10^{-8}$ m^3/kg, showing no significant correlation with any of the major elements (Appendix A14).

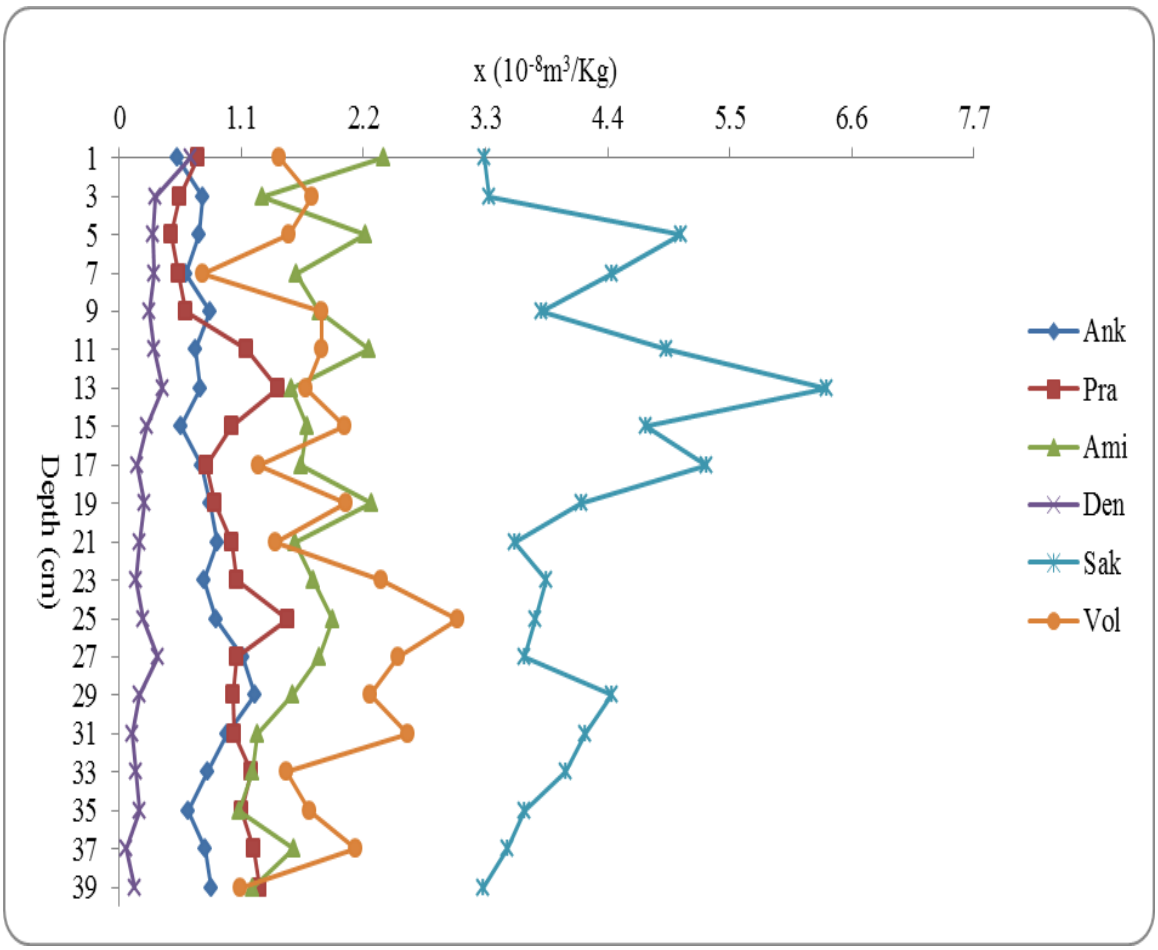

Figure 3.14. Density corrected magnetic susceptibility (x) profiles of the sediment cores from the Ankobra, Pra, Amisa, Densu, Sakumo II and Volta estuaries.

3.3.3 Sediment Composition and Provenance

3.3.3.1 Ankobra Estuary

3.3.3.1.1 Sediment Characterization and Mineralogy

Non-biogenic materials constituted about 100% of the core from the youngest section to the 26cm depth. A few (2-5%) biogenic materials mainly broken pieces of diatoms were seen below this depth. Monocrystalline quartz made about 85% of the entire core while feldspars and lithic fragments constituted close 15% (Plate 1). A few accessory minerals mainly amphiboles and micas were also seen at some sections of the core (Appendix A15).

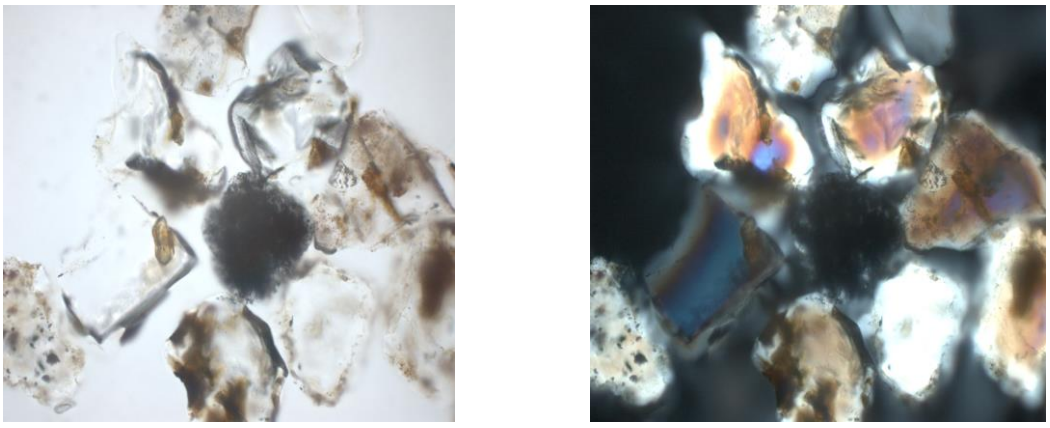

Plates 1. Microscopic images of quartz grains of smeared sections from the sediment core from the Ankobra estuary (left in plane polarized; Right in Cross polarized), Magnification; X60.

3.3.3.1.2 Major Element Composition, Provenance, and Weathering Histories

Silica (SiO_2) constituted close to about 80% of the core, while Al, the second most abundant major element in the core constituted between 6-10%. Iron (Fe) the third most abundant element constituted between 3-5% of the sediment, while all other major elements analyzed constituted less than 1% (Appendix A16). These results further support the results of the smear-slide analysis above, that the sediment was quartz (silicate) rich. Apart from depths 15 cm, 17 cm and 35 cm which had CIA indices of 54,

65 and 63 respectively, all sections of the core had CIA indices greater than 75. The Al_2O_3-CaO+Na_2O-K_2O (A-CN-K) diagram showed that this core fell within the intermediate and extreme weathered fraction and consisted solely of clay mineral smectite (Fig. 3.15). The sediment had come under intensive weathering that depleted them of any feldspar hence supporting results from the smear-slide analysis. The discriminant function diagram for this core showed that all sediment in this core originated from a quartzose/recycled sedimentary provenance (Fig. 3.16).

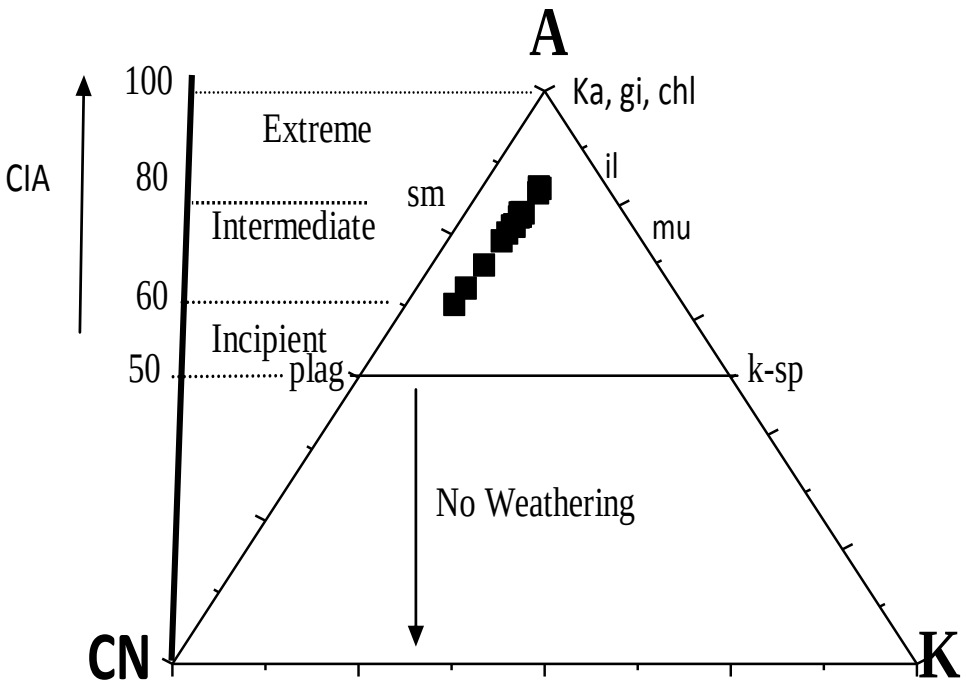

Figure 3.15. A-CN-K diagram showing composition of the sediment core from Ankobra Estuary. A=Al_2O_3; CN=CaO+Na_2O; K=K_2O (Molar proportions). {sm=smectite; plag=plagioclase; ka=kaolinite; chl=chlorite; il=illite; mu=muscovites; k-sp=potassium feldspar}

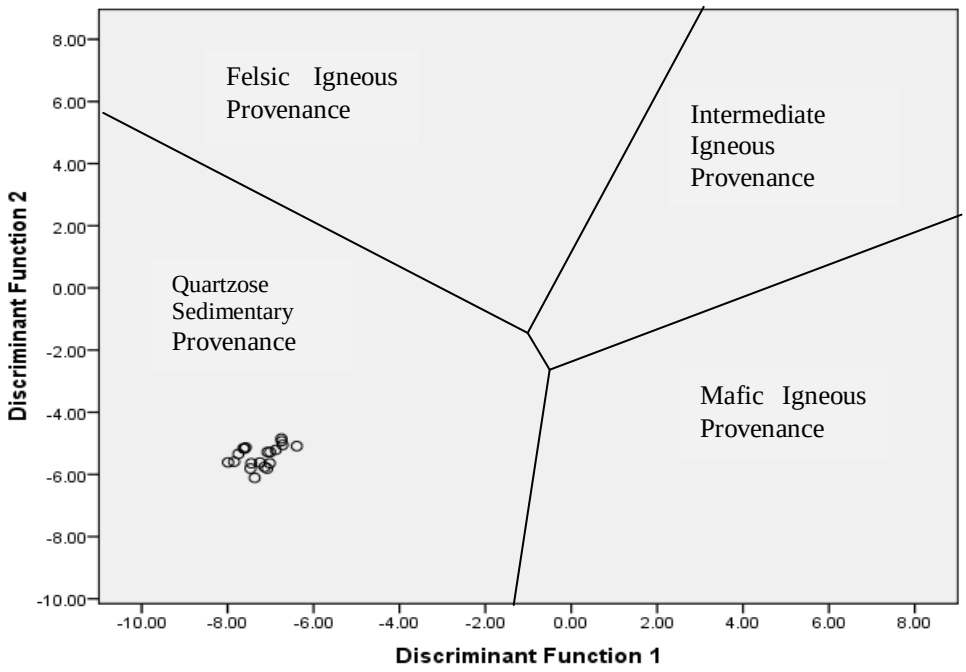

Figure 3.16. Discriminant function diagram for the provenance signatures of the sediment core from Ankobra estuary using major elements

3.3.3.2 Pra Estuary

3.3.3.2.1 Sediment Characterization and Mineralogy

Non-biogenic materials constituted about 95% of the core while biogenic components constituted less than 4%. Sponge spicules were the most abundant fossils found in this core. Quartz grains were the most abundant mineral framework constituting between 80% and 85% of the core (Plate 2). Lithic fragments and feldspars constituted less than 20% of the core. A few micas and amphiboles were seen in some sections of the core (Appendix 17).

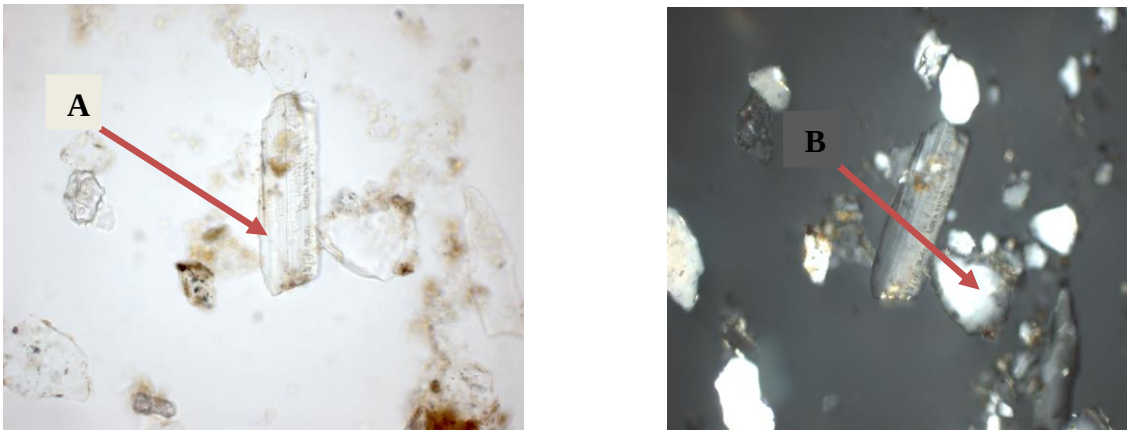

Plates 2. Microscopic images of smeared sections from the sediment core from the Pra estuary in plane polarized (left) Cross polarized (right) lights. (a) Feldspar, (b) Monocrytalline quartz Magnification; X60.

3.3.3.2.2 Major Element Composition, Provenance and Weathering Histories

Silica (SiO_2) was the most abundant element constituting between 75%-80% of the core. Aluminum (Al) was the second most abundant element in the core constituting about 8%-13% While Iron (Fe) made about 3%-6% of the core. Potassium (K) constituted between 0.7% -1%. The concentrations of all the other elements were below 1% (Appendix A18). CIA values ranged between 81 and 88 from the youngest to the oldest section. The Al_2O_3-CaO+Na_2O-K_2O (A-CN-K) diagram showed that the sediment fell within the extremely weathered region and consisted solely of clay mineral smectite (Fig. 3.17). There were no muscovites present in the core. The discriminant function diagram for this core indicated that most of the sediment took their source from a quartzose sedimentary provenance while a few originated from a mafic igneous provenance (Fig. 3.18).

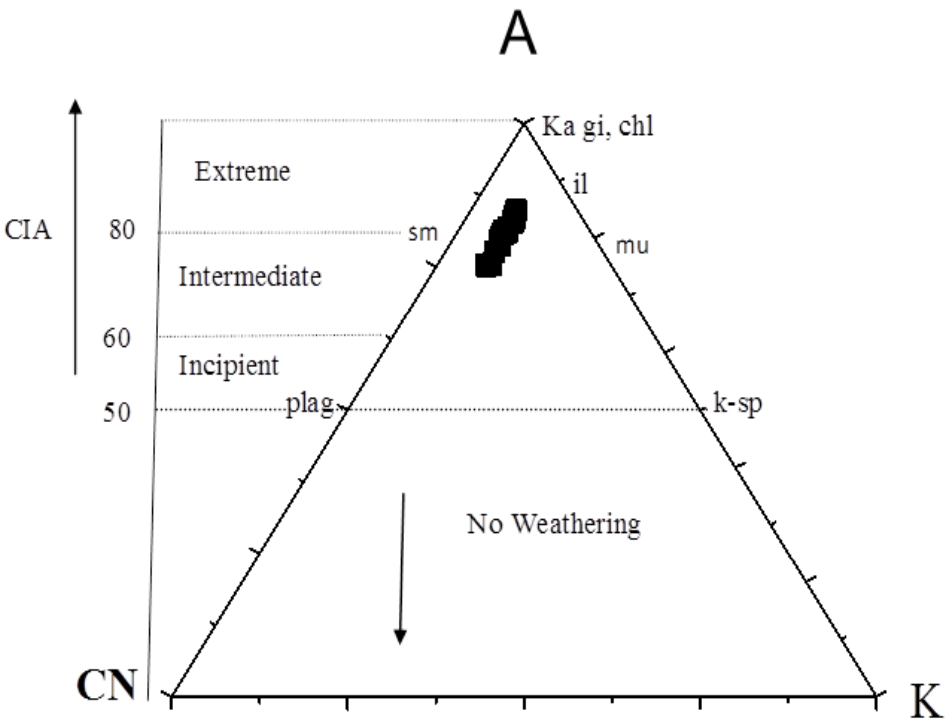

Figure 3.17. A-CN-K diagram showing composition of the sediment core from Pra estuary. $A=Al_2O_3$; $CN=CaO+Na_2O$; $K=K_2O$ (Molar proportions). {sm=smectite; plag=plagioclase; ka=kaolinite; chl=chlorite; il=illite; mu=muscovites; k-sp=potassium feldspar}

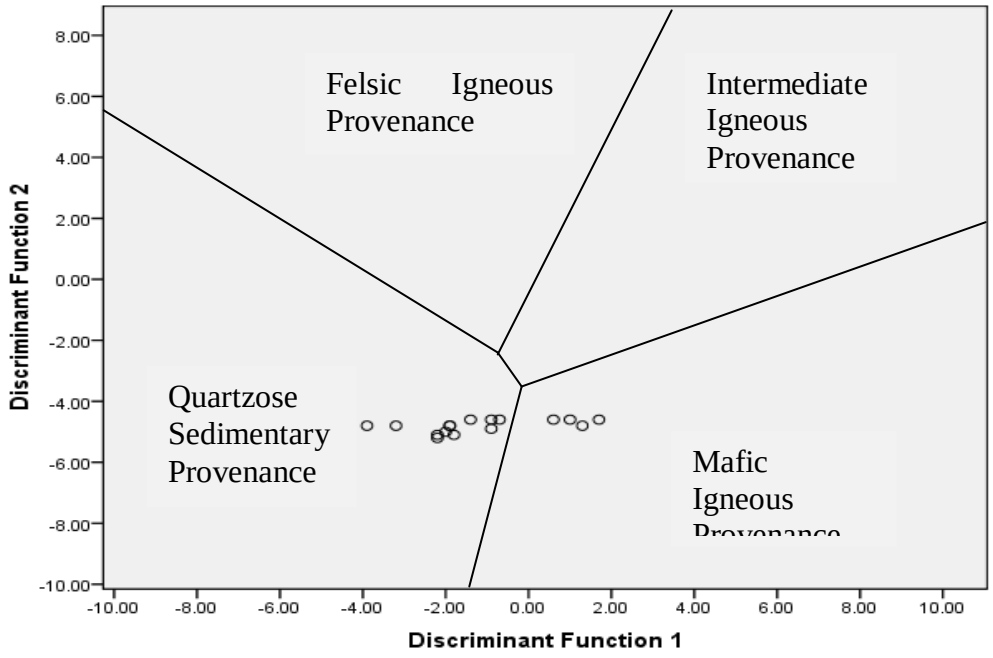

Figure 3.18. Discriminant function diagram for the provenance signatures of the sediment core from Pra estuary using major elements.

3.3.3.3 Amisa Estuary

3.3.3.3.1 Sediment Characterization and Mineralogy

Non-biogenic materials constituted the bulk of the core varying between 80 and 95% while biogenic materials constituted between 2 and 20%. Broken pieces of diatoms, radiolarians and sponge spicules were the most dominant fossil pieces identified. Quartz grains constituted between 40 and 60% while Accessory minerals made between 30 and 35% (Appendix A19).

3.3.3.3.2 Major Element Composition, Provenance and Weathering Histories

Silica (SiO_2) varied between 61% and 68%. Again, Al (13-19%) was the second most abundant major element after Si followed by S which constituted close to between 5% and 7%. Iron (Fe) was the next most abundant element after S varying between 5% and 6%. Iron (Fe) varied between 1.5% and 2.18% while K followed Na with values varying between 1.24% and 1.45%. The concentration of Mg was comparatively high in this core varying between 0.89% and 1.14%. Calcium (Ca) and all other elements were below 1% (Appendix A20). CIA ranged between 77 and 84 from the youngest to oldest section of the core. The Al_2O_3-CaO+Na_2O-K_2O (A-CN-K) diagram showed that the sediment fell within the extremely weathered region and consisted solely of clay mineral Illite (Fig. 3.19). Most of the sediment had come under intensive weathering that completely depleted them of any feldspar and left behind clay minerals. The discriminant function diagram indicated all the sediment took their source from mafic igneous provenance therefore supporting the results of the smear slide analysis (Fig. 3.20).

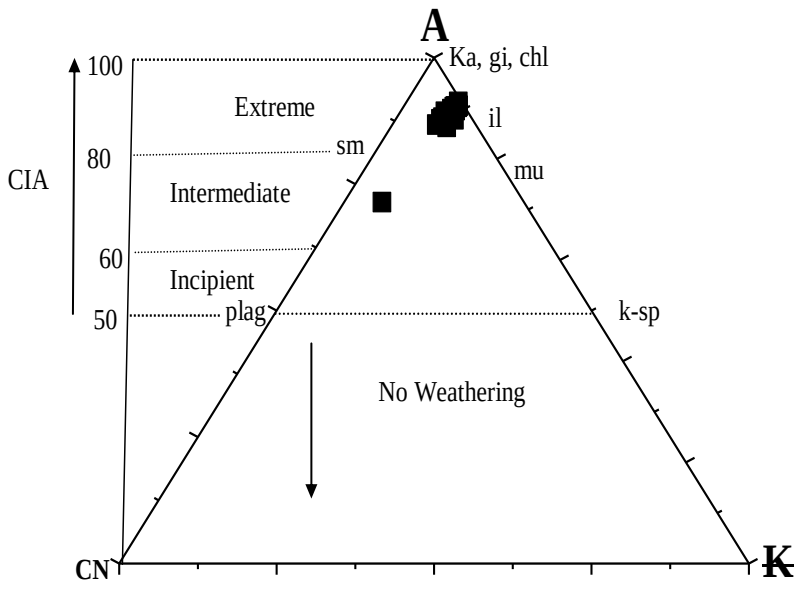

Figure 3.19. A-CN-K diagram showing composition of the sediment core from Amisa estuary. $A=Al_2O_3$; $CN=CaO+Na_2O$; $K=K_2O$ (Molar proportions). {sm=smectite; plag=plagioclase; ka=kaolinite; chl=chlorite; il=illite; mu=muscovites; k-sp=potassium feldspar}

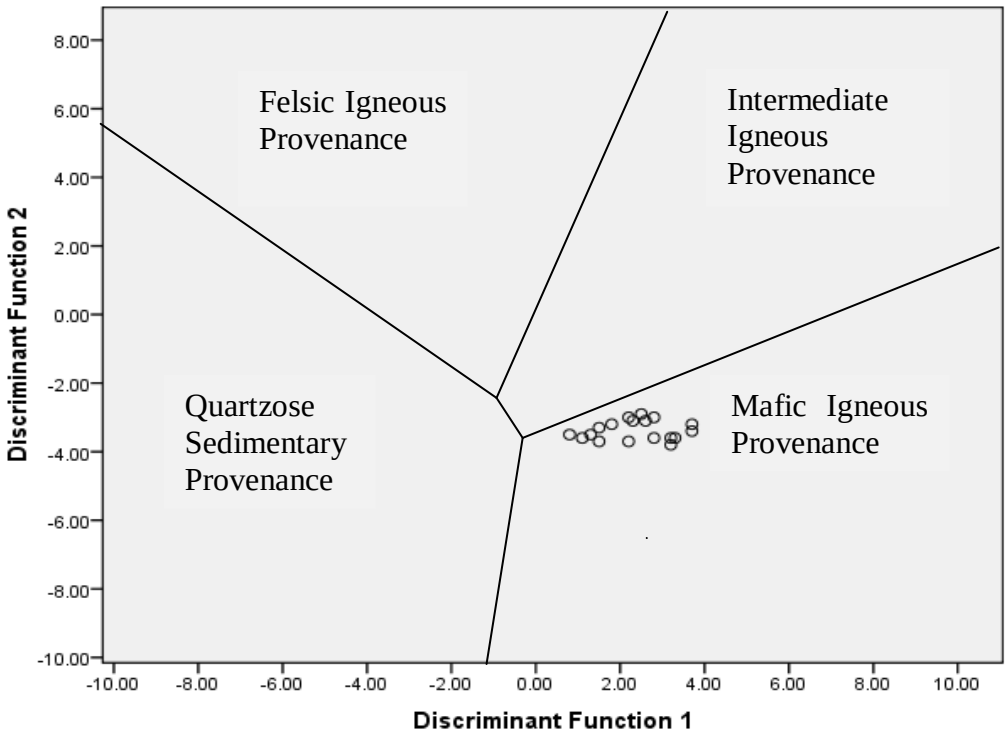

Figure 3.20. Discriminant function diagram for the provenance signatures of the sediment core from Amisa estuary using major elements.

3.3.3.4 Densu Estuary

3.3.3.4.1 Sediment Characterization and Mineralogy

Non-biogenic materials constituted between 67 and 95% of core and consisted of quartz (85-90%), feldspars (5-15%), and very few accessory minerals. This core was rich in biogenic materials (5-33%). This richness was observed from depths 3cm to 29cm. Well preserved pennate diatoms were the most abundant fossil organisms (Appendix A21). Broken pieces of centric diatoms were also present as well as radiolarians. Preserved and broken sponge spicules were also seen at some sections. Microscopic images of minerals and representative fossils are shown in Plate 3.

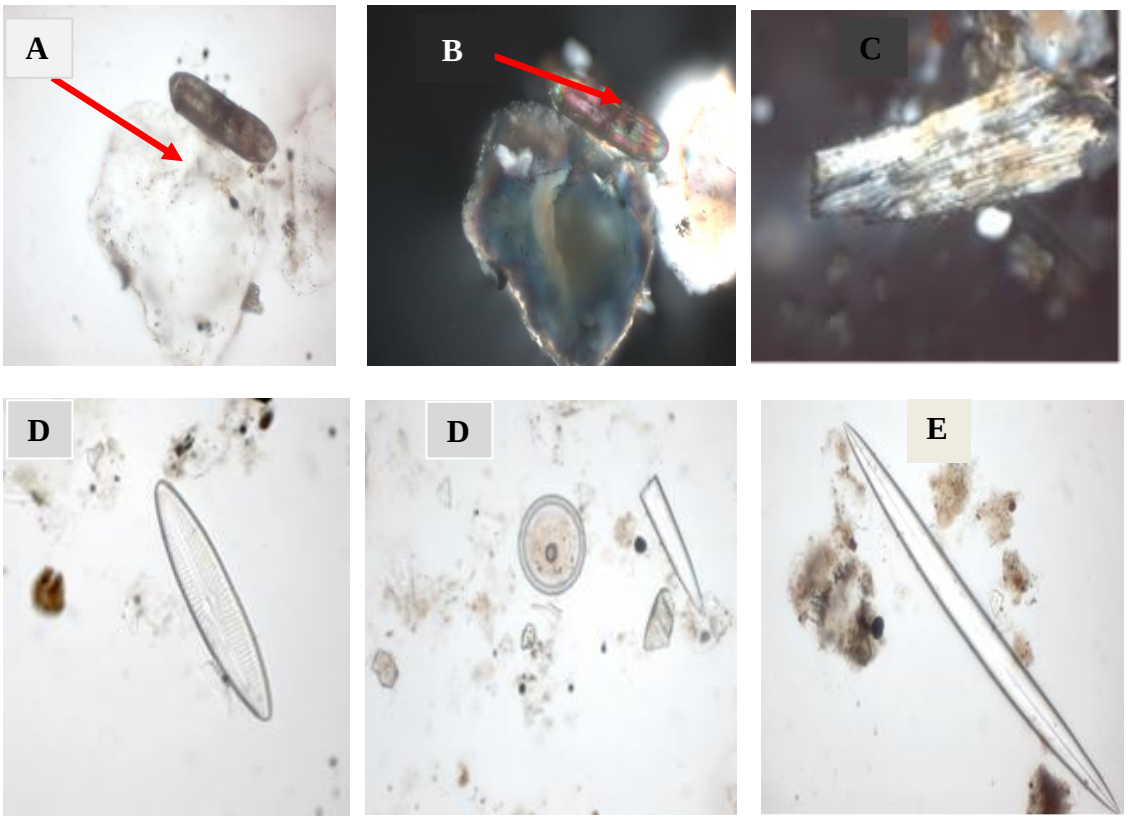

Plates 3. Minerals and Representative fossils from the Densu estuary in plane (upper left) and cross (upper right) polarized light: (a) Monocrystalline quartz; (b) accessory mineral; (c) Muscovite; (d) pennate diatom; (e) centric diatom; (f) sponge spicule; Magnification; x60

3.3.3.4.2 Major Element Composition, Provenance, and Weathering histories

Silica (SiO_2) made the bulk of the sediment (66.77-89.27%), followed by Al with values varying between 4.63-11.36%. Compositions of S and Fe were almost the same varying between 1% and 10%. Sodium (Na) was the next after S and Fe constituting between 1%-2% of the core while K followed with values varying between 0.8% and 1%. Proportions of other elements were below 1% (Appendix A22). Low CIA values varying between 63 and 75 were estimated for this core. The Al_2O_3-CaO+Na_2O-K_2O (A-CN-K) diagram showed that the sediment fell mostly within the incipient to intermediate weathering region (Fig. 3.21). The discriminant function diagram indicated that almost all the sediment took their source from a quartzose/recycled sedimentary provenance (Fig. 3.22).

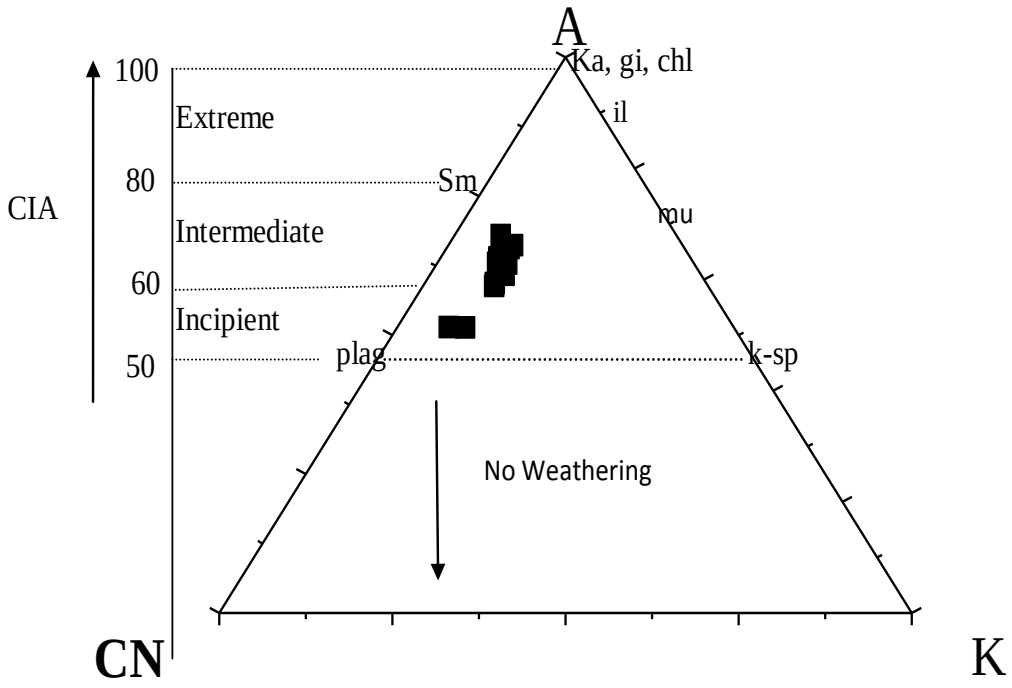

Figure 3.21. A-CN-K diagram showing composition of the sediment core from Densu estuary. A=Al_2O_3; CN=CaO+Na_2O; K=K_2O (Molar proportions). {sm=smectite; plag=plagioclase; ka=kaolinite; chl=chlorite; il=illite; mu=muscovites; k-sp=potassium feldspar}

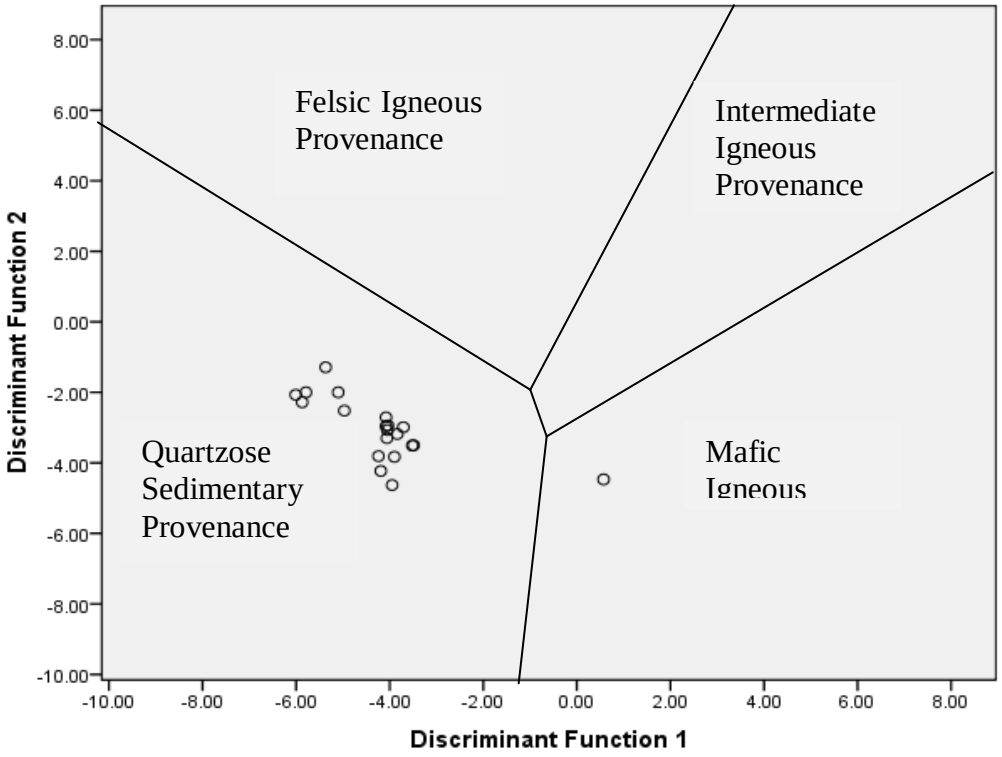

Figure 3.22. Discriminant function diagram for the provenance signatures of the sediment core from the Densu estuary using major elements.

3.3.3.5 Sakumo II Estuary

3.3.3.5.1 Sediment Characterization and Mineralogy

Non-biogenic materials constituted about 90 to 97% of the sediment while 3 to 10% was of biogenic origin. Broken pieces and a few preserved diatoms constituted the main biogenic component while quartz (mainly polycrystalline) varying between 30% and 60% constituted the main non-biogenic component (Plate 4). Feldspars formed about 5% while accessory minerals constituted between 15 and 60% of the non-biogenic materials (Appendix A23).

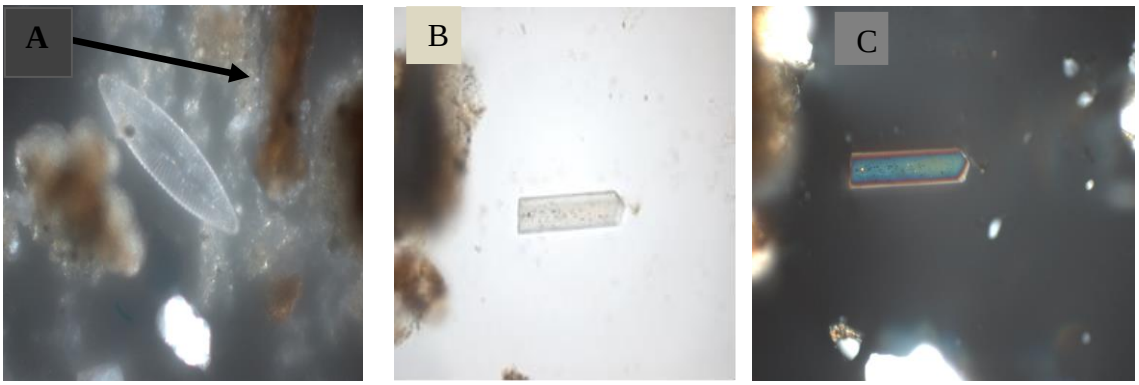

Plates 4. Microscopic images from different sections of the core from the Sakumo II estuary: (a) Polycrystalline quartz grains and pennate diatom; (b) Accessory mineral Amphibole in plane and cross (c) polarized light; magnification X60

3.3.3.5.2 Major Element Composition, Provenance and Weathering Histories

Silica (SiO_2) constituted the bulk of the sediment (59.75-70.16%). Al ranged between 12.41-16.71%. The S and Fe compositions were almost the same ranging between 3.76% and 8.24%. Magnesium (Mg) and Na was the next after S and Fe constituting between 2%-3% of the core while K followed with values ranging between 0.95% and 1.5%. Proportions of other elements were below 1% (Appendix A24). High CIA values varying between 77 and 83 were estimated for this core. The Al_2O_3-CaO+Na_2O-K_2O (A-CN-K) diagram showed that the sediment fell mostly within the incipient to intermediate and consisted solely of potassium feldspars and muscovites (Fig. 3.23). The A-CN-K indicated that most of the sediment had come under intensive weathering prior to deposition. The discriminant function diagram indicated almost all the sediment took their source from a mafic sedimentary provenance (Fig. 3.24).

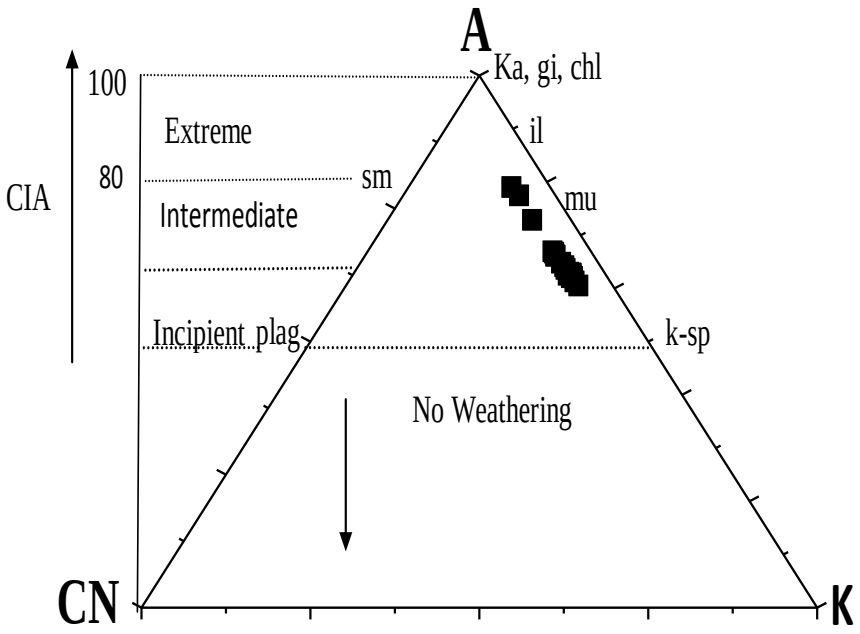

Figure 3.23. A-CN-K diagram showing composition of the sediment core from Sakumo II estuary. A=Al_2O_3; CN=CaO+Na_2O; K=K_2O (Molar proportions). {sm=smectite; plag=plagioclase; ka=kaolinite; chl=chlorite; il=illite; mu=muscovites; k-sp=potassium feldspar}

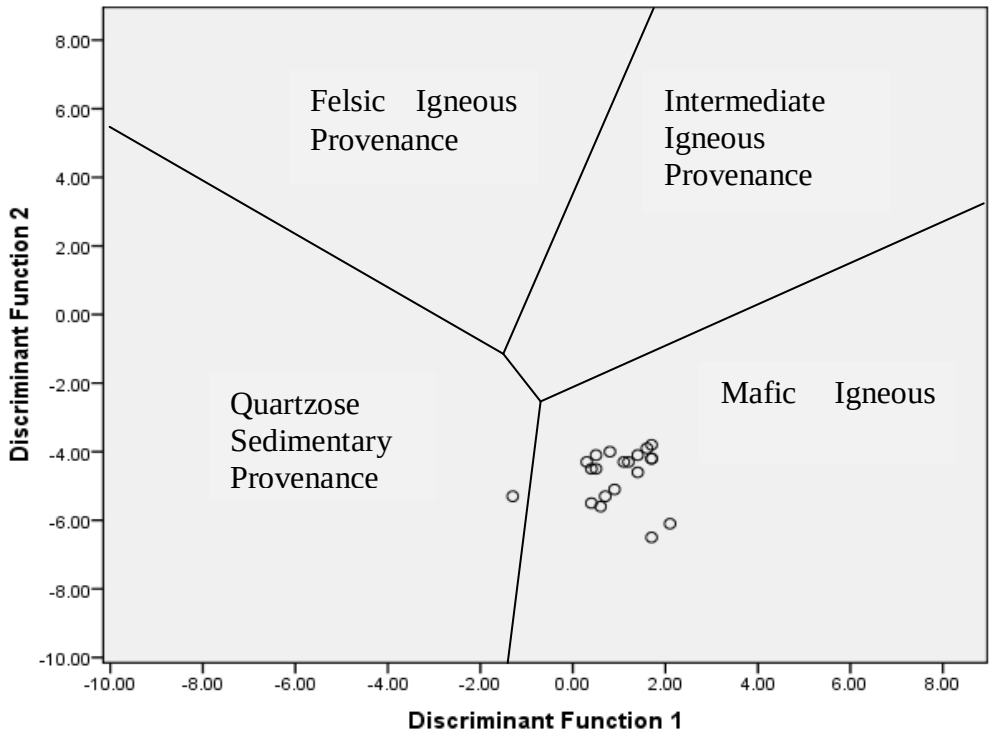

Figure 3.24. Discriminant function diagram for the provenance signatures of the sediment core from Sakumo II estuary using major elements.

3.3.3.6 Volta Estuary

3.3.3.6.1 Sediment Characterization and Mineralogy

Biogenic materials constituted 5% and 20% with sponge spicules forming the bulk of the biogenic materials. Some forams were also seen in this particular estuary (Plate 5). Non-biogenic materials constituted 80% to 95% of the core. Quartz made the bulk of non-biogenic materials varying between 55% and 80%. Feldspars constituted 5-10% of the core while lithics formed 10-25% of the core (Appendix A25).

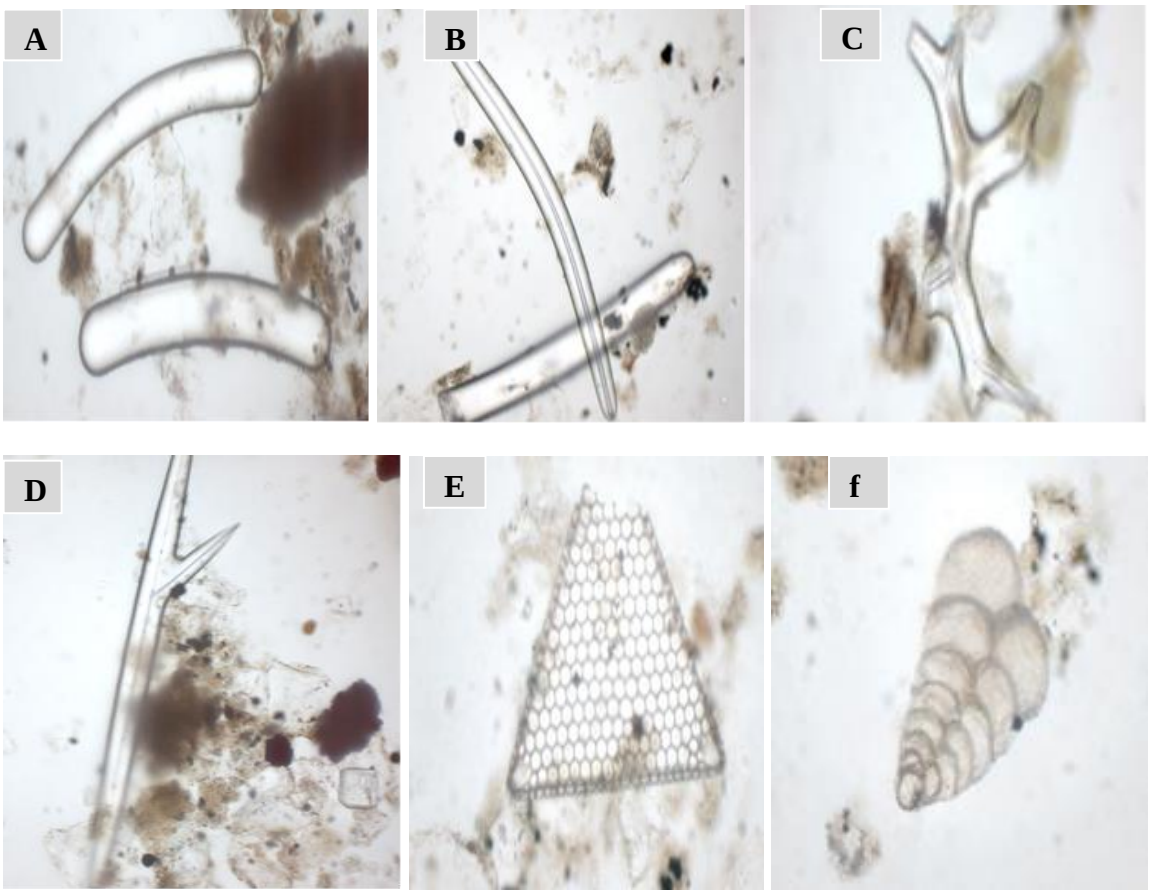

Plates 5. Microscopic images of representative fossils from the Volta estuary under plane polarized light: (a, b, c, d) sponge spicules; (e, f) forams; x60.

3.3.3.6.2 Major Element Composition, Provenance and Weathering Histories

Silica (SiO_2) made the bulk of the sediment (70.65%-87.82%) while Al varied between 5.56 and 14.97%. Iron (Fe) was the next abundant element after Al forming 2.23% to 5.79% of the core. Sulphur was the next after Fe, varying between 0.81% and 2.75% while K, Na and Ca followed with values varying between 0.3% and 1.5%. Proportions of other elements were below 1% (Appendix A26). High CIA values ranging between 71 and 81 were estimated for this core. The Al_2O_3-CaO+Na_2O-K_2O (A-CN-K) diagram showed that the sediment fell mostly within the intermediate weathering region and consisted solely of smectite (Fig. 3.25). The A-CN-K indicated that most of the sediment had come under intensive weathering prior to deposition. The discriminant function diagram indicated that almost all the sediment took their source from a quartzose/recycled sedimentary provenance (Fig. 3.26).

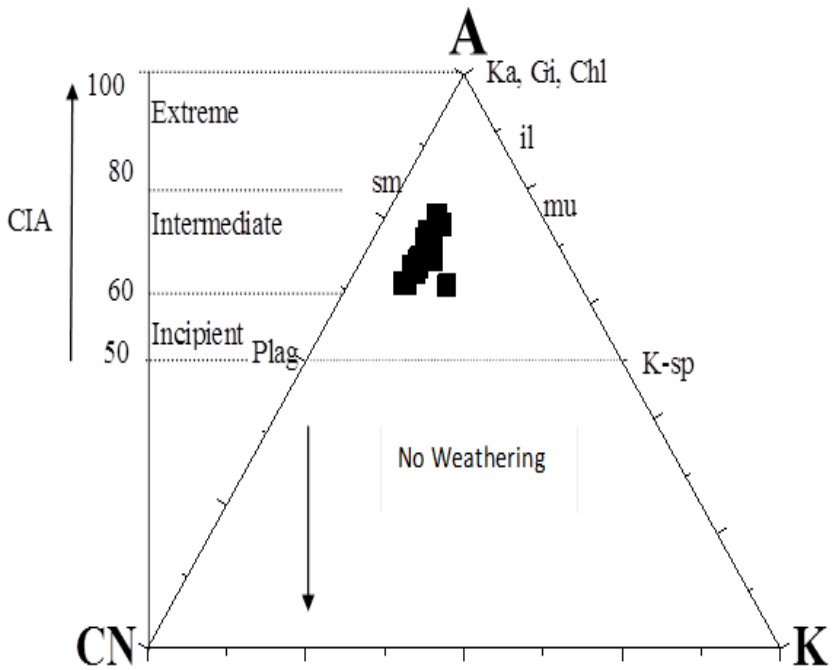

Figure 3.25. A-CN-K diagram showing composition of the sediment core from the Volta estuary. A=Al_2O_3; CN=CaO+Na_2O; K=K_2O (Molar proportions). {sm=smectite; plag=plagioclase; ka=kaolinite; chl=chlorite; il=illite; mu=muscovites; k-sp=potassium feldspar}

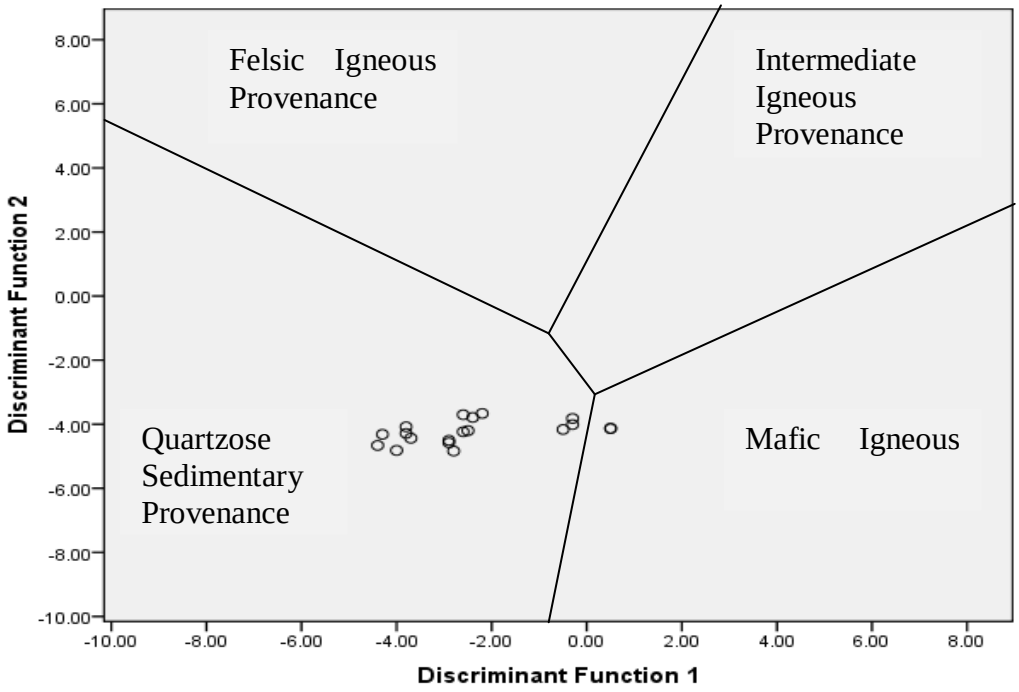

Figure 3.26. Discriminant function diagram for the provenance signatures of the sediment core from the Volta estuary using major elements.

3.4 Discussion

Grain size is a fundamental property of every sedimentary material that may help reveal their origin and history, particularly the dynamics of transport and deposition (Syvitski, 1991). The mean size is an indication of the magnitude of the force or energy, applied by water or wind to move the grains (Kamaruzzaman *et al*., 2002). Mean values and percent composition of size fractions pointed to the fact that cores from the Ankobra, Pra and Volta estuaries were dominated by very fine sand and coarse silt suggesting deposition of these grains under both fluvial and calm tidal conditions respectively (Kamaruzzan *et al*., 2002).

The highly disturbed profiles observed in the Ankobra and Pra could also be attributed to the intense activities of illegal gold mining operations in their watershed (Tsikata, 1997). The domination of the cores from Amisa and Sakumo II by fine silt also suggested their grains were deposited under calm tidal conditions while the fine sand-dominated sediment from the Densu estuary may be indicative of fluvial transportation under high energy conditions.

Generally, only the finest grains associated with high porosity are deposited in the zone of least energy (Dalrymple, 1992). Although some of the cores seem to coincide with very calm depositional processes, which in fact should have allowed for more selection of the grains to be deposited, large sorting or standard deviation values suggesting poor sorting (Ashok and Munkar, 2009) were rather estimated for all the cores. Mixing processes within the estuaries themselves could have accounted for the poorly sorted nature of the grains (Pizzuto, 1995).

All mineral grains are "susceptible" to becoming magnetized in the presence of a magnetic field, and magnetic susceptibility (MS) is an indicator of the strength of this transient magnetism within a material sample (Ellwood *et al.*, 2008). MS in sediment is generally considered to be an indicator of iron, ferromagnetic or clay mineral concentration. Basically there are three types of magnetic behavior into which all minerals can be divided, ferromagnetic, paramagnetic, and diamagnetic (Thompson and Oldfield, 1986). In the very low inducing magnetic fields that are generally applied, MS is largely a function of the concentration and composition of the magnetizable material in a sample (Ellwood *et al.*, 2008). Ferromagnetic minerals such as titanomagnetites have volume susceptibilities of the order of 500 to 5000 x $I0^{-6}$SI and tend to dominate the

susceptibility if they occur in sufficient abundance. Paramagnetic minerals such as amphiboles, pyroxenes, chlorites, rhodochrosite, clays, particularly chlorite, smectite and illite and other iron or manganese-bearing minerals have susceptibilities typically of 0.1 to 50 x $I0^{-6}$SI; these minerals may also dominate susceptibility if they occur in considerable amounts. Diamagnetic minerals such as, calcite and quartz have no net magnetic moments and produce small negative susceptibilities (0.05 to 0. 5 x $I0^{-6}$ S1) when exposed to a magnetic field. These organic compounds typically acquire a very weak negative MS when placed in inducing magnetic fields (Ellwood *et al.*, 2008). That means their acquired MS is opposed to the low magnetic field that is applied hence, the presence of these diamagnetic minerals reduces the MS in a sample (Ellwood *et al.*, 2008).

Values from this study as compared with Hunt *et al.*, (1995) and Thompson and Oldfield (1986) showed all sediments from all six estuaries consisted of paramagnetic and diamagnetic minerals. The nearly negative mass susceptibility recorded in the Ankobra, Pra and Densu core is an indication that this core is mostly dominated diamagnetic (non-iron bearing) minerals which in this case could be quartz as was seen in the microscopic analysis and also organic matter in the case of the Densu. The value 1 as recorded from some sections of the Ankobra and most sections of Pra core also suggest the presence of paramagnetic (iron-bearing) minerals such as orthopyroxenes, olivines and amphiboles (Thompson and Oldfield, 1986).

Although one would have expected that the anoxic nature of the sediment from the Densu (characterized by heavy smells of H_2S during the sampling period) would have resulted in the diagenetic formation of ferromagnetic minerals such as magnetite,

hematites etc. with very high MS values, the presence of high amounts of quartz, biogenic materials and pyrites in this core as revealed in the smear slide analysis, could have subdued the MS. Factors such as changes in biological productivity or organic carbon accumulation rates are known to naturally cause variabilities in MS values (Ellwood *et al*., 2008).

The peaking of MS values at some sections of the Ankobra and Pra cores could have resulted from high fluvial processes moving mineral rich detrital materials from adjacent lands into these estuaries which also was in agreement with the strongly positively correlation between MS and dominant detrital components and clay elements (K_2O, Fe_2O_3, TiO_2, Al_2O_3, and MgO) from these estuaries. The mass susceptibilities recorded for the Amisa, Sakumo and Volta cores suggest the domination of these cores by paramagnetic and iron-bearing minerals such as orthopyroxenes, olivines, and amphiboles as well as a few iron sulfides such as chalcopyrites and pyrites which was also supported by results of the correlation analysis.

High abundance of phytoplankton remains in buried sediment could be an indication of high productivity of surface waters at the time of sediment deposition as well as the health of the ecosystem. Results of the smear slide showed that the cores from Ankobra, Pra and to some extent Amisa were almost completely depleted in biogenic remains. Turbidity is known to be a major limiting factor of benthic primary production and nutrient uptake on estuarine intertidal sandflats (Pratt *et al*., 2012) and the high turbidity observed in the Ankobra and Pra estuaries could have resulted from activities of illegal mining.

The Ankobra and Pra watersheds are particularly known for intense illegal gold mining operations termed locally as ‘‘galamsey’’ since the early 80’s (Ofosu-Mensah, 2011). The activities of such operations have resulted in the continuous washing of muddy effluents into the rivers draining into these estuaries resulting in the extreme brownish coloring of the waters (observed during sampling), which could have hindered light penetration and primary production.

Additionally high fluvial discharge of sediment from the Ankobra and Pra rivers due to mining into their estuaries may have diluted the little biogenic materials that would have been buried with sediment. Unlike the Ankobra and Pra, the surface waters of the Densu and Volta estuaries were rather clear, transparent and productive, hence the richness of theirs cores with fossils of diatoms and sponge spicules as was observed in the smear slide analysis which is also in agreement with Sakshaug (1997).

Degradation of labile feldspars (low CIAs) from source rocks to secondary clay minerals (moderate to high CIAs) occurs during chemical weathering leading to formation of sediment chemical signatures which are preserved in the sedimentary record (Krissek and Horner, 1987). This study reflects moderate to high weathering conditions either in the original source terrane or during transportation for all cores. The high CIA values depict chemically dominated weathering processes which are unique to tropical terrane (Krissek and Horner, 1987).

The discriminant functions of Roser and Korsch (1988) used Al_2O_3, TiO_2, Fe_2O_3, MgO, CaO, Na_2O, and K_2O compositions of sediment to discriminate among four sedimentary provenances namely: (i) Mafic Igneous provenance sediment formed in oceanic island

arc; (ii) Intermediate Igneous provenance sediment formed in mature island arc; (iii) Felsic Igneous provenance sediment formed in active continental margin; and (iv) Quartzose or Recycled provenance formed in passive continental margin.

In this study, all sediment from the Ankobra, Densu and Volta cores plotted within the recycled continental or quartzose sedimentary provenance section of the diagram. This result suggests that sediment from the Ankobra estuary are all recycled continental materials formed in a passive tectonic setting, which have undergone intense geochemical transformations. Such sediment are rich in quartzites, phyllites, grits and conglomerates, and schists which are characteristic of the Lower Birimian rocks underlying Prestea, Awaso, Asankragua, Bogoso and Esiama areas (Junner *et al.*, 1942) known for intense illegal gold mining.

Sediment entering the Densu estuary could have been derived from recycled sedimentary materials of coming from the Bortianor, Kokrobite and Nyanyanu areas which are underlain by Togo series rocks. These rocks comprise marine series of shales, sandstones, limestones, and sandstones which are mostly recycled (Amuzu, 1975). Just like those of the Densu, the sediment entering the estuary of the Volta River could have been derived from the Akosombo, Akuse, Kpong, Osudoku, Fute, lolonya, Akplabanya, Anyanui, Kpando, Kpeme, Big Ada areas also underlain by Togo series rocks (Amuzu, 1975).

Results showed that all sediment from the Sakumo II and the Amisa estuaries took their source from mafic igneous origins implying that sediment from the core from the Sakumo II could have been derived from the Tema, Sakumono, Afienya, and Lashibi

areas whose rocks are mainly acidic ortho and para gneisses, schists and migmatites rich in mafic minerals such as garnets, hornblendes and biotites. Sediment from the core from the estuary of the Amisa River could have been derived from the Asebu, Abakrampa, Enyan Denkyira areas whose rock composition varies from Granite, biotites, muscovites, granodiorites, pegmatites and aplites with biotite schist pendants (Dickson and Benneh, 1980).

About 85% of the sediment from the core from the Pra estuary could have been derived from the Obuasi, Dunkwa, Bogoso, Fosu, Twifo Praso, Tarkwa Takoradi, Sekondi and Inchaban areas whose rocks consist of quartzites, phyllites, grits, conglomerates (Dickson and Benneh, 1980) while 20% could have originated the Shama and Aboadze areas whose rocks comprise metamorphosed lavas, pyroclastic rocks, hypabyssal basic intrusives, phyllites and greywackes (Dickson and Benneh, 1980).

CHAPTER FOUR

RECONSTRUCTION OF TRACE METAL ACCUMULATION HISTORIES USING SEDIMENT CORES FROM SIX GHANAIAN ESTUARIES

4.1 Introduction

Estuaries are natural systems that act as important conduits of materials from the terrestrial environments into coastal areas and deeper parts of the ocean (Mil- Homens *et al.,* 2009). In addition, they provide substrates to benthic invertebrates, feeding area for nektonic, epibenthic invertebrates, migratory birds and nursing grounds to fishes (Burgos and Rainbow, 2001). They thus represent an important ecological compartment with respect to both the aquatic and terrestrial environments (Morillo *et al*., 2009).

Intense industrial activities accompanied by rapid population growth since the 19th century has resulted in the release of enormous amounts of trace metals known to negatively affect the ecology of estuaries (Vale *et al.*, 2008). Available literature shows that part of the trace metals introduced into estuaries are further exported and deposited on adjacent shelf and slopes of the marine environment (Queralt *et al.*, 1999; Mil-Homens *et al.*, 2009).

Naturally, they serve as important zones of sediment transfer between fluvial and marine systems, often forming sinks for sediment and contaminants moving downstream, alongshore or landwards (Ridgway and Shimmield, 2002). As sediments get accumulated in the estuarine environment over time, they amass a lot of information about their sources, predominantly the temporal variations in their rates of supply (Cheevaporn and Mokkongpai, 1996). The need to obtain data on the variations in their source supply, especially those due to man are key and chronological studies of sediment cores are required to document such changes (Cheevaporn and Mokkongpai, 1996).

The use of estuarine and marine sediment cores to document environmental changes over time, particularly in understanding historical metal fluxes is well researched, with the examination of ^{210}Pb profiles in sediment cores being one of the most widely accepted and validated methods for studying recent accumulation trends (Ruiz-Fernández *et al.*, 2009a; Diaz-Asencio *et al.*, 2009; Xu *et al.*, 2009; Hung and Hsu, 2004; Cundy *et al.*, 2001; Ruiz-Fernández *et al.*, 2004).

Although metal pollution of some estuaries and other nearshore systems arising from Gold mining operations in Ghana date back to the 19th Century (Ofosu-Mensah, 2011), metal pollution due to industrialization is comparatively recent dating back to the latter part of the 20th century, around 1961 (La Verle, 1994). The birth of industrial age in Ghana in the early 60s saw the rapid development of industries along the coastal belt that have led to some negative impacts on our coastal water bodies. Many estuaries, particularly those located in heavily industrialized and populated regions of the country, have become dumping and waste discharge points for these large numbers of industries and residents. Consequently, the environmental quality of our estuaries and adjacent continental shelf has experienced degradation from the beginning of our industrialization to present.

Natural geochemical cycling of trace metals into these estuaries and their adjacent shelf are also expected to have changed over time. Long-term monitoring data, a key to understanding temporal changes in nearshore environmental quality and geochemical cycling of trace metals into these systems are rather expensive to collect, hence missing. In the absence of long-term monitoring data however, data obtained from the

sedimentary record can be used to provide retrospective information on the past characteristics of the aquatic environment (Ruiz-Fernández and Hillaire-Marcel, 2009).

To date however, all geochemical studies on trace metals in Ghana's nearshore and coastal environments have focused on spatial assessments in surface sediment and biota which are unable to tell us how these systems have been impacted over time. Apart from a study conducted by Sorensen *et al.* (2003) to investigate historical trends in sedimentation and nutrient fluxes using sediment cores from the Keta lagoon, no study has yet been conducted to investigate historical trends in metal pollution using sediment cores from Ghanaian estuarine environments. Thus, literature on the use of ^{210}Pb in dating sediment and understanding metal accumulation rates in Ghana is rather scarce.

An ongoing worldwide project by the Group Experts on the Scientific Aspects of Marine Pollution (GESAMP) Working Group 39 to develop a database for assessing historical trends of organic and inorganic contaminants in sediment cores from all the large marine ecosystems (LMES) world-wide has revealed that none of such studies has yet been conducted in Ghana and many other West African countries (Ruiz-Fernandez, Pers Comm). The need to apply the ^{210}Pb sediment dating method to the studying of trace metal accumulation patterns over time in Ghanaian coastal environment is therefore long overdue and the importance of this current study cannot be overemphasized.

Based on the above gaps, the study proposed the following alternate hypotheses that:

I. The metal concentrations in the Ankobra, Pra, Amisa, Densu Sakumo II and Volta estuaries have changed since industrialization (after 1960) and are within background geochemical levels;
II. Trace metals in the estuaries are naturally derived;

III. Trace metals accumulation patterns in adjacent continental shelf and deep-sea areas are similar to those in estuaries.

4.1.1 Aim and Objectives

The study evaluated temporal changes in trace metal accumulation rates as reflected in the sedimentary record of the Ankobra, Pra, Amisa, Densu, Sakumo II and Volta estuaries using ^{210}Pb sediment dating technique. Specifically:

I. Estimated sedimentation rates and ages of the sediment core from each estuary using the CRS model validated with CIC-CSR model (Appleby and Oldfield, 1978; Appleby *et al.*, 1979);

II. Evaluated temporal changes in metal concentration in each estuary during the last 100-200 years;

III. Quantified any temporal enrichment in metal concentrations over geochemical background levels using the enrichment factor and anthropogenic accumulation fluxes;

IV. Explained possible sources of metals in each estuary using cluster and provenance analysis;

V. Compared metal accumulation patterns in the estuarine sediments to that of the adjacent shelf and deep-sea areas.

4.2 Materials and Methods

4.2.1 Estuarine Study Sites and Sampling Procedure

Information pertaining to the description of the estuarine study sites and sediment coring protocols can be assessed from section 3.2.1 of chapter 3. Site description and sampling protocols for the continental shelf and deep-sea areas are given below.

4.2.1.1 Continental Shelf and Deep-Sea Areas

The study was carried out at the Western end of the Ghanaian continental shelf on two North-South transects which lie in close proximity to the Ankobra and Pra estuaries. The transects; A and B were located about 235.38km and 151.01km away from the Ghana/Cote d'Ivoire border respectively (Fig. 4.1). The coastline of Ghana, measuring about 536 km long, stretches from longitude 3° 06'W to 1° 10'E and lies between latitudes 4° 30' and 6° 6'N (Koranteng, 1995)). The continental shelf varies in width from approximately 13km to 80km, typical of many shelf regions along the African coast (Koranteng, 1995). The shelf drops sharply into the Cote d'Ivoire enscarpment just beyond the 145-250m depth contour and narrows in width progressively from the western end towards the east (Google Maps, 2014). The ocean floor on the continental shelf of Ghana has distinct areas of mud, hard rocks and mixed deposits which are potential sinks for trace metals and other particulate materials (Koranteng, 1995). As a result of rapid urbanization, the coastal zone has become a home to over 80% of the country's industries with the majority of these industries discharging their wastes and sewage directly into the ocean and estuaries (Armah and Amlalo, 1997). Untreated effluent and debris from small-scale mining operators are discharged directly into major rivers that enter the western end of the shelf via their estuaries, potentially threatening the ecological integrity of the coastal zone (Hayford *et al.*, 2008).

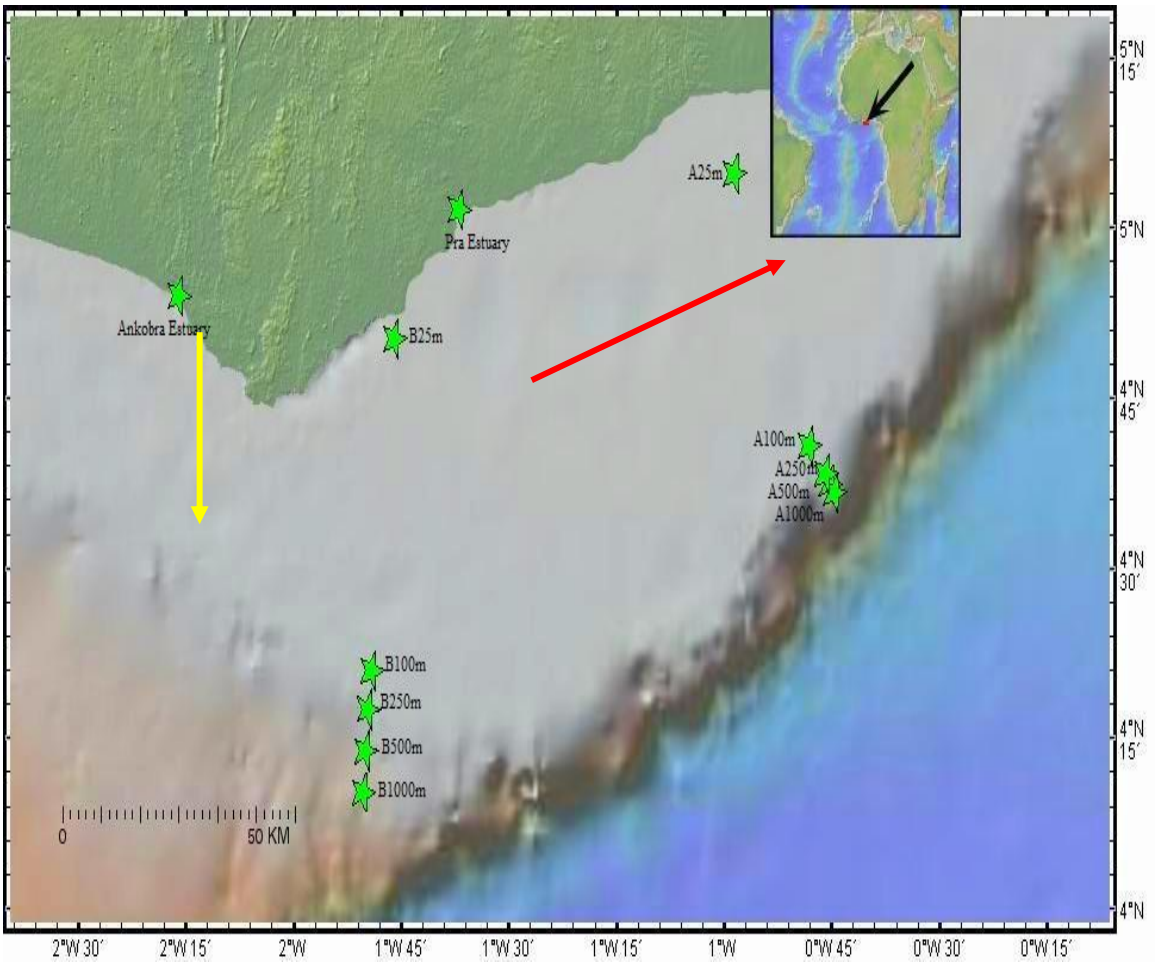

Figure 4.1. Map of the Western Continental Shelf of Ghana showing sampling locations and estuaries: Yellow arrow shows undercurrent direction; red arrow shows surface (Guinea Current) direction (Koranteng, 1984)

4.2.1.2 Field Sampling Procedure

Surface sediment samples from the continental shelf were taken using a Van Veen grab with adjustable weight and opening of 0.1m^2 deployed from the R/V Fridtjoff Nansen in April 2010. Samples were taken along two north to south transects (about 100km apart) in the western Gulf of Guinea. At each location, sediment samples were taken at depths of about 25m, 100m, 250m, 500m and 1000m along two transects. A total of 10 sites, 5 along each transect were analyzed.

4.2.2 Radionuclide Analysis of Cores

See section 3.2.2 for sediment coring protocols. Analysis of ^{210}Pb and other radionuclides in sediment cores followed the method of Takesue and Swarzenski (2011). Sample preparation for gamma analysis was carried out at MLML. Sediment cores sectioned at 2cm intervals were oven dried at 60^{o}C to constant weight and homogenized to fine powders. Samples were transferred into tarred gamma vials, tapped down, filled to exactly the 10mL line, capped, sealed and the weight noted. Sealed sediment in gamma vials were stored for at least 3 weeks to prevent loss of ingrown ^{222}Rn, and to allow for secular equilibrium between ^{226}Ra and its short-lived daughter nuclides ^{214}Pb and ^{214}Bi which were used for dating.

Samples were sent to the United States Geological Survey laboratory in Santa Cruz, California for gamma counting. Counting was carried out on an ultra-low background, high purity germanium well detector, which provided low noise and excellent energy resolution at low to moderate energies. Analyses of Gamma rays were performed inside a large-diameter, low-background shield consisting of copper-lined lead which was flushed continuously with nitrogen gas to remove any residual radon (Rn) buildup. Lead-210 (^{210}Pb) was measured by its gamma peak at 46.5 keV, ^{226}Ra was measured by its indirect peaks at 351.87 (^{214}Pb) and 609.31 (^{214}Bi), and ^{137}Cs was measured by its peak at 661 keV (Takesue and Swarzenski, 2011).

The counting of each sample lasted for 24 hours on average. The excess ^{210}Pb was calculated by subtracting supported ^{210}Pb (^{226}Ra) from total ^{210}Pb. Absolute activities were determined by using calibrated (RGU-1, RGTh-, and IAEA radioactive standards)

sediment samples in the same geometry (1-10 mL). Counting errors were less than 12 percent.

4.2.3 Trace Metal Analysis

4.2.3.1 Total Mercury Analysis

Total Hg (organic and inorganic) in sediment was analyzed using the DMA 80 automatic mercury analyzer (Milestone, Inc.) at the Marine Pollution Studies Laboratory of MLML. Unlike the ICP-MS and other techniques, the DMA-80 requires no sample preparation, hence reduces the contamination of samples prior to analysis. As Hg volatilizes at low temperatures, it is likely that some Hg in the samples may be subject to loss when using sample preparation methods that require enormous amount of heating.

The DMA-80 has been referenced in USEPA method SW-846 7473 which employs a sequence of thermal decomposition, gold amalgamation and atomic absorption spectrophotometry. In this method, controlled heating in an oxygenated decomposition furnace was used to liberate mercury from pulverized sediment which was carried through flowing oxygen to the catalytic section of the furnace where oxidation is completed and halogens and nitrogen/sulfur oxides are trapped. The remaining decomposition products were further carried to a gold coated amalgamator column that selectively trapped the mercury in each sample. Heating of the amalgamator column released mercury vapor which was carried by flowing oxygen through absorbance cells positioned in the light path of a single wavelength atomic absorption spectrophotometer. Absorbance (peak height) was measured at 253.7 nm and it was proportional to the mercury concentration in the sediment sample.

About 0.6g of homogenized sediment was used for each sample analysis in the DMA-80 direct Hg analyzer. All samples were run in triplicates and Hg concentrations reported in μgg^{-1}. For quality control and assurance purposes, two empty sample "boats" were placed inside the DMA at the beginning of each run to ensure that the instrument is running well and to clean any residual mercury from previous runs. This was followed by high and low checks using certified reference material (CRM) 1944 and 2702 respectively to check percent recoveries of mercury by the instrument.

Where recoveries were over 105%, a new batch of empty sample boats were run again to clean the instrument followed by a low or high check depending on which one failed. One or two initial calibration blanks (ICB), followed by three method blanks were run following high and low checks before the introduction of actual samples. In between every ten samples continuous calibration blanks (CCB) and continuous calibration verifications (CCV) were ran to check against any instrumental drifts. Then also for every batch of 20 samples, there was one sample run as duplicate, a selected sample with known concentration was spiked with prepared standard to check percent recovery. A CCB and CCV run were again made at the end of each batch of 20 sample runs.

4.2.3.2 Analysis of other Trace Metals

Digestion of sediment (samples, BCSS-1 SRM, method blanks) for trace metals has already been described in section 3.2.5. Digested sediments, method blanks and multi-element standards of trace metals of interest (As, Cd, Cr, Mo, V, Cu, and Zn as justified in section 2.2.2) were quantified via a Perkin-Elmer Element 2 high resolution Inductively Coupled Plasma Mass Spectrometry (ICP-MS).

4.2.4 Total Organic Carbon (TOC) analysis

Total organic carbon was analyzed to help explain any variability in trace metal enrichment in each estuary. TOC analysis was carried out on every section of each core using the method outlined in Hunter (2006). Samples for the analysis were oven dried at 60^{o}C and homogenized into fine powders using an agate mortar and pestle. Between 5000-10000µg of sample was weighed into pre-dried aluminum "boats" and introduced into a 440 elemental analyzer (Exeter Analytical, Inc.) at Moss Landing Marine Laboratories. The 440 elemental analyzer combusts the sediment sample in an oxygen environment around 800^{o}C. The combustion process reduces, separates and mixes the evolving gas with a helium carrier gas into CO_2, N_2 and H. Thereafter, it utilizes a four wire Wheatstone bridge thermal conductivity differential to report values of Carbon, nitrogen and hydrogen (Hunter, 2006). Detection limit of the analyzer was 0.20µg/mg for carbon. Calibration of the analyzer was made using L-Cystine standard purchased from J. T Baker Chemical Co. For quality control and quality assurance purposes, blanks, appropriate blanks and filters were run at the beginning of each batch of runs. Four L-cystine standards were run and the average values for carbon and nitrogen were compared with known values of the standard. Acceptable limits for instrumentally reported standards were less than ±1.0% of the known value and a coefficient of variation of the four standards were 0.5% or less. Also two L-cystine and two BCSS-1 (National Research Council Canada, 1995) standards were run after every 25 samples and at end of each instrumental run as known, to assure against instrumental drift or depletion of combustion/reduction tube chemicals.

4.2.5 ^{210}Pb Dating of Estuarine Sediment Cores

Counted depths (z) were dated using the CRS model and validated with CF-CSR model (Appleby and Oldfield, 1978) using sedimentation rates and annual ^{210}Pb (Excess) deposition onto the sediment. As ^{137}Cs was not detected in most of the cores, the choice of it as a model validator could not be established in the study. The study therefore validated the CRS model used in dating the cores by comparing average sedimentation rates estimated using this model to those estimated using the CF-CSR model.

The CF-CSR model predicts an exponential decay for ^{210}Pbexcess activity versus the cumulative mass depth (m) as;

$$A(m) = A(0)\, e^{(-\lambda m/w)} \qquad 4\text{-}1$$

Where λ is the radioactive decay constant (0.03114) year^{-1}for ^{210}Pb, w is the sedimentation rate in gcm^{-2}y^{-1}. The constant sedimentation rate, for the entire core is estimated from the best fit to the data set.

Unlike the CF-CSR model where one sedimentation rate was estimated from the best fit to the data set for each estuary, the CRS model allowed the sedimentation rate to vary and the total ^{210}Pb flux inventory ($\sum$) for each core was used in dating the sediment cores. This required a compensation for the incompleteness of the ^{210}Pbexcess profile for each core (Laissaoui *et al.*, 2008). This was done by extrapolating the lower portion of ^{210}Pbexcess from ^{210}Pbexcess vs mass depth plot of the CF-CSR model (Laissaoui *et al.*, 2008). The cores were then dated using the equations below;

$$A(z) = A(0)\, e^{-\lambda t} \qquad 4\text{-}2$$

Where A (z) is ^{210}Pbex at depth z, and A (0) is the total ^{210}Pbex activity flux of the entire core. Both A (z) and A (0) were determined by an integration of the ^{210}Pb profile, leaving the sediment age t as a function of depth z as;

$$t = \frac{1}{\lambda} Ln \frac{(Ao)}{(Az)} \qquad 4\text{-}3$$

The changing sedimentation rate (w in $gcm^{-2}yr^{-}1$) was then estimated from the equation below;

$$w = \frac{\lambda A}{C} \qquad 4\text{-}4$$

Where A is the cumulative ^{210}Pb activity flux (dpm/cm^2) and C is the excess ^{210}Pb activity (dpm/g) at a particular depth.

Sediment accumulation rates (w) of ^{210}Pb were calculated after transforming depth scales into cumulative dry mass (M) using the dry bulk density (DBD) to correct for compaction (Appleby and Oldfields, 1992). To calculate DBD, the water content of each sediment section was determined after drying at 60^{o}C to constant weight and the porosity estimated. The porosity (ϕ), dry bulk density (DBD), cumulative dry mass per depth (M) of each sample were calculated by assuming a solid density of 2.50 g cm^{-3} as adopted from Swarzenski *et al.* (2006) as follows:

$$\phi = F_w / [F_w + (1 - F_w)\rho_w / \rho_s] \qquad 4\text{-}5$$

$$DBD = [(1 - \phi) * 2.5] \qquad 4\text{-}6$$

$$M = \sum [(1 - \phi)\rho_s * \delta_\times] \qquad 4\text{-}7$$

Where F_w is the fraction of water in the wet sediment [=1-(dry weight/wet weight)], ρ_w is the density of pore water (assumed to be 1.0 gcm^{-3}), and ρ_s is the density of dry

sedimentary particles (assumed to be 2.5 gcm^{-3}) and δ_x is the thickness of the layer (2 cm).

4.2.6 Statistical Analysis

The main hypotheses of the study were tested using the student's T-test (assuming unequal variances) by comparing mean metal concentrations before and after 1960 using the Microcal Origin 8 software. Cluster Analysis (CA) using Ward's approach was carried out in SPSS software (version 13 for Windows) to evaluate similarities in trace metal concentration. CA was carried out on the standardized datasets (whose mean and standard deviation were set to zero and one, respectively – Z score) to minimize the effect by the difference in measured units, and variance, and to render the data dimensionless. Spearman correlation was also used in identifying significant correlations among the various metals analyzed.

4.2.7 Estimation of Trace Metal Enrichment in Sediment

In order to identify trace metal enrichments in sediment during the period covered by ^{210}Pb-derived geochronologies, enrichment factors (EFs) were calculated using Al as a normalization tracer for natural, mineralogical and grain size variability, according to the following formula below;

$$EF = [(C_n/C_{Al})_{\text{Sample}} / (C_n/C_{Al})_{\text{Reference Sample}}] \quad 4\text{-}8$$

Where $(C_n/C_{Al})_{\text{Sample}}$ is the heavy metal to Al ratio in the samples of interest, and $(C_n/C_{Al})_{\text{Reference Sample}}$ is the heavy metal to Al ratio in the selected reference sample (Zhang *et al.*, 2007). According to Sutherland (2000), five contamination categories can be recognized on the basis of the enrichment factor: EF<2, depletion to mineral enrichment; 2≤EF<5,

moderate enrichment; 5≤EF<20, significant enrichment; 20≤EF<40, very high enrichment; and EF>40, extremely high enrichment.

4.2.8 Historical Contribution of Human Activities to Trace Metal Levels in the Estuarine Sediment

To quantify anthropogenic contributions to trace metals in each estuary, the mass accumulation fluxes (MAFs) and geochemical baseline accumulation fluxes (BFs) of the enriched metals were calculated using measured concentrations and the sedimentation rates from each estuary (for MAFs). Geochemical background concentrations were taken from Rudnick and Gao (2003). The anthropogenic fluxes (AF) were calculated by subtracting the BFs from MAFs with values greater than zero depicting anthropogenically enhanced metal enrichment in the sediment (Bing *et al.*, 2011).

4.3 Results

4.3.1 CF-CSR Sedimentation Rates and Annual 210Pb input into Sediments

For the sediment cores from the Ankobra, Pra, Densu and Volta estuaries, the excess ^{210}Pb was near 0.00 dpmg^{-1} at depths 10 cm, 16 cm and 40 cm respectively. The excess ^{210}Pb was 4.41 dpmg^{-1} at 26 cm and 4.45 dpmg^{-1} at 16cm for sediment cores from the Amisa and Sakumo II estuaries (Appendices B1–B6).

All six cores showed an exponential decline in their excess ^{210}Pb activities with depth (CMD) (Fig. 4.2). The excess ^{210}Pb activity of the Ankobra estuary varied between 3.12 dpmg^{-1} and 0.27 dpmg^{-1} while that of Pra and Amisa estuaries varied between 1.77 dpmg^{-1} and 0.11 dpmg^{-1}, and 6.18 dpmg^{-1} and 4.41 dpmg^{-1} respectively. The excess ^{210}Pb activity of the Densu estuary varied between 5.78 dpmg^{-1} and 0.25 dpmg^{-1} while that of

the Sakumo II and Volta estuaries varied between 9.44 and 3.80 dpmg^{-1} and, 2.0 and 0.00 dpmg^{-1} respectively (Fig. 4.2).

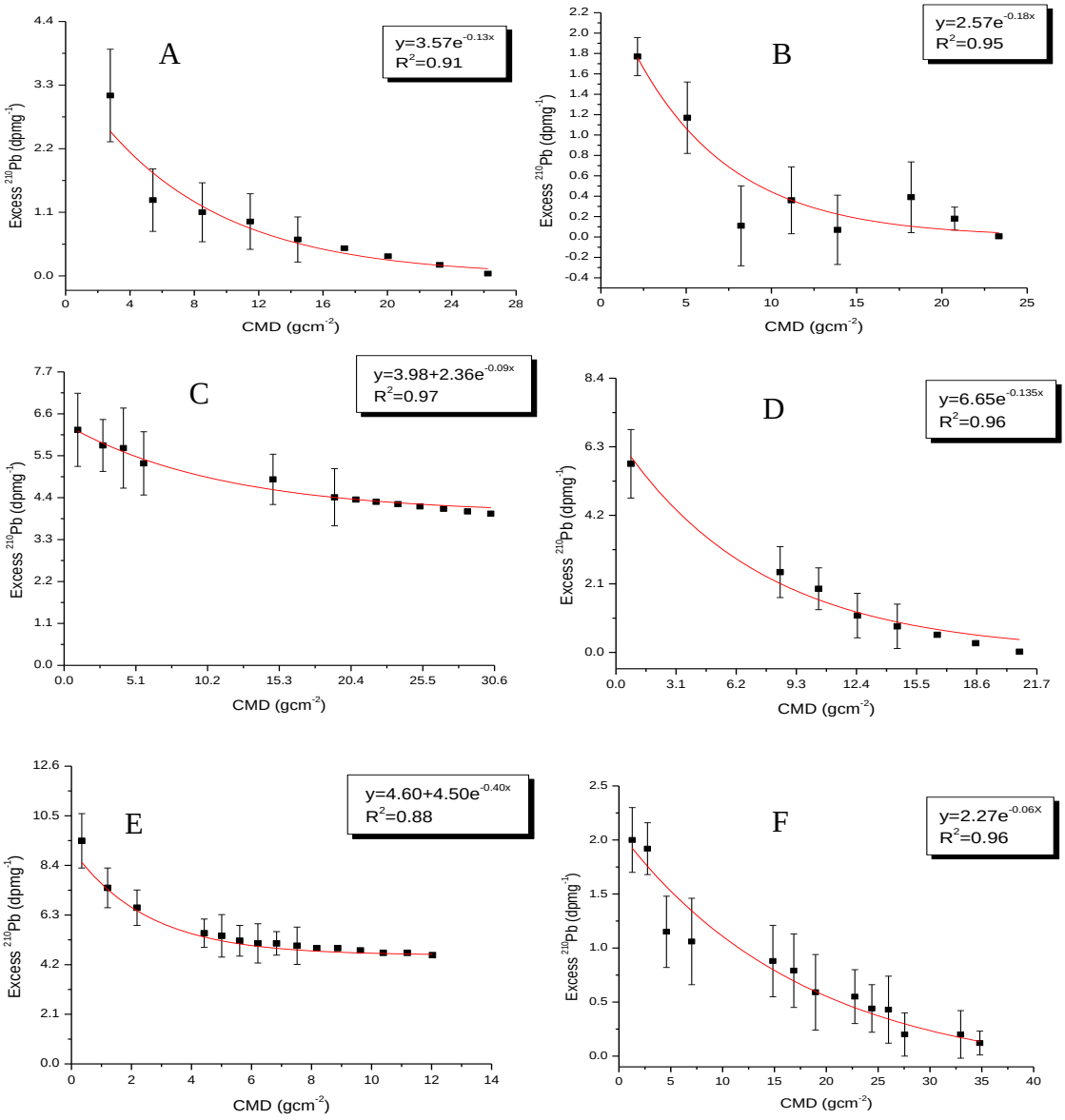

Figure 4.2. Excess ^{210}Pb activity versus mass depth from the; (a) Ankobra, (b) Pra, (c) Amisa, (d) Densu, (e) Sakumo II and (f) Volta estuaries.

The CF-CSR sedimentation rates (w) estimated from the best fit to data (from Fig. 4.2) were 0.24±0.1 gcm^{-2}y^{-1}, 0.17±0.02 gcm^{-2}y^{-1}, 0.35±0.1 gcm^{-2}y^{-1}, 0.23±0.1 gcm^{-2}y^{-1}, 0.10±0.02 gcm^{-2}y^{-1} and 0.52±0.2 gcm^{-2}y^{-1} for the Ankobra, Pra, Amisa, Densu, Sakumo II and Volta estuaries respectively (Table 4.1). Thus based on the CF-CSR model, the Sakumo II estuary had the least sedimentation rate (0.1 gcm^{-2}y^{-1}) while the Volta estuary

recorded the highest sedimentation rate of about 0.52 $gcm^{-2}y^{-1}$. Likewise, the annual CF-CSR ^{210}Pbexcess (F) input onto the sediment from each estuary, estimated from F=A(0)w (Laissaoui *et al.*, 2008) were 0.84±0.20 $dpmcm^{-2}y^{-1}$, 0.45±0.10 $dpmcm^{-2}y^{-1}$, 4.80±1.00 $dpmcm^{-2}y^{-1}$, 1.56±0.08 $dpmcm^{-2}y^{-1}$, 4.96±1.2 $dpmcm^{-2}y^{-1}$ and 1.18±0.05 $dpmcm^{-2}y^{-1}$ for the Ankobra, Pra, Amisa, Densu, Sakumo II and Volta estuaries respectively (Table 4.1).

Table 4.1. Summary of CF-CSR sedimentation rates and Annual ^{210}Pb (excess) input (F) for all six estuaries

Estuaries	Sedimentation Rate ($gcm^{-2}y^{-1}$)	Annual ^{210}Pb input into Sediment ($dpmcm^{-2}y^{-1}$)
Ankobra	0.24±0.10	0.84±0.20
Pra	0.17±0.02	0.45±0.10
Amisa	0.35±0.10	4.80±1.00
Densu	0.23±0.10	1.56±0.08
Sakumo II	0.10±0.02	4.96±1.0
Volta	0.52±0.20	1.18±0.05

4.3.2 CRS sedimentation Rates and Annual ^{210}Pb (F) Input into Sediments

By extrapolating from the lower portion of the exponential fit for each core (from Fig. 4.2 above), total ^{210}Pb inventory (excess) estimated for each core were 20.46 $dpmcm^{-2}y^{-1}$, 9.00 $dpmcm^{-2}y^{-1}$, 151.55 $dpmcm^{-2}y^{-1}$, 24.76 $dpmcm^{-2}y^{-1}$, 60.96 $dpmcm^{-2}y^{-1}$ and 38.85 $dpmcm^{-2}y^{-1}$ for the Ankobra, Pra, Amisa, Densu, Sakumo II and Volta estuaries respectively. The Pra estuary recorded the least inventory while the Amisa recorded the highest inventory. Extrapolations further indicated that, the sediment cores from the Amisa and Sakumo II cores had excess ^{210}Pb activities beyond the 40cm depth (maximum depth in this study).

Based on the above total ^{210}Pb inventories (excess), average CRS sedimentation rates varying between 0.94 and 0.04 gcm^{-2}y^{-1}, 1.37 and 0.04 gcm^{-2}y^{-1}, 0.78 and 0.03 gcm^{-2}y^{-1}, 1.85 and 0.1 gcm^{-2}y^{-1}, 0.43 and 0.01 gcm^{-2}y^{-1}, and 0.89 and 0.03 gcm^{-2}y^{-1} were estimated for the Ankobra, Pra, Amisa, Densu, Sakumo II and Volta estuaries respectively (Fig. 4.3). Again using the CRS model, the Sakumo II estuary recorded the least average sedimentation rate (0.20±0.01 gcm^{-2}y^{-1}) while the Volta estuary recorded the highest average sedimentation rate (0.54±0.36 gcm^{-2}y^{-1}) (Table 4.2).

Additionally, the CRS F estimated from F= λ∑A (Laissaoui *et al.*, 2008), where A is the total ^{210}Pb inventory (excess) yielded 0.68±0.2 dpmcm^{-2}y^{-1}, 0.28±0.1 dpmcm^{-2}y^{-1}, 4.70+0.8 dpmcm^{-2}y^{-1}, 0.77±0.2 dpmcm^{-2}y^{-1},4.96±1.0 dpmcm^{-2}y^{-1} and 1.21±0.1 dpmcm^{-2}y^{-1} for the Ankobra, Pra, Amisa, Densu, Sakumo II and Volta estuaries respectively (Table 4.2).

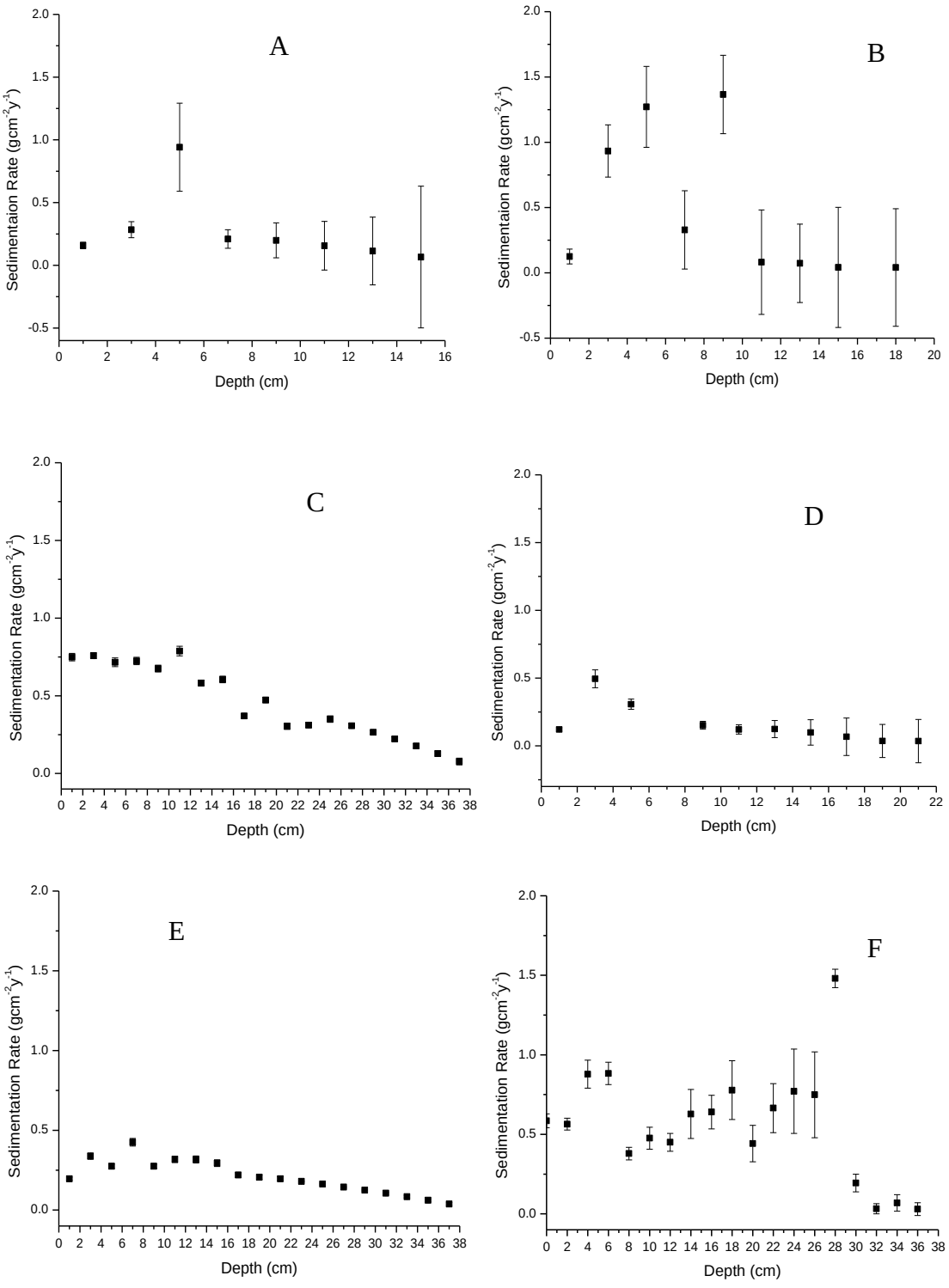

Figure 4.3. Estimated CRS sedimentation rates from the; (a) Ankobra, (b) Pra, (c) Amisa, (d) Densu, (e) Sakumo II and (f) Volta estuaries.

Table 4.1. Summary of CRS sedimentation rates (Averages) and Annual ^{210}Pb (excess) input (F) for all six estuaries

Estuaries	Sedimentation Rate ($gcm^{-2}y^{-1}$)	Annual ^{210}Pb input into Sediment ($dpmcm^{-2}y^{-1}$)
Ankobra	0.24±0.10	0.63±0.30
Pra	0.47±0.20	0.28±0.10
Amisa	0.43±0.02	4.70±0.80
Densu	0.31±0.13	0.77±0.20
Sakumo II	0.20±0.01	1.89±0.20
Volta	0.54±0.36	1.21±0.10

4.3.3 CRS Ages of Cores

The CRS model enabled dating of the first 10cm of the Ankobra core to about 148 years old (2003-1855 AD). Dates below this depth were extrapolated using the average sedimentation rate of 0.24±0.10$gcm^{-2}y^{-1}$ from the CRS model (1855-1681 AD) which dated the entire core to about 322years. This age however which appeared to be too old when using the ^{210}Pb sediment dating method (100-200 years). Due to this the core was dated up to about 197 years (2003-1813AD) which corresponded to the 30cm (Fig. 4.4A).

The CRS model dated the first 16cm of the Pra core to 38 years old (2010-1971 AD). Dates below the 16cm depth were extrapolated using the average sedimentation rate of 0.47±0.20 $gcm^{-2}y^{-1}$ from the CRS model, which brought the entire core to about 121 years old (1971-1888 AD) (Fig 4.4B).

Additionally, the CRS model dated the entire Amisa core to about 74 years (2011-1937 AD) (Fig 4.4C). The sedimentation rates from the CRS model enabled the dating of the first 20cm of the Densu core to about 59 years old (2011-1951 AD). Dates below this depth were extrapolated using the average sedimentation rate of 0.31±0.13 $gcm^{-2}y^{-1}$ from the CRS model (1951-1849) to bring the entire core to 159 years (Fig 4.4D).

Again, the sedimentation rates from the CRS model were used to date the entire Sakumo II core to about 81 years (2011-1929 AD) (Fig 4.4E) .Finally, the sedimentation rates from the CRS model enabled the dating of the entire sediment core from the Volta estuary to about 71 years old (2010-1939 AD) (Fig 4.4 F).

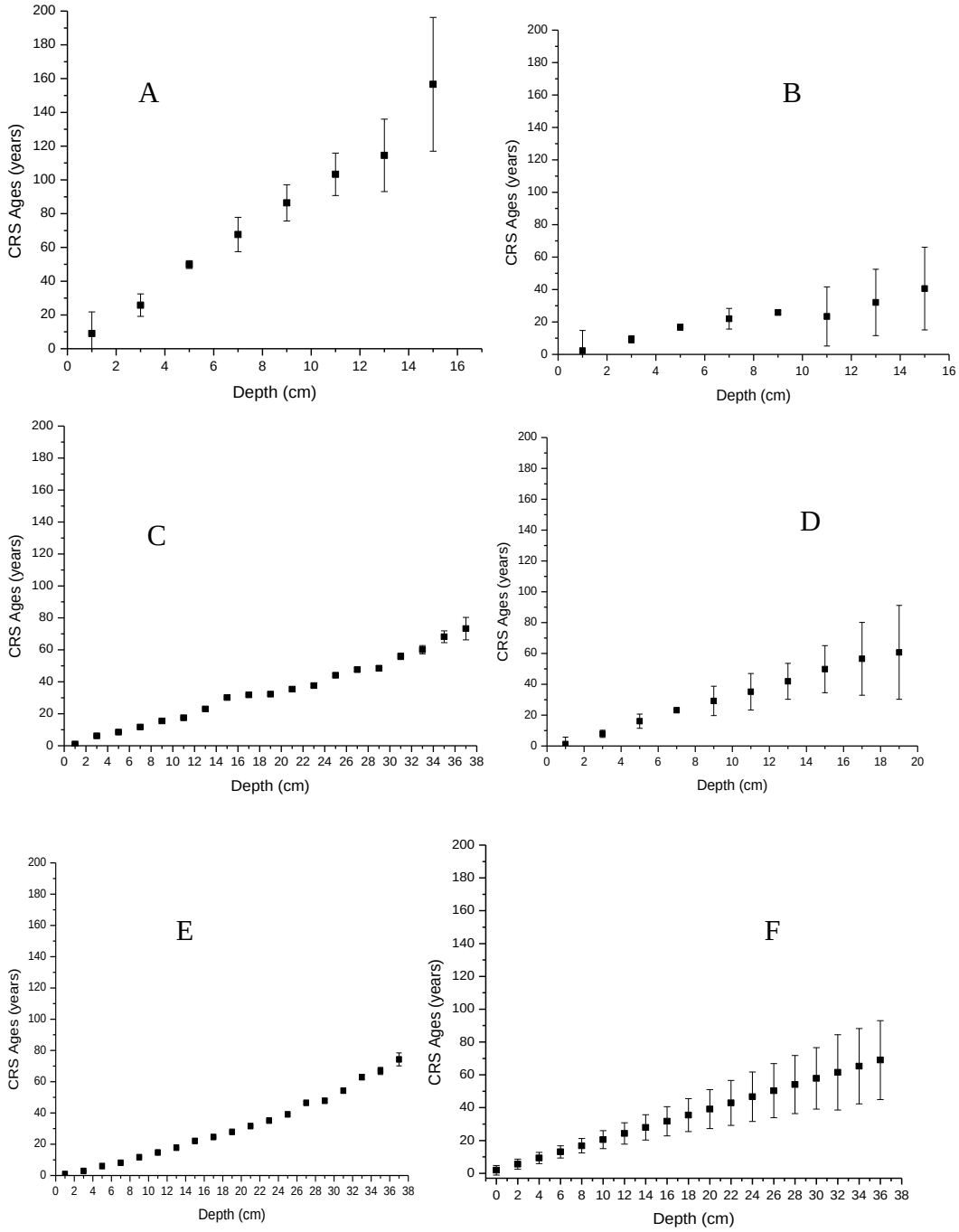

Figure 4.4. Modelled CRS ages of the cores from the; (a) Ankobra, (b) Pra, (c) Amisa, (d) Densu, (e) Sakumo II, and (f) Volta estuaries.

4.3.4 Temporal Variations in Trace Metal Concentrations

4.3.4.1 Ankobra Estuary

A few of the trace metal showed high down-core variability while others did not. Concentrations of Cd, Hg and Mo varied slightly from 0.06 to 0.15 μg^{-1}, 0.12 to 0.24 μg^{-1} and 0.54 to 1.70 μg^{-1} between 1840 and 2003 AD respectively (Fig. 4.5A). On the contrary, the concentrations of Pb, Cu and Zn varied greatly from 6.55 to 13.92 μg^{-1}, 11.40 to 25.11 μg^{-1}, and 42.81 to 79.78 μg^{-1} between 1840 and 2003 AD respectively (Fig. 4.5B). Just as Pb, Cu and Zn, high variabilities were seen in the levels of Cr (from 60.30 to 139.16 μg^{-1}), V (from 44.75 to 106 μg^{-1}) and As (from 69.40 to 142.71 μg^{-1}) over the same period (Fig 4.5C). The concentrations of trace metals in the sediment core from the Ankobra estuary followed the trend As >Cr>V>Zn>Cu>Pb>Mo>Hg>Cd. Results of the independent T-test to compare mean metal concentrations before and after industrialization was significant for only Mo (t=2.42; p=0.03) and Zn (t=2.65; p=0.02) (Appendix B7). For both metals, the means before industrialization were greater than after industrialization.

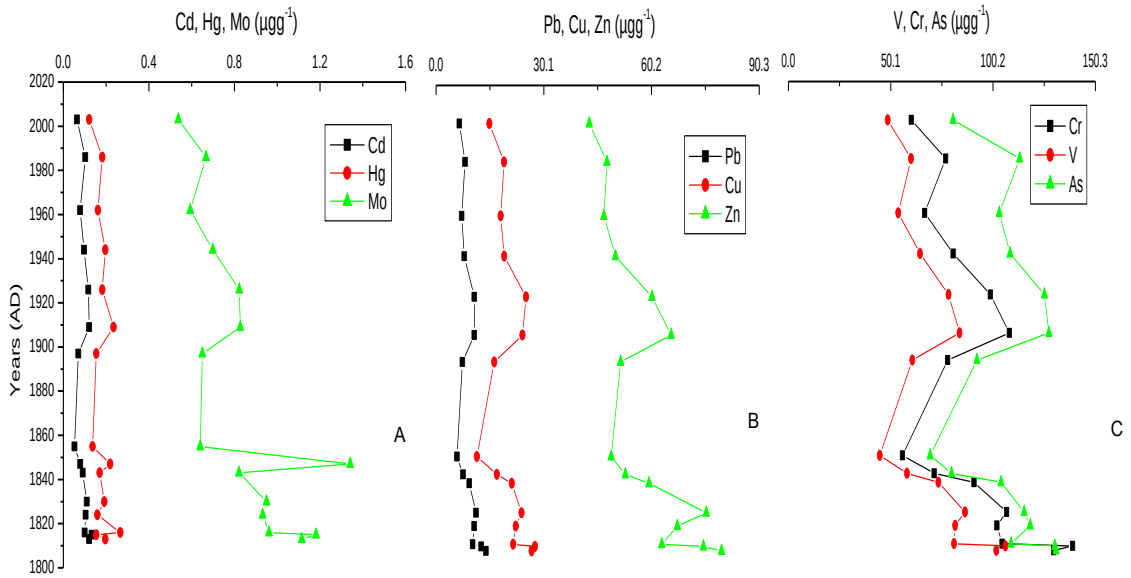

Figure 4.5. Temporal profiles of trace metal concentrations in the sediment core from the Ankobra estuary: (a) Cd, Hg & Mo; (b) Pb, Cu & Zn; (c) Cr, V & As.

4.3.4.2 Pra Estuary

With the exception of some slight variability that was observed in the concentrations of Cd and Hg ranging from 0.05 to 0.11 μg^{-1} and from 0.12 to 0.33 μg^{-1} respectively between 1950 AD and 1980 AD, their concentrations were quite homogenous (Fig. 4.6A). Slight variabilities were seen in the concentrations of Pb and Cu ranging from 7.35 to 15.33 μg^{-1} and 17.00 to 31.75 μg^{-1} respectively, while Zn showed high variability in concentration (ranging from 40.91 to 80.46 μg^{-1}) between 1890 and 2011 AD (Fig. 4.6B). High variabilities in concentrations were seen from 1890 to about 1980 AD for V and As ranging from 53.55 to 113.79 μg^{-1} and 22.66 to 46.64 μg^{-1} respectively between 1890 and 2010 AD (Fig. 4.6C). Concentrations of the trace metals in this core followed the trend Cr>V>Zn>As>Cu>Pb>Mo>Hg>Cd. The T-test was significant for all trace metals Mo (t=5.17; p=0.00), Cd (t=3.13; p=0.01), Pb (t=3.98; p=0.00), Cr (t=2.39; p=0.03), Cu (t=2.32; p=0.03), Zn (t=3.37; p=0.00), and As (t=4.13; p=0.00) (Appendix B8). Mean concentrations of trace metals prior to industrialization were higher than means after industrialization.

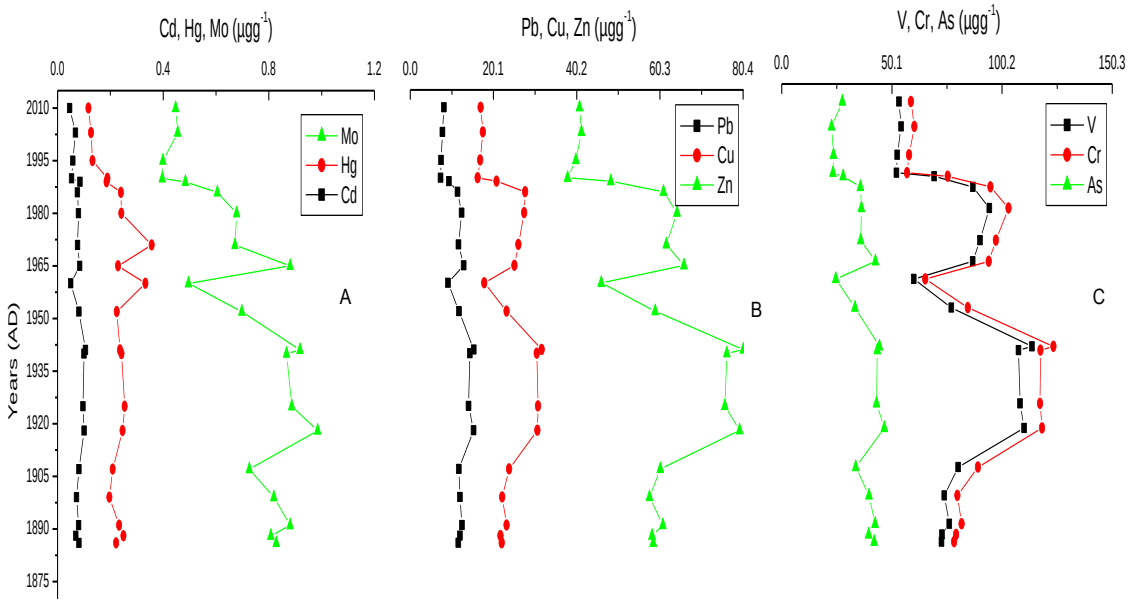

Figure 4.6. Temporal profiles of trace metal concentrations in the sediment core from the Pra estuary: (a) Cd, Hg & Mo; (b) Pb, Cu & Zn; (c) Cr, V & As.

4.3.4.3 Amisa Estuary

Though the concentrations of Mo, ranging from 1.57 to 1.99 μg^{-1} showed some high peaks between 1935 AD and 1950 AD, almost no variability was seen in the concentrations of Cd and Hg, ranging from 0.05 to 0.08 μg^{-1} and 0.12 to 0.14 μg^{-1} respectively between 1935 and present (Fig. 4.7A). Similar down-core concentrations were also seen for Pb, Cu and Zn ranging from 21.66 to 24.92 μg^{-1} 18.41 to 22.24 μg^{-1} and 66.48 to 74.84 μg^{-1} respectively between 1940 AD and AD 2010 (Fig. 4.7B). The concentration of As was slightly homogenous ranging from 10.54 to 14.46 μg^{-1} between 1935 and 2011 AD, while slight variations in concentrations were observed for V and Cr ranging 68.72 to 81.12μg^{-1} and 79.22 to 93.43μg^{-1} respectively between 1940 and 2010AD (Fig. 4.7C). Mean concentrations of trace metals in this core followed the trend Cr>V>Zn>Pb>Cu>As>Mo>Hg>Cd. The T-test was significant for Cd (t=7.39; p=0.00), Cu (t=3.19; p=0.00), As (t=-4.49; p=0.00) and Hg (t=2.23; p=0.03) (Appendix B9). The mean trace metal concentrations prior to industrialization were greater for Cd, Cu and Hg.

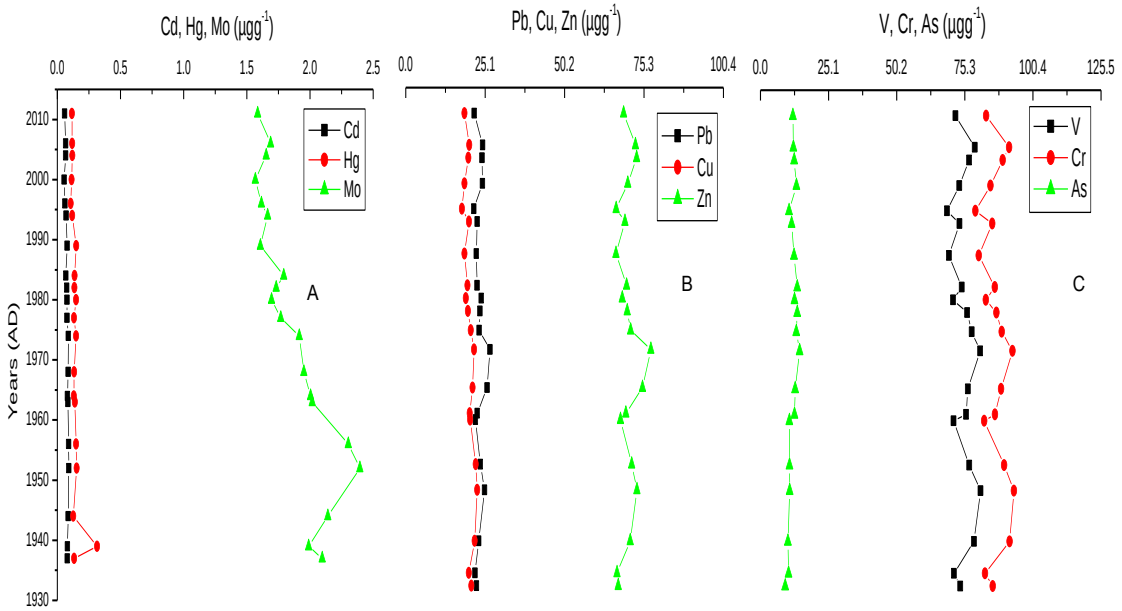

Figure 4.7. Temporal profiles of trace metal concentrations in the sediment core from Amisa estuary: (a) Cd, Hg & Mo; (b) Pb, Cu & Zn; (c) Cr, V & As.

4.3.4.4 Densu Estuary

Apart from a sharp peak corresponding to 1960 AD, the concentrations of Hg (from 0.03 to 0.17 μg^{-1}) and Cd (from 0.03 to 0.13 μg^{-1}) did not vary much over time. The concentrations of Mo (from 0.83 to 1.08 μg^{-1}) were almost homogenous from 1840 AD until about 2000 AD where levels increased sharply to present (Fig. 4.8A). Sharp increases were seen in the concentrations of Pb (from 10.07 to 21.45 μg^{-1}), Cu (from 11.54 to 29.38 μg^{-1}) and Zn (from 31.60 to 70.11 μg^{-1}) over the last 10 years (Fig. 4.8B). Similarly, sharp increases were also observed in V (from 27.51 to 66.04 μg^{-1}), Cr (from 34.57 to 74.02 μg^{-1}) and As (from 3.41 to 10.08 μg^{-1}) concentrations from 2000 AD to recent (Fig. 4.8C). Concentrations of trace metals in this core followed the trend Cr>Zn>V>Cu>Pb>As>Mo>Hg>Cd. The T- test was significant for Mo (t=-2.66; p=0.02), Cd (-4.20; p=0.00), Pb (t=-3.05; 9=0.01), Cr (t=-2.25; p=0.04), V (t=-11.58; p=0.00), Zn (t=-2.7; p=0.02), and As (t=-2.34; p=0.03) (Appendix B10). Means after industrialization were significantly higher than means prior to industrialization.

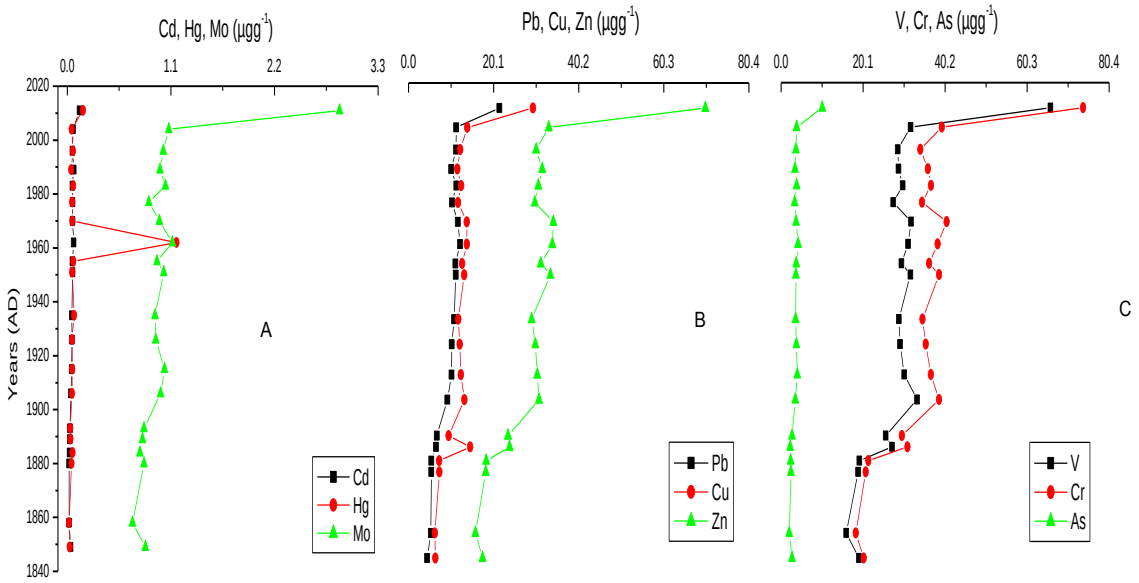

Figure 4.8. Temporal profiles of trace metal concentrations in the sediment core from Densu estuary: (a) Cd, Hg & Mo; (b) Pb, Cu & Zn; (c) Cr, V & As.

4.3.4.5 Sakumo II Estuary

Although the concentrations of Mo appear to have increased steadily from 3.65 to 5.40 μg^{-1} within the last 20 years, no variability was seen in the concentrations of Cd (between 0.10 and 0.17 μg^{-1}) and Hg (between 0.20 and 0.35 μg^{-1}) through time (Fig 4.9A). Just as was seen for Mo, the concentrations of Zn, Cu and Pb appeared to have increased progressively from 79.77 to 126.99 μg^{-1}, 39.31 to 49.49 μg^{-1} and 35.87 to 41.17 μg^{-1} respectively within the last 20 years (Fig. 4.9B). The concentrations of As were almost homogenous down the core ranging from 4.29 to 4.91 μg^{-1} while V and Cr appeared to have increased gradually from 72.39 to 90.26 μg^{-1} and 81.91 to 103.62 μg^{-1} respectively during the past 20 years (Fig. 4.9C). Concentrations of trace metals in this core followed the trend Cr>Zn>V>Cu>Pb>As>Mo>Hg>Cd. The T-test was significant for Cd (t=-3.86; p=0.00), Cu (t=-2.46; p=0.04), Zn (-3.66; p=0.01) and Hg (-3.70; p=0.01) (Appendix B11). The means after industrialization were significantly greater than prior to industrialization.

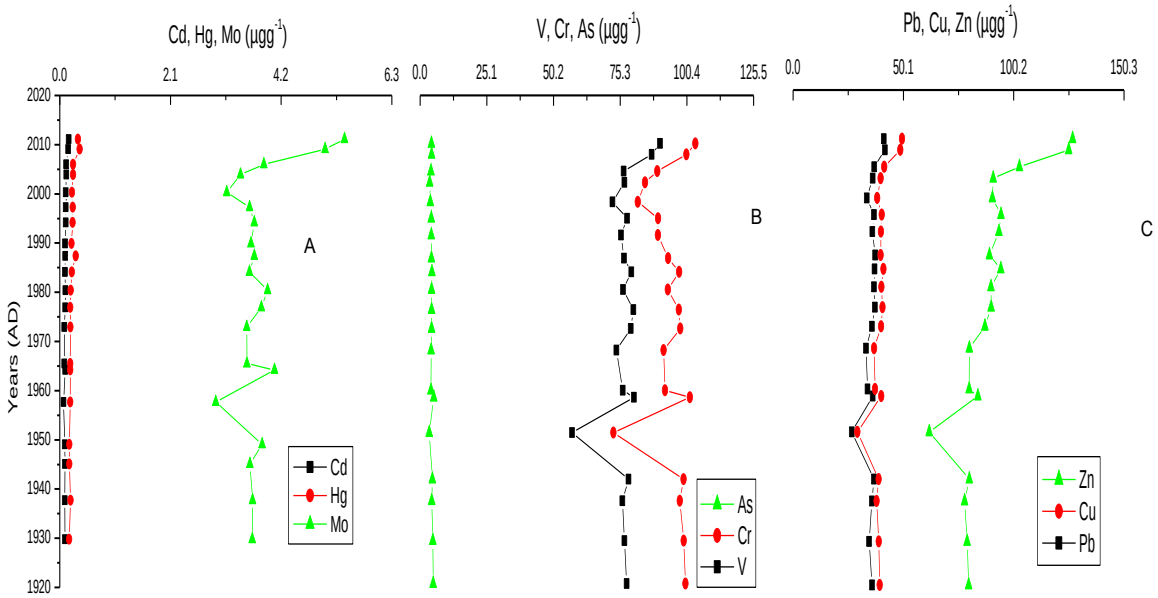

Figure 4.9. Temporal profiles of trace metal concentrations in the sediment core from Sakumo II estuary: (a) Cd, Hg & Mo; (b) Pb, Cu & Zn; (c) Cr, V & As.

4.3.4.6 Volta Estuary

Apart from two sharp peaks that corresponded to 1965 AD and 2003 AD for Hg, the concentrations of Hg, ranging from 0.04 to 0.09 μg^{-1}, Mo, ranging from 0.51 to 0.84 μg^{-1} and Cd, ranging from 0.02 to 0.04 μg^{-1} were nearly homogenous from 1940 to 2010 AD (Fig. 4.10A). Slight variabilities were seen in the concentrations of Pb (ranging from 12.75 to 15.20 μg^{-1}), Cu (ranging from 13.14-26.72 μg^{-1}) and Zn (ranging from 21.44-54.67 μg^{-1}) levels were also observed down-core (Fig. 4.10B). Similarly, slight variations were seen in the concentration of As (ranging from 4.76-7.41 μg^{-1}), while V and Cr concentrations varied greatly from 27.37 to 87.21 μg^{-1} and 32.77 to 85.38 μg^{-1} respectively between 1940 and 2010 AD (Fig. 4.10C). Concentrations of trace metals in this core followed the trend Cr>V>Zn>Cu>Pb>As>Mo>Hg>Cd. The T-test was not significant for any of the trace metals analyzed, implying there was no significant change in their concentrations before and after industrialization (Appendix B12).

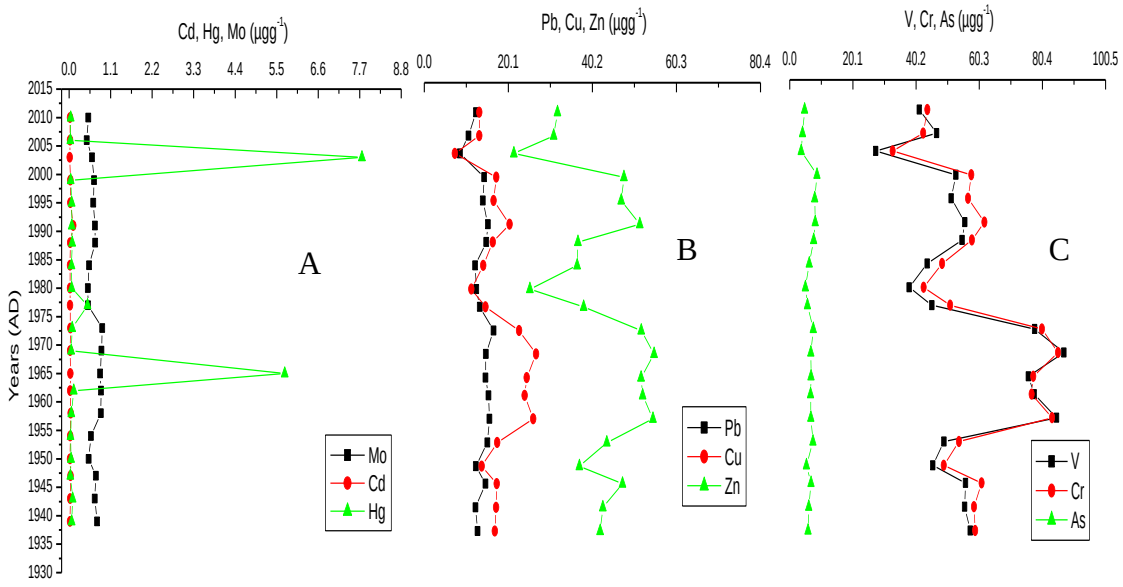

Figure 4.10. Temporal profiles of trace metal concentrations in the sediment core from Volta estuary: (a) Cd, Hg & Mo; (b) Pb, Cu & Zn; (c) Cr, V & As.

4.3.5 Temporal Variations in Estuarine Metal Enrichments Factors (EF)

4.3.5.1 Ankobra Estuary

Significant enrichment of Hg (5.2<EF≤8.4) and extremely high enrichments of As (69.3<EF≤114.3) were observed since 1800 AD while moderate enrichments were seen for Cr (3.9<EF≤4.5). All other elements were within background geochemical levels (EF<2) (Fig. 4.11).

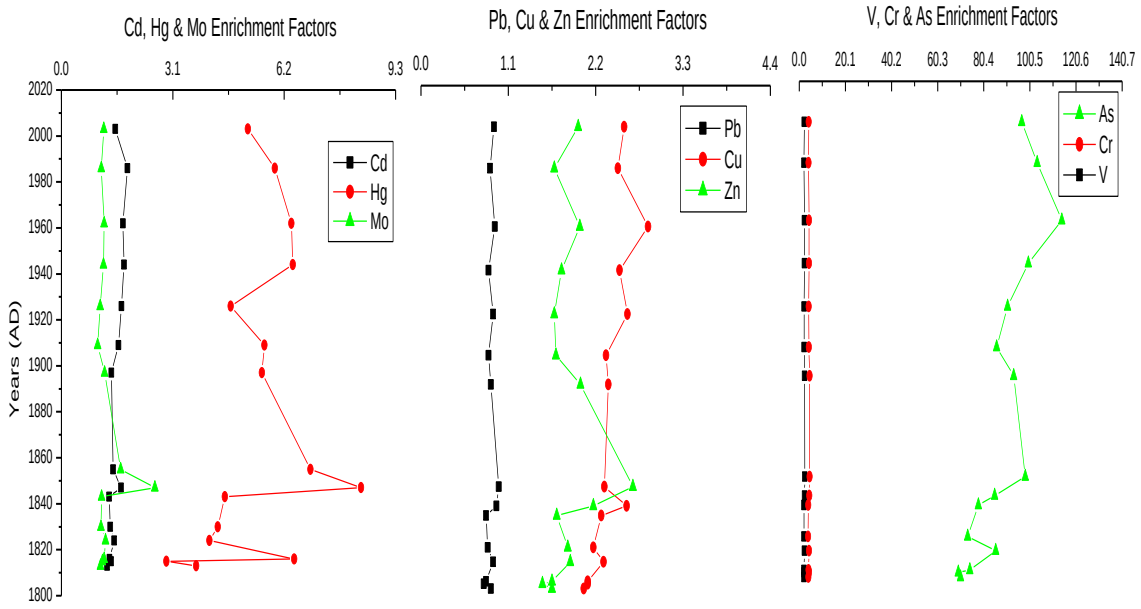

Figure 4.11. Temporal profiles of trace metal enrichment factors in the sediment core from the Ankobra estuary.

4.3.5.2 Pra Estuary

Similar to the core from Ankobra, significant enrichment of Hg (5.0<EF≤9.4) were observed between 1950 AD and 1995 AD while very high enrichment of As (20.0<EF≤30.0) were observed since 1890 AD to present. Again a moderate enrichment was observed for Cr (3.0<EF≤3.3) while all other trace metals were within background geochemical levels (EF<2) (Fig. 4.12).

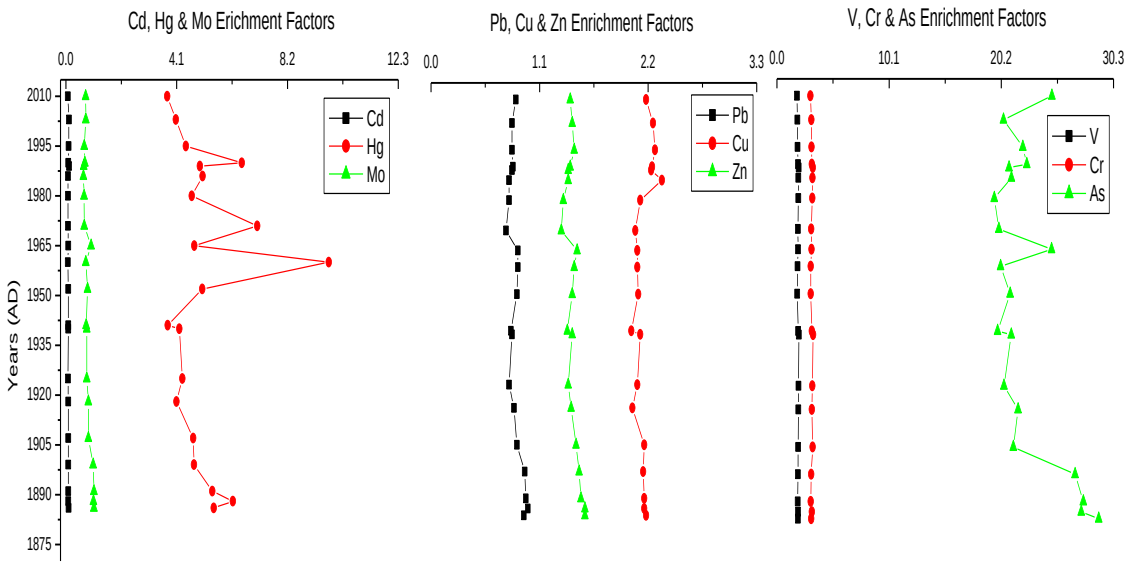

Figure 4.12. Temporal profiles of trace metal enrichment factors in the sediment core from the Pra estuary.

4.3.5.3 Amisa Estuary

Significant enrichment of Hg (EF=6.2) was only observed around 1940 AD while significant enrichment of As (5.0<EF≤7.0) was observed after 1960 AD. All other trace metals were within background geochemical levels (EF<2) (Fig. 4.13.)

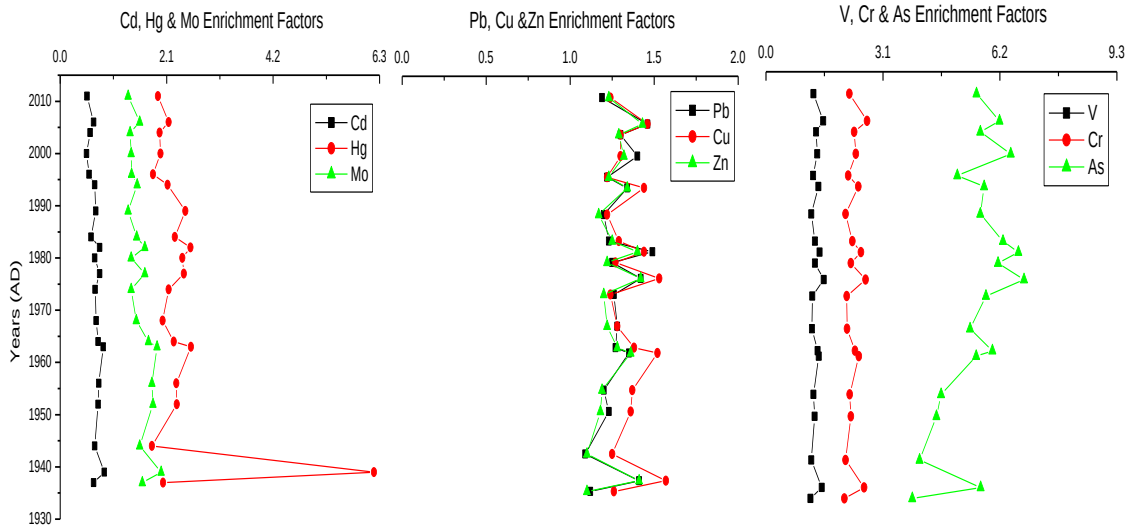

Figure 4.13. Temporal profiles of trace metal enrichment factors in the sediment core from the Amisa estuary.

4.3.5.4 Densu Estuary

Extremely high enrichment of Hg (EF=44.8) was observed around 1965 AD while As (5.0<EF≤6.5) seemed to be showing significant enrichment towards the last 10 years. All other elements until 2000 AD were within geochemical background levels (EF<2) and seemed to be showing potentials for significant enrichment after this date (Fig. 4.14).

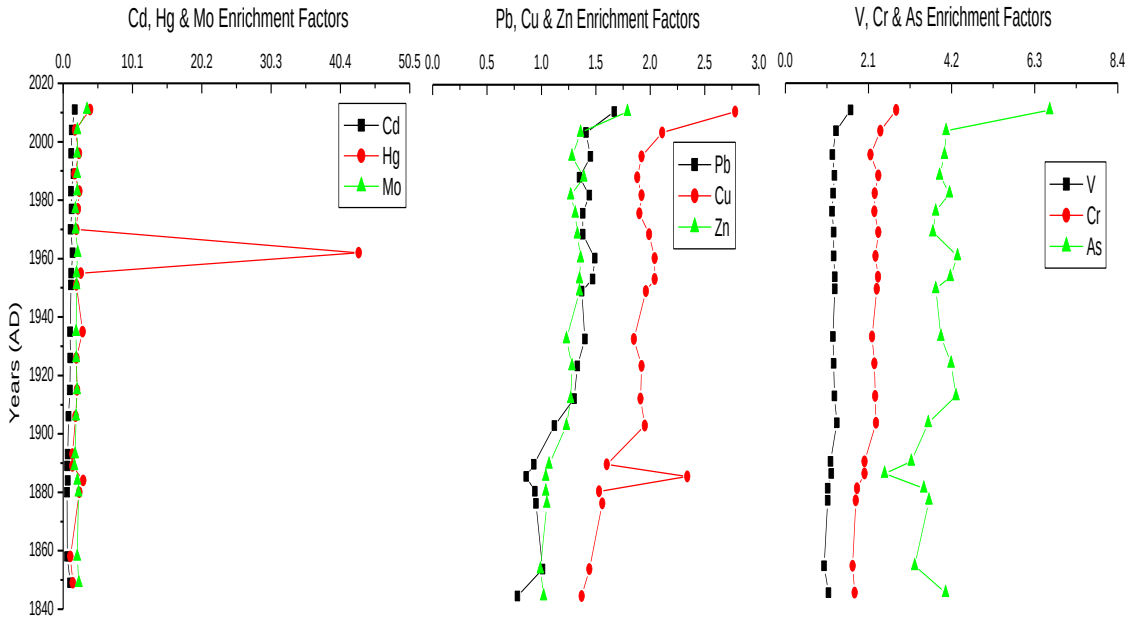

Figure 4.14. Temporal profiles of trace metal l enrichment factors in the sediment core from the Densu estuary.

4.3.5.5 Sakumo II Estuary

Significant enrichment of Hg (5.0<EF≤6.2) was observed from around 2005 AD to recent. An increasing enrichment towards the last 10 years was seen for most of the trace metals with Mo, Cu and As showing potentials of significant enrichment (Fig. 4.16).

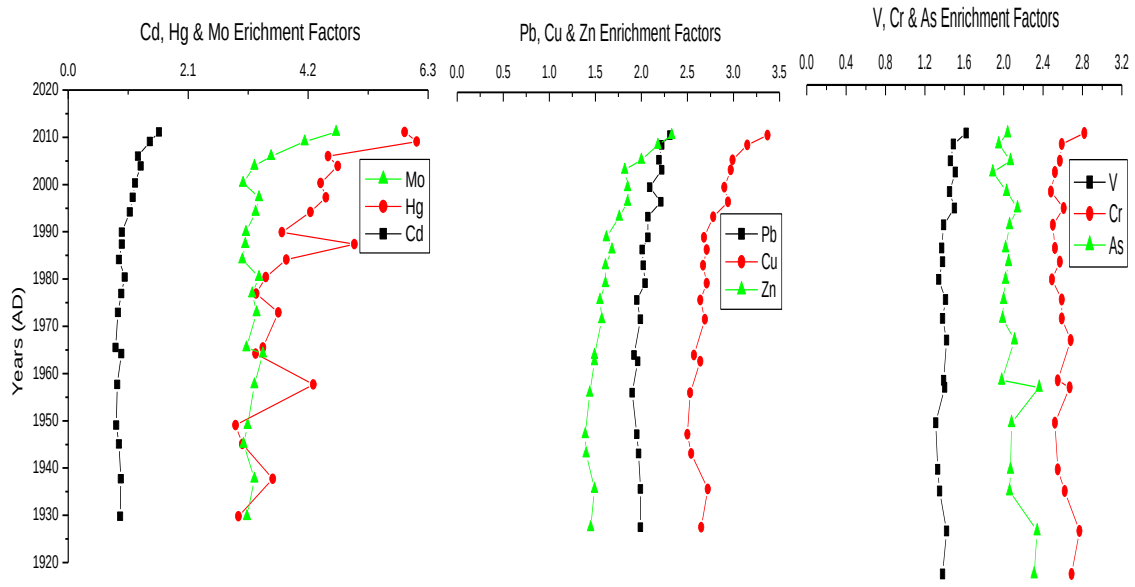

Figure 4.15. Temporal profiles of trace metal enrichment factors in the sediment core from the Sakumo II estuary.

4.3.5.6 Volta Estuary

Extremely high enrichment of Hg (EF =100.1 and 392.9) was observed at around 1964 AD and 2004 AD respectively while significant enrichment of As (EF=5.9 and 7.0) was observed at around 1965 AD and 1995 AD respectively. Apart from these sharp peaks for Hg and As, their levels in addition to all other trace metals were within background geochemical levels (EF<2) (Fig. 4.17).

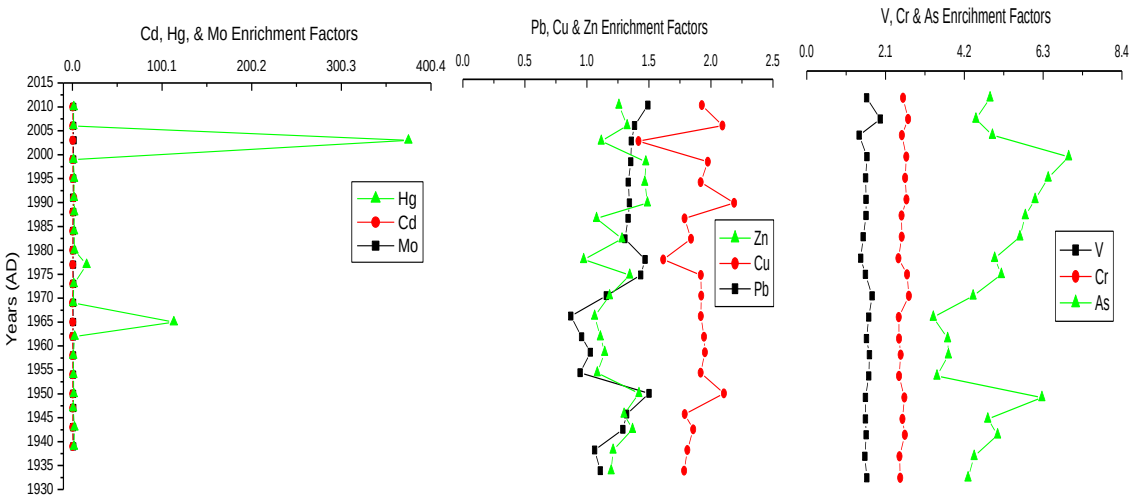

Figure 4.16. Temporal profiles of trace metal trace metal enrichment factors in the sediment core from the Volta estuary.

4.3.6 Historical Excess Flux of Trace Metal in Estuaries

Historical excess fluxes of metals whose enrichment factors were above two (2) were estimated and cores from all estuaries except the Volta showed an increasing profile in their excess fluxes of trace metals from oldest to the youngest sections (Fig. 4.18). For the sediment core from the Ankobra estuary, excess fluxes varied from 0.13 to 3.80 $\mu gcm^{-2}y^{-1}$ for Cu, 3.33 to 95.29 $\mu gcm^{-2}y^{-1}$ for As, 0.22 to 5.04 $\mu gcm^{-2}y^{-1}$ for V and 0.01 to 0.09 $\mu gcm^{-2}y^{-1}$ for Hg (Fig. 4.18A).

In the Pra estuary, excess fluxes varied from 2.39 to 55.12 $\mu gcm^{-2}y^{-1}$ for Cr, 1.65 to 35.42 $\mu gcm^{-2}y^{-1}$ for As and 0.01 to 0.20 $\mu gcm^{-2}y^{-1}$ for Hg (Fig. 4.18B), while in the Amisa estuary excess fluxes varied from 1.31 to 42.94 $\mu gcm^{-2}y^{-1}$ for Cr, 0.20 to 8.13 $\mu gcm^{-2}y^{-1}$ for As and 0.02 to 0.06 $\mu gcm^{-2}y^{-1}$ for Hg (Fig 4.18C).

In the Densu estuary, excess fluxes varied from 0.0 to 0.22 $\mu gcm^{-2}y^{-1}$ for Mo, 0.0 to 10.26 $\mu gcm^{-2}y^{-1}$ for Cr, 0.10 to 0.98 $\mu gcm^{-2}y^{-1}$ for As and 0.0 to 0.11 $\mu gcm^{-2}y^{-1}$ for Hg (Fig. 4.18D), while in the Sakumo II, excess fluxes varied from 0.03 to 1.32 $\mu gcm^{-2}y^{-1}$

for Mo, 0.24 to 8.33 µgcm^{-2}y^{-1} for Pb, 0.33 to 11.71 µgcm^{-2}y^{-1} for Cu, 0.36 to 24.73 µgcm^{-2}y^{-1} for Zn, 0.04 to 0.712 µgcm^{-2}y^{-1} for As and 0.002 to 0.11 µgcm^{-2}y^{-1} for Hg (Fig. 4.18E). Finally, in the Volta, excess fluxes varied between 0.44 µgcm^{-2}y^{-1} and 71.76 µgcm^{-2}y^{-1} for Cr and 0.11 µgcm^{-2}y^{-1} and 5.90 µgcm^{-2}y^{-1} for As (Fig. 4.18F).

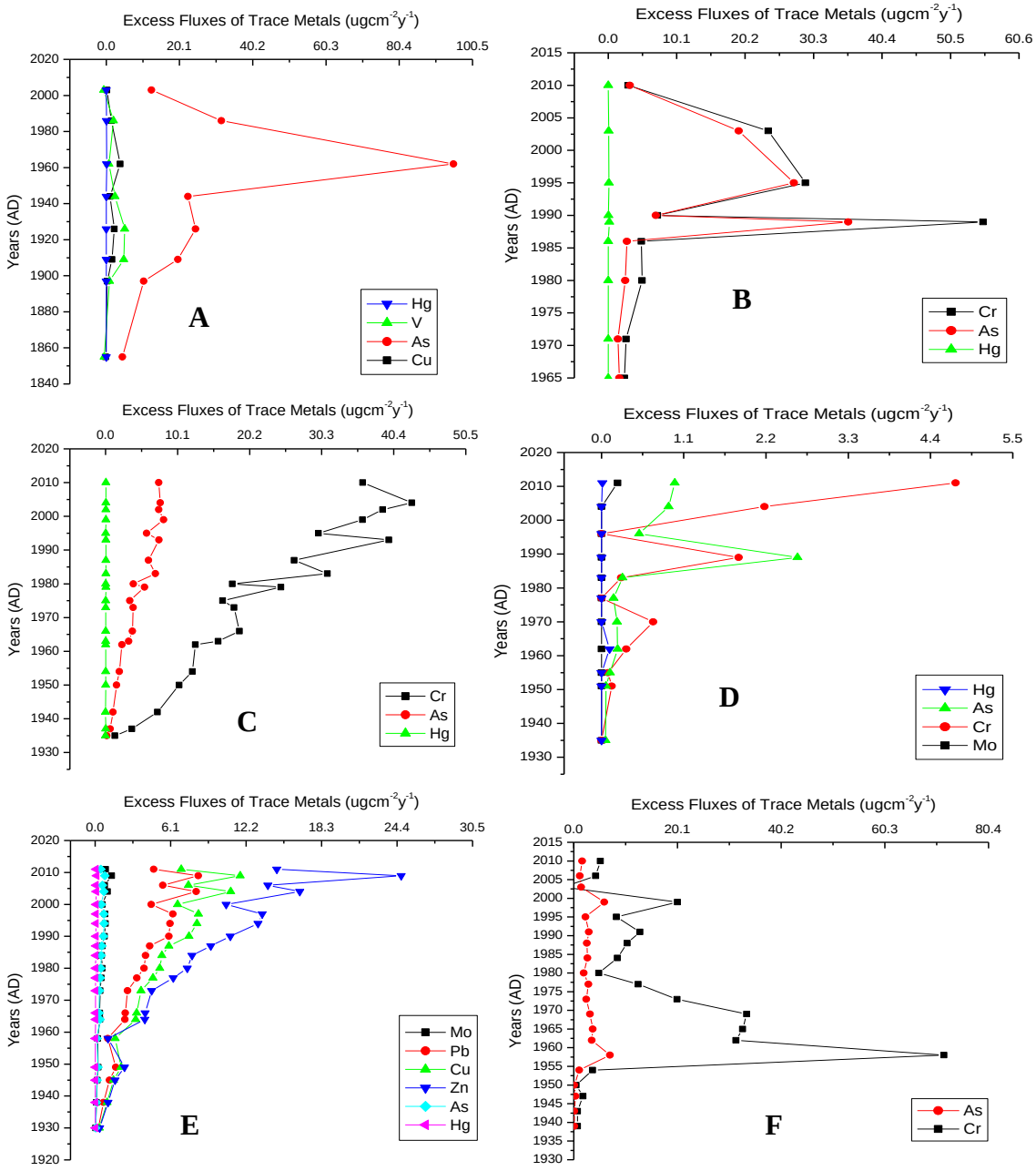

Figure 4.18. Historical anthropogenic accumulation fluxes of trace metals into the: (a) Ankobra; (b) Pra; (c) Amisa; (d) Densu; (e) Sakumo II and (f) Volta estuaries.

4.3.7 Correlations between Trace Metals, Aluminum (Al) and Organic carbon (OC)

4.3.7.1 Ankobra Estuary

Results of cluster analysis revealed that Al grouped together with V, Cr, Pb, Cd, Zn, Cu, As but not with Hg (Fig. 4.19). None of the trace metals grouped with OC. Spearman correlation confirmed strong positive correlations between Al and V (r=0.98; p=0.00; n=20), Cr (r=0.99; p=0.00; n=20), Pb (r=0.98; p=0.00; n=20), Zn (0.94; p=0.00; n=20), Cu (r=0.96; p=0.00; n=20), Mo (r=0.61; p=0.02; n=20), As (r=0.87; p=0.00; n=20), but not Hg (r=0.18; p=0.78; n=20) (Appendix B13).

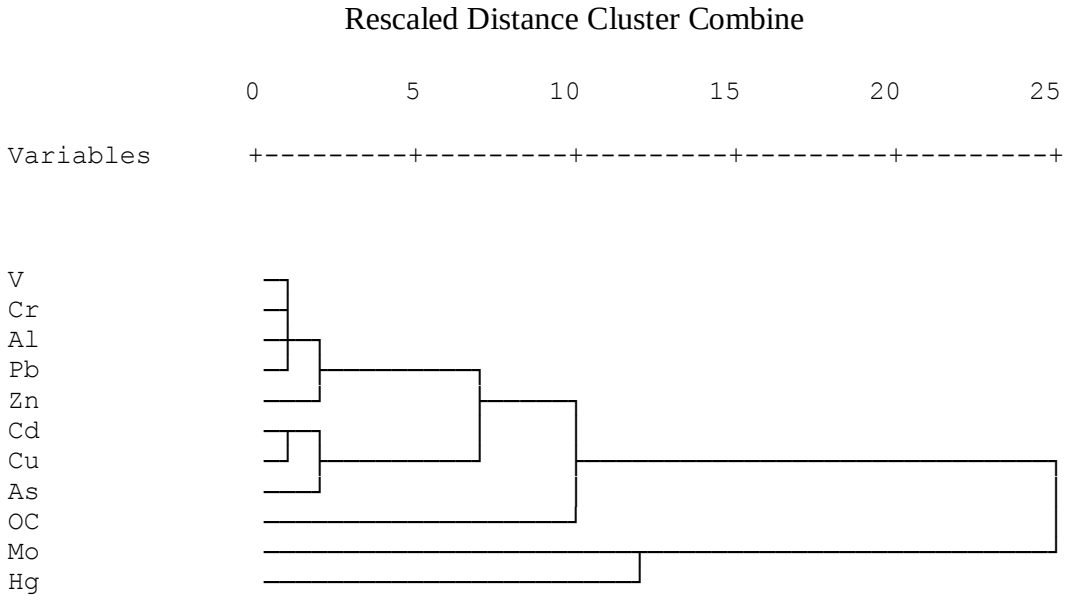

Figure 4.19. Cluster Analysis of Al, OC and trace metals in the sediment core from the Ankobra estuary.

4.3.7.2 Pra Estuary

Again, Al grouped together with V, Cr, Pb, Cd, Zn, Cu, As but not with Hg (Fig. 4.20). Similarly, none of the trace metals grouped with OC. Here again, spearman correlation confirmed strong positive correlations between Al and V (r=0.99; p=0.00; n=20), Cr (r=0.99; p=0.00; n=20), Cu (r=0.99; p=0.00; n=20), Pb (r=0.95; p=0.00; n=20), Zn

(r=0.98; p=0.00; n=20), Cd (r=0.89; p=0.00; n=20), As (r=0.84; p=0.00; n=20), Mo (r=0.81; p=0.00; n=20), but not Hg (r=0.55; p=0.06; n=20) (Appendix B14)

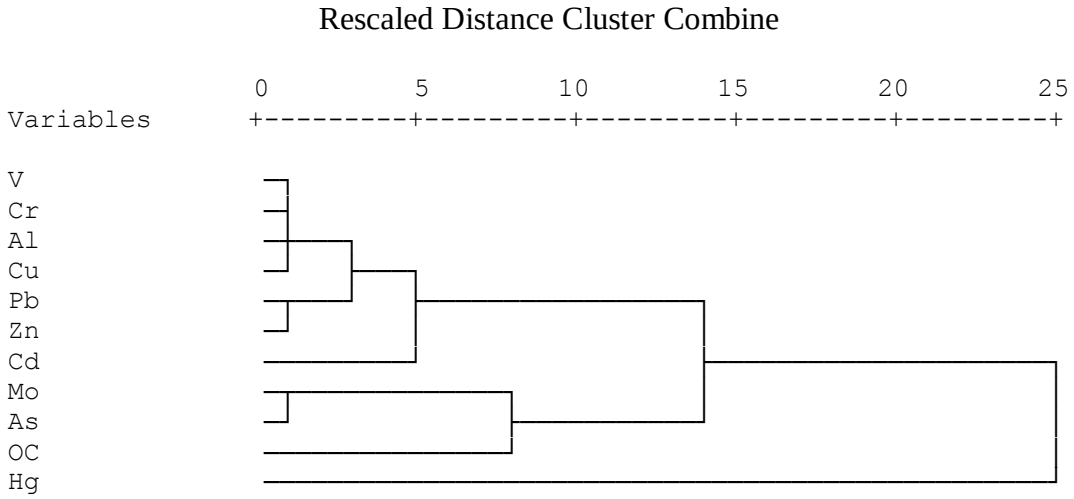

Figure 4.20. Cluster Analysis of Al, OC and trace metals in the sediment core from the Pra estuary.

4.3.7.3 Amisa Estuary

Unlike the Ankobra and Pra, Al grouped together with only V, Cr, Cu, Pb, Zn but not Hg, Cd, Mo, and As (Fig. 4.21). In this estuary, As grouped with OC. Spearman correlation confirmed positive correlations between Al and V (r=0.58; p=0.01; n=20), Cr (r=0.59; p=0.01; n=20), Cu (r=0.56; p=0.01; n=20), Pb (r=0.52; p=0.02; n=20), Zn (r=0.63; p=0.00; n=20) but not Mo (r=0.43; p=0.07; n=20), Cd (r=0.44; p=0.06; n=20), As (r=0.09; p=0.70; n=20) and Hg (r=-0.23; p=0.31; n=20) (Appendix B15).

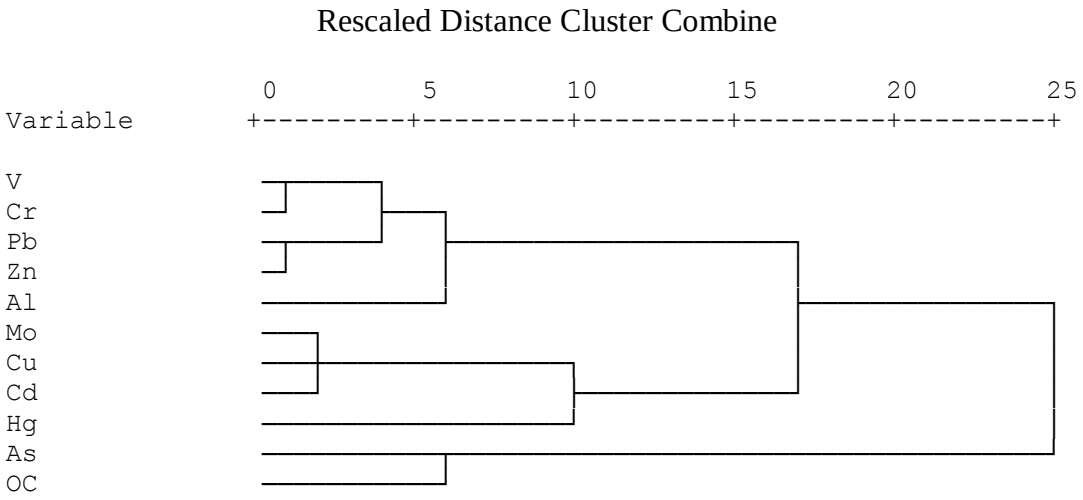

Figure 4.21. Cluster Analysis of Al, OC and trace metals in the sediment core from the Amisa estuary.

4.3.7.4 Densu Estuary

Aluminum (Al) grouped together with all trace metals except Hg (Fig. 4.22). Spearman correlation confirmed strong positive correlations between Al and Mo (r=0.89; p=0.00; n=20), Cd (r=0.91; p=0.00; n=20), Pb (r=0.95; p=0.00; n=20), V (r=0.99, p=0.00; n=20), Cr (r=0.98; p=0.00; n=20), Cu (r=0.98; p=0.00; n=20), Zn (r=0.99; p=0.00; n=20), As (r=0.92; p=0.00; n=20) but not Hg (r=0.12; p=0.42; n=20) (Appendix B16).

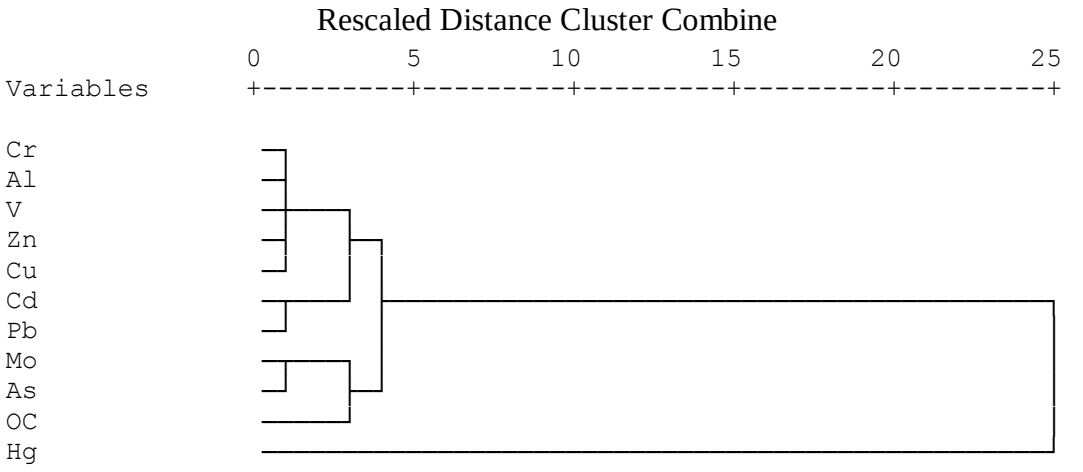

Figure 4.22. Cluster Analysis of Al, OC and trace metals in the sediment core from the Densu estuary.

4.3.7.5 Sakumo II Estuary

Interestingly, Al did not group together with any of the trace metals in this estuary. Groupings however existed between: Zn, Cd and Hg; Pb, Cu and V; OC, As and Cr (Fig. 4.23). Spearman correlation revealed none of the metals correlated with Al ($p>0.05$). Cadmium (Cd), Zn and Hg were highly correlated with each other ($p<0.05$), while Pb, Cu and V also correlated ($p<0.05$) with each other. Arsenic (As), OC and Cr also correlated strongly ($p<0.05$) with each other (Appendix B17).

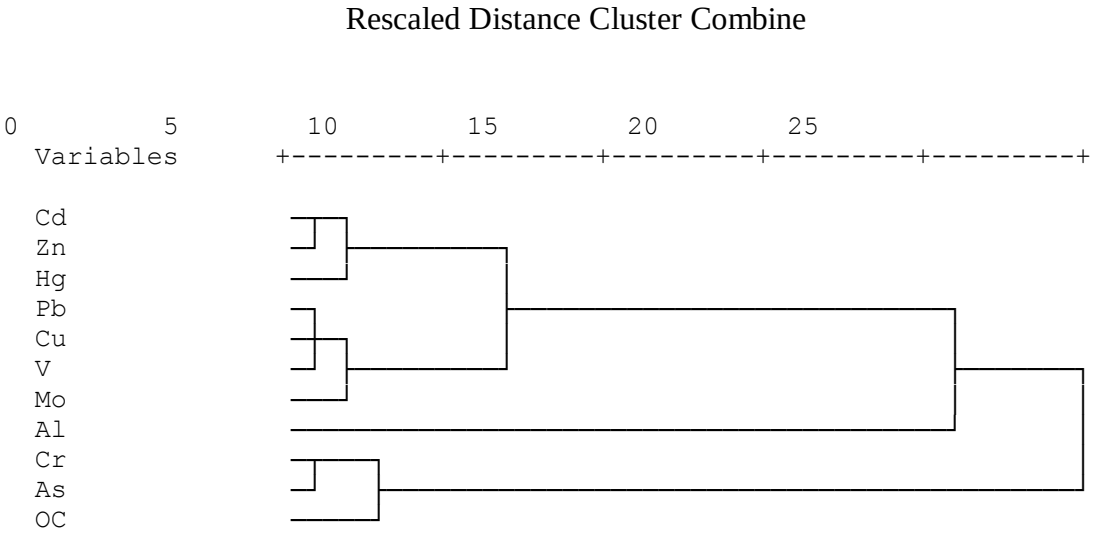

Figure 4.23. Cluster Analysis of Al, OC and trace metals in the sediment core from the Sakumo II estuary.

4.3.7.6 Volta Estuary

Clustering occurred between Al and Cr, V, Cu only (Fig. 4.24). Spearman correlation (Appendix B18) confirmed strong positive correlations existed between Al and Pb ($r=0.76$; $p=0.00$; $n=20$), Mo ($r=0.90$; $p=0.00$; $n=20$), V ($r=0.98$; $p=0.00$; $n=20$), Cr ($r=0.99$; $p=0.00$; $n=20$), Cu ($r=0.88$; $p=0.00$; $n=20$), As ($r=0.52$; $p=0.02$; $n=20$) but not Hg ($r=-0.13$; $p=0.56$; $n=20$) and Cd ($r=0.21$; $p=0.38$; $n=20$).

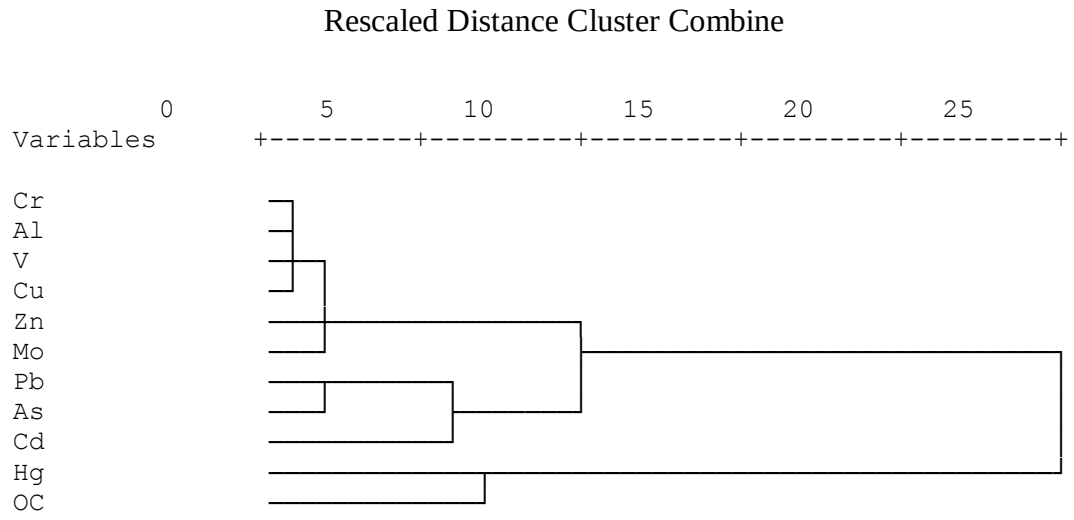

Figure 4.24. Cluster Analysis of Al, OC and trace metals in the sediment core from the Volta estuary

4.3.8 Trace Metal Accumulation Patterns in Estuarine, Nearshore and Deep-sea Sediment

Levels of trace metals analyzed in the estuarine sediments showed similar accumulation patterns in the nearshore and deep-sea environments (Fig. 4.25). For instance, where enrichments were observed in the estuarine sediments for As, similar levels were seen in the nearshore (B25m) environment (Fig. 4.25B)

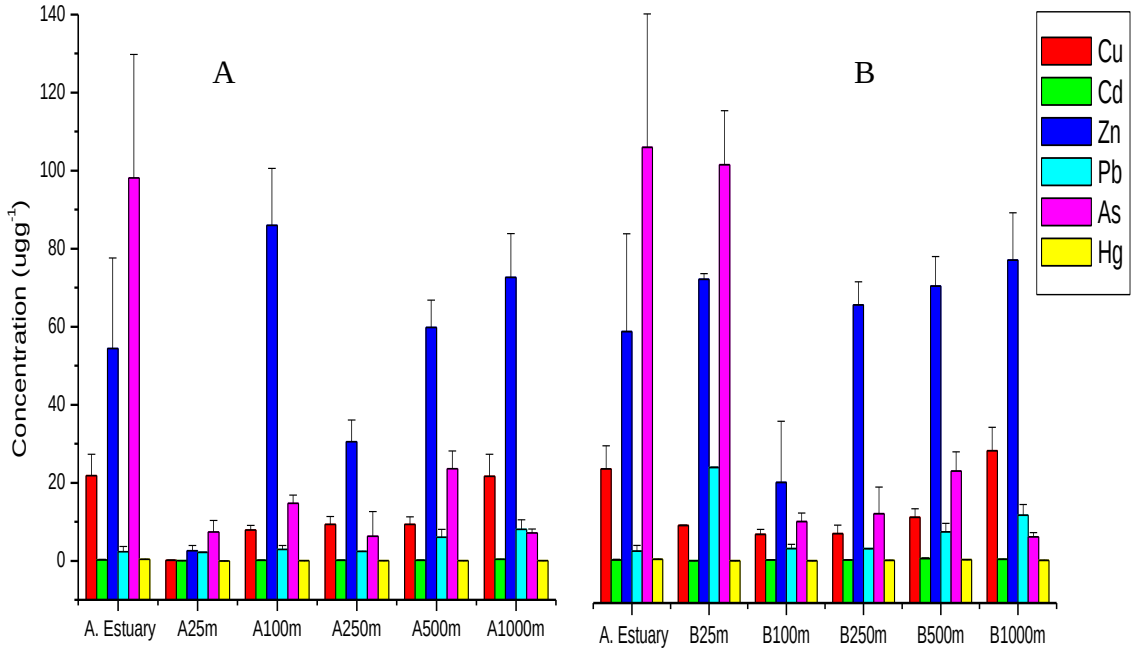

Figure 4.25. Metal Concentration across estuarine and shelf sediment: (a) Ankobra estuary and Continental Shelf Transect A; (b) Ankobra estuary and Continental Shelf Transect B.

4.4 Discussion

4.4.1 Radionuclide profiles, sedimentation rates and geochronologies

Apart from the core from the Pra estuary which showed slightly different average sedimentation rates for the CRS and CF-CSR models, the average sedimentation rates for the cores from all other five estuaries using the CRS model were in agreement with those established using the CIC-CSR model. The CRS model was further validated by comparing the annual ^{210}Pb input into the sediment using both the CRS and CIC-CSR models. Here also values were comparable for all cores using both models, except for those from Densu and Sakumo II which showed some slight variations in their annual input. These two validation approaches confirmed the validity of results obtained using the CRS model in dating the cores.

The low activities of ^{210}Pb recorded in this study could be attributed to the effect of different factors such as low atmospheric ^{210}Pb fluxes and low production of ^{210}Pb from decay of parent ^{226}Ra dissolved in shallow waters (Ruiz-Fernández and Hillaire-Marcel, 2009). The clear exponential decline in excess ^{210}Pb concentration in the Amisa, Densu and Sakumo II cores with depth suggests an almost constant sediment accumulation rate throughout the datable portions of the cores from these estuaries (O'Reilly *et al.*, 2011). This was seen in the almost constant sedimentation rates estimated from these estuaries with very small errors.

Although the cores from the Ankobra, Pra and Volta also exhibited exponential declines in their excess ^{210}Pb concentration, the huge errors associated with these declines suggested their actual sedimentation rate may have varied (Kim *et al.*, 2004). Factors like bioturbation, compaction and sudden environmental disturbances, such as strong storms or water currents in estuaries can produce such changes in sedimentation rates (Bricker-

Urso *et al.*, 1989). These irregular sedimentation rates of the Ankobra and Pra estuaries could further be attributed to artisanal gold mining (legal and illegal) activities in their watersheds. For instance, illegal mining popularly called 'galamsey' in Ghana has posed several environmental concerns in recent times (Amankwah, 2013). Beside contamination of the country's major waters resources with mercury and other associated trace metals (Hilson and Pardie, 2006), the act of 'galamsey' has introduced tons of sediment into the rivers draining into these estuaries through the washing of soil mixed with gold on sluice boxes (Amankwah, 2013). This could have varied the sediment delivery into these rivers and their estuaries leading to the observed sedimentation rates in this study.

All six cores were dated using the constant rate of supply (CRS) model (Appleby and Oldfield, 1978) because using this model to calculate trace metal fluxes is straightforward if the inventory of excess ^{210}Pb in the sedimentary column is comparable with that expected from atmospheric deposition (Cochran *et al.*, 1998). As no data are available for atmospheric fluxes of ^{210}Pb in the study areas, sediment inventory of excess ^{210}Pb were compared to those estimated for some locations in the Equatorial Atlantic which indicated a ^{210}Pb atmospheric flux of <0.5 dpm cm^{-2} year^{-1} (15°–55°S,) and 0.18 dpm cm^{-2} year^{-1} (13°05'N, 54°00'W) (Turekian *et al.*, 1977). Sediment inventory of ^{210}Pb from this study were quite higher than the atmospheric fluxes from these studies. This may be a result of various factors such as local precipitation, and the fact that the flux itself may have changed over time. Atmospheric flux of ^{210}Pb may vary from place to place depending on factors such as rainfall regime or the geographical location (Appleby, 1998).

The variabilities in this study may be strongly related to the amount and seasonality of precipitation, because wet deposition of ^{210}Pb (precipitation and scavenging) is more efficient than dry deposition, except at desert areas (Preiss *et al.*, 1996).

The estimated ages for all sections of the different cores showed an exponential increase with depth, probably due to compaction effect resulting from the progressive decrease of water content and organic content in all the cores (French *et al.*, 1994).

4.4.2 Accumulation Trends, Contamination Status and Sources of Trace Metal in Estuarine Sediment

Though the core from the Ankobra estuary did not show any distinct trend in temporal profiles of all trace metals analyzed, results revealed moderate enrichments of sediment with V, Cu and extreme contamination of the estuary with Hg and As. Calculated excess fluxes of As, Hg, Cu and V (using sedimentation rates) were greater than zero implying that these metals were derived through human activities or some other source that are human related (Bing *et al.*, 2011).

The extreme contamination of the Ankobra estuary with Hg and As could be due to intense mining activities, particularly those arising from artisanal gold mining in the upstream of the Ankobra River. Geochemical provenance assessment of the sediment revealed about 80% of the sediment in this estuary could have originated from Prestea, Awaso, Asankragua, Bogoso and Esiama which are important gold mining areas.

Gold mining has been identified as an important anthropogenic source of Hg emission into the environment (Villas Boas *et al.*, 2001). In the face of the documented dangers of gold mining with Hg, it continues to be utilized in artisanal gold mining throughout the

world, especially in South America, Africa, Asia and North America (Lacerda and Salomons, 1998). Being an important gold mining country dating back as far as the 19th century, artisanal gold mining with Hg in the country has intensified since the last 100 years regardless of the passing of Mercury law in 1933 to ban Ghanaians gold miners from using it (Tsikata, 1997; Akabzaa and Dramani, 2001). High levels of Hg (attributed to artisanal gold mining) in the range of 0.00625-0.0573µgg^{-1}, 0.00273-0.0498µgg^{-1}and 0.0130.0333µgg^{-1}have for instance been reported in sediments from the Lower Pra, Offin and Upper Pra Rivers respectively (Donkor *et al.*, 2006).

Though most environmental As problems are the result of mobilization under natural conditions, man has had an important additional impact through mining, combustion of fossil fuels, the use of arsenical pesticides, herbicides and crop desiccants and its use as an additive to livestock feed, particularly for poultry (Smedley and Kinniburg, 2002). Just as many countries in the world, Ghana's gold is associated with sulphide mineralization, particularly arsenopyrite (Smedley and Kinniburg, 2002). Arsenic (As) mobilizes in the local environment as a result of arsenopyrite oxidation, induced and exacerbated by intense mining activities in mining towns of Ghana (Smedley and Kinniburg, 2002). Studies have confirmed high concentrations of As in soils and rivers close to some key mining towns of Ghana (Bowell, 1992; 1993).

In addition to As and Hg, gold mining has also been regarded as a significant source of Pb and other heavy metal contamination of the environment owing to activities such as mineral exploitation, ore transportation, smelting and refining, disposal of the tailings and waste waters around mines (Essuman *et al.*, 2007). These perhaps could have resulted in the moderate enrichment of the Ankobra estuary with Cr, V and Cu.

Similar to the core from the Ankobra estuary, the core from the Pra estuary showed no trend in temporal profiles of all trace metals analyzed though the concentrations of all trace metals seemed to have decreased after 1960 or post- industrialization. Results revealed moderate enrichment with Cr and extreme contamination of the estuary with Hg and As. Using the sedimentation rates, the excess fluxes estimated for Cr, Hg and As were greater than zero implying they were not naturally derived. Provenance analysis of the sediment from the Pra estuary revealed most of it originated from the Obuasi, Dunkwa, Bogoso, Fosu, Twifo Praso, and Tarkwa which are all known areas of intense gold mining. The contamination of the Pra estuary with Hg and As could therefore be due to gold mining activities as previously discussed.

An increasing trend in temporal profiles of trace metal concentrations was seen in both Densu and Sakumo II estuaries for all trace metals analyzed. However no enrichment was seen in the sediment concentrations of Cd, Pb, V, and Zn for Densu. Moderate enrichment of the Densu sediment with Cr and Mo was seen with signs of extreme enrichment of the sediment with As since the last 20 years. Excess fluxes of Cr, Mo and As were greater than zero implying these metals are not naturally derived, with provenance analysis of the sediment revealing they were mostly derived from the immediate townships surrounding the estuary. The Densu estuary is located in the heavily urbanized part of Accra where tons of waste discharged by residence into the estuary could have led to the anoxic state of the sediment (characterized by the smell of H_2S during sampling). This reduced state of the sediment could have resulted in the enrichment of the sediment from the Densu estuary with Mo and As.

Arsenic (As), Mo, V, Cr, U and Re are oxyanion-forming elements whose mobilizations are dependent on the pH and redox state of the aquatic environment (Rajeeva *et al.*, 2012; Kinniburg and Smedley, 2002; Azcue and Nriagu, 1995). Relative to the other oxyanion-forming elements, As and Mo are among the most redox controlled in the environment because of their ability to be highly mobile under reduced conditions (Kinniburg and Smedley, 2002).

The solubility of the redox sensitive elements (Mo, Mn) for instance varies as a function of redox potential and are strongly coupled (Elbaz-Poulichet *et al.*, 2005). Above the redox transition zone, Mn precipitates as MnOx incorporating MoO_4^{2-}. When reduced MnOx releases Mn^{2+} and MoO_4^{2-} leading to an increased concentration in the overlying waters with MoO_4^{2-} diffusing into sediment layers and getting transformed into MoS_4^{-} (Erickson and Helz, 2000). Molybdenum (Mo) then forms Mo–Fe–S clusters of cuboid on pyrite followed by the reduction of Mo (VI) to stabilize this structure (Vorlicek *et al.*, 2004). For these reasons, Mo is generally enriched relative to crustal values in anoxic sediment.

The core from the Sakumo II showed no enrichment in sediment concentrations of Cd and V, although moderate enrichments were seen for Pb, Cu, Cr, Mo, As and Zn with significant enrichment of the estuary's sediment with Hg since the last 35 years. Estimated excess fluxes of all metals, except for V were greater than zero implying these metals were enriched in the estuary as result of anthropogenic activities. Provenance analysis of the sediment revealed they were likely to have originated from the Tema, Sakumono, Afienya, and Lashibi townships which are homes to about 80% of Ghana's industries. The geochemical enrichment of the sediment with these metals could

therefore be attributed mostly to industrial discharges, although a change in the redox state of the estuarine sediment characterized by strong H_2S smell during sampling could have played a role in the high levels of both Mo and As reported. As explained previously, As and Mo are among the most redox controlled in the environment because of their ability to be highly mobile under reduced conditions. Similarly, the areas surrounding this estuary just as the Densu experience very high vehicular traffic which could have resulted in the enrichment of their sediments with the trace metals.

Just as the Ankobra and Pra, the core from the Volta did not show any distinct trend in the temporal profiles of all trace metals analyzed. No metal enrichments were seen in the sediment concentrations of Mo, Cu Cd, Pb, V, and Zn. Moderate enrichments were however seen for Cr while As appeared to be extremely enriched at a few sections of the core. Estimated excess fluxes of Cr and As showed they were added to the estuary as a result of anthropogenic activities. Provenance analysis of the sediment revealed they might have originated from the Akosombo, Akuse, Kpong, Osudoku, Fute, lolonya, Akplabanya, Anyanui, Kpando, Kpeme and Big Ada townships which are among the less industrialized and urbanized part of the country. This obviously may be the reason why the levels of Mo, Cu Cd, Pb, V, and Zn were still within geochemical backgrounds. Though results showed that Cr maybe anthropogenically derived, a strong correlation of the metal with Al also suggest some natural addition to the estuarine the sediment.

The presence and peaking of Hg in unacceptably high concentrations is some sections of the Densu, Amisa and Volta cores could be attributed solely to episodic dumping or natural release into the atmosphere.

Interestingly and contrary to all the other cores that have been discussed above, trace metal concentrations of the core from the Amisa estuary appeared not to have changed over time. No enrichments in sediment concentrations of Mo, Cd, Pb, Cu, Zn and V were seen in the core although moderate enrichment was seen for Cr while As seemed to be significantly enriched. Provenance analysis of the sediment showed they may have been derived from the Asebu, Abakrampa, Enyan and Denkyira townships which also are relatively not industrialized.

Similar trace metal accumulation patterns observed in the Ankobra estuary reflected in the sediments from the nearshore and deep-sea areas of the Ghana Coast possibly due to the export of trace metals from the estuarine environments into the continental shelf by the action of currents (Libes, 2009).

CHAPTER FIVE

ECOTOXICOLOGICAL RISK ASSESSMENT OF TRACE METALS IN SEDIMENTS FROM THE ANKOBRA, SAKUMO II AND VOLTA ESTUARIES

5.1 Introduction

Effective environmental management practices for pollutants are dependent on a clear understanding of the fate of the pollutants in the environment as well as their ecotoxicological risks (Lei *et al.,* 2008). To restrict the use of a particular chemical and protect the environment, traditional risk assessment methods compared predicted no effect concentrations (PNEC) to predicted or observed environmental concentrations (PEC) to generate a hazard quotient (HQ) (Naito *et al.,* 2002).

This hazard quotient or point estimate method is only useful to counter the presumption of a potential for adverse effects which belongs in the early stages or tiers of a risk assessment (Lei *et al.,* 2008). The approach can be termed protective to some extent in the use of conservative assumptions and parameter estimates to assure that no situations where adverse effect would be expected to occur would wrongly be declared safe (Van Straalen and Denneman, 1989). The HQ approach however, cannot under any circumstance be used to establish a level of risk as the quotient is based on point estimates from a concentration-response vector (Aldenberg and Slob, 1993). Futhermore, the term 'risk' implies an element of likelihood, and likelihood is reported as probabilities, which cannot be established from point estimates.

Based on the aforementioned lapses that could present shortfalls in the decision making and management process, probabilistic risk assessment (PRA) also known as the tiered approach is becoming the most important and recommended method for assessing ecotoxicological risks of contaminants (SETAC, 1994: ECOFRAM, 1999). PRA allows the risk assessor to include estimates of uncertainty as well as stochastic properties of both exposures and responses in the risk assessment process to generate more reliable results for management purposes (Solomon *et al.,* 1996). The use of PRA recognizes that

there are no absolutes in risk assessment (i.e. there are never any situations where there is no risk of effect and there are few situations where there is complete certainty that a given level of effect will occur), instead, there is a continuum of potential exposure and effect situations and a range of certainty can be reported (Solomon and Jones, 2000). This allows the risk manager to make the decisions as to the degree of overlap between the exposure and effects function that is acceptable and the level of certainty required in a particular situation (Solomon and Jones, 2000). The risk manager can also derive criteria for the protection of a percentage of individuals of potential species for a particular contaminant of potential hazard.

5.1.1 Justification

The accumulation trends of metals in sediments of Ghanaian estuaries have not been widely studied. A study was therefore undertaken to understand the accumulation rates and temporal changes of metal concentrations in the Ankobra, Pra, Amisa, Densu, Sakumo II and Volta estuaries. Major findings of the study (reported previously) revealed increasing enrichment of some metals in the sediment of the Ankobra, Pra, and Sakumo II during the last 150 years while the Amisa, and Volta estuaries did not show any signs of anthropogenic metal enrichments. The Ankobra and Pra were enriched with metals known to be associated with mining operations, while the Sakumo II was enriched with metals arising solely from the discharge of industrial effluents.

In the aquatic environment however, sediment are in intimate contact with the water column phase and stay in quasi-equilibrium between the sediment and water column. Thus depending on the hydrodynamics of the system and the kinetics of the metals, metals bound to the sediment phase could be released back into the water column and vice versa where they are made available to fauna and flora. This is particularly true for

estuaries which by nature are controlled by complex hydrodynamics and whose sediment is often in suspension due to mixing (Ridgway and Shimmield, 2002). This means that high sediment metal concentrations of estuaries as reported in this study have higher likelihoods of posing risks not only to the benthic fauna but also to those in the water column.

By envisaging the risks these increasing sediment metal concentrations are likely to pose to both sediment and water column organisms, the study spatially assessed the levels of sediment metals in the Ankobra (enriched with metals associated with gold mining), Sakumo II (highly urbanized and industrialized) and Volta (control site) estuaries based on the findings of temporal assessments and metal accumulation rates. The results of this study have been used to deepen our understanding of the potential ecotoxicological risks that the elevated metal levels may pose to the ecology of these estuaries and nearby ecosystems. The study also seeks to develop acceptable criterion of metal levels in estuaries in which the current concentrations of trace metal are likely to pose potential risks.

5.1.2 Aim and Objectives

This study used the three tiered approach of AQUARISK to assess the ecological risks of As, Cd, Cu, Hg, Pb and Zn levels in the Ankobra, Sakumo II and Volta estuaries. Specifically:

I. This study presents an initial hazard screening of each metal by comparing measured concentrations to sediment quality guidelines using probability distributions.

II. Probability density functions were used to derive site specific acceptability criteria for species protection in estuaries where potential concerns for metals have been established

III. Risk maps were generated for metals of potential concern in estuaries where they pose risks.

5.2 Materials and Methods

5.2.1 Field Sampling Protocols

Surficial sediment samples were taken from the Ankobra (n=32), Sakumo II (n=24) and Volta (n=31) estuaries using an Ekman grab in August and September 2013. Maps of sampling sites at the Ankobra, Sakumo II and Volta estuaries are shown below (Fig. 5.1, 5.2 & 5.3). Samples were kept frozen at -4^{o}C soon after they were brought to the laboratory.

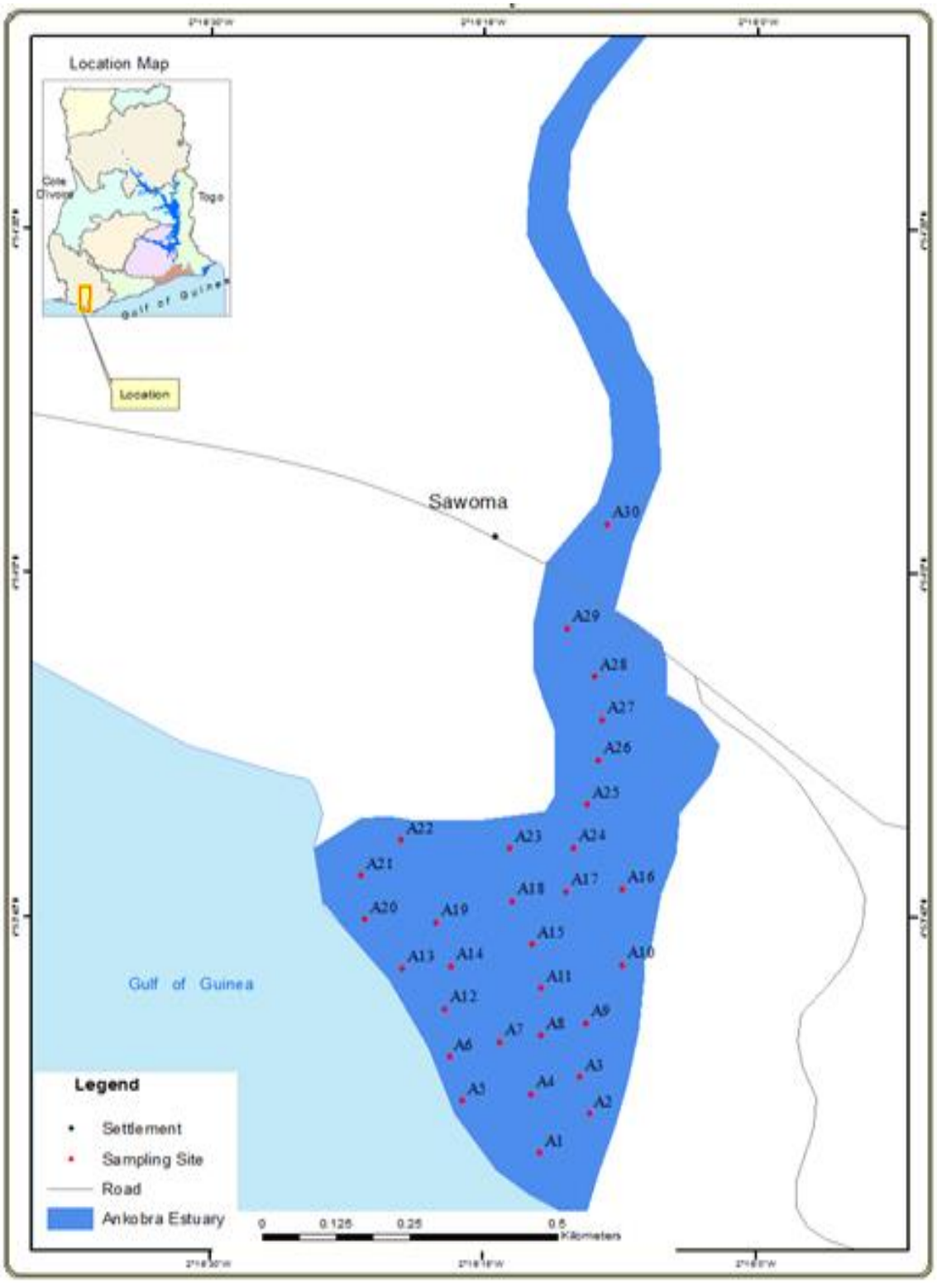

Figure 5.1. Map showing sampling locations in the Ankobra estuary

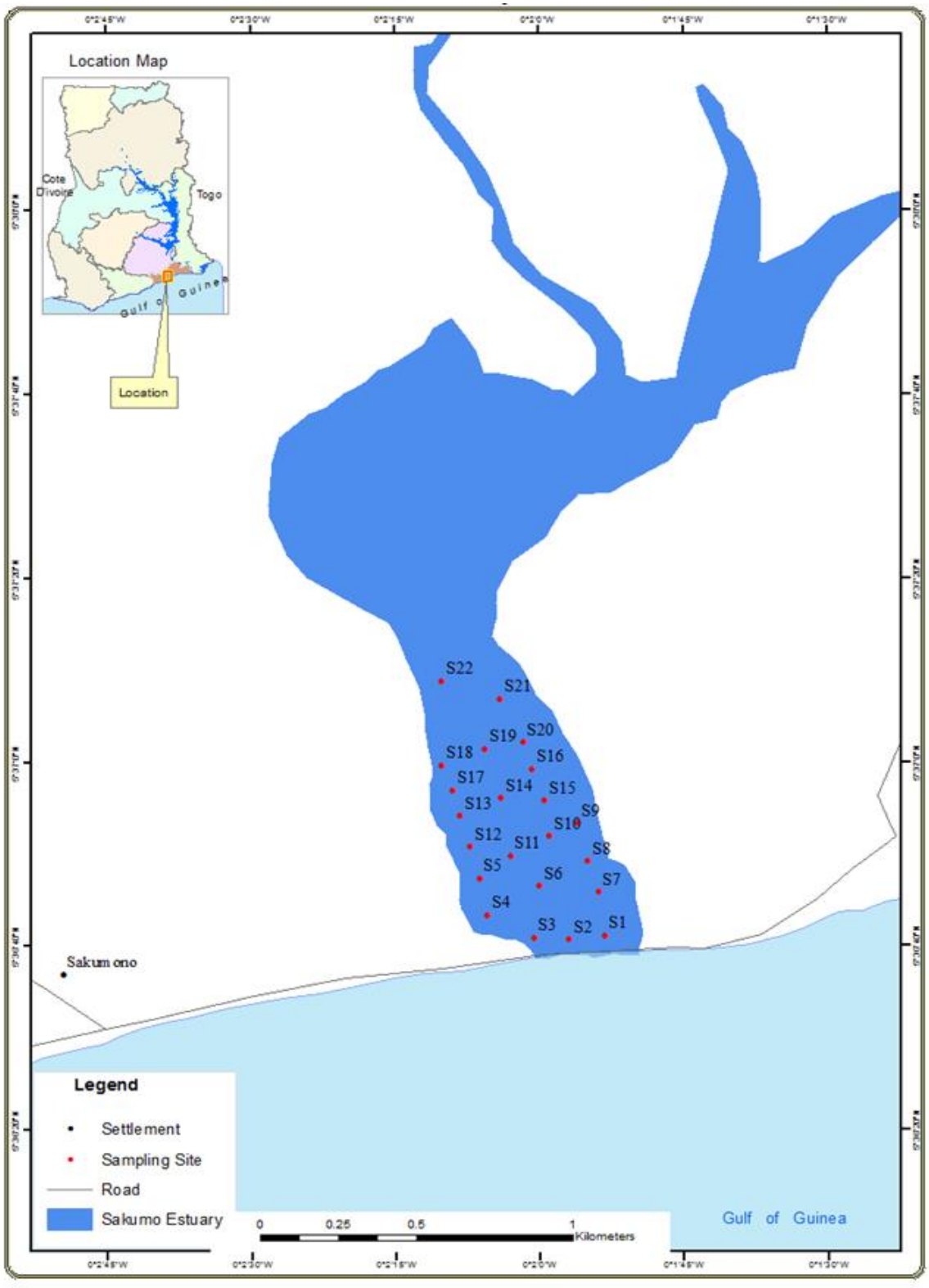

Figure 5.2. Map showing sampling locations in the Sakumo II estuary

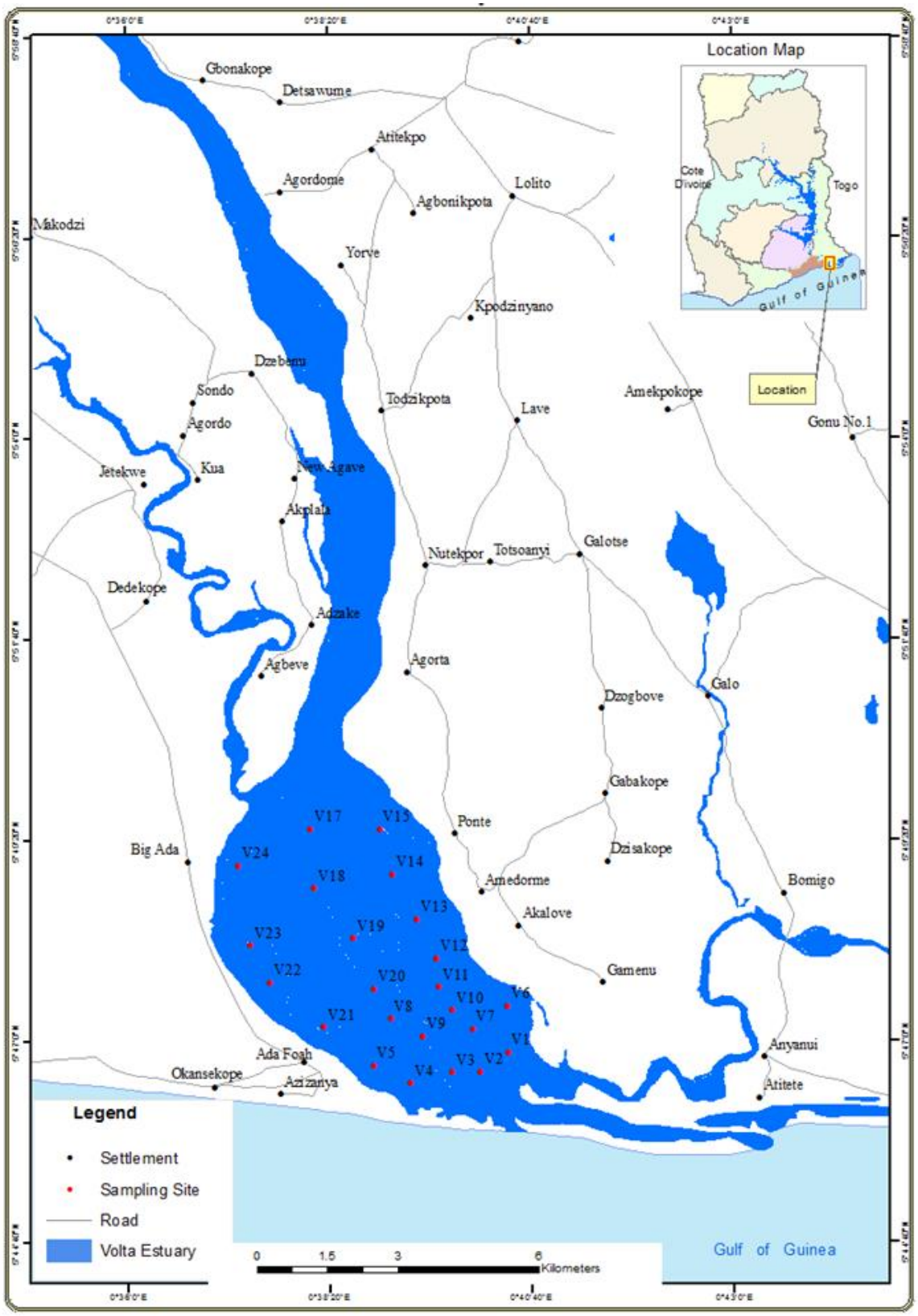

Figure 5.3. Map showing sampling locations in the Volta estuary

5.2.2 Sample Preparation and Analysis

Sediments were dried to constant weight at 60^{o}C, sieved and the fraction below 63µm retained for analysis. Sediments including the estuarine sediment standard reference material (SRM) 1646a and blanks were digested following the digestion protocol for soil samples for the Milestone Acid Digestion Microwave ETHOS 900. About 1.5g of sediment was weighed into acid washed 100ml polytetraflouroethylene (PTFE) Teflon bombs. Six (6)mL of concentrated nitric acid (HNO_3, 65%), 3ml of concentrated hydrochloric acid (HCL,35%) and 0.25mL of hydrogen peroxide (H_2O_2, 30%) was added to each sample in a fume chamber. Samples were microwave digested for 26 minutes using milestone microwave labstation ETHOS 900, INSTR: MLS-1200. The digestate was made up to 20mL with double distilled water and analyzed for the presence of total As, Cd, Cu, Hg, Zn, and Pb using the VARIAN AA 240FS- Atomic Absorption Spectrometer in an acetylene- air flame at the Ghana Atomic Energy Commission (GAEC). Blanks, Duplicates, SRM, and standards were analyzed as quality controls.

5.2.3 Marine and Freshwater Spiked Sediment Toxicity Test Data

A literature review of data on marine and freshwater spiked sediment toxicity test data (dose derived data) for risk analysis from the Australian and New Zealand Environment Conservation Council (ANZECC) and the Agriculture and Resources Management Council of Australia and New Zealand (ARMCANZ) database were used for tier 2 and 3 risk analysis (Appendices C1-C5). Data on spiked sediment toxicity test on marine, estuarine and freshwater organisms do not exist for Ghana and most African countries hence the choice of secondary data for this study. The study however chose tests that

utilized broad taxonomic genera such as invertebrates, diatoms, bivalves, *tilapia sp* which have been reported in our estuaries.

The study also took into consideration the temperature at which organisms were affected for the different endpoints chosen for each test so as to ensure that vast differences in temperature do not exist for test organisms and temperatures recorded for the estuaries in this study. Where test organisms for a particular element have not been reported in any of our estuaries, the element was not used in the subsequent tiers of the risk analysis.

5.2.4 Probabilistic Ecotoxicological Risk Assessment

Probabilistic ecotoxicological risk assessment was carried out following the procedure of Twinning *et al.* (2008). Metal concentrations in sediment were first screened by comparing with NOAA's sediment quality guidelines (SQG) in a tier 1 risk analysis using AQUARISK for contaminants of potential concern (COPC). This was followed by detailed probabilistic analysis on each metal of potential concern by fitting cumulative probability density functions using log-normal and Burr Type III distributions to both the concentration and effect data or dose derived data (DRD).

A test for normality of log-transformed data was used to assess the validity of the log-normal assumption while a test for normality of deviations from the fitted distributions was used to test for the normality of the deviations of the discrete cumulative distribution functions formed by the data points from the hypothesized log-normal or Burr Type III distribution curve in AQUARISK. Once the distribution parameters and their uncertainties were assessed, critical values were derived from the log-normal or Burr Type III distributions for comparison with the SQG.

The critical values were the median hazardous concentration (HC) affecting 5%, 25% and 50% of species and the 95% lower confidence limit ($HC_{n;\ 95}$). AQUARISK further estimated the degree (probability) to which the contaminant data are likely to exceed the $HC_{5;95}$, $HC_{25;95}$ and $HC_{5;95}$ criteria, the average percent (%) of species that are likely be adversely affected by the COPC (i.e. risk to aquatic species), the percent reduction in concentration required to achieve a tolerable level of chemical concentration of the $HC_{5;95;}$ $HC_{25;95}$ and $HC_{50;95}$, and finally the target concentration required to achieve the set criteria.

5.2.5 Risk Mapping

The results of trace metal analyses for the Ankobra and Sakumo II estuaries were used to generate risk maps of metals of potential concern using MATLAB. Since the concentration data were irregularly spaced, Kriging was used to produce interpolated metal concentrations at nodal points on a fine grid covering each estuary. Parameters for describing risk-concentration distributions from the AQUARISK modeling and the measured metal concentrations were used to calculate a risk estimate (% species likely to be adversely affected) for each metal using the cumulative distribution function of the Burr Type III distribution (Twinning *et al.*, 2008):

$$Y_i = 1/\left[1+\left(b/X_i\right)^c\right]^k \qquad 5\text{-}1$$

Where Y_i is the estimated proportion of species likely to be adversely affected by the metal (X); X_i is the interpolated metal concentration at any individual node; and b, c, and k are the parameters (annex, C.) of the Burr Type III distribution for each metal derived using AQUARISK.

5.3 Results

5.3.1 Screening for Contaminants of Potential Concern

5.3.1.1 Ankobra Estuary

Results showed that Cu, Cd, Zn and Pb were not of potential concern because their values were lower than the sediment quality guideline (SQG) (Fig 5.4), hence were "screened out" of the analysis while Hg and As were "screened in" for further tier analysis since their levels were beyond the SQG. These results are in agreement with geochemical analysis which classified As and Hg as extremely enriched beyond natural background levels (See Fig. 4.11). Results of trace metal concentrations are shown in Appendix C7.

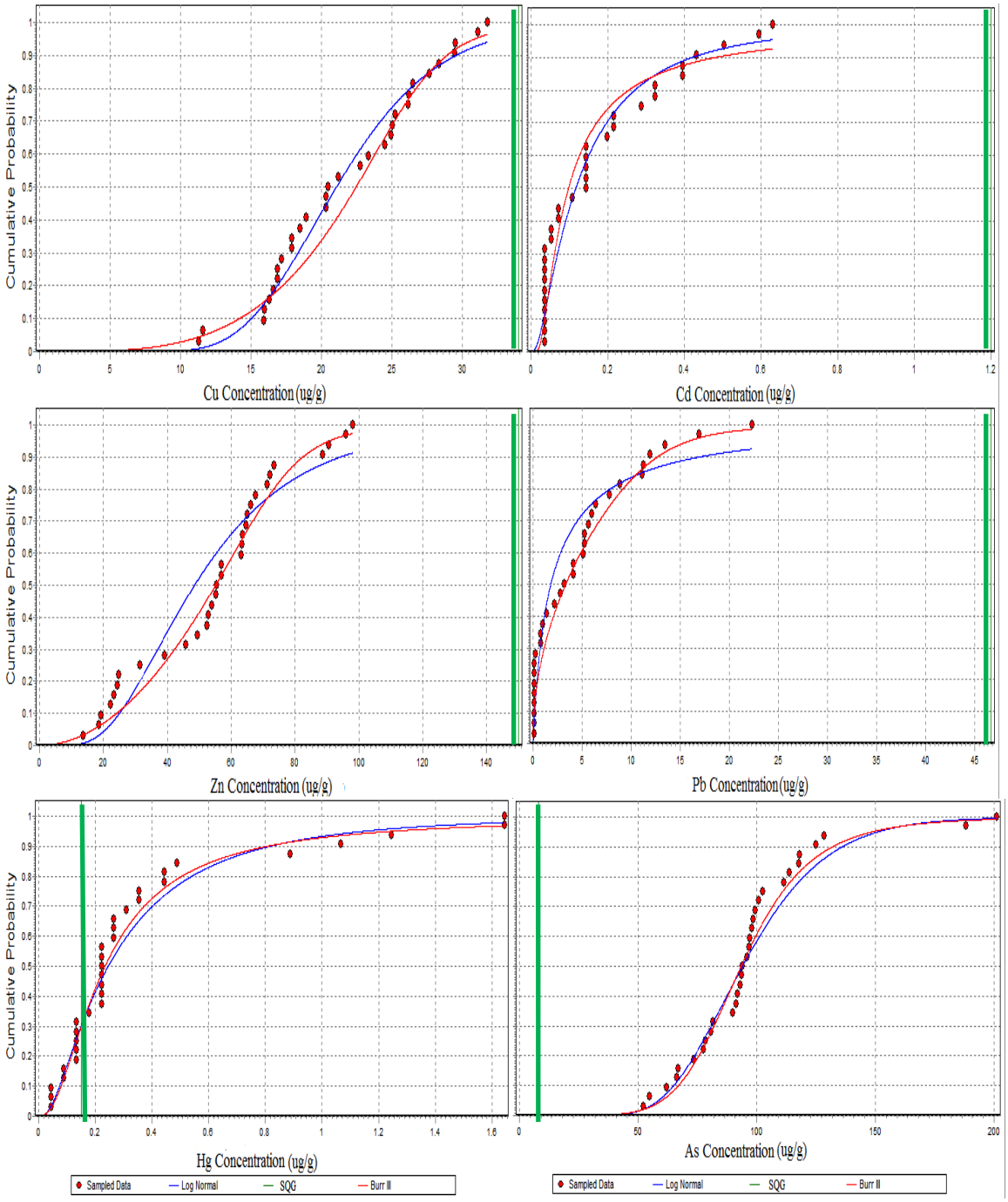

Figure 5.4. Probabilistic Hazard Screening of Metals in the Ankobra estuary using AQUARISK.

5.3.1.2 Sakumo II Estuary

For this estuary, Cu, Cd, Pb and Hg were all beyond the SQG hence "screened in" for higher tier analysis, while Zn and As were not of potential concern hence "screened out" of the analysis (Fig 5.5). Again these results are in agreement with those of the geochemical analysis which classified these metals as moderately enriched beyond background levels (See Fig. 4.15). Results of trace metal concentrations are shown in appendix C8.

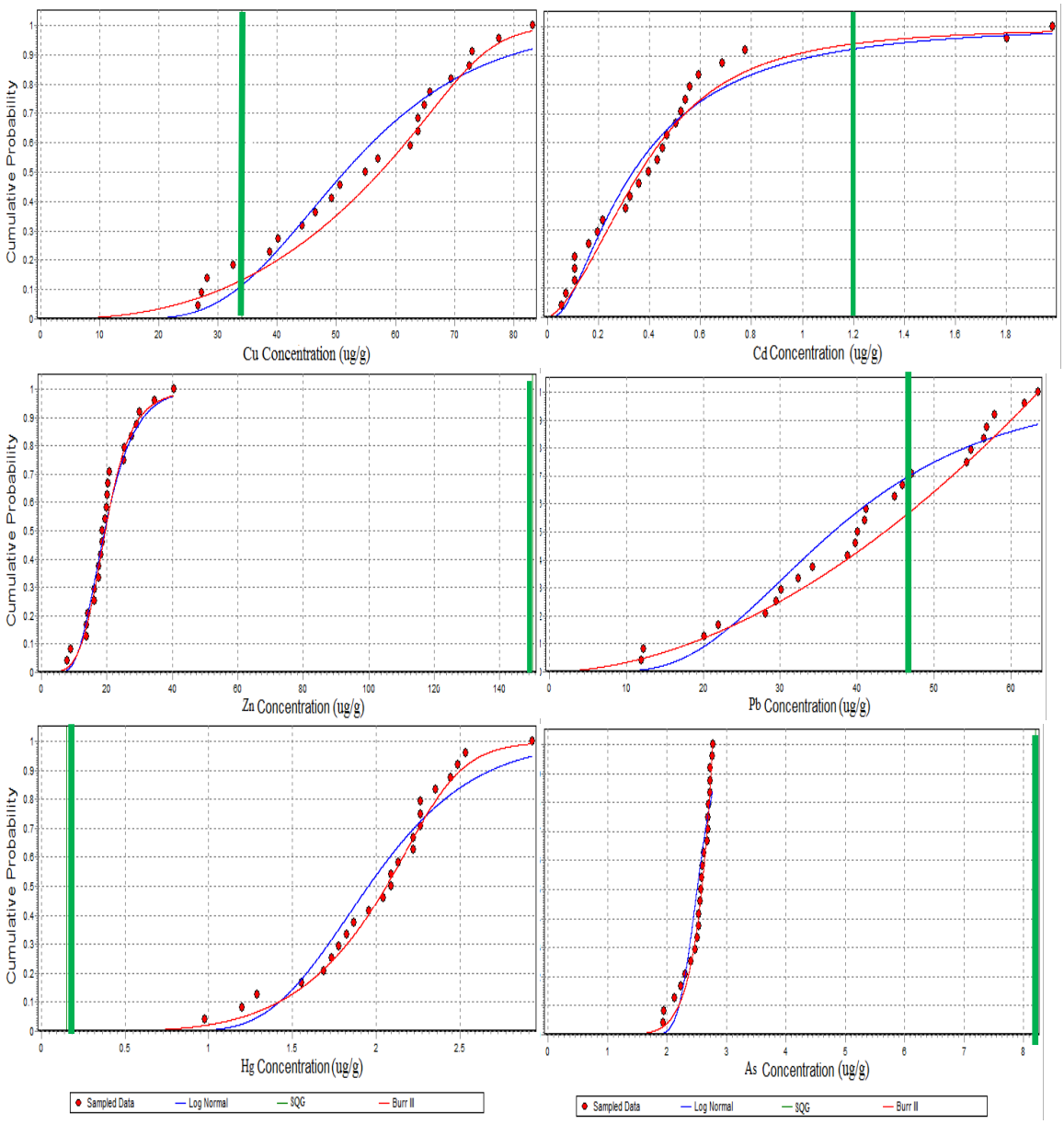

Figure 5.5. Probabilistic Hazard Screening of Metals in the Sakumo II estuary using AQUARISK.

5.3.1.3 Volta Estuary

For this estuary, none of the metals analyzed were of potential concern since they all fell below the SQG (Fig 5.6). This again was in agreement with results of the geochemical studies which classified these metals as being within background geochemical levels (See Fig. 4.16). None of the metals in this estuary was retained for higher tier analysis in AQUARISK. Results of trace metal concentrations are shown in appendix C3.

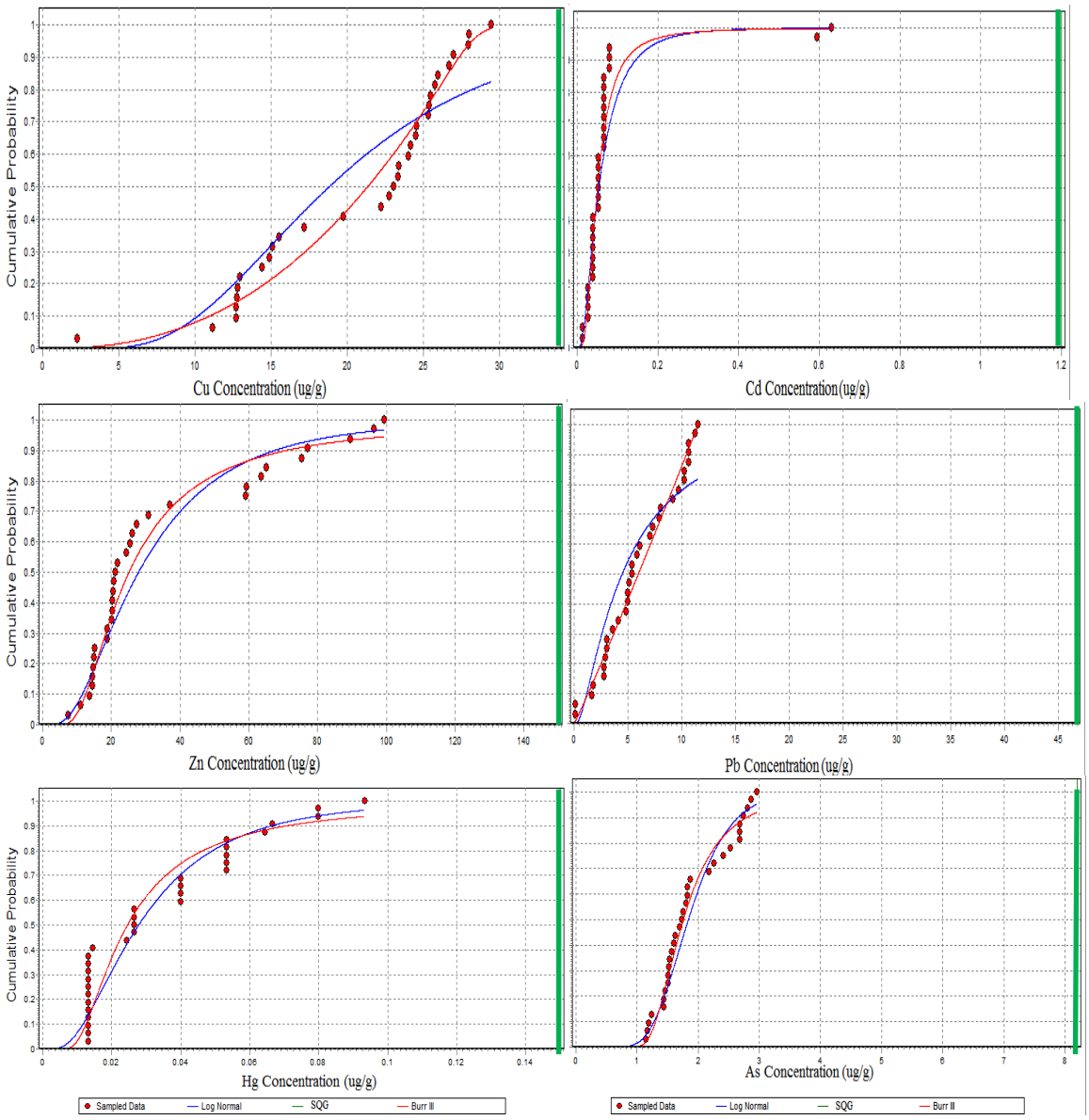

Figure 5.6. Probabilistic Hazard Screening of Metals in the Volta estuary using AQUARISK.

5.3.2 AQUARISK Estimates of the Hazardous Concentrations (HC) of Metals in Sediment Likely to Affect 5, 25 or 50% of Species for the 95 Percent Confidence Limit

5.3.2.1 Ankobra Estuary

Result showed that for As, the probabilities of exceeding the $HC_{5;95}$, $HC_{25;95}$ and $HC_{50;95}$ criteria in the Ankobra estuary are 1 based on the current levels recorded in this study (Table 5.1). The current concentrations of As are likely to affect 79%, 75.8% and 70.2% for the $HC_{5;95}$, $HC_{25;95}$ and $HC_{50;95}$ respectively. AQUARISK estimated the percent reduction in As level required to meet the $HC_{5;95}$, $HC_{25;95}$ and $HC_{50;95}$ to be 99.9%, 97.8% and 94.2% respectively with target concentrations of 0.1, 2.1 and 5.5ugg^{-1} respectively (Table 5.1). For Hg, the probabilities of exceeding $HC_{5;95}$, $HC_{25;95}$ and $HC_{50;95}$ are 0.8, 0.1 and 0.0 respectively. The current concentrations of Hg in the estuary are likely to affect 65%, 2.1% and 0% for the $HC_{5;95}$, $HC_{25;95}$ and $HC_{50;95}$. AQUARISK estimated the percent reduction in Hg level required to meet the $HC_{5;95}$, and $HC_{25;95}$ to be 90.5% and 12.7% respectively with target concentrations of 0.0 and 0.2 ugg^{-1} respectively (Table 5.1).

Table 5.1. AQUARISK Estimates of the $HC_{5;95}$, $HC_{25;95}$ and $HC_{50;95}$ criteria for the Ankobra Estuary

Hazard	Probability of Exceedence: CI=95%			% Species Affected: CI=95%			Reduction Required: CI=95%			Target Concentration (ugg^{-1}): CI= 95%			
	HC_5	HC_{25}	HC_{50}	HC_5	HC_{25}	HC_{50}	HC_5	HC_{25}	HC_{50}	HC_5	HC_{25}	HC_{50}	This Study
As	1.0	1.0	1.0	79.0	74.8	70.2	99.9	97.8	94.2	0.1	2.1	5.5	97.6±32.5
Hg	0.8	0.1	0.0	65.0	2.1	0.0	80.5	12.7	0.0	0.0	0.2	0.5	0.4±0.2

5.3.2.2 Sakumo II Estuary

Result showed that for Cd the probabilities of exceeding the $HC_{5;95}$, $HC_{25;95}$ and $HC_{50;95}$ criteria in this estuary are 1 based on the current levels recorded in this study. The current concentrations of Cd are likely to affect 77.6%, 76.2% and 72.9% for the $HC_{5;95}$, $HC_{25;95}$ and $HC_{50;95}$ respectively. AQUARISK estimated the percent reduction in Cd level required to meet the $HC_{5;95}$, $HC_{25;95}$ and $HC_{50;95}$ criteria to be 100%, 99.8% and 99.2% respectively with target concentrations of 0.0, 0.0 and 0.0 ug/g respectively (Table 5.2). Similarly for Pb, the probabilities of exceeding the $HC_{5;95}$, $HC_{25;95}$ and $HC_{50;95}$ in the this estuary are 1 based on the current levels recorded in this study. The current concentrations of Pb in this estuary are likely to affect 99.3%, 89.2% and 85.1% for the $HC_{5;95}$, $HC_{25;95}$ and $HC_{50;95}$ criteria respectively. AQUARISK estimated the percent reduction in Pb level required to meet the $HC_{5;95}$, $HC_{25;95}$ and $HC_{50;95}$ criteria to be 100%, 99.9% and 99.6% respectively with target concentrations of 0.0, 0.1 and 0.1 ug/g respectively (Table 5.2). Also for Hg, the probabilities of exceeding the $HC_{5;95}$, $HC_{25;95}$ and $HC_{50;95}$ criteria in this estuary are 1, 1 and 0.3 respectively based on the current levels recorded in this study. The current concentrations of Hg in the estuary are likely to affect 39.7% 38.2 5.7% for the $HC_{5;95}$, $HC_{25;95}$ and $HC_{50;95}$ criteria respectively. AQUARISK estimated the percent reduction in Hg level required to meet the $HC_{5;95}$, $HC_{25;95}$ and $HC_{50;95}$ criteria to be 96.3%, 73.8% and 24.2% respectively with target concentrations of 0.1, 0.5 and 1.5 ug/g respectively (Table 5.2). Finally for Cu, the probabilities of exceeding $HC_{5;95}$, $HC_{25;95}$ and $HC_{50;95}$ criteria in this estuary are all 1 based on the current levels recorded in this study. The current concentrations of Cu in the estuary are likely to affect 97.8%, 82.3% and 60.5% for the $HC_{5;95}$, $HC_{25;95}$ and $HC_{50;95}$ criteria respectively. AQUARISK estimated the percent reduction in Cu level required to

meet the $HC_{5;95}$, $HC_{25;95}$ and $HC_{50;95}$ criteria to be 100%, 89.2% and 70.3 with target concentrations of 0.0, 0.1 and 5.0 ug/g respectively (Table 5.2).

Table 5.2. AQUARISK Estimates of the $HC_{5;95}$, $HC_{25;95}$ and $HC_{50;95}$ criteria for the Sakumo II estuary

	Probability of Exceedence: CI=95%			% Species Affected: CI=95%			Reduction Required: CI=95%			Target Median Concentration (ug/g): CI= 95%			
Hazard	HC_5	HC_{25}	HC_{50}	HC_5	HC_{25}	HC_{50}	HC_5	HC_{25}	HC_{50}	HC_5	HC_{25}	HC_{50}	This Study
Cu	1.0	1.0	1.0	97.8	82.3	60.5	100.0	89.2	70.5	0.0	0.1	5.0	54.2±17.1
Cd	1.0	1.0	1.0	77.6	76.2	72.9	100.0	99.8	99.2	0.0	0.0	0.0	0.5±0.3
Pb	1.0	1.0	1.0	99.3	89.2	85.1	100.0	99.9	99.6	0.0	0.1	0.1	40.8±14.1
Hg	1.0	1.0	0.3	39.7	38.3	5.7	96.3	73.8	24.2	0.1	0.5	1.5	2.0±0.4

5.3.3 Risk Mapping of Metals of Potential Concern to Biota

5.3.3.1 Ankobra Estuary

Results showed that for this estuary, As appeared to be of high risk to the entire estuary with risk probabilities ranging from 0.74 in the marine zone to 0.88 in the freshwater zone (Fig. 5.7A). The lowest risk areas were within the brackish zone while the highest risk areas were towards the riverine section. Although Hg was of low risk to species than As, just as the former risk probabilities increased towards the freshwater zone ranging from 0.05 in the marine zone to 0.35 in the freshwater zone (Fig. 5.7B)

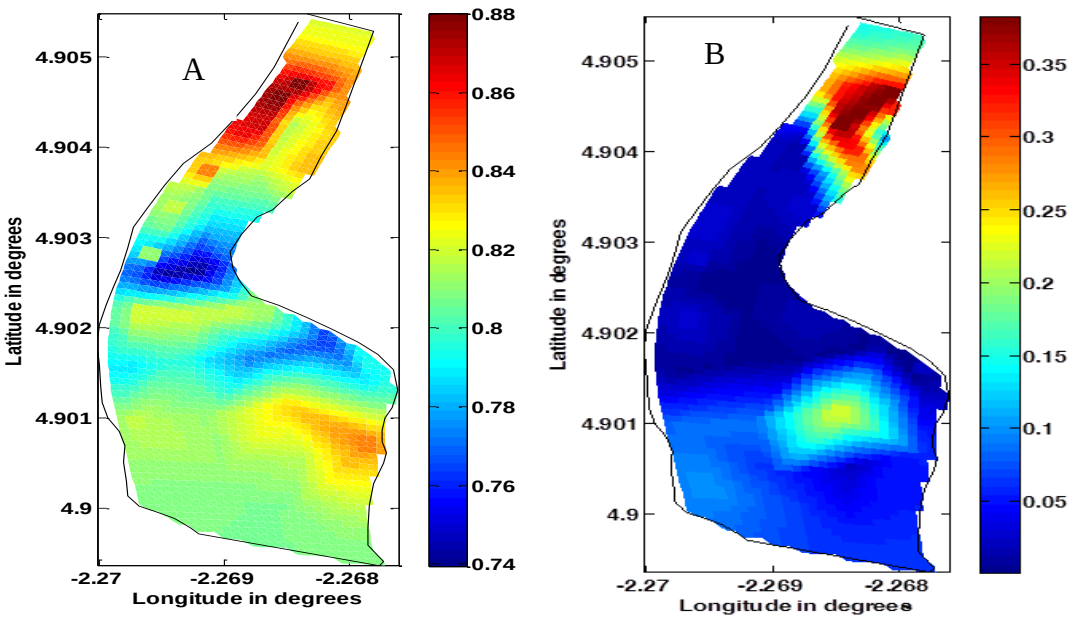

Figure 5.7. Maps of potential risk of (a) As and (b) Hg to biota in the Ankobra estuary.

5.3.3.2 Sakumo II Estuary

Cadmium (Cd) appeared to be of high risk to the biota in the entire estuary with probabilities ranging from 0.65 in the freshwater zone to 0.9 in the marine zone (Fig 5.8A). Highest risks were seen towards the marine zone. Risk probabilities of Hg in this estuary ranged from 0.35 (in the brackish zone) to 0.55 in most other areas of the estuary (Fig. 5.8B). Risk probabilities of Cu ranged from 0.1 in the freshwater zone to 0.8 in the marine zone with (Fig. 5.8C). Almost all areas of the estuary with exception of a very small area towards the marine section were within the lowest risk areas for Cu. Finally, risk probabilities of Pb ranged from 0.1 in the brackish region to 0.9 in the marine region (Fig. 5.8D). Just as Cd, and Hg, Pb was of high risk to almost the entire estuary.

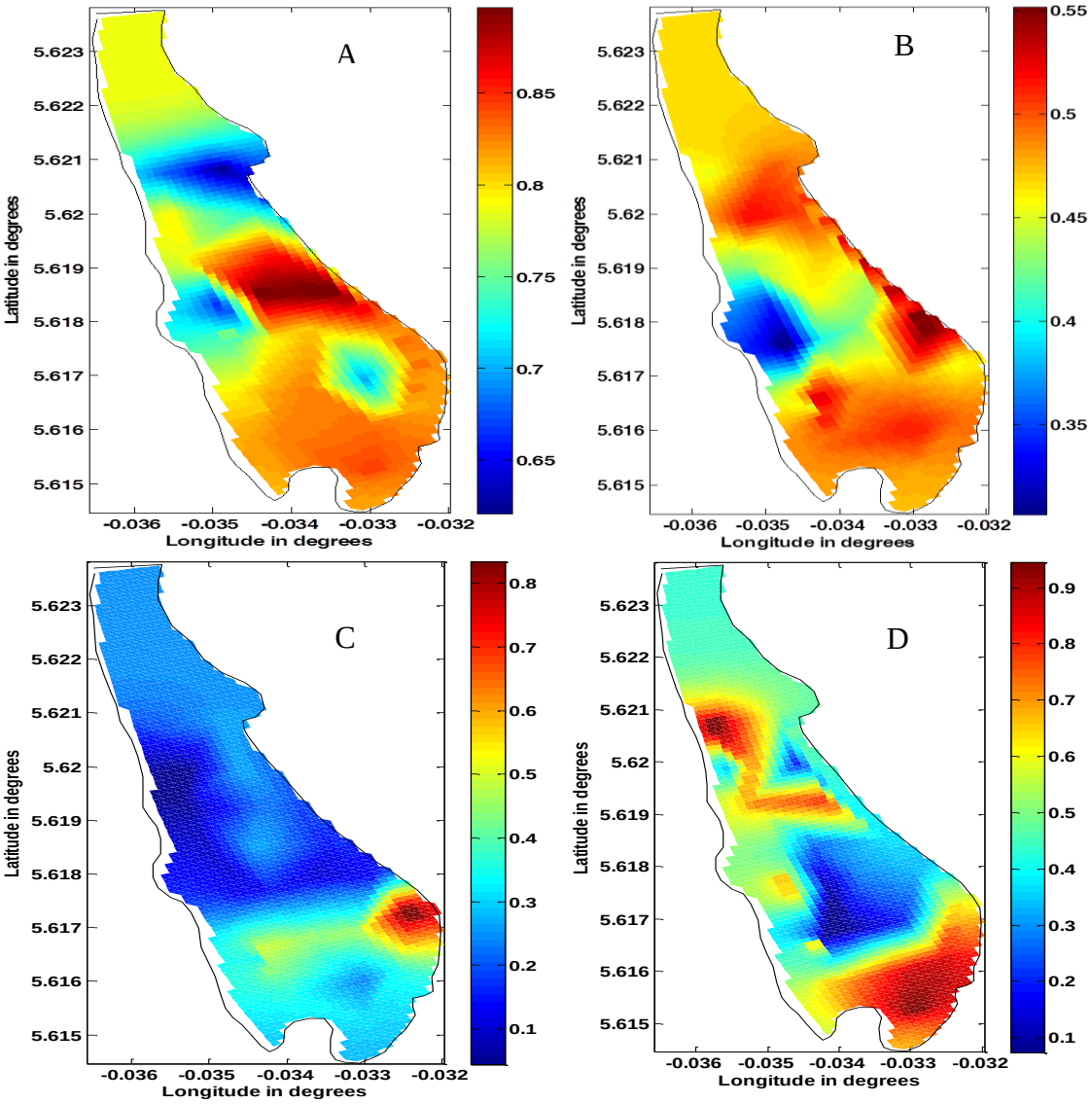

Figure 5.8. Maps of potential risk of (a) Cd, (b) Hg, (c) Cu and (d) Pb to biota in the Sakumo II estuary.

5.4 Discussion

As results obtained in the geochemical assessments indicated that As and Hg were extremely enriched in the sediments, the ecotoxicological risk analysis of the sediments from the Ankobra estuary also identified As and Hg as contaminants of potential concern while Cd, Zn and Pb were not. Highest risk probabilities of both As and Hg were seen in the freshwater zone of the estuary indicating that the source of these metals could be upstream of the Ankobra estuary. This again is in agreement with the results of provenance analysis which suggested that the sediments could have originated from the Pestea, Awaso, Asankragua, Bogoso and Esiama areas which are upstream of the Ankobra River (See section 3.4)

Ecotoxicological risk assessment of the sediments from the Sakumo II estuary identified Cu, Cd, Pb and Hg as contaminants of potential concern to the biota in the estuary. Similar to the Ankobra, these results are in agreement with the results of the geochemical assessments which described the sediment as being moderately enriched with these metals (see Fig. 4.15). Contrary to the Ankobra estuary however, risks of trace metals cut across the entire estuary particularly the marine zone, suggesting sources within the immediate surroundings of the estuary. This again confirms the results of the provenance analysis which suggested that the sediment in the Sakumo II estuary are derived from the Tema, Sakumono, Afienya and Lashibi areas, which are in close proximity to the estuary.

Apart from Cu, that might be useful to organisms when in low levels; As, Cd, Hg and Pb are highly toxic metals which have no known biological requirements, thus their presence in the sediment in such high levels are threatening (Gill *et al.*, 1999; Storelli *et al*., 2005; Julshamn *et al*., 2008).

Mercury (Hg) for instance, has been listed as a high priority pollutant due to its persistence in the environment and high toxicity to organisms at all levels of the food chain (Jiang *et al.*, 2006). Marine organisms exposed to different Hg concentrations in laboratory experiments have shown several effects such as: hormonal and gonadal alteration; changes in hematological parameters; histopathological alterations in liver and kidneys; and decreasing of enzymatic activities (Berntssen *et al.*, 2004; Gill *et al.*, 1999).

Just as Hg, Pb is neither essential nor beneficial to aquatic organisms with all existing data showing that its metabolic effects are rather adverse (Berg *et al*., 2000; Storelli *et al*., 2005; Lahaye, 2006; Julshamn *et al*., 2008). It is a metabolic poison that affects behavior, as well as the hematopoietic, vascular, nervous, renal, and reproductive systems of aquatic organisms (Eisler, 1988).

CHAPTER SIX

CONCLUSIONS AND RECOMMEDATIONS

6.1 Conclusions

Provenance, trace metal accumulation and ecotoxicological risk of trace metals in sediments from the Ankobra, Pra, Amisa, Densu, Sakumo II and Volta estuaries were studied using petrographical, geochemical, and ^{210}Pb dating techniques. From the study, the following conclusions were made.

The study revealed that sediment cores from all six estuaries were subjected to extreme weathering prior to deposition and exhibited high maturity as observed in their clay mineralogy. Results of the provenance analysis showed that sediments from the Ankobra, Densu and Volta originated exclusively from recycled/quartzose sedimentary environments while those from the Amisa and Sakumo II were exclusively derived from mafic igneous sources. The core from the Pra however consisted of sediments derived from both recycled/quartzose sedimentary and mafic igneous environments.

A clear exponential decline in excess ^{210}Pb concentrations in the Amisa, Densu and Sakumo II cores with depth suggested a constant sediment accumulation rate throughout the datable portions of the cores from these estuaries. The study suggests the cores from the Ankobra, Pra and Volta could be responding to anthropogenic disturbances and that, their actual sedimentation rates may have varied.

Based on metal concentrations and EFs, it is also concluded that, the Ankobra, Pra, and to some extent the Amisa estuaries have been impacted with gold mining operations through the release of high levels of As and Hg from their watershed over time. Except for V and Cd, the levels of Mo, Zn, Pb, As, Hg and Cu were enriched beyond background geochemical levels in the Sakumo II and these enrichments were attributed to rapid urbanization and industrialization in it watershed since the last 50 years.

Though the core from the Densu estuary showed an increasing trend in the concentrations of all metals analyzed in the last 10 years, EFs showed that apart from Mo and As, the estuary has not seen any enrichment in metal levels beyond geochemical background levels. The historical enrichment of the sediment from the Densu estuary with Mo and As was attributed to changes in redox conditions driven by the overly urbanized nature of the watershed rather than industrialization.

Comparatively, the metal concentrations in the Volta estuary were within geochemical background level. However, sharp peaks in the levels of Hg in some sections of this core and that of the Amisa and Densu were attributed primarily to episodic inputs of total Hg to the sediment.

Trace metal accumulations patterns in the estuarine sediment were reflected also in the nearshore and deep-sea sediments. This study did not however, assess any geochemical linkages between these systems.

AQUARISK estimates indicated that As and Hg in sediments posed ecotoxicological risk to the biota of the Ankobra estuary while Cd, Pb, Hg and Cu posed risk to the biota of the Sakumo II estuary. None of the trace metals analyzed posed ecotoxicological risks to the biota of the Volta estuary. To achieve atleast a 75% species protection in the Ankobra estuary, a significant percent reduction of about 97.8% and 12.7% in the current levels of As and Hg respectively are required. Additionally, to achieve atleast a 75% species protection in the Sakumo II, a significant percent reduction of about 99.8%, 99.9%, 73.8% and 89.2% in the current levels of Cd, Pb, Hg and Cu respectively will be required.

6.2 Recommendations

This study is the first ever of its kind using sediment cores to reconstruct metal pollution histories in estuarine environments of Ghana.

The study recommends that more coring studies be carried out at the different parts of each estuary as this will help bring out any information that may have been lost in the preliminary study.

The study should also be extended to other estuarine environments in Ghana to assess any temporal variations to their trace metal supply and to know if these other environments have also been impacted with urbanization and industrialization.

The use of AQUARISK in assessing ecotoxicological risks of trace metals in the selected estuaries have been very successful although it is the first time the approach has been used in Ghana. It is recommended that this study is extended to other nearshore environments that were not part of the study for an in-depth understanding of the fate of trace metals in such environments and allow for proper management and monitoring plans.

Future studies in trace metal assessments in sediment should incorporate provenance analysis of the sediment as this have been very useful in understanding the source of metals in this study.

CHAPTER SEVEN

7.0 REFERENCES

Abdel-Sabour, M. F. (2007). Chromium in receiving environment in Egypt (an overview). *Journal of Environment, Agriculture and Food Chemistry*. 6: 2178–2198.

Abdul, H.B.O. and Subrahmanyam, M. N. V. (1998). Trace metal concentrations in the crab *macrophthalmus depressus* and sediment on the Kuwait coast. *Environmental Monitoring and Assessment*, 53: 297–304.

Aitchison, J.C. (1985). Stephens Subgroup (upper Maitai parison of the chemistry of the conglomerate Group) in the Countess Range-Mararoa River area. N.Z. matrix. *Journal of Geology and Geophysics*, 28: 767 (abstract).

Akabzaa T., and Daramani A. (2001). *Impact of mining sector in Ghana: A study of the Tarkwa Mining Region.* Report to SAPRI. 117pp.

Aldenberg, T., and Slob, W. (1993). Confidence limits for hazardous concentrations based on logistically distributed NOEC toxicity data. *Ecotoxicology and Environmental Safety*, 25: 48-63.

Amankwah, E. (2013). Impact of illegal mining on water resources for domestic and irrigation purposes. *ARPN Journal of Earth Sciences*, 2 (3): 117-121.

Amuzu, A.T. (1975). *Survey of water quality of the River Densu*. A research report presented to the Water Resources Research Unit of the CSIR, Accra, Ghana. 57pp.

Anani, C., Moradeyo, M., Atta-Peters, D., Kutu, J., Asiedu, D., and Boamah, D. (2013). Geochemistry and provenance of sandstones from Anyaboni and surrounding areas in the voltaian basin, Ghana. *International Research Journal of Geology and Mining*, 6: 206-212.

Anderson, J. B. (1985). *Antarctic glacial marine sedimentation: a core workshop*. Geological Society of America, Annual meeting, Orlando, Florida, 66 pp.

Antipov, A.N., Lyalikova, N.N., Khiznjak, T.V., and L'vov, N.P. (1999). Some properties of dissimilatory nitrate reductases lacking molybdenum and molybdenum factors. *Biochemistry (Moscow)*, 64: 483–487.

Appleby, P. G. (2001). Chronostratigraphic techniques in recent sediments. In *Tracking environmental change using lake sediments, basin analysis, coring, and chronological techniques, development in paleoenvironmental research*, ed. W.L. Last and J.P. Smol. Dordrecht: Kluwer Academic Publishers. 171-203 pp.

Appleby, P. G., and F. Oldfield. 1983. The assessment of 210Pb data from sites with varying sediment accumulation rates. *Hydrobiologia*, 103: 29-35.

Appleby, P.G. (1998). Dating of sediments and determination of sedimentation rate. Proceedings of a seminar held in Helsinki, 2–3 April 1997. 149pp.

Appleby, P.G. and Oldfield, F. (1992): *Application of ^{210}Pb to sedimentation studies. In: Uranium-series Disequilibrium: Applications to Earth, Marine & Environmental Sciences* (eds. M. Ivanovich & R.S. Harmon), Oxford University Press, Oxford: 731-778 pp.

Appleby, P.G., and Oldfield, F. (1978): The calculation of ^{210}Pb dates assuming a constant rate of supply of unsupported ^{210}Pb to the sediment. *Catena*, 5: 1-8.

Appleby, P.G., Oldfield, F., Thompson, R., Huttunen, P., and Tolonen, K. (1979). Pb-210 dating of annually laminated lake-sediments from Finland. Nature, 280: 53–55

Armah, A.K. and Amlalo, D.S. (1998). Coastal Zone Profile of Ghana. Gulf of Guinea Large Marine Ecosystem Project. Ministry of Environment, Science & Technology. 111pp.

Armstrong-Altrin, J.S., Lee, Y.I., Kasper-Zubillaga, J.J., Carranza-Edwards, A., Garcia, D., Eby, N., Balaram, V., and Cruz-Ortiz, N.L. (2012). Geochemistry of beach sands along the western Gulf of Mexico, Mexico: Implication for provenance. *Chemie der Erde / Geochemistry*, 72: 345-362.

Arnold, W. R., Santore, R. C., and Cotsifas, J. S. (2005). Predicting copper toxicity in estuarine and marine waters using the Biotic Ligand Model. *Marine Pollution Bulletin,* 50: 1634-1640.

Ashokk, S., and Mankar, R.S. (2009). Grain Size Analysis and Depositional Pattern of Upper Gondwana Sediment Early Cretaceous of Salbardi Area, Districts Amravati, Maharashtra and Betul, Madhya Pradesh. *Journal Geological Society of India,* 73: 393-406.

Asiedu, D.K., Dampare, S. B., Asamoah Sakyi, P., Banoeng-Yakubo, B., Osae, S., Nyarko B. J. B. and Manu, J. (2004). Geochemistry of Paleoproterozoic metasedimentary rocks from the Birim diamondiferous field, southern Ghana: Implications for provenance and crustal evolution at the Archean-Proterozoic boundary. *Geochemical Journal*, 38: 215-228.

Azcue, J.M., and Nriagu, J.O. (1995). Impact of abandoned mine tailings on the arsenic concentrations in Moira Lake, Ontario. *Journal of Geochemical Explorations*, 52: 81–89.

Bakele, B. (2011). Geochemistry of lower sandstone in Blue Nile Gorge Mesozoic sedimentary sequences: Implication for provenance composition and paleoclimate. A master's thesis submitted to Addis Ababa University, June, 2011.

Barry, B., Obuobie, E., Andreini, M., Andah, W. and Pluquet, M. (2005). Volta River Basin Synthesis. Comprehensive Assessment of Water Management in Agriculture, IWMI. Pp. 198

Bartell, S.M., Lefebvre, G., Kaminski, G., Carreau, M., and Campbell, K.R. (1999). An ecosystem model for assessing ecological risks in Québec Rivers, lakes, and reservoirs. *Ecological Modelling*, 124: 43–67.

Berg, V., Ugland, K. I., Hareide, N. R., Groenningen, D., and Skaare, J. U. (2000) Mercury, cadmium, lead, and selenium in fish from a Norwegian fjord and off the coast, the importance of sampling locality. *Journal of Environmental Monitoring*, 2: 375-377.

Berntssen, M.H.G., Hylland, K., Julshamn, K., Lundebye, A.-K., Waagbø, R. (2004). Maximum levels of organic and inorganic mercury in fish feed. *Aquaculture Nutrition*. 10: 83–97.

Berry, W.J., Boothman, W.S., Serbst, J.R., and Edwards, P.A. (2004). Predicting the toxicity of Cr in sediment. *Environmental Toxicology, Chemosphere*, 23: 2981–2992.

Bing, H.J., Wu, Y.H., Sun, Z.B., and Yao, S.C. (2011). Historical trends of heavy metal contamination and their sources in lacustrine sediment from Xijiu Lake, Taihu Lake Catchment, China. *Journal of Environmental Sciences*, 23(10): 1671–1678.

Blake, A. C., Chadwick, D. B., Zirino A., and Rivera-Duarte, I. (2004). Spatial and Temporal Variations in Copper Speciation in San Diego Bay. *Estuaries*, 27: 437-447.

Blanton, M.L., Gardiner, W.W., and Dirkes, R.L. (1995). Grain-size distribution and contaminant association. Prepared for U.S. Department of Energy under contract of DE-AC06-76RLO 1830, pp. 53

Boughton, D.A., Smith, E.R., and O'Neill, R.V. (1999). Regional vulnerability: a conceptual framework. *Ecosystem Health*, 5: 312–322.

Bowell, R.J. (1992). Supergene gold mineralogy at Ashanti, Ghana: implications for the supergene behaviour of gold. *Mineralogical Magazine*, 56: 545–560.

Bowell, R.J. (1993). Mineralogy and geochemistry of tropical rain forest soils: Ashanti, Ghana. *Chemical Geology*, 106: 345–348.

Brand, L. E., Sunda, W. G., and Guillard, R. R. L. (1986). Reduction of marine phytoplankton reproduction rates by copper and cadmium. *Journal of Experimental Marine Biology and Ecology*, 96: 225-250.

Bricker-Urso, S., Nixon, S.W., Cochran, J.K., Hirschberg, D. J., and Hunt, C. (1989). Accretion rates and sediment accumulation in Rhode Island salt marshes. *Estuaries*, 12: 300–317.

Brown, N. L., Lee, B. T. O., and Silver, S. (1994). Bacterial transport and resistance to copper. In H. Sigel and A. Sigel [eds.], *Metal ions in biological systems*. V. 30. Marcel Dekker. 405-435pp

Bruland, K.W. (1992). Complexation of cadmium by natural organic ligands in the central North Pacific. *Limnology and Oceanography*, 37: 1,008–1,017.

Bubb, J,M., and Lester J.N (1991). Impact of heavy metals on rivers and implications for man and the environment. *Science of Total Environment*, 100: 207-258.

Buhl, K. J., and Hamilton, S. J. (1990). Comparative toxicity of inorganic contaminants related by placer mining to early life stages of salmonids. *Ecotoxicology and Environmental Safety*, 20: 325-342.

Burbridge, D.J., Iris Koch, I., Zhang, J., and Reimer, K.J. (2012). Chromium speciation in river sediment pore water contaminated by tannery effluent. Chemosphere, 89: 838–843.

Burgos, M., and Rainbow, P. (2001). Availability of cadmium and zinc from sewage sludge to the flounder, Platichthys flesus, via a marine food chain. *Marine Environmental Research*, 51: 417–439.

Burmaster, D. E., and Harris R. H. (1993). The magnitude of compounding conservatisms in Superfund risk assessments. *Risk Analysis*, 13: 131-134.

Butler, A., and Carter-Franklin, J.N. (2004). The role of vanadium bromoperoxidase in the biosynthesis of halogenated marine natural products. *Natural Products Reports*, 21: 180–188.

Callahan M. A., Slimak M. W. and Gabel N. W. (1979). Water- Related Environmental Fate of 129 Priority Pollutants. Rep. EPA-40/4, U.S. Environmental Protection Agency, Washington DC. 29pp.

Campbell, P.G.C. (1995). Interactions between trace metals and aquatic organisms: A critique of the free-ion activity model, In A. Tessier and D. R. Turner (eds.), Metal Speciation and Bioavailability in Aquatic Systems. John Wiley and Sons, London, U.K. p. 45-97.

Carroll, J.L., Lerche, I., Abraham, J.A., and Cisar, D.J. (1995). Model determined sediment ages from 210Pbprofiles in un-mixed sediment. *Nuclear Geophysics*, 9: 553–565.

CCME (Canadian Council of Ministers of the Environment) (1996). A framework for ecological risk assessment: general guidance. Ottawa, ON, Canada. Available from ccme.ca/assets/pdf/pn_1195_e.pdf. [accessed 11 December 2010].

Chakrapani, G.J. (2005). Factors controlling variations in river sediment loads. *Current Science,* 88(4): 569–575.

Chapman, P. M., and Mann, G. S. (1999). Sediment quality values (SQVs) and ecological risk assessment (ERA). *Marine Pollution Bulletin*, 38: 339-344.

Cheevaporn, V., and Mokkongpai., P. (1996). Pb-210 Radiometric dating of estuarine sediments from the eastern coast of Thailand. *Journal of Science and Society*, 22: 313-324.

Chen, S.Q., and Chen, B. (2012b). Network environ perspective for urban metabolism and carbon emissions: a case study of Vienna, Austria. *Environmental Science and Technology*, 46: 4498–4506.

Chen, S.Q., Chen, B., and Fath, B.D. (2013). Ecological risk assessment on the system scale: A review of state-of-the-art models and future perspectives. *Ecological Modelling*, *250*: 25– 33.

Chen, S.Q., Fath, B.D., Chen, B., and Su, M.R. (2011). Evaluation of the changed properties of aquatic animals after dam construction using ecological network analysis. *Procedia Environmental Sciences*, 5: 114–119.

Christian, R.R., Brinson, M.M., Dame, J.K., Johnson, G., Peterson, C.H., and Baird, D. (2009). Ecological network analyses and their use for establishing reference domain in functional assessment of an estuary. *Ecological Modelling*, 220: 3113–3122.

Chung, J., Zasoski, R.J., and Lim, S. (1994). Kinetics of chromium(III) oxidation by various manganese oxides. Korean J. Agric. Chem. Patterson, R.R., S. Fendorf, and M. Fendorf. 1997. *Reduction of Biotechnology*, 37:414–420.

Coale, K. H., and Bruland K.W. (1988). Copper complexation in the northeast Pacific. *Limnology and Oceanography*, 33: 1084-1101.

Cochran, J.K., D.J. Hirschberg, J. Wang, and C. Dere. (1998). Atmospheric deposition of metals to coastal waters (Long Island Sound, New York U.S.A.): evidence from saltmarsh deposits. *Estuarine, Coastal and Shelf Science*, 46: 503–522.

Cohen, A.S., Palacios-Fest, M.R., McGill, J., Swarzenski, P., Verschuren, D., Sinyinza, R., Songori, T., Kakagozo, B., Syampila, M., O'Reilly, C.M. and Alin S.R. (2005). Paleolimnological investigations of anthropogenic environmental change in Lake Tanganyika: I. An introduction to the project. *Journal of Paleolimnology*, 34:1-18.

Collier, R.W. (1985). Molybdenum in the Northeast Pacific Ocean. *Limnology and Oceanography*, 30: 1351–1354.

Comber, S.D.W., Gardner, M.J., Gunn, A.M., Whalley, C. (1996). Kinetics of trace metal sorption to estuarine suspended particulate matter. *Chemosphere*, 33 (6): 1027–1040.

Condie, K. C. (1993): Chemical composition and evolution of the upper continental crust: Contrasting results from surface samples and shales. *Chemical Geology*, 104: 1–37.

Covelli, S., Langone, L., Acquavita, A., Piani, R., and Emili, A. (2012). Historical flux of mercury associated with mining and industrial sources in the Marano and Grado Lagoon (northern Adriatic Sea) *Estuarine, Coastal and Shelf Science*, pp 1-13 (in press).

Cox, R., Lowe, D.R. and Cullers, R.L. (1995). The influence of sediment recycling and basement composition on evolution of mudrock chemistry in the southwestern United States: *Geochimica et Cosmochimica Acta*, 59: 2919–2940.

Crook, K.A.W. (1974). Lithogenesis and geotectonic: the significance of compositional variation in flysch arenites (greywackes). *Society of Economic Paleontologist and Mineralogist's Special Publication*, 19: 304–310.

Crusius, J., Calvert, S., Pedersen, T., and Sage, D. (1996). Rhenium and molybdenum enrichments in sediment as indicators of oxic, suboxic and sulfidic conditions of deposition. *Earth Planetary Science Letters*, 145: 65–78.

Cundy, A.B., Croudace, I.W., Alejandro Cearreta, A., and Irabien, M.J. (2003) Reconstructing historical trends in metal input in heavily-disturbed, contaminated estuaries: studies from Bilbao, Southampton Water and Sicily. *Applied Geochemistry*, 18: 311–325.

Cutter, G. A. (1992). Kinetic controls on metalloid speciation in seawater. *Marine Chemistry*, 40: 65–80.

Dahl, T. W., Chappaz A., Fitts J. P., and Lyons T. W. (2013). Molybdenum reduction in a sulfidic lake: evidence from X-ray Absorption Fine-Structure Spectroscopy. *Geochimica. Cosmochimica et Acta*, 103: 213–231.

Dale, V.H., Biddinger, G.R., and Newman, M.C. (2008). Enhancing the ecological risk assessment process. *Integrated Environmental Assessment and Management*, 4: 306–313.

Dalrymple, R.W., Zaitlin, B.A., and Boyd, R. (1992). Estuarine facies models: conceptual basis and stratigraphic implications. Journal of Sedimentary Petrology, 62: 1130–1146.

De Angelis, D.L., Bartell, S.M., and Brenkert, A.L. (1989). Effects of nutrient recycling and food chain length on resilience. *The American Naturalist*, 134: 778–805.

De Schamphelaere, K. A. C., Heijerick, D. G., and Janssen, C. R. (2002). Refinement and field validation of a biotic ligand model predicting copper toxicity to *Daphnia magna*. *Comparative Biochemistry and Physiology*, 133: 243-258.

Debrah, C. (1999). Speciation of Heavy Metals in waters and sediment from the Densu Basin. M.Phil Thesis, Department of Chemistry, University of Ghana,Legon. 155pp.

Delfino, J.J. and otto, R.G. (1986). Trace metal transport in two tributaries of the Upper Chesapeake Bay the Susquehanna and Bush rivers. *Marine Chemistry*, 20: 29 44.

Díaz-Asencio, M., Alonso-Hernández, C.M., Bolanos-Álvarez, Y., Gómez-Batista, M., Pinto, V., Morabito, R., Hernández-Albernas, J.I., Eriksson, M., and Sanchez-Cabeza, J.A. (2009). One century sedimentary record of Hg and Pb pollution in the Sagua estuary (Cuba) derived from 210Pb and 137Cs chronology. *Marine Pollution Bulletin*, 59: 108-115.

Dickinson, W. R., Beard, L. S., Brakenridge, G. R., Erjavec, J. L., Ferguson, R. C., Inman, K. F., Lindberg, F. A., and Ryberg P. T. (1983). Provenance of North American Phanerozoic sandstones in relation to tectonic setting. *Geological Society of America Bulletin*, 94: 222-235.

Dickinson, W.R. (1985) Interpreting provenance relations from detrital modes of sandstones; In: *Provenance of Arenites* (ed.) Zuffa G G (New York: D. Reidel Publ. Co.), pp. 333–361.

Dickinson, W.R., and Suczek, C.A., 1979. A plate tectonic and sandstone compositions. *Bulletin of American Association of Petrologist and Geologists*, 63: 2164–2182.

Dickinson, W.R., Beard, S., Brakenbridge, F., Erjavec, J., Ferguson, R., Inman, K., Knepp, R., Lindberg, P., Ryberg, P. (1983). Provenance of North American Phanerozoic sandstones in relation to tectonic setting. *Geological Society of America Bulletin* 64: 233–235.

Dickson, K. B. and Benneh G. (1980). *A New Geography of Ghana*. Longmans Group Limited, London. 173pp

Donkor, A. K., Nartey V. K., Bonzongo, J. C., and D. K. Adotey (2006). Artisanal Mining of Gold with Mercury in Ghana. *West Africa Journal of Applied Ecology*, 9: 0855-4307

Duester, L., Vink, J.P.M., and Hirner, A.V. (2008). Methylantimony and arsenic species in sediment pore water tested with the sediment or fauna incubation experiment. *Environment, Science and Technology*, 42: 5866-5871

Duzgoren-Aydin, N.S., Aydin, A. and Malpas, J. (2002). Re-assessment of chemical weathering indices: case study of pyroclastic rocks of Hong Kong. *Engineering Geology* 63: 99–119.

ECOFRAM (1999). ECOFRAM Aquatic and Terrestrial Final Draft Reports, USEPA, www.epa.gov/oppefed1/ecorisk/ index.htm Accessed June 1, 2013.

Eggleston, M.R. (2012). Impact of Sediment Resuspension Events on the Availability of Heavy Metals in Freshwater Sediment. Master's thesis submitted to the department of Natural Resources and Environment, at the University of Michigan. 94pp

EHC (Environmental Health Criteria) 135 (1995). International Programme on Chemical Safety. pp. 173.

EHC (Environmental Health Criteria) 200 (1998). International Programme on Chemical Safety. pp. 150.

Ehrlich, H.L. (1996). *Geomicrobiology.* 3rd Edn., Marcel Dekker, New York. 719pp

Eisler, R. (1988). Lead hazards to fish, wildlife, and invertebrates: a synoptic review Contaminant Hazard Reviews. *Biological report,* 85: 1-14.

Eisler, R. (1993). Zinc hazards to fish, wildlife and invertebrates. A synoptic review. US fish and wildlife biological report. 29(10). pp. 106.

Elbaz-Poulichet, F., Seidel, J. L., Jezequel, D., Metzger, E., Prevot, F., Simonucci, C., Sarazin, G., Viollier, E., Etcheber, H., and Jouanneau, J.M. (2005). Sedimentary record of redox-sensitive elements (U, Mn, Mo) in a transitory anoxic basin (the Thau lagoon, France), *Marine Chemistry*, 95: 271–281.

Ellwood, B.B., Tomkin, J.H., Ratcliffe, K.T., Wright M., and Kafafy, A.M. (2008). High-resolution magnetic susceptibility and geochemistry for the Cenomanian/Turonian boundary GSSP with correlation to time equivalent core. *Palaeogeography, Palaeoclimatology, Palaeoecology*, 261: 105-126.

Emerson, S., and Huested, S.S. (1991). Ocean anoxia and the concentrations of molybdenum and vanadium in seawater. *Marine Chemistry*, 34: 177–196.

Erdogan, M. (2009). Monitoring and statistical assessment of heavy metal pollution in sediment along izmir bay using icp-ms. A PhD Thesis Submitted to the Graduate School of Engineering and Sciences of İzmir Institute of Technology. 130pp

Erickson, B.E., and Helz, G.R., (2000). Molybdenum (VI) speciation in sulfidic waters: stability and lability of thiomolybdates. *Geochimica et Cosmochimica Acta*, 64: 1149–1158.

Essumang, D., Dodoo, K., Obiri, D. K., and Yaney, J. Y. (2007). Arsenic, Cadmium, and Mercury in Cocoyam (Xanthosoma sagititolium) and Watercocoyam

(Colocasia esculenta) in Tarkwa, a Mining Community. *Bulletin of Environmental Contamination and Toxicology*, 79: 377-379.

European Commission (1996). Technical guidance documents in support of the Commission Directive 93/67/EEC on risk assessment for new noticed substances and the Commission Regulation EC/ 1488/94 on risk assessment for existing substances. Luxembourg. 337pp.

Fath, B.D. (2004). Network analysis in perspective: comments on WAND: an ecological network analysis user friendly tool. *Environmental Model and Software*, 19: 341–343.

Fath, B.D., and Patten, B.C. (1999). Review of the foundations of network environ analysis. *Ecosystems*, 2: 167–179.

Fedo, C. M., Nesbitt, H.W., and Young, G. M., (1995). Unraveling the effects of potassium metasomatism in sedimentary rocks and paleosols, with implications for paleoweathering conditions and provenance. *Geology*, 23: 921-924.

Fendorf, S., Eick, M.J., and Grossl, P. (1997). Arsenate and chromate retention mechanisms on goethite. 1 Surface structure. E*nvironment, Science and Technology*, 31: 315-319.

French, P.W., Allen, J.R.L., and Appleby, P.G. (1994). 210-Lead dating of a modern period salt marsh deposit from the Severn Estuary (southwest Britain), and its implications. *Marine Geology*, 118: 327– 334.

Friedmann, A.S., Watzin, M.C., Brinck-Johnsen, T. and Leiter, J.C. (1996). Low levels of dietary methylmercury inhibit growth and gonadal development in juvenile walleye (*Stizostedion vitreum*). *Aquatic Toxicology.* 35: 265-278.

Garcia-Orellana, J. Cañas, L., Masqué, P., Obrador, B., Olid, C., and Pretus, J. (2011). Chronological reconstruction of metal contamination in the Port of Maó (Minorca, Spain). *Marine Pollution Bulletin*, 62: 1632–1640.

Garnier-Laplace, J., K. Beaugelin-Seiller, R., Gilbin, C., Della-Vedova, O., Jolliet, and Payet, J., (2009). A Screening Level Ecological Risk Assessment and ranking method for liquid radioactive and chemical mixtures released by nuclear facilities under normal operating conditions. *Radioprotection*, 44: 903-908.

Gill, G.A., Bloom, N.S., Cappellino, S., Driscoll, C.T., Mason, R.P., Rudd, J.W.M. (1999). Sediment-water fluxes of mercury in Lavaca Bay, Texas. *Environment, Science and Technology*, 33: 747–756.

Gilmour, C.C., Henry, E.A., and Mitchell, R. (1992). Sulfate stimulation of mercury methylation in fresh-water sediment. *Environment, Science and Technology*, 26: 2281–2287.

Gobas, F.A. (1993). A model for predicting the bioaccumulation of hydrophobic organic chemicals in aquatic food-webs: application to Lake Ontario. *Ecological Modelling*, 69: 1–17.

Hagan, G.B., Ofosu, F.G., Hayford, E.K., Osae, E.K., and Oduro-Afriyie, K. (2011). Heavy Metal Contamination and Physico-Chemical Assessment of the Densu River Basin in Ghana. *Research Journal of Environmental and Earth Sciences*, 3: 385-392.

Hakanson, L. (1980). An ecological risk index for aquatic pollution control. A sedimentological approach. *Water Research*, 14: 975-1001.

Hamdan, J., and Burnham, C. P. (1996). The contribution of nutrients from parent material in three deeply weathered soils of Peninsular Malaysia. *Geoderma*, 74: 219–233.

Hansmann, W., and Köppel, V. (2000) Lead-isotopes as tracers of pollutants in soils. *Chemical Geology*, 171:123–44.

Haq, B.U.,and Boersma, A. (1998). Introduction to Marine Micropaleontology. Elsevier, New York. 376pp.

Hatje, V., Birch, G.F., and Hill, D.M. (2001). Spatial and temporal variability of particulate trace metals in Port Jackson Estuary, Australia. *Estuarine, Coastal and Shelf Science*, 53: 63-77.

Hayford, E. K., Amin, A., Osae, E.K., and Kutu, J. (2008). Impact of Gold Mining on Soil and some Staple Foods Collected from Selected Mining Communities in and around Tarkwa-Prestea Area. *West African Journal of Applied Ecology, 14: 1-12*

Helz, G. R., Bura-Nakic E., Mikac N., and Ciglenecki I. (2011) New model for molybdenum behavior in euxinic waters. *Chemical Geology*, 284: 323–332.

Helz, G. R., Vorlicek T. P., and Kahn M. D. (2004) Molybdenum scavenging by iron monosulfide. *Environment, Science and Technology*, 38: 4263–4268.

Helz, G.R., Miller, C.V., Charnock, J.M., Mosselmans, J.F.W., Pattrick, R.A.D., Garner, C.D., and Vaughan, D.J. (1996). Mechanism of molybdenum removal from the sea and its concentration in black shales: EXAFS evidence. *Geochimica et Cosmochimica. Acta*, 60: 3631–3642.

Herut, B., and Amir Sandler, A. (2006). Normalization methods for pollutants in marine sediment: review and recommendations for the Mediterranean. IOLR Report H18 Submitted to UNEP/MAP. 23pp.

Hicks, R., Caldas, L.Q., Dare, P.R., and Hewitt, P.J. (1986) Cardio-toxic and broncho constrictor effects of industrial metal fumes containing barium. *Archives of toxicology, Supplement* 9: 416–420.

Hill, R.A., Chapman, P.M., Mann, G.S., and Lawrence, G.S. (2000). Level of Detail in Ecological Risk Assessments. *Marine Pollution Bulletin*, 40: 471-477.

Hilson, G., Hilson, C.J., and Pardie, S. (2007). Improving awareness of mercury pollution in small-scale gold mining communities: challenges and ways forward in rural Ghana. Environmental Research 103 (2): 275-287.

Hirayama, K., Kageyama, S., and Unohara, N. (1992). Mutual separation and preconcentration of vanadium (V) and vanadium (IV) in natural waters with chelating functional group immobilized silica gels followed by determination of vanadium by inductively coupled plasma atomic emission spectrometry. *Analyst*, 117: 13–17.

Hirose, K., (2006). Chemical Speciation of trace metals in seawater: A review. *Analytical Sciences*, 22: 1055-1061.

Ho, T.Y., Quigg, A., Finkel, Z.V., Milligan, A.J., Wyman, K., Falkowski, P.G., Morel, F.M.M. (2003). The elemental composition of some marine phytoplankton. *Journal of Phycology*, 39: 1145–1159.

Hoffman, D.J., Rattner, B.A., Burtons Jr., G.A., and Cairns Jr., J. (2003) *Handbook of Ecotoxicology*. 2nd ed. Lewis Publishers, Portland, OR: SciTech Book News. 1250pp.

Holland, H.D., Turekian, K.K. (Eds.) (2003). *Treatise on Geochemistry,* 2nd Edition, Elsevier. 9144pp

Holm, T.R., and Curtiss, C.D. (1989). A comparison of oxidation reduction potentials calculated from the As(V)/As(III) and Fe(III)/Fe(II) couples with measured platinum-electrode potentials in groundwater. *Journal of Contamination and. Hydrology*, 5: 67–81.

Hope, B.K. (1997). An assessment of the global impact of anthropogenic vanadium. *Biogeochemistry*, 37: 1–13.

Horowitz, A.J. (1991). A primer on sediment-trace element chemistry. Lewis Publishers, Chelsea, Michigan. 136pp.

Huang, P.C., Su, P.H, Chen, H.Y, Huang, H.B., Tsai, J.L, Huang, H.I, and Wang, S.L. (2012). Childhood blood lead levels and intellectual development after ban of leaded gasoline in Taiwan: a 9-year prospective study. *Environment International*, 40: 88-96.

Hung, J.J., and Hsu, C.L. (2004). Present state and historical changes of trace metal pollution in Kaoping coastal sediment, southwestern Taiwan. *Marine Pollution Bulletin*, 49: 986–998.

Hunter, K.A., Kim, J.P., and Croot, P.L. (1997). Biological roles of trace metals in natural waters. *Environmental Monitoring and Assessement*, 44: 103-147.

Jetter, H. W. (2000). Determining the ages of recent sediments using measurements of trace radioactivity. *Terra et Aqua*, 78: 21-28

Jiang, G. B., Shi, J. B., and Feng, X. B. (2006). Mercury pollution in China. *Environment, Science and Technology*, 40: 3672–3678.

Johnsson, M. J. (1993). Tectonic versus chemical-weathering controls on the composition of fluvial sands in tropical environments. *Sedimentology*, 37: 713-726.

Julshamn, K., Duinker, A., Frantzen, S., Torkildsen, L., and Maage, A. (2008). Organ distribution and food safety aspects of cadmium and lead in great scallops, Pecten maximus l., and horse mussels, Modiolus modiolus l., from Norwegian waters. *Bulletin of Environmental Contamination and Toxicology*, 80: 385-389.

Junner, N. R., Hirst T. and Service H. (1942). *Tarkwa Goldfield*. Memoir No.6. Gold Coast Geological Survey. 75pp.

Kamaruzzaman, B. Y., Shazili, N. A. M., and Mohd Lokman, H. (2002). Particle size distribution in the bottom sediment of the Kemaman River Estuarine System, Terengganu, Malaysia. *Pertanika Journal of Agriculture*, 25: 149-155.

Kampa, M., and Castanas, E. (2008). Human health effects of air pollution. *Environmental Pollution*, 151: 362-367.

Kasper-Zubillaga, J.J., Dickinson, W.W. (2001), Discriminating depositional environments of sands from modern source terranes using modal analysis: *Sedimentary Geology*, 143: 149-167.

Kennish, M.J., ed. (1997) *Practical Handbook of Estuarine and Marine Pollution*. Boca Raton, USA: CRC Press: 524 pp.

Kesse, G. O. (1985). *The Mineral and Rock Resources of Ghana*. AA/ Balkema/Rotterdam/ Boston. 610pp.

Kim, G., Alleman, L.Y., and Church, T.M. (2004). Accumulation records of radionuclides and trace metals in two contrasting Delaware salt marshes. *Marine Chemistry*, 87: 87– 96.

Koranteng, K. A. (1984). A trawling survey off Ghana. CECAF/TECH/84/63 CECAF Project, Dakar: (FAO); 72pp.

Koranteng, K.A. (1995). Fish and fisheries of three coastal lagoons in Ghana. Global Environmental Facility and Ghana Coastal Wetlands Management Project. GW/A /SF2/3 285pp.

Korsch, R.J. (1984). Geological aspects of the Torlesse complex, south coast of Wellington. Geological Society of New Zealand Miscellaneous Publications, 31B: 67-90.

Kozelka, P.B., and Bruland, K. (1998). Chemical speciation of dissolved Cu, Zn, Cd, Pb in Narragansett Bay, Rhode Island. Marine Chemistry, 60: 267–282.

Krissek, L. A., and Horner, T. C. (1988). A preliminary study of REE distributions in mudrocks of the Permian Beacon Supergroup, Central Transantarctic Mountains: Evidence for early development and preservation of LREE enrichment: *American Association of Petroleum Geologists Bulletin*, 72: 208 pp.

Krissek, L.A., and T.C. Homer. (1987). Provenance evolution recorded by fine-grained Permian clastics, central Transantarctic Mountains. Antarctic Journal of the United States, 22(5): 26-28.

Kwei, E. A. (1974). The coastal lagoons in Ghana and the ecology of the crab, Callinectes latimanus (Rathburt). (PhD Thesis.) University of Ghana. 344 pp.

La Verle, B. (1994). *Ghana: A country study*. Washington, D.C., Federal Research Division, Library of Congress.

Laar, C., Fianko, J.R., Akiti, T.T ., Osae, S. and Brimah, A.K. (2011). Determination of heavy metals in the blackchin tilapia from the Sakumo Lagoon, Ghana. *Research Journal of Environment and Earth Sciences*, 3(1): 8-13.

Lacerda L. D. and Salomons W. (1998). *Mercury from Gold and Silver Mining: A chemical Time Bomb?* Springer-Verlag Berlin Heidelberg Publishers, New York. 146pp.

Lahaye, V., Bustamante P., Dabin W., Van Canneyt O., Dhermain F., Cesarini C., Pierce G.J., and Caurant F. (2006). New insights from age determination on toxic element accumulation in striped and bottlenose dolphins from Atlantic and Mediterranean waters. *Marine Pollution Bulletin*, 52: 1219–1230.

Laird, M.G., 1972. Sedimentology of the Greenland Group in the Paparoa Range, West Coast, South Island. *New Zealand Journal of Geology and Geophysics*, 15: 372-393.

Laissaoui, A., Benmansour, M., Ziad, N., Ibn, M.M., Abril, J.M., and Mulsow, S. (2008). Anthropogenic radionuclides in the water column and a sediment core from the Alboran Sea: application to radiometric dating and reconstruction of historical water column radionuclide concentrations. *Journal of Paleolimnology*, 40(3): 823-833

Landis, C.A., (1980). Little Ben Sandstone, Maitai Group (Permian): nature and extent in the Holly- ford-Eglington region, South Island, New Zealand. *New Zealand Journal of Geology and Geophysics*, 23: 551-567.

Lei, M., Liao, B., Zeng, Q., Qin, P., and Khan, S. (2008). Fraction distribution of lead, cadmium, copper, and zinc in metal contaminated soil before and after extraction with disodium ethylenediaminetetraacetic acid. *Communications in Soil Science and Plant Analysis*, 39: 1963–1978.

Leonard, A., and Gerber, G. B. (1989). Zinc toxicity: does it exist? *Journal of the American College of Toxicology*, 8:1285-1290.

Libes, S. (2009). *An introduction to marine biogeochemistry*. 2nd Edition, Elsevier Academic Press. 928pp.

Liu, M., Lia, Y., Zhanga, W., and Wang, Y. (2013). Assessment and Spatial distribution of zinc pollution in agricultural soils of Chaoyang, China. *Procedia Environmental Sciences*, 18: 283 – 289.

Lotze, H.K., and Worm, B. (2009). Historical baselines for large marine animals. *Trends in Ecological Evolutions*, 24: 254-262.

Luo, Q.Y., Zhao, W., Zhang, F., and Zhang, Z.Z. (2011). Analyses on blood lead testing of 0 through 6-year-old children in Meizhou, Guangdong Province. Xian Dai Yu Fang Yi Xue, 38: 614–615.

Mackay, D. (1991). *Multimedia Environmental Fate Models*: *The Fugacity Approach*. Lewis Publishers, Boca Raton, FL. 272pp.

MacKinnon, T.C. (1983). Origin of the Torlesse terrane and coeval rocks. South Island, New Zealand. *Bulletin of the Geological Society of America*, 94: 967-985.

Martins, S.E., and Bianchini, A. (2008). Copper accumulation and toxicity in the Plata pompano *Trachinotus marginatus* Cuvier 1832 (Teleostei, Carangidae). *Pan-American Journal of Aquatic Sciences,* 3: 384-390.

McLennan, S.M. (1993). Weathering and global denudation: *Journal of Geology*, 101: 295– 303.

McLennan, S.M., Hemming, S., McDaniel, D.K., and Hanson, G.N. (1993): Geochemical approaches to sedimentation, provenance, and tectonics. Processes Controlling the Composition of Clastic Sediment, Geological Society of America, Colorado. Geological Society of Americal. *Special publication*, 284: 21–40.

Melamed, D. (2005). Monitoring arsenic in the environment: A review of science and technologies with the potential for field measurements. *Analytica Chimica Acta*, 532: 1-13.

Merian, E. (1991). *Metal and their compound in the environmen*t. Weinheim Verlag chemie, Weinheeim, 365pp.

Mielke, H.W., Gonzales, C.R., Powell, E., Jartun, M., and Mielke Jr., P.W. (2007). Nonlinear association between soil lead and blood lead of children in

metropolitan New Orleans, Louisiana: 2000-2005. *Science of the Total Environment*, 388: 43-53.

Mil-Homens, M., Branco, V., Vale, C., Boer, W., Alt-Epping, U., Abrantes, F., and Vicente, M. (2009). Sedimentary record of anthropogenic metal inputs in the Tagus prodelta (Portugal). *Continental Shelf Research*, 29: 381-392.

Morel, F.M.M., Hudson, R.J.M., and Price, N.M. (1991). Limitation of productivity by trace metals in the sea. *Limnology and Oceanography*, 36: 1742-1755.

Morford J. L., Martin W.R., Kalnejais L., Francois R., Bothner M. and Karle I.-M. (2007). Insights on geochemical cycling of U, Re and Mo from seasonal sampling in Boston Harbor, Massachusetts, U.S.A. *Geochimica et Cosmochimica Acta*, 71(4): 895-917.

Morillo, J., Usero, J., and Rojas, R. (2008). Fractionation of metals and As in sediment from a biosphere reserve (Odiel salt marshes) affected by acidic mine drainage. *Environmental Monitoring and Assessment*, 139: 329–337.

Morris, A.W. (1975). Dissolved molybdenum and vanadium in the northeast Atlantic Ocean. *Deep-Sea Research*, 22: 49–54.

Morton, B., and Blackmore, G. (2001). South China Sea. *Marine Pollution Bulletin*, 42: 1236-1263.

Naito, W., Miyamoto, K., Nakanishi, J., Masunaga, S. and Bartell, S. (2002). Application of an Ecosystem Model for Aquatic Ecological Risk Assessment of Chemicals for a Japanese Lake. *Water Research*, 36: 1–14.

Nameroff, T.J., Balistrieri, L.S., and Murray, J.W. (2002). Suboxic trace metal geochemistry in the eastern tropical North Pacific. *Geochemica et Cosmochimica Acta*, 66: 1139–1158.

Nesbitt, H. W. and Young, G. M. (1996). Petrogenesis of sediment in the absence of chemical weathering: effects of abrasion and sorting on bulk composition and mineralogy. *Sedimentology*, 43: 341-358.

Nesbitt, H. W., Fedo, C. M. and Young, G. M. (1997). Quartz and feldspar stability, steady and non-steadystate weathering, and petrogenesis of siliclastic sands and muds. *Journal of Geology*, 105: 173–191.

Nesbitt, H.W. and Young, G.M. (1982). Early Proterozoic climates and plate motions inferred from major element chemistry of Lutites. *Nature*, 299: 715-717.

Nesbitt, H.W., and Young, G.M. (1984). Prediction of some weathering trends of plutonic and volcanic rocks based on thermodynamic and kinetic considerations. *Geochimica et Cosmochimica Acta*, 48: 1523-1534.

Nesbitt, H.W., and Young, G.M. (1989). Formation and diagenesis of weathering profiles: *Journal of Geology*, 97: 129–147.

Nesbitt, H.W., Young, G.M., McLennan, S.M. and Keays, R.R. (1996). Effects of chemical weathering and sorting on the petrogenesis of siliciclastic sediment, with implications for provenance studies. *Journal of Geology*, 104: 525-542.

Nriagu, J. O. and Wong, H. K. (1983). Selenium Pollution of lakes near the smelters of Sudbury, Ontario, *Nature*, 301: 55-57.

Nriagu, J.O. (1990), Human influence on the global cycling of trace metals. *Palaeogeography, Palaeoclimatology and Palaeoecology*, 82: 113 – 120.

Nriagu, J.O. and Pacyna, J.M. (1988). Quantitative assessment of worldwide contamination of air, water and soils by trace metals. *Nature*, 333: 134-139.

O'Reilly J, Vintró, L.L., Mitchell, P. (2011). ^{210}Pb-dating of a lake sediment core from Lough Carra (Co. Mayo, western Ireland): Use of paleolimnological data for

chronology validation below the ^{210}Pb dating horizon. *Journal of Environmental Radioactivity*, 102: 495–499.

Ofosu-Mensah, E.A. (2011). Gold mining and the socio-economic development of Obuasi in Adanse. *African Journal of History and Culture*, 3(4): 54-64,

Osae, S., Asiedu, D.K., Yakubo, B., Koeberl, C., Dampare, S.B. (2006). Provenance and tectonic setting of Late Proterozoic Buem sandstones of southeastern Ghana: Evidence from geochemistry and detrital modes. *Journal of African Earth Science*, 44: 85–96.

Pacyna, J.M., and Pacyna, E.G. (2001). An assessment of global and regional emissions of trace metals to the atmosphere from anthropogenic sources worldwide. *Environmental Reviews*, 9: 269-298.

Pan, K., and Wang, W.X. (2012). Trace metal contamination in estuarine and coastal environments in China. *Science of the Total Environment*, 421–422, 3–16.

Parizanganeh, A. (2008). Grain size effects on trace metals along the Iranian Coast of the Caspian Sea. Proceeding of Taal 2007 World Lake Conference, 329-336 pp.

Park, R.A., Clough, J.S., and Wellman, M.C. (2008). AQUATOX: modeling environmental fateand ecological effects in aquatic ecosystems. *Ecological Modelling*, 213: 1–15.

Parker, A. (1970). An index of weathering for silicate rocks. *Geological Magazine*, 103: 501-504.

Pennington, W., T. C. Tutin, R. S. Cambray, J. D. Eakins, and D. D. Harkness. 1976. Radionuclide dating of recent sediments of Blelham Tarn. *Freshwater Biology*, 6: 317-331.

Pettersson, L., Andersson, I., and Gorzsas, A. (2003). Speciation in peroxovanadate systems. *Coordination Chemistry Revews*, 237: 77–87.

Pizzuto, J. E. (1995). Downstream fining in a network of gravel-bedded rivers, *Water Resources Research*, 31: 753– 759.

Pratt, D.R., Pilditch, C.A., Lohrer, A.M., and Thrush S.F. (2012),. The effects of short-term increases in turbidity on sandflat microphytobenthic productivity and nutrient fluxes. http://dx.doi.org/10.1016/j.seares.2013.07.009. (in press)

Preiss, N., Mélières, M.A., and Pourchet, M. (1996). A compilation of data on lead-210 concentration in surface air and fluxes at the airsurface and water-sediment interfaces. *Journal of Geophysical Research*, 101(22): 28847–28862.

Preziosia, D.V., and Pastorok, R.A. (2008). Ecological food web analysis for chemical risk assessment. *Science of the Total Environment,* 406: 491–502.

Price, J. R., and Velbel M. A. (2003). Chemical weathering indices applied to weathering profiles developed on heterogeneous felsic metamorphic parent rocks. *Chemical Geology*, 202: 397-416.

Queralt, I., Barreiros, M.A., Carvalho, M.L., Costa, M.M., (1999). Application of different techniques to assess sediment quality and point source pollution in low-level contaminated estuarine recent sediments (Lisboa coast, Portugal). *Science of Total Environment,* 241 (1–3): 39–51.

Rajeeva, R., Rekha, R., Ashay, B., Shivadhar, S., and Madhusudan, C. (2012). Speciation of arsenic across water-sediment interface of Falgu river. *American Journal of Environmental Science*, 8: 615-621.

Randall, P.M., Chattopadhyay S. (2013). Mercury contaminatedsedimentites- An evaluation of remedial options. *Environmental Research*, 125: 131–149.

Rehder, D. (2000). Vanadium nitrogenase. *Journal of Inorganic Biochemistry*, 80: 133–136.

Reimann, C., and de Caritat, P. (2005). Distinguishing between natural and anthropogenic sources of element in the environment: regional geochemical surveys versus enrichment factors. *Science of the Total Environment, 337*: 91-107.

Rice, H.W., and Morel, F.M.M. (1990). Availability of well-defined iron colloids to the marine diatom *Thalassiosira weissflogii*. *Limnology and Oceanography*, 35: 652–662.

Ridgway, J., and Shimmield, G. (2002). Estuaries as repositories of historical contamination and their impact on shelf seas. *Estuarine, Coastal and Shelf Science*, 55: 903–928.

Ritson, P.I., Bouse, R.M., Flegal, A.R., and Luoma, S.N. (1999). Stable lead isotopic analyses of historic and contemporary lead contamination of San Francisco Bay estuary. *Marine Chemistry*, 64: 71–83.

Robbins, J.A. (1978). Geochemical and Geophysical applications of radioactive lead isotopes. In: Nriago, J.P. (Ed.), Biochemistry of Lead in the Environment. Elsevier, Amsterdam, 285–393pp.

Robinson, L.A., Rogers, S., and Frid, C.L.J. (2010). Methodology for assessing the status of species and habitats at the OSPAR Region scale for the OSPAR Quality Status Report. (Contract No: C-08-0007-0085 for the Joint Nature Conservation Committee). University of Liverpool, Liverpool and Centre for the Environment, Lowestoft. Fisheries and Aquaculture Science. 250pp.

Rosenberg, R., and Costlow, J.D. (1979). Delayed response to irrevisisble non-genetic adaptation to salinity in early development of the brachyuran crab *Rhithropanopeus harrisii* and some notes on adaptation to temperature. *Ophelia*, 18: 97-112.

Roser, B. P., and Korsch, R. J., (1986). Determination of tectonic setting of sandstones and mudstones suites using SiO_2 content and K_2O/Na_2O ratio: *Journal of Geology*, 94: 635-650.

Roser, B.P., and Korsch, R.J. (1988). Provenance signature of sandstone-mudstone suite determined using discriminant function analysis of major element data. *Chemical Geology*. 67: 119–139.

Roy, P.D., Caballero, M., Lozano, R., Smykatz-Kloss, W. (2008). Geochemistry of Late Quaternary sediments from Tecocomulco lake, central Mexico: implication to chemical weathering and provenance: *Chemie der Erde-Geochemistry*, 68: 383-393.

Rudnick, R.L., and Gao, S. (2003) The Composition of the Continental Crust, pp. 1-64. In The Crust (ed. R.L. Rudnick) Vol. 3, Treatise on Geochemistry (eds. H.D. Holland and K.K. Turekian), Elsevier-Pergamon, Oxford. 1–64pp

Ruiz-Fernández, A.C., Frignani, M., Hillaire-Marcel, C., Ghaleb, B., Arvizu, M.D., Raygoza-Viera, J.R., Páez-Osuna, F. (2009a). Trace metals (Cd, Cu, Hg and Pb) accumulation recorded in the intertidal mudflat sediments of three coastal lagoons in the Gulf of California, Mexico. *Estuaries and Coasts*, 32: 551–564.

Ruiz-Fernández, A.C., Páez-Osuna, F., Machain-Castillo, M.L., Arellano-Torres, E. (2004). ^{210}Pb geochronology and trace metal fluxes (Cd, Cu and Pb) in the Gulf of Tehuantepec, South Pacific of Mexico. *Journal of Environmental Radioactivity*, 76 (1–2): 161–175.

Ruiz-Fernandeza, A.C., Hillaire-Marcel, C., and Paez-Osuna F., Ghaleba, B., Soto-Jimenez M. (2003). Historical trends of metal pollution recorded in the sediment of the Culiacan River Estuary, Northwestern Mexico. *Applied Geochemistry*, 18: 577-588.

Ruxton, B.P. (1968). Measures of the degree of chemical weathering of rocks. *Journal of Geology*, 76: 518–527.

Sadiq, M. (1988). Thermodynamic solubility relationships of inorganic vanadium in the marine environment. *Marine Chemistry*, 23: 87–96.

Sakshaug, E. (1997). Biomass and productivity distributions and their variability in the Barents Sea. *ICES Journal of Marine Science*, 54: 341–350.

Salomons, W. (1995). Environmental impact of metals derived from mining activities: Processes, predictions, prevention. *Journal of Geochemical Exploration*, 52: 5-23.

Santschi, P. H., Lenhart, J. J., and Honeyman, D. (1997). Heterogeneous processes affecting trace metal contaminant distribution in estuaries: The role of natural organic matter. *Marine Chemistry*, 8: 99-125.

Schäfer, J., Blanc, G., Lapaquellerie, Y., Maillet, N., Maneux E., and Etcheber, H. (2002). Ten-year observation of the Gironde tributary fluvial system: fluxes of suspended matter, particulate organic carbon and cadmium, *Marine Chemistry*, 79: 229–242.

Schiff, K., and Gossett. R. (1998). Southern California Bight 1994 Pilot Project: III Sediment Chemistry. Technical Report 306. Southern California Coastal Water Research Project. Westminster, CA. 260pp

Schropp, S.J., Windom, H.L. (1988). A Guide to the Interpretation of Metal Concentrations in Estuarine Sediments. Coastal Zone Management Section, Florida, 1-44pp.

Schulz, H.D. and Zabel M. (2006). *Marine Geochemistry*. 2nd ed. Springer-Verlag Berlin Heideberg, Germany.

Schwab, F.L. (1975). Framework mineralogy and chemical composition of continental margin type sandstone. *Geology*, 3: 487–490.

Schwertmann, U and G. Pfab (1994). Structural vanadium in synthetic geothite, *Geochimica et Cosmochimica Acta*, 58: 4349-4352.

Senesi, G.S. , Baldassarre, G., Senesi, N., and Radina, B. (1999). Trace element inputs into soils by anthropogenic activities and implications for human health. *Chemosphere*, 39: 343–77.

SETAC (Society for Environmental Toxicology and Chemistry) (1994). Pesticide Risk and Mitigation. Final Report of the Aquatic Risk Assessment and Mitigation Dialog Group, SETAC Foundation for Environmental Education, Pensacola, FL. 220 pp.

Shkolnik, M. Y. (1984). *Trace elements in plants*. Developments in Crop Science, Elsevier. 6: 463pp

Siddiq, M. (1989). Nickel sorption and speciation in a marine environment. *Hydrobiologia*, 176: 225-232.

Siddique, A., Mumtaz, M., Zaigham, N.A., Mallick, K.A., Saied, S., Zahir, E., and Khwaja, H.A. (2009). Heavy metal toxicity levels in the coastal sediment of the Arabian Sea along the urban Karachi (Pakistan) region. *Marine Pollution Bulletin*, 58: 1406–1414.

Siddique, A., Mumtaz, M., Zaigham, N.A., Mallick, K.A., Saied, S., Zahir, E., and Khwaja, H.A. (2009). Heavy metal toxicity levels in the coastal sediment of the Arabian Sea along the urban Karachi (Pakistan) region. *Marine Pollution Bulletin*, 58: 1406–1414.

Sinex, S. A. & Helz, G. R. (1981). Regional geochemistry of trace elements in Chesapeake Bay sediment. *Environmental Geology*, 3: 315–323.

Singh, P. and Rajamani, V. (2001). REE geochemistry of recent clastic sediment from the Kaveri floodplains, southern India: Implications to source weathering and sedimentary processes. *Geochimica Cosmochimica Acta*, 65: 3093-3108.

Smedley, P.L., and Kinniburgh, D.G. (2002). A review of the source, behaviour and distribution of arsenic in natural waters. *Applied Geochemistry*, 17: 517–568.

Solomon, K. R., and Sibley P. (2002). New concepts in ecological risk assessment: where do we go from here? *Marine Pollution Bulletin*, 44: 279–285.

Solomon, K.R., Baker, D.B., Richards, P., Dixon, K.R., Klaine, S.J., La Point, T.W., Kendall, R.J., Giddings, J.M., Giesy, J.P., Hall, L.W.J., Weisskopf, C., and Williams, M. (1996). Ecological risk assessment of atrazine in North American surface waters. *Environmental Toxicology and Chemistry*, 15: 31-36

Solomon, K.R., Giesy, J.P., and Jones, P. (2000). Probabilistic risk assessment of agrochemicals in the environment. *Crop Protection*, 19: 649-655.

Sonke, J.S., Lars-Eric Heimburger, L.E., and Dommergue, A. (2013). Mercury biogeochemistry: Paradigm shifts, outstanding issues and research needs. C. R. *Geoscience*, 345: 213–224.

Sorensen, T.H., Volund, G., Armah, A.K., Christiansen, C., Jensen, L.B., Pedersen, J.T. (2003). Temporal and Spatial variations in Concentrations of Sediment Nutrients and Carbon in the Keta Lagoon, Ghana. *West African Journal Applied Ecology*, 4: 91-105.

Storelli, M.M., Storelli, A., Giacominelli-Stuffler, R., Marcotrigiano, G.O., (2005). Mercury speciation in the muscle of two commercially important fish, hake (*Merluccius merluccius*) and striped mullet (*Mullus barbatus*) from the Mediterranean sea: estimated weekly intake. *Food Chemistry*, 89: 295–300.

Sunda, W.G. (1989). Trace metal interactions with marine phytoplankton. *Biological Oceanography*, 6: 411-442.

Sunda, W.G., and Huntsman, S.A. (1995). Cobalt and zinc inter-replacement in marine phytoplankton: biological and geochemical implications. *Limnology and Oceanography*, 40: 1404–1417.

Sutherland, R. A. (2000): Bed sediment associated trace metals in an urban stream, Oahu, Hawaii. *Environmental Geology*, 39: 611- 637.

Swarzenski, P.W., Baskaran, M., Rosenbauer, R.J Orem and W.H. (2006). Historical trace elements distribution in sediments from the Mississippi River Delta. *Estuaries and Coasts*, 29: 1094–1107.

Syvitski, J.P.M. (1991). Principles, methods and application of grain size analysis. Cambridge University Press, 368pp.

Syvitski, J.P.M., Peckham, S.D., Hilberman, R., and Mulder, T. (2003). Predicting the terrestrial flux of sediment to the global ocean: a planetary perspective. *Science*. 162: 5-24.

Szava-Kovats, R.C. (2008). Grain-size normalization as a tool to assess contamination in marine sediment: Is the <63 lm fraction fine enough? *Marine Pollution Bulletin*, 56: 629–632.

Takesue, R.K., and Swarzenski, P.W. (2011), More than 100 years of background-level sedimentary metals, Nisqually River Delta, South Puget Sound, Washington: U.S. Geological Survey. Open-File Report 2010-1329, 13pp.

Taylor, S.W., Kammerer, B., and Bayer, E. (1997). New perspectives in the chemistry and biochemistry of the tunichromes and related compounds. *Chemistry Reviews*, 97: 333–346.

Thompson, R., and Oldfield, F. (1986). *Environmental Magnetism*, Allen and Unwin, London. 227pp.

Tribovillard, N., Riboulleau A., Lyons T., and Baudin F. (2004) Enhanced trapping of molybdenum by sulfurized marine organic matter of marine origin in Mesozoic limestones and shales. *Chemical Geological*, 213: 385–401.

Tripathi, J.K., and Rajamani, V. (2003). Geochemistry of Delhi quartzites: implications for the provenance and source area weathering. *Journal of the Geological Society of India* 62: 215 –226.

Tsikata F. S. (1997). The vicissitudes of mineral policy in Ghana. *Resource Policy* 23 (1–2): 9–14

Turekian, K. K., Nozaki, Y. and Benninger, L. K. (1977). Geochemistry of atmospheric radon and radon products. Annu. Rev. *Earth and Planetary Science*, 5: 227–255.

Turnbull, I.M. (1979). Petrography of the Caples terrane of the Thomson Mountains, northern Southland. New Zealand. *New Zealand Journal of Geology and Geophysics*, 22:709-727.

Twining, J., Creighton, N., Hollins, S., and Szymczak, R. (2008). Probabilistic Risk Assessment and Risk Mapping of Sediment Metals in Sydney Harbour Embayments. Human and Ecological Risk Assessment: *An International Journal*, 14: 1202 -1225.

Twining, J., Perera, J., Vu Nguyen, V., and Brown, P. (2005). Computer code for aquatic ecological risk assessment (version 3.2) technical reference manual. Australian Nuclear Science and Technology Organisation, ANSTO/M-127 Vol.1. 38 pp.

Ullrich, S.M., Tanton, T.W., and Abdrashitova, S.A. (2001). Mercury in the aquatic environment: a review of factors affecting methylation. *Critical Reviews in Environment, Science and Technology*, 31: 241–293.

UNEP (United Nations Environmental Programme) (2008). Draft final review of scientific information on lead. UNEP Chemical Branch, DTIE. 99pp

UNEP (United Nations Environmental Programme) (2013). Global Mercury Assessment 2013: Sources, Emissions, Releases and Environmental Transport. UNEP Chemicals Branch, Geneva, Switzerland. 44pp

US (ACOE) Army Corps of Engineers, (1996). Risk assessment handbook. Volume II: Environmental evaluation. Manual EM, Washington, DC. 200: 1-4pp

US (EPA) Environmental Protection Agency (1998). Guidelines for ecological risk assessment. Risk Assessment Forum, Washington, D.C. EPA/630/R-95/002F.

USEPA (United States Environmental Protection Agency), (2004). Aquatox (Release 2). Modeling Environmental Fate and Ecological Effects in Aquatic Ecosystems, Technical Documentation. U.S. Environmental Protection Agency, Washington, DC. 2: 10pp.

Valavanidis, A., and Viachogianni, T. (2010). Metal Pollution in Ecosystems. Ecotoxicology Studies and Risk Assessment in the Marine Environment. *Science advances on Environment, Toxicology and Ecotoxicology issues*, 1-14 pp.

Vale, C., Canário, J., Caetano, M., Lavrado, J., Brito, P. (2008). Estimation of the anthropogenic fraction of elements in surface sediments of the Tagus Estuary (Portugal). *Marine Pollution Bulletin*, 56: 1364–1367.

Van Straalen, N.M., and Denneman C.A.J.. (1989). Ecotoxicological evaluation of soil quality criteria. *Ecotoxicology, Environment and Safety*,18: 241-251.

Villas Boas, R. C, Beinhoff, C. and da Silva, A. R. (2001). Mercury in the Tapajos basin. UNIDO Workshop in Belem, Para, Brazil. 203pp.

von Eynatten, H., Barcelo-Vidal, C., Pawlowsky-Glahn, V. (2003). Composition and discrimination of sandstones: a statistical evaluation of different analytical methods. *Journal of Sedimentary Research*, 73: 47–57

Vorlicek T. P., Kahn M. D., Kasuya Y., and Helz G. R. (2004) Capture of molybdenum in pyrite-forming sediment; role of ligand-induced reduction by polysulfides. *Geochimica et Cosmochimica Acta*, 68: 547–556.

Wang, B., Yu, G., Jun, H., Wang, T., and Hu, H.Y. (2010). Probabilistic ecological risk assessment of DDTs in the Bohai Bay based on a food web bioaccumulation model. *Science of the Total Environment*, 409: 495–502.

Wang, D., and Sañudo-Wilhelmy, S.A. (2008). A rapid method of separating different chemical species of dissolved vanadium in seawater. *Marine Chemistry*, 112: 72–80.

Water Resources Commission (2012). Pra River Basin-Integrated Water Resources Managemen Plan. 53pp.

Weatherley, A. H., Lake, P. S., and Rogers, S.C. (1980). Zinc pollution and the ecology of the freshwater environment. In Nriagu, J. O. editor. Zinc in the environment. Part I: ecological cycling. John Wiley, New York. 337-417pp

Weltje, G.J. (2004). Ternary sandstone composition and provenance: an evaluation of the Dickinson model. *Geological Society of London's Special* Publications, 264: 79–99.

Weltje, G.J. and von Eynatten, H. (2004). Quantitative provenance analysis of sediment: review and outlook. *Sedimentary Geology*, 171: 1 – 11.

Wiener, J.G. and Spry, D.J. (1996). Toxicological significance of mercury in freshwater fish. In: Environmental Contaminants in Wildlife. Beyer, W.N., G.H. Heinz, and A.W. Redmon-Norwood (eds). Lewis Publisher, Boca Raton, FL. 297-339pp

Xu, B., Yang, X., Gu, Z., Yanhui Zhang, Y., Chen, Y.M., and Lv, Y. (2009). The trend and extent of heavy metal accumulation over last one hundred years in the Liaodong Bay, China. *Chemosphere*, 75: 442–446.

Yan, D.T., Chen, D.Z., Wang, Q.C. and Wang, J.G. (2010). Large-scale climatic fluctuations in the latest Ordovician on the Yangtze block, south China. *Geology*, 38: 599–602.

Yang, X.G., Wang, K., Lu, J., and Crans, D.C. (2003). Membrane transport of vanadium compounds and interaction with the erythrocyte membrane. *Coordination Chemistry Reviews*, 273: 103–111.

Yen, J.Y., and Lundberg, N. (2006). Sediment compositions in offshore southern Taiwan and their relations to the source rocks in Modern Arc-Continent Collision Zone. *Marine Geology*, 225: 247-63.

Yue, T.X., Wang, Y.A., Chen, S.P., Liu, J.Y., Qiu, D.S., and Deng, X.Z. (2003). Numerical simulation of population distribution in China. *Population Environment*, 25: 141–63.

Zhang, L., Liu, J., Li, Y., and Zhao, Y. (2013). Applying AQUATOX in determining the ecological risk assessment of polychlorinated biphenyl contamination in Baiyangdian Lake, North China. *Ecological Modelling*, 265: 239– 249.

Zhang, M., Reardon, E.J. (2007). Removal of B, Cr, Mo, and Se from wastewater by incorporation into hydrocalumite and ettringite. *Environment, Science and Technology*, 37(13): 2947–2952.

Zheng, Y., Anderson, R.F., van Geen, A., and Kuwabara, J. (2000). Authigenic molybdenum formation in marine sediment: a link to porewater sulfide in the Santa Barbara Basin. *Geochimica et. Cosmochimica Acta*, 64: 4165–4178.

Zobrist, J., Dowdle, P.R., Davis, J.A., and Oremland, R.S. (2000). Mobilization of arsenite by dissimilatory reduction of adsorbed arsenate. *Environment, Science and Technology*, 34: 4747-4753.

APPENDIX A

Appendix A1. Preparation of core sections for analysis

Appendix A2. Sediments Digestions Methods

Methods	Steps
1 (Two steps)	2ml of H_2O_2 + sample cooked to dryness in Teflon beakers; 2ml of 6N HCL+ 2ml of 14N HNO_3 + 1ml of 26N HF cooked to dryness in Teflon beakers; and made up to 10ml (1ml HNO_3 + 9ml Milli Q)
2 (Three steps)	2ml of H_2O_2 + sample cooked to dryness; 2ml of 6N HCL + 2ml of 14N HNO_3 cooked to dryness; 1ml of 6N HCL + 1ml of 26N HF cooked to dryness; and made up to 10ml (1ml HNO_3 +9ml Milli Q)
3 (Four steps/Bomb digestion)	2ml of H_2O_2 cooked to dryness in Teflon beakers; 2ml of 6N HCL + 2ml of 14N HNO_3 in Teflon bombs; Add 1ml of 6N HCL + 1ml of 26N HF cooked to dryness in Teflon bombs; and made up to 10ml (1ml HNO_3 +9ml Milli Q
4 (Four steps)	1ml of H_2O_2 cooked to dryness; 1 ml of H_2O_2 cooked to dryness; 2ml of 6N HCL + 14N HNO_3 cooked to dryness; 1ml of 6N HCL +2ml of 26N HF cooked to dryness; and made up 10ml (1ml HNO_3 +9ml Milli Q)

Appendix A3. Grain size analysis of the sediment core from the Ankobra estuary

Depth (cm)	Mean **(µm)**	Mode **(µm)**	Mean/Median Ratio	SD **(µm)**	Variance **(µm)**	Skewness	Kurtosis	Descrition
0-2	36.97	96.49	0.72	3.40	11.57	-1.88	4.25	Coarse silt, poorly sorted
2-4	37.83	80.07	0.75	3.43	11.73	-1.84	3.89	Coarse silt, poorly sorted
4-6	28.71	55.13	0.71	3.73	13.91	-1.45	2.37	Medium silt, poorly sorted
6-8	33.30	55.13	0.71	3.40	11.55	-1.72	3.58	Coarse silt, poorly sorted
8-10	28.11	50.22	0.73	3.48	12.10	-1.38	2.29	Medium silt, poorly sorted
10-12	30.70	87.90	0.65	3.69	13.59	-1.42	1.82	Medium silt, poorly sorted
12-14	33.64	55.24	0.81	3.23	10.42	-2.04	4.80	Coarse silt, poorly sorted
14-16	36.89	96.49	0.71	3.64	13.26	-1.73	2.73	Coarse silt, poorly sorted
16-18	38.36	96.49	0.74	3.45	11.87	-1.59	2.75	Coarse silt poorly sorted
18-20	38.26	87.90	0.75	3.86	14.89	-1.04	0.71	Coarse silt, poorly sorted
20-22	30.81	96.49	0.73	3.59	12.89	-1.27	1.71	Medium silt, poorly sorted
22-24	27.47	55.27	0.70	3.70	13.68	-1.26	1.34	Medium silt, poorly sorted
24-26	31.75	96.49	0.72	3.67	13.48	-1.31	1.81	Coarse silt, poorly sorted
26-28	30.70	87.90	0.65	3.69	13.59	-1.42	1.82	Medium silt, poorly sorted
28-30	28.95	96.49	0.74	3.84	14.72	-1.07	0.96	Medium silt, poorly sorted
30-32	28.71	55.13	0.71	3.73	13.91	-1.45	0.96	Medium silt, poorly sorted
32-34	30.75	105.90	0.73	2.86	8.19	-2.63	8.12	Medium silt, poorly sorted
34-36	31.86	96.49	0.59	3.92	15.37	-1.33	1.31	Coarse silt, poorly sorted
36-38	31.86	96.49	0.59	3.92	15.37	-1.33	1.31	Coarse silt, poorly sorted
38-40	30.81	96.49	0.73	3.59	12.89	-1.27	1.71	Medium silt, poorly sorted

Appendix A4. Grain size analysis of the sediment core from the Pra estuary

Depth (cm)	Mean **(µm)**	Mode **(µm)**	Mean/Meidan Ratio	SD **(µm)**	Variance **(µm)**	Skewness	Kurtosis	Description
0-2	39.27	66.44	0.74	3.54	12.55	-1.57	3.06	Coarse silt, poorly sorted
2-4	25.66	60.52	0.71	3.50	12.24	-1.41	1.98	Medium silt, poorly sorted
4-6	41.17	60.52	0.78	3.42	11.70	-1.70	4.01	Coarse silt, poorly sorted
6-8	25.60	50.22	0.71	3.49	12.17	-1.44	2.17	Medium silt, poorly sorted
8-10	34.91	55.13	0.77	3.49	12.17	-1.59	3.42	coarse silt, poorly sorted
10-12	25.54	55.13	0.71	3.51	12.29	-1.53	2.58	Medium silt, poorly sorted
12-14	35.22	60.52	0.74	3.55	12.60	-1.54	2.99	Coarse silt, poorly sorted
14-16	15.90	37.97	0.78	3.30	10.92	-1.12	0.93	Medium silt, poorly sorted
16-18	23.61	50.22	0.76	3.33	11.12	-0.98	0.92	Medium silt, poorly sorted
18-20	26.78	59.35	0.73	3.35	11.21	-1.95	4.72	Coarse silt, poorly sorted
20-22	27.61	50.22	0.73	3.74	14.00	-1.09	1.12	Medium silt, poorly sorted
22-24	33.10	55.13	0.74	3.93	15.43	-1.16	1.62	Coarse silt, poorly sorted
24-26	25.88	50.22	0.74	3.74	13.96	-1.02	0.96	Medium silt, poorly sorted
26-28	25.58	96.49	0.69	3.61	13.03	-1.21	1.17	Medium silt, poorly sorted
28-30	31.46	60.52	0.71	4.08	16.61	-0.98	0.63	Coarse silt, poorly sorted
30-32	27.10	96.49	0.66	3.76	14.13	-1.16	0.86	Medium silt, poorly sorted
32-34	34.34	60.52	0.76	3.54	12.53	-1.71	3.31	Coarse silt, poorly sorted
34-36	35.62	60.52	0.67	3.53	12.45	-1.76	3.50	Coarse silt, poorly sorted
36-38	31.82	60.52	0.70	3.55	12.62	-1.69	3.45	Coarse silt, poorly sorted
38-40	26.66	50.22	0.74	3.54	12.55	-1.09	-0.34	Medium silt, poorly sorted

Appendix A5. Grain size analysis of the sediment core from the Amisa estuary

Depth (cm)	**Mean (µm)**	**Mode (µm)**	**Mean/Median Ratio**	**SD (µm)**	**Variance (µm)**	**Skewness**	**Kurtosis**	**Description**
0-2	22.49	125.90	0.64	3.32	10.99	-1.10	0.96	Medium Silt, Poorly Sorted
2-4	25.02	105.90	0.63	3.78	14.27	-1.01	0.60	Medium Silt, Poorly Sorted
4-6	20.69	105.90	0.55	3.32	10.99	-0.99	0.46	Medium Silt, Poorly Sorted
6-8	17.29	66.44	0.75	3.49	12.21	-0.99	0.41	Medium Silt, Poorly Sorted
8-10	16.50	66.44	0.75	3.45	11.90	-1.00	0.42	Medium Silt, Poorly Sorted
10-12	18.34	66.44	0.74	3.48	12.10	-0.99	0.37	Medium Silt, Poorly Sorted
12-14	17.29	66.44	0.75	3.49	12.21	-0.99	0.41	Medium Silt, Poorly Sorted
14-16	18.37	66.44	0.72	3.50	12.22	-0.99	0.55	Medium Silt, Poorly Sorted
16-18	18.35	66.44	0.73	3.49	12.17	-0.99	0.43	Medium Silt, Poorly Sorted
18-20	16.50	66.44	0.75	3.45	11.90	-0.99	0.42	Medium Silt, Poorly Sorted
20-22	18.05	66.44	0.72	3.47	12.03	-0.99	0.49	Medium Silt, Poorly Sorted
22-24	18.14	66.44	0.74	3.43	11.76	-0.99	0.56	Medium Silt, Poorly Sorted
24-26	17.98	66.44	0.73	3.49	12.20	-0.99	0.41	Medium Silt, Poorly Sorted
26-28	18.70	66.60	0.73	3.45	11.91	-0.99	0.64	Medium Silt, Poorly Sorted
28-30	18.05	66.44	0.72	3.47	12.03	-0.97	0.49	Medium Silt, Poorly Sorted
30-32	17.23	66.44	0.76	3.49	12.18	-0.97	0.35	Medium Silt, Poorly Sorted
32-34	20.69	185.40	0.55	4.61	21.22	-0.95	0.39	Medium Silt, Poorly Sorted
34-36	25.29	105.90	0.70	3.32	10.99	-1.00	0.46	Medium Silt, Poorly Sorted
36-38	18.34	66.44	0.74	3.48	12.10	-0.97	0.37	Medium Silt, Poorly Sorted
38-40	18.34	66.44	0.74	3.48	12.10	-0.97	0.37	Medium Silt, Poorly Sorted

Appendix A6. Grain size analysis of the sediment core from the Densu estuary

Depth (cm)	Mean (μm)	Mode (μm)	Mean/Median Ratio	SD (μm)	Variance (μm)	Skewness	Kurtosis	Description
0-2	88.33	185.40	0.72	3.09	9.57	-2.39	7.15	Very fine sand, poorly sorted
2-4	77.53	140.10	0.73	3.67	13.45	-1.56	4.28	Very fine sand, poorly sorted
4-6	85.10	127.60	0.78	3.93	15.42	-1.32	2.94	Very fine sand, poorly sorted
6-8	85.74	140.10	0.75	3.54	12.52	-1.76	4.36	Very fine sand, poorly sorted
8-10	78.55	140.10	0.74	3.60	12.92	-1.46	2.78	Very fine sand, poorly sorted
10-12	69.84	127.60	0.73	3.73	13.88	-1.59	3.18	Very fine sand, poorly sorted
12-14	73.58	140.10	0.70	3.53	12.43	-1.80	4.06	Very fine sand, poorly sorted
14-16	75.32	127.60	0.76	3.89	15.12	-1.33	2.85	Very fine sand, poorly sorted
16-18	75.49	127.60	0.76	3.73	13.93	-1.45	3.07	Very fine sand, poorly sorted
18-20	81.41	127.60	0.76	3.45	11.90	-1.78	4.51	Very fine sand, poorly sorted
20-22	49.25	127.60	0.62	3.57	12.74	-1.88	3.92	Coarse Silt, poorly sorted
22-24	53.93	153.80	0.60	3.74	13.96	-1.79	3.52	Coarse Silt, poorly sorted
24-26	78.86	140.10	0.76	3.75	14.03	-1.51	3.19	Very fine sand, poorly sorted
26-28	73.73	140.10	0.69	3.77	14.24	-1.71	3.05	Very fine sand, poorly sorted
28-30	75.69	140.10	0.70	3.41	11.61	-1.93	4.64	Very fine sand, poorly sorted
30-32	68.28	140.10	0.66	3.22	10.36	-2.19	5.55	Very fine sand, poorly sorted
32-34	68.54	140.10	0.64	3.29	10.80	-2.12	4.91	Very fine sand, poorly sorted
34-36	88.33	185.40	0.72	3.09	9.57	-2.39	7.15	Very fine sand, poorly sorted
36-38	83.15	185.40	0.71	3.03	9.15	-2.45	7.15	Very fine sand, poorly sorted
38-40	85.10	127.60	0.78	3.93	15.42	-1.32	2.94	Very fine sand, poorly sorted

Appendix A7. Grain size analysis of the sediment core from the Sakumo II estuary

Depth (cm)	Mean **(µm)**	Mode **(µm)**	Mean/Median Ratio	SD **(µm)**	Variance **(µm)**	Skewness	Kurtosis	Description
0-2	23.55	105.90	0.74	3.68	13.54	-0.90	0.35	Medium Silt, Poorly Sorted
2-4	16.05	66.44	0.79	3.26	10.60	-0.93	0.51	Medium Silt, Poorly Sorted
4-6	16.66	66.44	0.79	3.40	11.57	-0.91	0.39	Medium Silt, Poorly Sorted
6-8	13.68	60.54	0.82	3.20	10.26	-0.79	0.23	Fine Silt, poorly sorted
8-10	16.56	66.44	0.79	3.40	11.57	-0.91	0.39	Fine Silt, poorly sorted
10-12	13.18	55.13	0.82	3.12	9.75	-0.82	0.33	Fine Silt, poorly sorted
12-14	13.08	55.13	0.81	3.12	9.75	-0.82	0.33	Fine Silt, poorly sorted
14-16	13.11	60.52	0.85	3.19	10.16	-0.72	0.14	Fine Silt, poorly sorted
16-18	14.31	60.52	0.83	3.26	10.63	-0.78	0.16	Fine Silt, poorly sorted
18-20	14.29	60.52	0.83	3.26	10.63	-0.78	0.16	Fine Silt, poorly sorted
20-22	14.31	60.52	0.83	3.26	10.63	-0.78	0.16	Fine Silt, poorly sorted
22-24	12.48	55.13	0.85	3.12	9.73	-0.72	0.14	Fine Silt, poorly sorted
24-26	12.78	55.13	0.87	3.12	9.73	-0.72	0.14	Fine Silt, poorly sorted
26-28	9.43	37.97	0.87	3.13	9.82	-0.62	-0.11	Fine Silt, poorly sorted
28-30	13.08	55.13	0.81	3.12	9.75	-0.82	0.33	Fine Silt, poorly sorted
30-32	6.28	21.69	0.68	2.86	8.20	-0.69	-0.25	Very Fine Silt, poorly sorted
32-34	6.28	21.69	0.68	2.86	8.20	-0.69	-0.25	Very Fine Silt, poorly sorted
34-36	5.56	5.35	0.94	3.28	10.73	-0.32	-0.52	Very Fine Silt, poorly sorted
36-38	10.12	55.13	0.68	3.12	9.76	-0.69	-0.49	Fine Silt, poorly sorted
38-40	10.12	55.13	0.68	3.12	9.76	-0.69	-0.49	Fine Silt, poorly sorted

Appendix A8. Grain size analysis of the sediment core from the Volta estuary

Depth (cm)	**Mean (µm)**	**Mode (µm)**	**Mean/Median Ratio**	**SD (µm)**	**Variance (µm)**	**Skewness**	**Kurtosis**	**Description**
0-2	64.94	153.80	0.72	3.25	10.55	-2.20	5.77	Very fine sand, poorly sorted
2-4	64.94	153.80	0.72	3.25	10.55	-2.20	5.77	Very fine sand, poorly sorted
4-6	66.41	153.80	0.74	3.12	9.71	-2.36	6.82	Very fine sand, poorly sorted
6-8	61.41	140.10	0.72	3.19	10.19	-2.13	5.40	Coarse silt, poorly sorted
8-10	58.51	72.94	0.81	3.96	15.65	-1.23	2.25	Coarse silt, poorly sorted
10-12	40.25	96.49	0.71	3.29	10.80	-1.78	3.50	Coarse silt, poorly sorted
12-14	63.27	80.07	0.80	3.52	12.37	-1.63	3.71	Coarse silt, poorly sorted
14-16	48.93	105.90	0.88	3.36	11.30	-1.64	2.83	Coarse silt, poorly sorted
16-18	74.98	87.90	0.85	3.24	10.52	-1.89	5.70	Very fine sand, poorly sorted
18-20	62.33	127.60	0.75	3.02	9.14	-2.40	7.19	Coarse silt, poorly sorted
20-22	70.58	96.49	0.73	3.94	15.50	-1.26	2.76	Very fine sand, poorly sorted
22-24	36.82	105.90	0.66	3.46	11.99	-1.85	3.77	Coarse silt, poorly sorted
24-26	26.73	55.13	0.69	4.23	17.88	-0.82	0.24	Medium Silt, Poorly Sorted
26-28	20.09	72.94	0.73	3.61	13.04	-0.85	0.13	Medium Silt, Poorly Sorted
28-30	24.55	105.90	0.68	3.79	14.33	-1.06	0.64	Medium Silt, Poorly Sorted
30-32	25.02	50.22	0.71	4.33	18.78	-0.81	0.25	Medium Silt, Poorly Sorted
32-34	56.84	153.80	0.69	3.53	12.47	-1.80	3.65	Coarse silt, poorly sorted
34-36	56.99	153.80	0.72	3.52	12.38	-1.65	3.09	Coarse slit, poorly sorted
36-38	60.60	140.10	0.74	3.42	11.68	-1.85	4.23	Coarse slit, poorly sorted
38-40	62.95	127.60	0.75	3.47	12.01	-1.76	4.02	Coarse slit, poorly sorted

Appendix A9. Correlations between MS and Major elements from the Ankobra estuary (*Correlation is significant at the 0.05 level; **Correlation is significant at the 0.01 level; n=20)

		MS	Li	Na	Mg	Al	P	S	K	Ca	Ti	Mn	Fe
MS	P. Correlation	1	.390*	.128	.551**	**.833****	**.766****	.462*	**.807****	**-.021**	.593**	.469*	**.818****
	Sig. (1-tailed)		.045	.295	.006	.000	.000	.020	.000	.466	.003	.018	.000
Li	P. Correlation		1	.132	.244	.663**	.378	.122	.672**	-.104	.375	.347	.535**
	Sig. (1-tailed)			.289	.150	.001	.050	.304	.001	.331	.052	.067	.008
Na	P. Correlation			1	.288	.289	.085	.295	.316	-.473*	-.039	.508*	.218
	Sig. (1-tailed)				.109	.108	.361	.103	.087	.018	.435	.011	.178
Mg	P.Correlation				1	.524**	.896**	.888**	.526**	.430*	.366	.771**	.845**
	Sig. (1-tailed)					.009	.000	.000	.009	.029	.056	.000	.000
Al	P. Correlation					1	.745**	.353	.997**	-.191	.598**	.579**	.882**
	Sig. (1-tailed)						.000	.064	.000	.210	.003	.004	.000
P	P. Correlation						1	.738**	.737**	.323	.579**	.668**	.960**
	Sig. (1-tailed)							.000	.000	.083	.004	.001	.000
S	P. Correlation							1	.352	.446*	.054	.811**	.666**
	Sig. (1-tailed)								.064	.024	.411	.000	.001
K	P. Correlation								1	-.192	.584**	.600**	.879**
	Sig. (1-tailed)									.209	.003	.003	.000
Ca	P. Correlation									1	-.216	.253	.157
	Sig. (1-tailed)										.180	.141	.254
Ti	P. Correlation										1	.054	.617**
	Sig. (1-tailed)											.410	.002
Mn	P. Correlation											1	.715**
	Sig. (1-tailed)												.000
Fe	P. Correlation												1
	Sig. (1-tailed)												

Appendix A10. Correlations between MS and Major elements from the Pra estuary (*Correlation is significant at the 0.05 level; **Correlation is significant at the 0.01 level; n=20)

		MS	Li	Na	Mg	Al	P	S	K	Ca	Ti	Mn	Fe
MS	P. Correlation	1	.709**	-.522**	.696**	.658**	.616**	.538**	.610**	.155	.682**	.478*	.707**
	Sig. (1-tailed)		.000	.009	.000	.001	.002	.007	.002	.258	.000	.017	.000
Li	P. Correlation		1	-.596**	.809**	.745**	.709**	.630**	.674**	.029	.727**	.643**	.813**
	Sig. (1-tailed)			.003	.000	.000	.000	.001	.001	.452	.000	.001	.000
Na	P. Correlation			1	-.570**	-.520**	-.607**	-.651**	-.441*	-.237	-.684**	-.435*	-.627**
	Sig. (1-tailed)				.004	.009	.002	.001	.026	.157	.000	.028	.002
Mg	P. Correlation				1	.936**	.965**	.750**	.859**	.058	.821**	.871**	.988**
	Sig. (1-tailed)					.000	.000	.000	.000	.404	.000	.000	.000
Al	P. Correlation					1	.908**	.524**	.975**	-.148	.759**	.910**	.944**
	Sig. (1-tailed)						.000	.009	.000	.266	.000	.000	.000
P	P. Correlation						1	.770**	.818**	.069	.825**	.894**	.978**
	Sig. (1-tailed)							.000	.000	.387	.000	.000	.000
S	P. Correlation							1	.357	.585**	.782**	.571**	.759**
	Sig. (1-tailed)								.061	.003	.000	.004	.000
K	P. Correlation								1	-.275	.639**	.859**	.859**
	Sig. (1-tailed)									.121	.001	.000	.000
Ca	P. Correlation									1	.331	-.066	.062
	Sig. (1-tailed)										.077	.391	.397
Ti	P. Correlation										1	.757**	.869**
	Sig. (1-tailed)											.000	.000
Mn	P. Correlation												.898**
	Sig. (1-tailed)												.000
Fe	P. Correlation												1
	Sig. (1-tailed)												

Appendix A11. Correlations between MS and Major elements from the Amisa estuary (*Correlation is significant at the 0.05 level; **Correlation is significant at the 0.01 level; n=20)

		MS	Na	Mg	Al	P	S	K	Ca	Ti	Fe
MS	P. Correlation	1	.531**	-.393*	-.196	.178	-.405*	-.108	-.182	-.252	-.004
	Sig. (1-tailed)		.008	.043	.203	.226	.038	.325	.222	.141	.493
Na	P. Correlation		1	-.428*	-.101	.397*	-.735**	-.187	.072	-.265	.014
	Sig. (1-tailed)			.030	.335	.041	.000	.215	.382	.129	.477
Mg	P. Correlation			1	.823**	-.396*	.802**	.526**	.078	.733**	.654**
	Sig. (1-tailed)				.000	.042	.000	.009	.373	.000	.001
Al	P. Correlation				1	-.154	.416*	.509*	.240	.613**	.715**
	Sig. (1-tailed)					.258	.034	.011	.154	.002	.000
P	P. Correlation					1	-.623**	-.004	-.210	-.133	.041
	Sig. (1-tailed)						.002	.493	.187	.288	.432
S	P. Correlation						1	.341	.036	.574**	.365
	Sig. (1-tailed)							.071	.441	.004	.057
K	P. Correlation							1	-.165	.485*	.430*
	Sig. (1-tailed)								.244	.015	.029
Ca	P. Correlation								1	-.136	.038
	Sig. (1-tailed)									.283	.437
Ti	P. Correlation									1	.792**
	Sig. (1-tailed)										.000
Fe	P. Correlation										1
	Sig. (1-tailed)										

Appendix A12. Correlations between MS and Major elements from the Densu estuary (*Correlation is significant at the 0.05 level; **Correlation is significant at the 0.01 level; n=20)

		MS	Na	Mg	Al	P	S	K	Ca	Ti	Fe
MS	P. Correlation	1	.745**	.877**	.849**	.694**	.864**	.574**	.200	.737**	.867**
	Sig. (1-tailed)		.000	.000	.000	.000	.000	.004	.199	.000	.000
Na	P. Correlation		1	.892**	.861**	.713**	.871**	.644**	.136	.751**	.875**
	Sig. (1-tailed)			.000	.000	.000	.000	.001	.284	.000	.000
Mg	P. Correlation			1	.980**	.773**	.956**	.697**	.139	.876**	.971**
	Sig. (1-tailed)				.000	.000	.000	.000	.280	.000	.000
Al	P. Correlation				1	.800**	.941**	.756**	.085	.940**	.970**
	Sig. (1-tailed)					.000	.000	.000	.361	.000	.000
P	P. Correlation					1	.829**	.550**	.170	.720**	.839**
	Sig. (1-tailed)						.000	.006	.237	.000	.000
S	P. Correlation						1	.635**	.190	.827**	.991**
	Sig. (1-tailed)							.001	.211	.000	.000
K	P. Correlation							1	.111	.798**	.659**
	Sig. (1-tailed)								.321	.000	.001
Ca	P. Correlation								1	.024	.137
	Sig. (1-tailed)									.460	.282
Ti	P. Correlation									1	.876**
	Sig. (1-tailed)										.000
Fe	P. Correlation										1
	Sig. (1-tailed)										

Appendix A13. Correlations between MS and Major elements from the Sakumo II estuary (*Correlation is significant at the 0.05 level; **Correlation is significant at the 0.01 level; n=20)

		MS	Na	Mg	Al	P	S	K	Ca	Ti	Fe
MS	P. Correlation	1	.251	-.196	-.137	-.063	.009	.002	-.259	-.090	-.215
	Sig. (1-tailed)		.143	.204	.282	.396	.485	.497	.135	.353	.182
Na	P. Correlation		1	.494*	.252	-.113	-.322	.689**	.456*	.052	.015
	Sig. (1-tailed)			.013	.142	.318	.083	.000	.022	.413	.475
Mg	P. Correlation			1	.556**	.297	.050	.725**	.987**	.294	.547**
	Sig. (1-tailed)				.005	.101	.416	.000	.000	.104	.006
Al	P. Correlation				1	.822**	.625**	.693**	.555**	.876**	.916**
	Sig. (1-tailed)					.000	.002	.000	.006	.000	.000
P	P. Correlation					1	.879**	.315	.302	.835**	.942**
	Sig. (1-tailed)						.000	.088	.098	.000	.000
S	P. Correlation						1	.131	.087	.729**	.759**
	Sig. (1-tailed)							.290	.358	.000	.000
K	P. Correlation							1	.705**	.559**	.495*
	Sig. (1-tailed)								.000	.005	.013
Ca	P. Correlation								1	.282	.549**
	Sig. (1-tailed)									.114	.006
Ti	P. Correlation									1	.852**
	Sig. (1-tailed)										.000
Fe	P. Correlation										1
	Sig. (1-tailed)										

Appendix A14. Correlations between MS and Major elements from the Volta estuary (*Correlation is significant at the 0.05 level; **Correlation is significant at the 0.01 level; n=20)

		MS	Na	Mg	Al	P	S	K	Ca	Ti	Fe
MS	P. Correlation	1	.290	.428*	.499*	.559**	.112	.405*	.047	.220	.454*
	Sig. (1-tailed)		.107	.030	.013	.005	.318	.038	.423	.175	.022
Na	P. Correlation		1	.691**	.626**	.242	.615**	.550**	.823**	.825**	.604**
	Sig. (1-tailed)			.000	.002	.152	.002	.006	.000	.000	.002
Mg	P. Correlation			1	.970**	.477*	.825**	.772**	.718**	.856**	.965**
	Sig. (1-tailed)				.000	.017	.000	.000	.000	.000	.000
Al	P. Correlation				1	.500*	.734**	.840**	.599**	.783**	.954**
	Sig. (1-tailed)					.012	.000	.000	.003	.000	.000
P	P. Correlation					1	.002	.182	.060	.273	.646**
	Sig. (1-tailed)						.497	.221	.401	.122	.001
S	P. Correlation						1	.670**	.835**	.792**	.697**
	Sig. (1-tailed)							.001	.000	.000	.000
K	P. Correlation							1	.506*	.630**	.710**
	Sig. (1-tailed)								.011	.001	.000
Ca	P. Correlation								1	.920**	.603**
	Sig. (1-tailed)									.000	.002
Ti	P. Correlation									1	.792**
	Sig. (1-tailed)										.000
Fe	P. Correlation										1
	Sig. (1-tailed)										

Appendix A15. Smear-slide analysis of sediments from the Ankobra Estuary

Depth (cm)	Biogenic (%)	Terrigenous (%)	Biogenic Component	Non- Biogenic Component
0-2	0	100	nothing	75% Quartz, 10% Feldspar, 14% Lithics, 1% AM
2-4	0	100	nothing	80% Quartz, 5% Feldspar, 15% Lithics
4-6	0	100	nothing	80% Quartz, 5% Feldspar, 14% Lithics, 1% AM
6-8	0	100	nothing	80% Quartz, 5% Feldspar, 13% Lithics, 2% AM
8-10	0	100	nothing	90% Quartz, 5% Feldspar, 5% Lithics
10-12	0	100	nothing	85% Quartz, 5% Feldspar,10% Lithics
12-14	0	100	nothing	65% Quartz, 5% Feldspar, 30% Lithics
14-16	0	100	nothing	90% Quartz, 5% Feldspar, 5% Lithics
16-18	0	100	nothing	80% Quartz, 5% Feldspar, 15% Lithics
18-20	0	100	nothing	80% Quartz, 5% Feldspar, 15% Lithics
20-22	0	100	nothing	70% Quartz, 5% Feldspars, 25% Lithics
22-24	0	100	nothing	70% Quartz, 5% Feldspars, 25% Lithics
24-26	0	100	nothing	70% Quartz, 5% Feldspars, 25% Lithics
26-28	5	95	Broken pieces of diatoms	85% Quartz, 5% Feldspar, 10% Lithics
28-30	3	97	Broken pieces of diatoms	90% Quartz, 3% Feldspar, 7% Lithics
30-32	2	98	Broken pieces of diatoms	90% Quartz, 3% Feldspar, 7% Lithics
32-34	2	98	Broken pieces of diatoms	85% Quartz, , 5% Feldspar,10% Lithics,
34-36	2	98	Broken pieces of diatoms	90% Quartz, 3% Feldspar, 7% Lithics
36-38	2	98	Broken pieces of diatoms	90% Quartz, 3% Feldspar, 7% Lithics
38-40	2	98	Broken pieces of diatoms	90% Quartz, 3% Feldspar, 7% Lithics

Appendix A16. Major element composition of the core from the Ankobra Estuary

Depth (cm)	Li_2O %	Na_2O %	MgO %	Al_2O_3 %	P_2O_5 %	SO_3 %	K_2O %	CaO %	TiO_2 %	MnO %	Fe_2O_3 %	Rb_2O %	SrO %	SiO_2 %
0-2	0.00	0.65	0.46	6.26	0.07	0.18	0.59	0.28	0.39	0.04	3.06	0.00	0.01	88.00
2-4	0.00	0.80	0.51	8.22	0.07	0.26	0.75	0.36	0.37	0.04	3.51	0.00	0.01	85.07
4-6	0.00	0.62	0.48	6.79	0.08	0.20	0.63	0.38	0.40	0.04	3.27	0.00	0.01	87.09
6-8	0.00	0.67	0.49	8.18	0.08	0.21	0.75	0.33	0.39	0.05	3.50	0.00	0.01	85.32
8-10	0.01	0.61	0.51	10.39	0.09	0.24	0.94	0.32	0.52	0.05	4.19	0.00	0.01	82.12
10-12	0.01	0.58	0.54	11.15	0.10	0.27	0.99	0.34	0.57	0.05	4.43	0.00	0.01	80.95
12-14	0.01	0.44	0.52	7.43	0.09	0.51	0.68	0.64	0.39	0.04	3.78	0.00	0.01	85.45
14-16	0.00	0.30	0.52	5.30	0.08	0.28	0.50	1.14	0.34	0.04	3.33	0.00	0.01	88.15
16-18	0.00	0.41	0.57	7.06	0.10	0.49	0.67	1.14	0.34	0.05	3.80	0.00	0.01	85.36
18-20	0.01	0.51	0.58	10.04	0.10	0.44	0.89	0.92	0.45	0.06	4.40	0.00	0.01	81.58
20-22	0.01	0.56	0.62	11.83	0.11	0.52	1.06	0.94	0.45	0.07	5.03	0.00	0.01	78.77
22-24	0.00	0.54	0.59	10.41	0.11	0.43	0.95	0.78	0.48	0.07	4.72	0.00	0.01	80.90
24-26	0.01	0.60	0.61	11.04	0.11	0.63	0.94	0.76	0.42	0.07	4.70	0.00	0.01	80.10
26-28	0.01	0.61	0.63	14.16	0.12	0.57	1.21	0.56	0.52	0.08	5.50	0.01	0.01	76.01
28-30	0.00	0.62	0.66	14.03	0.13	0.64	1.19	0.57	0.58	0.06	5.65	0.00	0.01	75.85
30-32	0.00	0.48	0.65	9.29	0.12	0.48	0.82	0.72	0.73	0.05	4.81	0.00	0.01	81.84
32-34	0.01	0.52	0.68	9.83	0.12	0.59	0.86	0.73	0.55	0.05	5.01	0.00	0.01	81.05

34-36	0.00	0.55	0.61	5.69	0.09	0.56	0.55	1.23	0.39	0.06	3.82	0.00	0.01	86.41
36-38	0.00	0.64	0.59	7.47	0.10	0.80	0.69	0.67	0.34	0.08	3.91	0.00	0.01	84.69
38-40	0.00	0.92	0.82	11.02	0.13	1.07	1.00	0.84	0.44	0.10	5.63	0.00	0.01	78.00

Appendix 17. Smear-slide analysis of sediments from the Pra Estuary

Depth/cm	% Biogenic	% Non-biogenic	Biogenic Component	Non-biogenic Component
0-2	0	100	Nothing	80% Quartz, 5% Feldspar, 15% Lithics
2-4	2	98	Broken pieces of radiolaria	80% Quartz, 5% Feldspar, 15% Lithics
4-6	4	96	Sponge Spicules	75% Quartz, 5% Feldspar, 20% Lithics
6-8	0	100	Nothing	80% Quartz, 5% Feldspar, 15% Lithics
8-10	2	98	Sponge Spicules	80% Quartz, 3% Feldspar, 15% Lithics, 2%AM
10-12	2	98	Sponge Spicules	80% Quartz, 3% Feldspar, 15% Lithics, 2%AM
12-14	0	100	Nothing	80% Quartz, 5% Feldspar, 15% Lithics
14-16	0	100	Nothing	80% Quartz, 5% Feldspar, 15% Lithics
16-18	0	100	Nothing	80% Quartz, 5% Feldspar, 15% Lithics
18-20	2	98	Sponge Spicules	90% Quartz, 15% 10% lithics
20-22	2	98	Sponge Spicules	90% Quartz, 15% 10% lithics
22-24	2	98	Sponge Spicules	90% Quartz, 15% 10% lithics
24-26	4	96	Sponge Spicules	80% Quartz, 5% Feldspar,15% Lithics
26-28	2	98	Sponge Spicules	80% Quartz, 5% Feldspar,15% Lithics
28-30	2	98	Sponge Spicules	80% Quartz, 5% Feldspar,15% Lithics
30-32	2	98	Sponge Spicules	80% Quartz, 5% Feldspar,15% Lithics
32-34	2	98	Sponge Spicules	90% Quartz, 15% 10% lithics
34-36	2	98	Sponge Spicules	90% Quartz, 15% 10% lithics
36-38	2	98	Sponge Spicules	90% Quartz, 15% 10% lithics
38-40	2	98	Sponge Spicules	90% Quartz, 15% 10% lithics

Appendix A18. Major element composition of the core from Pra Estuary

Depth (cm)	Li_2O %	Na_2O %	MgO %	Al_2O_3 %	P_2O_5 %	SO_3 %	K_2O %	CaO %	TiO_2 %	MnO %	Fe_2O_3 %	Rb_2O %	SrO %	SiO_2 %
0-2	0.00	0.86	0.39	8.40	0.07	0.17	0.72	0.31	0.57	0.03	2.95	0.00	0.01	85.51
2-4	0.00	0.83	0.39	8.36	0.07	0.20	0.75	0.30	0.52	0.03	2.86	0.00	0.01	85.67
4-6	0.00	0.77	0.38	8.01	0.07	0.20	0.76	0.28	0.49	0.03	2.79	0.00	0.01	86.21
6-8	0.00	0.77	0.36	7.80	0.07	0.20	0.72	0.28	0.47	0.03	2.78	0.00	0.01	86.50
8-10	0.01	0.78	0.42	10.06	0.08	0.20	0.85	0.26	0.57	0.04	3.53	0.00	0.01	83.19
10-12	0.01	0.81	0.49	12.76	0.10	0.25	1.03	0.26	0.63	0.05	4.33	0.00	0.01	79.26
12-14	0.01	0.75	0.50	13.93	0.11	0.24	1.09	0.25	0.65	0.04	4.60	0.00	0.01	77.82
14-16	0.01	0.74	0.50	13.54	0.11	0.22	1.07	0.25	0.65	0.04	4.57	0.00	0.01	78.28
16-18	0.01	0.74	0.54	12.96	0.14	0.67	0.98	0.32	0.75	0.05	5.12	0.00	0.01	77.70
18-20	0.00	0.75	0.37	9.19	0.08	0.29	0.78	0.32	0.68	0.04	3.33	0.00	0.01	84.16
20-22	0.01	0.70	0.47	11.94	0.10	0.49	0.93	0.33	0.70	0.04	4.30	0.00	0.01	79.98
22-24	0.01	0.74	0.61	16.85	0.16	0.65	1.20	0.28	0.72	0.06	5.93	0.01	0.01	72.79
24-26	0.01	0.71	0.58	15.50	0.15	0.54	1.20	0.31	0.71	0.05	5.47	0.01	0.01	74.76
26-28	0.01	0.74	0.58	15.86	0.16	0.57	1.16	0.30	0.71	0.06	5.69	0.01	0.01	74.13
28-30	0.01	0.72	0.60	16.16	0.17	0.63	1.14	0.29	0.76	0.06	5.96	0.01	0.01	73.50
30-32	0.01	0.73	0.48	11.91	0.10	0.51	0.92	0.35	0.67	0.04	4.23	0.00	0.01	80.04
32-34	0.01	0.77	0.49	11.13	0.12	0.63	0.85	0.32	0.63	0.04	4.55	0.00	0.01	80.44
34-36	0.01	0.71	0.52	11.58	0.13	0.71	0.87	0.31	0.71	0.04	4.78	0.00	0.01	79.63

36-38	0.01	0.70	0.50	10.86	0.12	0.62	0.80	0.31	0.71	0.04	4.63	0.00	0.01	80.69
38-40	0.01	0.75	0.52	10.92	0.11	0.73	0.84	0.36	0.69	0.04	4.63	0.00	0.01	80.40

A19. Smear-slide analysis of sediments from the Amisa Estuary

Depth (cm)	**Biogenic (%)**	**Terrigenous (%)**	**Biogenic Component**	**Non-biogenic Component**
0-2	5	95	Broken pieces of Diatoms	40% Quartz, 50% AM 10% lithics
L	I	95	Broken pieces of Diatoms	40% Quartz, 50% AM, 10% lithics
4-6	10	90	Broken pieces of Diatoms	45% Quartz, 45% AM, 10% lithics
6-8	10	90	Both preserved and broken pieces diatoms	45% Quartz, 45% AM, 10% lithics
8-10	12	88	Mostly preserved pennate diatoms	40% Quartz, 50% AM, 10% lithics
10-12	5	95	Mostly broken pennate diatoms	40% Quartz, 50% AM, 10% lithics
12-14	5	95	Broken pieces of diatoms	40% Quartz, 50% AM, 10% lithics
14-16	4	96	Broken pieces of diatoms	40% Quartz, 50% AM, 10% lithics
16-18	15	85	Broken pieces of diatoms and radiolaria	60% Quartz, 20% AM, 20% lithics
18-20	20	80	broken radiolaria ,diatoms and sponge spicules	60% Quartz, 35% AM, 5% lithics
20-22	10	90	broken radiolaria. diatoms and sponge spicules	50% Quartz, 40% AM, 10% lithics
22-24	8	92	Mostly broken radiolaria	50% Quartz, 40% AM, 10% lithics
24-26	10	90	Mostly broken radiolaria	65% Quartz, 30% AM, 5% lithics
26-28	12	88	Mostly broken radiolaria	50% Quartz, 40% AM, 10 % lithics
28-30	10	90	Mostly broken radiolaria	40% Quartz, 40% AM, 20 % lithics
30-32	15	85	Mostly broken radiolaria	40% Quartz, 40% AM, 20 % lithics
32-34	10	90	Mostly broken radiolaria	40% Quartz, 40% AM, 20 % lithics
34-36	6	94	Mostly broken radiolaria	45% Quartz, 50% AM, 5 % lithics
36-38	8	92	Mostly broken radiolaria	60% Quartz, 35% AM, 5% lithics
38-40	8	92	Mostly broken radiolaria	60% Quartz, 35% AM, 5% lithics

Appendix A20. Major element composition of the core from Amisa Estuary

Depth (cm)	Al_2O_3 %	Li_2O %	Na_2O %	MgO %	P_2O_5 %	SO_3 %	K_2O %	CaO %	TiO_2 %	MnO %	Fe_2O_3 %	Rb_2O %	SrO %	SiO_2 %
0-2	16.15	0.01	2.18	1.02	0.12	4.95	1.35	0.40	0.70	0.02	6.38	0.01	0.01	66.72
2-4	14.72	0.01	1.87	0.89	0.11	4.34	1.31	0.32	0.68	0.02	6.08	0.01	0.01	69.65
4-6	16.43	0.01	1.95	0.96	0.12	4.52	1.42	0.39	0.71	0.02	6.52	0.01	0.01	66.93
6-8	15.34	0.01	2.02	0.93	0.17	3.89	1.35	0.45	0.73	0.02	6.78	0.01	0.01	68.29
8-10	15.63	0.01	2.04	0.89	0.16	3.56	1.31	0.38	0.66	0.02	6.15	0.01	0.01	69.17
10-12	14.97	0.01	1.96	0.88	0.13	4.83	1.31	0.28	0.72	0.02	6.41	0.00	0.01	68.46
12-14	16.39	0.01	1.98	0.95	0.11	4.94	1.28	3.07	0.67	0.02	6.33	0.01	0.02	64.23
14-16	16.22	0.01	2.15	1.03	0.11	5.73	1.33	0.41	0.72	0.02	6.73	0.01	0.01	65.52
16-18	14.15	0.01	1.87	0.95	0.11	5.46	1.26	0.45	0.70	0.02	6.31	0.00	0.01	68.70
18-20	16.59	0.01	1.67	1.01	0.11	6.23	1.34	0.48	0.70	0.02	6.65	0.01	0.01	65.16
20-22	14.49	0.01	1.71	0.97	0.12	5.80	1.29	0.41	0.74	0.02	6.64	0.01	0.01	67.78
22-24	18.68	0.01	1.98	1.14	0.12	6.59	1.39	1.00	0.76	0.02	7.28	0.01	0.01	61.00
24-26	17.76	0.01	1.90	1.10	0.11	6.64	1.33	0.80	0.78	0.02	6.90	0.01	0.01	62.62
26-28	15.75	0.01	1.69	1.06	0.12	6.82	1.33	0.53	0.70	0.02	6.54	0.01	0.01	65.43
28-30	14.43	0.01	1.62	1.00	0.11	7.14	1.42	0.48	0.70	0.02	6.28	0.01	0.01	66.76
30-32	17.40	0.01	1.61	1.09	0.11	7.14	1.33	0.73	0.73	0.02	6.62	0.01	0.01	63.19
32-34	17.88	0.01	1.60	1.16	0.12	7.54	1.45	0.67	0.78	0.02	6.88	0.01	0.01	61.87
34-36	18.68	0.01	1.70	1.18	0.11	6.85	1.45	0.67	0.76	0.02	6.66	0.01	0.01	61.87
36-38	13.68	0.01	1.72	0.95	0.11	6.55	1.30	0.64	0.70	0.02	5.99	0.01	0.01	68.32
38-40	17.68	0.01	1.57	1.14	0.11	7.03	1.30	0.63	0.73	0.02	6.49	0.01	0.01	63.27

Appendix A21: Smear-slide analysis of sediments from the Densu Estuary

Depth (cm)	% Biogenic	% non-biogenic	Biogenic Component	Non-biogenic Component
0-2	5	95	Broken pieces of diatoms, radiolaria, sponge spicules	90% Quartz, 10% Feldspar
2-4	10	90	Radiolaria, few broken diatoms and sponge spicule	90% Quartz, 10% Feldspar
4-6	30	70	Preserved pennate diatoms, broken centric diatoms	85% Quartz, 15% Feldspar
6-8	30	70	Preserved pennate diatoms, broken centric diatoms	85% Quartz, 15% Feldspar
8-10	25	85	Preserved pennate diatoms, broken centric diatoms	85% Quartz, 15% Feldspar
10-12	28	82	Preserved pennate diatoms, broken centric diatoms	85% Quartz, 15% Feldspar
12-14	30	70	Preserved pennate diatoms, broken centric diatoms	80% Quartz, 20% Feldspar
14-16	33	67	Preserved pennate diatoms, broken centric diatoms	85% Quartz, 15% Feldspar
16-18	18	88	Pennate and centric diatoms smaller in size	80% Quartz, 20% Feldspar
18-20	20	80	Pennate and centric diatoms smaller in size	80% Quartz, 20% Feldspar
20-22	20	80	Pennate and centric diatoms smaller in size	80% Quartz, 20% Feldspar
22-24	22	78	Pennate and centric diatoms smaller in size	85% Quartz, 15% Feldspar
24-26	25	75	Pennate and centric diatoms smaller in size	80% Quartz, 20% Feldspar
26-28	10	90	Mostly sponge spicules and a few centric diatoms	80% Quartz, 20% Feldspar
28-30	10	90	Mostly sponge spicules and a few centric diatoms	55% Quartz, 20% Feldspar
30-32	8	92	Only sponge spicules	90% Quartz, 10% Feldspar
32-34	6	94	Mostly broken sponge spicules	85% Quartz, 15% Feldspar
34-36	6	94	Broken sponge spicules and diatoms	65% Quartz, 35% Feldspar,
36-38	5	95	Broken sponge spicules	75% Quartz, 25% Feldspar
38-40	3	97	Broken sponge spicules	90% Quartz, 10% Feldspar,

Appendix A22: Major element composition of the core from Densu Estuary

Depth (cm)	Li_2O %	Na_2O %	MgO %	Al_2O_3 %	P_2O_5 %	SO_3 %	K_2O %	CaO %	TiO_2 %	MnO %	Fe_2O_3 %	Rb_2O %	SrO %	SiO_2 %
0-2	0.01	2.09	0.99	11.36	0.12	9.53	1.03	0.69	0.61	0.07	6.71	0.00	0.01	66.77
2-4	0.00	1.11	0.48	7.07	0.06	4.18	0.93	0.56	0.43	0.04	3.36	0.00	0.01	81.77
4-6	0.00	1.23	0.46	6.83	0.06	3.90	0.92	0.57	0.43	0.04	3.09	0.00	0.01	82.47
6-8	0.00	1.30	0.48	6.59	0.06	3.87	0.88	1.85	0.41	0.04	3.01	0.00	0.02	81.50
8-10	0.00	1.36	0.47	6.98	0.06	4.01	0.90	0.61	0.44	0.04	3.24	0.00	0.01	81.87
10-12	0.00	1.31	0.46	6.62	0.06	3.35	0.84	0.52	0.42	0.03	3.03	0.00	0.01	83.35
12-14	0.00	1.45	0.50	7.44	0.07	3.98	0.90	0.60	0.46	0.04	3.46	0.00	0.01	81.10
14-16	0.00	1.46	0.47	7.24	0.06	4.17	0.98	0.56	0.47	0.04	3.31	0.00	0.01	81.23
16-18	0.00	1.36	0.44	6.68	0.06	3.76	0.87	0.55	0.46	0.04	3.26	0.00	0.01	82.51
18-20	0.00	1.48	0.49	7.19	0.06	4.02	0.91	0.58	0.44	0.04	3.32	0.00	0.01	81.44
20-22	0.00	1.30	0.44	6.82	0.11	3.58	0.92	0.64	0.42	0.03	3.09	0.00	0.01	82.62
22-24	0.00	1.21	0.44	6.77	0.05	3.53	0.84	0.66	0.42	0.03	3.10	0.00	0.01	82.91
24-26	0.00	1.23	0.48	6.94	0.05	3.86	0.88	0.58	0.43	0.03	3.17	0.00	0.01	82.33
26-28	0.00	1.25	0.50	7.26	0.05	3.28	0.93	0.51	0.45	0.02	3.07	0.00	0.01	82.67
28-30	0.00	1.21	0.42	6.37	0.04	2.06	0.84	0.44	0.39	0.01	2.25	0.00	0.01	85.95
30-32	0.00	1.30	0.44	6.67	0.03	1.96	1.00	0.46	0.46	0.01	2.23	0.00	0.01	85.41
32-34	0.00	1.08	0.31	5.09	0.03	1.86	0.83	0.39	0.36	0.01	1.92	0.00	0.01	88.09
34-36	0.00	1.21	0.33	5.01	0.03	1.99	0.81	0.42	0.31	0.01	1.87	0.00	0.01	87.99
36-38	0.00	1.10	0.28	4.63	0.03	1.64	0.73	0.37	0.27	0.01	1.68	0.00	0.01	89.25
38-40	0.00	1.28	0.32	4.98	0.03	2.16	0.88	0.98	0.28	0.01	1.97	0.00	0.01	87.08

Appendix A23. Smear-slide analysis of sediments from the Sakumo II Estuary

Depth (cm)	Biogenic (%)	Terrigenous (%)	Biogenic Component	Non-Biogenic Component
0-2	10	90	Broken pieces of diatoms and sponge spicules	65% Quartz, 5% Feldspars, 30% AM
2-4	5	95	Broken pieces of diatoms	65% Quartz, 5% Feldspars, 30% AM
4-6	3	97	Broken pieces of diatoms	50% Quartz,1 5% Feldspar, 35% AM
6-8	2	98	Broken pieces of diatoms	50% Quartz, 15% Feldspar, 35% AM
8-10	2	98	Broken pieces of diatoms	50% Quartz, 15% Feldspar, 35% AM
10-12	3	97	Broken pieces of diatoms	50% Quartz, 15% Feldspar, 35% AM
12-14	5	95	Broken pieces of diatoms	65% Quartz, 5% Feldspars, 30% AM
14-16	3	97	Broken pieces of diatoms and sponge spicules	20% Quartz, 19% Feldspar, 60% AM,
16-18	2	98	Broken pieces of diatoms	40% Quartz, 5% Feldspar, 55% AM
18-20	3	97	Broken pieces of diatoms	40% Quartz, 5% Feldspar, 55% AM
20-22	6	94	Broken pieces of pennate and centric diatoms	40% Quartz, 5% Feldspar, 55% AM
22-24	3	97	Broken pieces of diatoms	40% Quartz, 5% Feldspar, 55% AM
24-26	8	92	Broken and few preserved centric and pennate diatoms	60% Quartz, 5% Feldspars, 35% AM
26-28	6	94	Broken pieces of centric and pennate diatoms	55% Quartz, 5% Feldspar, 40% AM
28-30	6	94	Mostly preserved pennate diatoms	55% Quartz, 5% Feldspar, 40% AM
30-32	6	94	Mostly preserved pennate diatoms	55% Quartz, 5% Feldspar, 40% AM
32-34	4	96	Mostly preserved pennate diatoms	55% Quartz, 5% Feldspar, 45% AM
34-36	4	96	Broken pieces of diatoms	55% Quartz, 5% Feldspar, 45% AM
36-38	4	96	Broken pieces of diatoms	55% Quartz, 5% Feldspar, 45% AM
38-40	5	95	Broken pieces of diatoms	55% Quartz, 5% Feldspar, 45% AM

Appendix A24: Major element composition of the core from Sakumo II Estuary

Depth (cm)	Al_2O_3 %	Li_2O %	Na_2O %	MgO %	P_2O_5 %	SO_3 %	K_2O %	CaO %	TiO_2 %	MnO %	Fe_2O_3 %	Rb_2O %	SrO %	SiO_2 %
0-2	15.78	0.01	0.92	2.24	0.32	5.51	1.05	1.37	0.99	0.11	8.24	0.01	0.01	63.46
2-4	16.61	0.01	1.12	2.29	0.31	5.39	1.07	1.40	1.00	0.11	8.10	0.01	0.02	62.58
4-6	14.91	0.01	1.33	2.16	0.27	4.70	1.08	1.32	0.93	0.09	7.09	0.01	0.02	66.10
6-8	14.41	0.01	1.87	1.99	0.25	4.51	1.15	1.14	0.91	0.07	6.64	0.01	0.02	67.04
8-10	14.18	0.01	1.98	1.90	0.24	4.14	1.10	1.13	0.89	0.07	6.39	0.01	0.02	67.96
10-12	14.74	0.01	2.27	2.31	0.27	4.63	1.19	1.39	0.96	0.10	6.94	0.01	0.02	65.17
12-14	15.42	0.01	2.37	2.57	0.29	4.94	1.18	1.49	0.95	0.11	7.48	0.01	0.02	63.19
14-16	15.95	0.01	2.52	2.62	0.28	4.51	1.20	1.57	0.94	0.11	7.44	0.01	0.02	62.84
16-18	16.31	0.01	2.55	2.74	0.29	4.67	1.19	1.69	0.95	0.11	7.68	0.01	0.02	61.82
18-20	16.13	0.01	2.52	2.78	0.29	4.55	1.20	1.75	0.97	0.11	7.86	0.01	0.02	61.82
20-22	16.14	0.01	2.79	2.86	0.29	4.89	1.25	1.93	0.94	0.11	7.70	0.01	0.02	61.09

22-24	16.27	0.01	2.70	2.81	0.29	4.70	1.28	1.73	0.98	0.11	7.74	0.01	0.02	61.38
24-26	14.72	0.01	2.36	2.60	0.26	4.10	1.10	1.52	0.92	0.09	7.15	0.01	0.02	65.16
26-28	15.56	0.01	2.48	2.61	0.25	3.96	1.24	1.57	0.92	0.09	6.99	0.01	0.02	64.32
28-30	16.34	0.01	2.53	3.18	0.29	4.90	1.35	2.02	0.97	0.12	7.87	0.01	0.02	60.41
30-32	12.41	0.01	1.79	2.44	0.22	3.76	0.95	1.52	0.72	0.09	5.92	0.01	0.01	70.16
32-34	16.71	0.01	2.47	3.33	0.28	4.91	1.31	2.20	0.98	0.13	7.93	0.01	0.02	59.75
34-36	16.06	0.01	2.08	3.14	0.28	4.21	1.27	2.00	0.94	0.12	7.72	0.01	0.02	62.15
36-38	15.38	0.01	1.91	3.13	0.28	4.60	1.20	1.97	0.94	0.12	7.66	0.01	0.02	62.78
38-40	15.98	0.01	2.02	3.26	0.28	4.65	1.24	2.12	0.98	0.13	7.79	0.01	0.02	61.54

Appendix A25: Smear-slide analysis of sediments from the Volta Estuary

Depth (cm)	**Biogenic (%)**	**non-biogenic (%)**	**Biogenic Component**	**Non-BiogenicComponent**
0-2	20	80	Mostly sponge spicules	90% Quartz, 5% Feldspar, 5%AM
2-4	20	80	Mostly sponge spicules	95% Quartz, 5% Feldspar
4-6	15	85	Mostly sponge Spicules	95% Quartz, 5%Feldspar
6-8	12	88	Sponge spicules and triceratium forams	90% Quartz, 5% Feldspar, 5%AM
8-10	10	90	Diatoms, forams and sponge spicules	90% Quartz, 5%Feldspar, 5%AM
10-12	12	88	Mostly sponge spicules	85% Quartz, 10%Feldspar, 5%AM
12-14	10	90	Mostly sponge spicules	75% Quartz, 10% Feldspar, 5% AM
14-16	10	90	Mostly sponge spicules	80% Quartz, 10% Feldspar, 10% AM
16-18	20	80	Mostly sponge spicules	90% Quartz, 10% Feldspar
18-20	10	90	Mostly sponge spicules	95% Quartz, 5% Feldspar
20-22	12	88	Mostly sponge spicules	60% Quartz, 10% Feldspar, 5% AM
22-24	8	92	Mostly sponge spicules	85% Quartz, 10% Feldspar, 5% AM
24-26	8	92	Mostly sponge spicules	85% Quartz, 10% Feldspar, 5% AM
26-28	6	94	Mostly sponge spicules	80% Quartz, 15% Feldspar, 5% AM
28-30	5	95	Mostly sponge spicules	85% Quartz, 10% Feldspar, 5% AM
30-32	15	85	Mostly sponge spicules	85% Quartz, 10% Feldspar, 5% AM
32-34	10	90	Mostly sponge spicules	85% Quartz, 10% Feldspar, 5% AM
34-36	12	88	Mostly sponge spicules	85% Quartz, 10% Feldspar, 5% AM
36-38	8	92	Mostly sponge spicules	85% Quartz, 10% Feldspar, 5% AM
38-40	8	92	Mostly sponge spicules	85% Quartz, 10% Feldspar, 5% AM

Appendix A26: Major element composition of the core from the Volta Estuary

Depth (cm)	**Al_2O_3 %**	**Li_2O %**	**Na_2O %**	**MgO %**	**P_2O_5 %**	**SO_3 %**	**K_2O %**	**CaO %**	**TiO_2 %**	**MnO %**	**Fe_2O_3 %**	**Rb_2O %**	**SrO %**	**SiO_2 %**
0-2	7.33	0.00	0.90	0.60	0.09	0.81	0.97	0.50	0.51	0.24	3.80	0.00	0.01	84.22
2-4	6.76	0.00	0.96	0.57	0.08	0.87	1.04	0.45	0.49	0.19	3.75	0.00	0.01	84.82
4-6	5.56	0.00	0.78	0.34	0.04	0.97	1.28	0.39	0.38	0.07	2.32	0.00	0.01	87.85
6-8	9.36	0.01	0.92	0.83	0.06	2.60	1.17	0.86	0.64	0.29	4.42	0.01	0.01	78.82
8-10	9.30	0.01	0.95	0.86	0.07	2.50	1.14	1.01	0.67	0.31	4.36	0.00	0.01	78.80
10-12	10.02	0.01	1.05	0.91	0.07	2.57	1.24	1.12	0.78	0.30	4.64	0.01	0.01	77.29
12-14	9.86	0.01	1.06	0.87	0.07	2.66	1.22	1.01	0.70	0.24	4.48	0.01	0.01	77.82
14-16	8.24	0.01	1.03	0.71	0.06	2.15	1.12	0.82	0.60	0.18	3.70	0.00	0.01	81.38
16-18	7.50	0.00	0.99	0.62	0.06	1.71	1.04	0.79	0.56	0.13	3.27	0.00	0.01	83.31
18-20	8.20	0.00	0.98	0.69	0.07	1.69	1.06	0.79	0.62	0.16	3.75	0.00	0.01	81.97
20-22	12.69	0.01	1.09	1.06	0.09	2.75	1.34	1.24	0.87	0.11	5.73	0.01	0.01	73.00
22-24	14.97	0.01	1.12	1.24	0.09	2.67	1.50	0.95	0.81	0.07	5.90	0.01	0.01	70.65

24-26	13.54	0.01	1.23	1.12	0.09	2.71	1.47	1.08	0.83	0.13	5.54	0.01	0.01	72.22
26-28	13.22	0.01	1.19	1.07	0.09	2.54	1.37	1.05	0.74	0.12	5.39	0.01	0.01	73.22
28-30	14.60	0.01	1.12	1.13	0.10	2.39	1.42	0.99	0.78	0.08	5.79	0.01	0.01	71.59
30-32	8.90	0.00	0.90	0.72	0.13	0.99	1.07	0.55	0.58	0.36	4.56	0.00	0.01	81.21
32-34	8.26	0.00	1.05	0.72	0.06	1.76	1.11	1.12	0.78	0.23	3.82	0.00	0.01	81.06
34-36	10.03	0.01	1.35	0.95	0.09	2.53	1.26	1.39	0.80	0.36	4.73	0.01	0.01	76.48
36-38	10.20	0.01	1.25	0.84	0.07	2.04	1.20	1.12	0.81	0.19	4.37	0.01	0.01	77.87
38-40	10.18	0.01	1.24	0.87	0.07	2.20	1.30	1.14	0.83	0.19	4.45	0.01	0.01	77.51

APPENDIX B

Appendix B1. Radionuclide records of sediment core of the Ankobra Estuary

Depth Interval (cm)	^{210}Pb (dpm/g)	Error	^{226}Ra (dpm/g)	Error	Excess ^{210}Pb (dpm/g)	Error	Dry Bulk Density (g/cm^3)
0-2	4.09	0.78	0.98	0.18	3.12	0.80	1.3893
2-4	2.2	0.52	1.12	0.14	1.10	0.54	1.3245
4-6	2.19	0.47	0.56	0.23	0.27	0.51	1.5351
6-8	1.81	0.47	0.92	0.10	0.94	0.48	1.4886
8-10	2.97	0.74	1.8	0.10	0.63	0.75	1.4784

Appendix B2. Radionuclide records of sediment core of the Pra Estuary

Depth Interval (cm)	^{210}Pb (dpm/g)	Error	^{226}Ra (dpm/g)	Error	Excess ^{210}Pb (dpm/g)	Error	Dry Bulk Density (g/cm^3)
0-2	3.37	0.68	1.59	0.11	1.77	0.69	1.0736
2-4	2.98	1.05	2.81	0.17	0.17	1.07	1.4614
4-6	3.86	1.38	3.75	0.17	0.11	1.40	1.5759
6-8	1.62	0.72	1.26	0.13	0.36	0.73	1.4761
8-10	2.50	0.84	2.42	0.15	0.07	0.86	1.3514
10-12	2.86	0.56	2.01	0.11	0.85	0.57	1.0007
12-14	2.45	0.54	2.06	0.08	0.39	0.55	1.1589
14-16	2.16	0.50	1.98	0.10	0.18	0.51	1.2722

Appendix B3. Radionuclide records of sediment core of the Amisa Estuary

Depth Interval (cm)	^{210}Pb (dpm/g)	Error	^{226}Ra (dpm/g)	Error	Excess ^{210}Pb (dpm/g)	Error	Dry Bulk Density (g/cm3)
0-2	9.04	0.93	2.01	0.16	6.18	0.96	0.4844
2-4	7.84	0.65	1.73	0.17	5.77	0.68	0.8939
4-6	7.51	1.02	1.63	0.13	5.70	1.05	0.7306
6-8	7.02	0.80	1.44	0.12	5.30	0.83	0.7204
8-10	7.03	0.74	1.67	0.16	5.32	0.76	0.7418
10-12	7.10	0.76	2.38	0.13	4.29	0.82	0.6848
12-14	7.54	0.67	1.81	0.13	5.43	0.72	0.7598
14-16	7.21	0.63	1.54	0.10	4.78	0.68	0.9258
16-18	8.75	0.65	1.70	0.13	7.00	0.69	0.7656
18-20	6.35	0.62	1.64	0.11	4.88	0.66	0.7192
20-22	8.59	1.18	2.07	0.15	6.74	1.25	0.7253
22-24	7.25	0.70	1.62	0.12	5.69	0.75	0.7032
24-26	6.19	0.70	1.95	0.13	4.41	0.75	0.7597

Appendix B4. Radionuclide records sediment core of the Densu Estuary

Depth Interval (cm)	^{210}Pb (dpm/g)	Error	^{226}Ra (dpm/g)	Error	Excess ^{210}Pb (dpm/g)	Error	Dry Bulk Density (g/cm^3)
0-2	6.87	1.03	0.97	0.16	5.78	1.05	0.385
2-4	2.15	0.59	0.90	0.13	1.21	0.60	0.8167
4-6	2.55	0.55	0.82	0.10	1.69	0.56	0.9974
6-8	0.89	0.52	0.63	0.08	0.25	0.53	1.0267
8-10	3.28	0.77	0.77	0.12	2.46	0.78	1.0065
10-12	3.33	0.62	1.23	0.11	1.95	0.64	0.9908
12-14	3.04	0.67	1.77	0.11	1.13	0.68	0.9997
14-16	2.85	0.66	1.91	0.14	0.80	0.68	1.0296

Appendix B5. Radionuclide records of sediment core of the Sakumo II Estuary

Depth Interval (cm)	^{210}Pb (dpm/g)	Error	^{226}Ra (dpm/g)	Error	Excess ^{210}Pb (dpm/g)	Error	Dry Bulk Density (g/cm^3)
0-2	10.84	1.13	1.40	0.20	9.44	1.15	0.1716
2-4	6.76	0.93	1.53	0.15	5.23	0.95	0.1921
4-6	8.55	0.92	2.40	0.16	6.15	0.94	0.2391
6-8	5.61	0.77	1.82	0.14	3.80	0.78	0.2308
8-10	7.39	0.74	1.78	0.14	5.61	0.75	0.2583
10-12	6.47	0.91	1.88	0.11	4.59	0.92	0.2656
12-14	5.80	0.93	1.43	0.15	4.37	0.95	0.2722
14-16	6.03	0.93	1.58	0.16	4.45	0.94	0.2939

Appendix B6. Radionuclide records of sediment core of the Volta Estuary

Depth Interval (cm)	^{210}Pb (dpm/g)	Error	^{226}Ra (dpm/g)	Error	Excess ^{210}Pb (dpm/g)	Error	Dry Bulk Density (g/cm^3)
0-2	3.95	0.62	1.95	0.13	2.00	0.63	0.6376
2-4	3.31	0.49	1.39	0.11	1.92	0.51	0.7391
4-6	2.70	0.58	1.55	0.12	1.15	0.59	0.9133
6-8	2.20	0.42	1.14	0.09	1.06	0.43	1.2195
8-10	3.87	0.73	1.69	0.14	2.18	0.74	1.021
10-12	3.53	0.79	2.03	0.11	1.49	0.79	0.9972
12-14	3.34	0.57	1.95	0.14	1.38	0.59	0.9661
14-16	2.75	0.93	1.86	0.11	0.88	0.93	0.9338
16-18	2.20	0.53	1.42	0.11	0.79	0.54	1.0089
18-20	1.85	0.66	1.26	0.12	0.59	0.67	1.0472
20-22	2.64	0.82	1.71	0.11	0.93	0.83	1.0132
22-24	2.39	0.52	1.84	0.11	0.55	0.53	0.8816
24-26	2.37	0.71	1.93	0.10	0.44	0.72	0.8203
26-28	2.41	0.71	1.99	0.10	0.43	0.71	0.8027
28-30	2.31	0.52	2.10	0.13	0.20	0.54	0.7853
30-32	3.31	0.52	1.94	0.10	1.37	0.53	0.7766
32-34	5.69	0.69	1.74	0.12	3.95	0.70	0.8611
34-36	2.57	0.68	2.37	0.11	0.20	0.69	1.0523
36-38	1.98	0.69	1.86	0.11	0.12	0.70	0.9305
38-40	2.21	0.69	2.21	0.11	0.00	0.70	0.9833

Appendix B7. Results of T-test analysis comparing metal concentrations before and after industrialization in the Ankobra Estuary

Element	Post-Mean	Pre-Mean	t	P (At 0.05 Sig. Level)
Mo	0.59±0.06	0.91±0.22	2.42	0.03
Cd	0.08±0.02	0.09±0.02	1.19	0.25
Pb	7.25±0.80	9.82±2.32	1.84	0.09
Cr	67.97±8.48	97.21±19.45	2.05	0.07
V	66.05±24.26	74.47±16.73	0.76	0.45
Cu	17.82±2.15	21.35±4.74	1.41	0.18
Zn	45.82±2.62	62.46±10.77	2.65	0.02
As	99.06±16.73	109.29±19.99	0.81	0.43
Hg	0.15±0.03	0.19±0.00	1.42	0.18

Appendix B8. Results of T-test analysis comparing metal concentrations before and after industrialization in the Pra Estuary

	Post-Mean	Pre-Mean	t	P (At 0.05 Sig. Level)
Mo	0.55±0.14	0.84±0.08	5.17	0.00
Cd	0.07±0.29	0.09±0.01	3.13	0.01
Pb	9.75±2.14	13.07±1.53	3.98	0.00
Cr	76.45±18.94	97.05±19.45	2.39	0.03
V	71.12±11.93	86.66±13.32	1.83	0.08
Cu	21.31±4.81	26.05±4.31	2.32	0.03
Zn	50.84±11.28	66.79±9.87	3.37	0.00
As	30.02±7.03	40.84±4.39	4.13	0.00
Hg	0.22±0.08	0.23±0.02	0.61	0.55

Appendix B9. Results of T-test analysis comparing metal concentrations before and after industrialization in the Amisa Estuary

	Post-Mean	Pre-Mean	t	P (At 0.05 Sig. Level)
Mo	1.62±0.00	2.18±0.02	7.399	0.00
Cd	0.07±0.00	0.09±0.00	1.94	0.06
Pb	23.38±2.11	23.15±1.41	-0.31	0.76
Cr	85.97±15.30	88.67±19.65	1.298	0.21
V	73.95±16.56	75.20±13.03	-1.82	0.09
Cu	19.69±1.10	26.04±1.53	3.199	0.00
Zn	70.39±9.15	66.79±19.48	-0.34	0.73
As	12.49±1.12	10.22±0.44	-4.49	0.00
Hg	0.12±0.00	0.17±0.00	2.23	0.08

Appendix B11. Results of T-test analysis comparing metal concentrations before and after industrialization in the Densu Estuary

	Post-Mean	Pre-Mean	t	P (At 0.05 Sig. Level)
Mo	1.01±0.00	0.88±0.01	-2.69	0.02
Cd	0.06±0.00	0.04±0.00	-4.2	0.00
Pb	11.14±0.53	8.00±3.9	-3.05	0.01
Cr	37.11±5.91	30.15±12.87	-2.25	0.04
V	41.73±17.5	30.16±8.09	-11.58	0.00
Cu	12.53±1.054	10.52±3.32	-1.86	0.08
Zn	31.94±3.32	25.19±8,22	-2.7	0.02
As	3.7±0.08	3.04±0.5	-2.34	0.03
Hg	0.21±0.15	0.04±0.00	-1.44	0.17

Appendix B12. Results of T-test analysis comparing metal concentrations before and after industrialization in the Sakumo II Estuary

	Post-Mean	Pre-Mean	t	P (At 0.05 Sig. Level)
Mo	3.81±0.37	3.69±0.01	-0.39	0.69
Cd	0.14±0.00	0.09±0.00	-3.86	0.00
Pb	38.97±8.05	35.74±0.81	-2.17	0.07
Cr	94.44±8.23	98.99±0.82	1.01	0.35
V	82.73±5.27	77.29±1.01	-1.82	0.18
Cu	44.84±5.22	38.76±0..32	-2.46	0.04
Zn	111.26±17.57	79.19±0.09	-3.66	0.01
As	4.27±0.243	4.66±0.05	1.51	0.16
Hg	0.31±0.00	0.18±0.00	-3.70	0.01

Appendix B13. Results of T-test analysis comparing metal concentrations before and after industrialization in the Volta Estuary

	Post-Mean	Pre-Mean	t	P (At 0.05 Sig. Level)
Mo	0.68±0.02	0.67±0.13	0.29	0.78
Cd	0.03±0.00	0.03±0.00	-0.27	0.78
Pb	13.50±2.53	13.77±1.12	0.28	0.78
Cr	58.27±16.27	60.88±14.12	0.35	0.74
V	55.43±17.66	58.08±20.87	0.32	0.73
Cu	17.30±5.56	18.10±6.13	0.31	0.76
Zn	41.29±1.23	44.59±4.56	0.68	0.51
As	6.37±1.22	6.35±0.59	-0.04	0.97
Hg	0.07±0.00	0.06±0.00	-0.07	0.47

Appendix B14. Spearman correlation analysis of trace metals in the Ankobra estuary (*correlation significant at 0.05, **correlation significant at 0.01 significance level)

	Mo	Cd	Pb	V	Cr	Cu	Zn	As	Hg	OC	Al
Mo	1	.524*	.623*	.640*	.628*	.555*	.673**	.328	.465	.413	.608*
		.045	.013	.010	.012	.032	.006	.233	.080	.126	.016
Cd		1	.903**	.903**	.903**	.966**	.785**	.959**	.436	.687**	.909**
			.000	.000	.000	.000	.001	.000	.104	.005	.000
Pb			1	.982**	.974**	.956**	.949**	.873**	.357	.765**	.984**
				.000	.000	.000	.000	.000	.191	.001	.000
V				1	.998**	.951**	.947**	.860**	.352	.749**	.994**
					.000	.000	.000	.000	.198	.001	.000
Cr					1	.944**	.932**	.861**	.352	.742**	.991**
						.000	.000	.000	.198	.002	.000
Cu						1	.859**	.943**	.375	.746**	.956**
							.000	.000	.168	.001	.000
Zn							1	.735**	.331	.675**	.939**
								.002	.228	.006	.000
As								1	.350	.632*	.870**
									.201	.012	.000
Hg									1	.129	.369
										.647	.176
OC										1	.778**
											.001
Al											1

Appendix B15. Spearman correlation analysis of trace metals in the Pra estuary (*correlation significant at 0.05, **correlation significant at 0.01 significance level)

	Mo	Cd	Pb	V	Cr	Cu	Zn	As	Hg	OC	Al
Mo	1	.795**	.948**	.804**	.794**	.789**	.903**	.974**	.412	.809**	.815**
		.000	.000	.000	.000	.000	.000	.000	.071	.000	.000
Cd		1	.876**	.895**	.895**	.887**	.902**	.791**	.280	.710**	.888**
			.000	.000	.000	.000	.000	.000	.232	.000	.000
Pb			1	.943**	.938**	.932**	.988**	.947**	.493*	.791**	.949**
				.000	.000	.000	.000	.000	.027	.000	.000
V				1	.999**	.992**	.979**	.834**	.503*	.710**	.998**
					.000	.000	.000	.000	.024	.000	.000
Cr					1	.993**	.976**	.823**	.492*	.700**	.997**
						.000	.000	.000	.028	.001	.000
Cu						1	.970**	.831**	.482*	.691**	.990**
							.000	.000	.032	.001	.000
Zn							1	.913**	.493*	.766**	.982**
								.000	.027	.000	.000
As								1	.409	.773**	.840**
									.074	.000	.000
Hg									1	.216	.510*
										.360	.022
OC										1	.707**
											.000
Al											1

Appendix B16. Spearman correlation analysis of trace metals in the Amisa estuary (*correlation significant at 0.05, **correlation significant at 0.01 significance level)

	Mo	Cd	Pb	V	Cr	Cu	Zn	As	Hg	OC	Al
Mo	1	.840**	.243	.502*	.526*	.867**	.306	-.452	.308	-.849**	.432
		.000	.316	.028	.021	.000	.203	.052	.199	.000	.065
Cd		1	.346	.457*	.460*	.824**	.345	-.203	.364	-.862**	.444
			.147	.049	.048	.000	.148	.404	.126	.000	.057
Pb			1	.727**	.731**	.544*	.909**	.480*	-.150	-.038	.523*
				.000	.000	.016	.000	.038	.540	.878	.022
V				1	.988**	.803**	.866**	.223	-.125	-.252	.582**
					.000	.000	.000	.359	.610	.298	.009
Cr					1	.825**	.866**	.161	-.124	-.275	.591**
						.000	.000	.509	.612	.255	.008
Cu						1	.658**	-.173	.144	-.689**	.558*
							.002	.479	.555	.001	.013
Zn							1	.426	-.217	-.095	.627**
								.069	.372	.699	.004
As								1	-.259	.431	.094
									.283	.065	.703
Hg									1	-.414	-.247
										.078	.308
OC										1	-.320
											.182
Al											1

Appendix B17. Spearman correlation analysis of trace metals in the Densu estuary (*correlation significant at 0.05, **correlation significant at 0.01 significance level)

	Mo	Cd	Pb	V	Cr	Cu	Zn	As	Hg	OC	Al
Mo	1	.887**	.861**	.945**	.902**	.915**	.939**	.983**	.156	.899**	.891**
		.000	.000	.000	.000	.000	.000	.000	.511	.000	.000
Cd		1	.955**	.916**	.933**	.889**	.958**	.931**	.269	.830**	.905**
			.000	.000	.000	.000	.000	.000	.252	.000	.000
Pb			1	.935**	.964**	.918**	.969**	.923**	.252	.802**	.947**
				.000	.000	.000	.000	.000	.283	.000	.000
V				1	.989**	.982**	.989**	.963**	.153	.883**	.987**
					.000	.000	.000	.000	.521	.000	.000
Cr					1	.974**	.991**	.940**	.176	.851**	.993**
						.000	.000	.000	.459	.000	.000
Cu						1	.969**	.924**	.177	.891**	.980**
							.000	.000	.456	.000	.000
Zn							1	.969**	.195	.878**	.979**
								.000	.411	.000	.000
As								1	.191	.871**	.924**
									.419	.000	.000
Hg									1	.086	.189
										.719	.424
OC										1	.849**
											.000
Al											1

Appendix B18. Spearman correlation analysis of trace metals in the Sakumo II estuary (*correlation significant at 0.05, **correlation significant at 0.01 significance level)

	Mo	Cd	Pb	V	Cr	Cu	Zn	As	Hg	OC	Al
Mo	1	.840**	.815**	.854**	.689**	.901**	.843**	.346	.701**	-.194	.544*
		.000	.000	.000	.001	.000	.000	.135	.001	.412	.013
Cd		1	.799**	.756**	.353	.911**	.960**	.008	.857**	.100	.263
			.000	.000	.127	.000	.000	.972	.000	.675	.263
Pb			1	.948**	.728**	.954**	.843**	.422	.636**	.000	.744**
				.000	.000	.000	.000	.064	.003	.999	.000
V				1	.833**	.939**	.787**	.516*	.563**	-.007	.768**
					.000	.000	.000	.020	.010	.978	.000
Cr					1	.661**	.392	.836**	.172	-.317	.902**
						.002	.087	.000	.469	.174	.000
Cu						1	.942**	.326	.773**	-.007	.602**
							.000	.161	.000	.976	.005
Zn							1	.039	.898**	.063	.351
								.869	.000	.791	.129
As								1	-.150	-.249	.749**
									.528	.290	.000
Hg									1	.017	.135
										.945	.571
OC										1	-.319
											.171
Al											1

Appendix B19. Spearman correlation analysis of trace metals in the Volta estuary (*correlation significant at 0.05, **correlation significant at 0.01 significance level)

	Mo	Cd	Pb	V	Cr	Cu	Zn	As	Hg	OC	Al
Mo	1	.200	.656**	.888**	.907**	.853**	.792**	.505*	.085	-.340	.904**
		.399	.002	.000	.000	.000	.000	.023	.722	.142	.000
Cd		1	.412	.189	.252	.333	.444*	.493*	-.171	-.071	.207
			.071	.424	.283	.151	.050	.027	.472	.765	.381
Pb			1	.747**	.810**	.813**	.847**	.828**	-.432	-.499*	.759**
				.000	.000	.000	.000	.000	.057	.025	.000
V				1	.987**	.975**	.872**	.484*	-.176	-.304	.984**
					.000	.000	.000	.031	.458	.193	.000
Cr					1	.982**	.913**	.578**	-.170	-.390	.990**
						.000	.000	.008	.475	.089	.000
Cu						1	.932**	.591**	-.197	-.311	.975**
							.000	.006	.406	.182	.000
Zn							1	.757**	-.277	-.362	.879**
								.000	.237	.117	.000
As								1	-.354	-.411	.522*
									.125	.072	.018
Hg									1	.210	-.132
										.373	.579
OC										1	-.396
											.084
Al											1

APPENDIX C

Appendix C1. Marine and Freshwater Spiked Sediment Toxicity Test Dataset for Copper (ANZECC/ARMCANZ)

Sp Latin Name	Sp Common Name	Trophic	Effect	Endpoint	Conc (ug/L)	Temp	Hardness Range	pH	Year	Author
Invertebrates	Invertebrates	2	ABD	NR	3	19.7	57	8.53	1989	Clements,W.H.,
Invertebrates	Invertebrates	2	MOR	LC50	6	20	53 - 57		1989	Clements,W.H., J.L.Farris,
Invertebrates	Invertebrates	2	ABD	NR	9	22	60	9.28	1989	Clements,W.H.,
Invertebrates	Invertebrates	2	POP	NR	10.7 - 29.7	24	65 - 68		1990	Clements,W.H.,
Invertebrates	Invertebrates	2	POP	NR	11.3 - 31.3	26	75 - 80		1990	Clements,W.H.,
Invertebrates	Invertebrates	2	ABD	NR	12	22	153	8.82	1989	Clements,W.H.,
Invertebrates	Invertebrates	2	MOR	LC50	15	20	150		1989	Clements,W.H., J.L.Farris,
Lumbriculus variegatus	Oligochaete	5	MOR	LC50	35	22	44 - 47**		1993	West,C.W., V.R.Mattson,
Gastropoda	Snails, limpets	2	ABD	NR	40	18	95 - 120		1990	Winner,R.W.,
Invertebrates	Invertebrates	2	ABD	NR	40	18	95 - 120		1990	Winner,R.W.,
Bivalvia	Bivalve, clam, mussel	2	ABD	NR	40	18	95 - 120		1990	Winner,R.W.,
Invertebrates	Invertebrates	2	ABD	NR	6.3E-7 - 7.7E-6 M				1987	Hawkins,P.R. and
Invertebrates	Invertebrates	2	ABD	NR	120	4	88 - 352		1976	Geckler,J.R.,
Skeletonema costatum	Diatom	1	TH MOR	NR-LE	150	13			1976	Braek,G.S., A.Jensen, and
Nitzschia acicularis	Diatom	1	PGR	EC100	4.0 umol/L	20		8.2	1989	Luderitz,V. and A.Nicklisch
Stephanodiscus rotula	Diatom	1	PGR	EC100	4.0 umol/L	20		8.2	1989	Luderitz,V. and A.Nicklisch
Nitzschia palea	Diatom	1	PGR	EC50	520	24			1989	Gowrinathan,K.P.
Cyclotella meneghiniana	Diatom	1	PGR	EC50	530	24			1989	Gowrinathan,K.P.
Nitzschia obtusa	Diatom	1	PGR	EC50	640	24			1989	Gowrinathan,K.P.
Cyclotella meneghiniana	Diatom	1	PGR	EC50	740	24			1989	Gowrinathan,K.P.
Mystus bleekeri	Catfish	3, 5	MOR	LC50	776	25	232 - 250	7.5	1988	Khangarot,B.S. and P.K.Ray
Velesunio angasi	Mussel	2	MOR	LC50	7800	24			1983	Skidmore,J.F. and I.C.Firth
Velesunio angasi	Mussel	2	MOR	LC50	<7800	24			1983	Skidmore,J.F. and I.C.Firth
Velesunio angasi	Mussel	2	MOR	LC50	<7800	24			1983	Skidmore,J.F. and I.C.Firth
Asterionella formosa	Diatom	1	BMS	NR	5.9 - 7.05 M	16		6.8	1981	McKnight,D.

Appendix C2. Marine and Freshwater Spiked Sediment Toxicity Test Dataset for Hg (ANZECC/ARMCANZ)

Latin Name	Sp Common Name	Trophic	Effect	Endpoint	Temp (C)	Hardness (mg/L)	pH	Conc (ug/L)	Year	Author
Tilapia zillii	Tilapia	3, 4	MOR	LC50				190	1986	El-Sebae,A.H., M.A.El-Amayem,
Ictalurus punctatus	Channel catfish	3, 5	MOR	LC50*	23	22	8.7	310	1958	Clemens,H.P. and K.E.Sneed
Ictalurus punctatus	Channel catfish	3, 5	MOR	LC50*	23	22	8.7	310	1958	Clemens,H.P. and K.E.Sneed
Ictalurus punctatus	Channel catfish	3, 5	MOR	LC50*	20	22	8.7	350	1958	Clemens,H.P. and K.E.Sneed
Ictalurus punctatus	Channel catfish	3, 5	MOR	LC50*	20	22	8.7	360	1958	Clemens,H.P. and K.E.Sneed
Ictalurus punctatus	Channel catfish	3, 5	MOR	LC50*	16.5	22	8.7	370	1958	Clemens,H.P. and K.E.Sneed
Ictalurus punctatus	Channel catfish	3, 5	MOR	LC50*	16.5	22	8.7	370	1958	Clemens,H.P. and K.E.Sneed
Ictalurus punctatus	Channel catfish	3, 5	MOR	LC50*	16.5	22	8.7	370	1958	Clemens,H.P. and K.E.Sneed
Ictalurus punctatus	Channel catfish	3, 5	MOR	LC50*	23	22	8.7	370	1958	Clemens,H.P. and K.E.Sneed
Ictalurus punctatus	Channel catfish	3, 5	MOR	LC50*	24	22	8.7	370	1958	Clemens,H.P. and K.E.Sneed
Ictalurus punctatus	Channel catfish	3, 5	MOR	LC50*	24	22	8.7	370	1958	Clemens,H.P. and K.E.Sneed
Ictalurus punctatus	Channel catfish	3, 5	MOR	LC50*	24	22	8.7	370	1958	Clemens,H.P. and K.E.Sneed
Ictalurus punctatus	Channel catfish	3, 5	MOR	LC50*	24	22	8.7	370	1958	Clemens,H.P. and K.E.Sneed
Ictalurus punctatus	Channel catfish	3, 5	MOR	LC50*	23	22	8.7	374	1958	Clemens,H.P. and K.E.Sneed
Ictalurus punctatus	Channel catfish	3, 5	MOR	LC50*	20	22	8.7	460	1958	Clemens,H.P. and K.E.Sneed
Ictalurus punctatus	Channel catfish	3, 5	MOR	LC50*		22	8.7	470	1958	Clemens,H.P. and K.E.Sneed
Ictalurus punctatus	Channel catfish	3, 5	MOR	LC50*	23	22	8.7	490	1958	Clemens,H.P. and K.E.Sneed
Ictalurus punctatus	Channel catfish	3, 5	MOR	LC50*	24	22	8.7	490	1958	Clemens,H.P. and K.E.Sneed
Ictalurus punctatus	Channel catfish	3, 5	MOR	LC50	25			580	1959	Clemens,H.P. and K.E.Sneed
Ictalurus punctatus	Channel catfish	3, 5	MOR	LC50	25			600	1959	Clemens,H.P. and K.E.Sneed
Ictalurus punctatus	Channel catfish	3, 5	MOR	LC50	25			780	1959	Clemens,H.P. and K.E.Sneed
Ictalurus punctatus	Channel catfish	3, 5	MOR	LC50*		22	8.7	850	1958	Clemens,H.P. and K.E.Sneed
Ictalurus punctatus	Channel catfish	3, 5	MOR	LC50*	20	22	8.7	870	1958	Clemens,H.P. and K.E.Sneed
Nais sp	Oligochaete	5	MOR	LC50*	17	50	7.6	1000	1973	Rehwoldt,R., L.Lasko, C.Shaw,
Ictalurus punctatus	Channel catfish	3, 5	~MO	LC0		22	8.7	1000	1958	Clemens,H.P. and K.E.Sneed
Ictalurus punctatus	Channel catfish	3, 5	MOR	LC50*	20	22	8.7	1400	1958	Clemens,H.P. and K.E.Sneed
Ictalurus punctatus	Channel catfish	3, 5	MOR	LC50	25			1500	1959	Clemens,H.P. and K.E.Sneed

Ictalurus punctatus	Channel catfish	3, 5	MOR	LC50*	20	22	8.7	1600	1958	Clemens,H.P. and K.E.Sneed
Latin Name	Sp Common Name	Trophic	Effect	Endpoint	Temp(C)	Hardness(mg/L)	pH	Conc(ug/L)	Year	Author
Ictalurus punctatus	Channel catfish	3, 5	MOR	LC50*		22	8.7	1610	1958	Clemens,H.P. and K.E.Sneed
Ictalurus punctatus	Channel catfish	3, 5	MOR	LC50*		22	8.7	1710	1958	Clemens,H.P. and K.E.Sneed
Ictalurus punctatus	Channel catfish	3, 5	MOR	LC50*	16.5	22	8.7	1810	1958	Clemens,H.P. and K.E.Sneed
Nais sp	Oligochaete	5	MOR	LC50*	17	50	7.6	1900	1973	Rehwoldt,R., L.Lasko, C.Shaw,
Ictalurus punctatus	Channel catfish	3, 5	MOR	LC50*	10	22		2020	1958	Clemens,H.P. and K.E.Sneed
Ictalurus punctatus	Channel catfish	3, 5	MOR	LC50*	23	22	8.7	2180	1958	Clemens,H.P. and K.E.Sneed
Ictalurus punctatus	Channel catfish	3, 5	MOR	LC50*	10	22		2210	1958	Clemens,H.P. and K.E.Sneed
Ictalurus punctatus	Channel catfish	3, 5	MOR	LC50	25			2300	1959	Clemens,H.P. and K.E.Sneed
Ictalurus punctatus	Channel catfish	3, 5	MOR	LC50*	10	22		2430	1958	Clemens,H.P. and K.E.Sneed
Ictalurus punctatus	Channel catfish	3, 5	MOR	LC50	25			2700	1959	Clemens,H.P. and K.E.Sneed
Ictalurus punctatus	Channel catfish	3, 5	MOR	LC50*	10	22		2810	1958	Clemens,H.P. and K.E.Sneed
Ictalurus punctatus	Channel catfish	3, 5	MOR	LC50*	16.5	22	8.7	2810	1958	Clemens,H.P. and K.E.Sneed
Ictalurus punctatus	Channel catfish	3, 5	MOR	LC50*	16.5	22		2960	1958	Clemens,H.P. and K.E.Sneed
Ictalurus punctatus	Channel catfish	3, 5	MOR	LC50	25			3300	1959	Clemens,H.P. and K.E.Sneed
Ictalurus punctatus	Channel catfish	3, 5	MOR	LC50	25			3300	1959	Clemens,H.P. and K.E.Sneed
Ictalurus punctatus	Channel catfish	3, 5	MOR	LC50	25			3400	1959	Clemens,H.P. and K.E.Sneed
Ictalurus punctatus	Channel catfish	3, 5	MOR	LC50*		22	8.7	3660	1958	Clemens,H.P. and K.E.Sneed
Ictalurus punctatus	Channel catfish	3, 5	MOR	LC50*	23	22	8.7	3750	1958	Clemens,H.P. and K.E.Sneed
Ictalurus punctatus	Channel catfish	3, 5	MOR	LC50*	24	22	8.7	3750	1958	Clemens,H.P. and K.E.Sneed
Ictalurus punctatus	Channel catfish	3, 5	MOR	LC50*	23	22	8.7	4018	1958	Clemens,H.P. and K.E.Sneed
Ictalurus punctatus	Channel catfish	3, 5	MOR	LC50	25			4100	1959	Clemens,H.P. and K.E.Sneed
Ictalurus punctatus	Channel catfish	3, 5	MOR	LC50*	10	22		4120	1958	Clemens,H.P. and K.E.Sneed
Ictalurus punctatus	Channel catfish	3, 5	MOR	LC50*	20	22	8.7	5000	1958	Clemens,H.P. and K.E.Sneed
Ictalurus punctatus	Channel catfish	3, 5	MOR	LC50*	23	22	8.7	5000	1958	Clemens,H.P. and K.E.Sneed
Ictalurus punctatus	Channel catfish	3, 5	MOR	LC50*	23	22	8.7	5000	1958	Clemens,H.P. and K.E.Sneed
Ictalurus punctatus	Channel catfish	3, 5	~MO	NR		22	8.7	5000	1958	Clemens,H.P. and K.E.Sneed
Lamellidens marginalis	Mussel	2	MOR	LC50				5000	1991	Raj,A.I.M. and P.S.Hameed

Ictalurus punctatus	Channel catfish	3, 5	MOR	LC50*	10	22	8.7	5790	1958	Clemens,H.P. and K.E.Sneed
Ictalurus punctatus	Channel catfish	3, 5	MOR	LC50*	23	22	8.7	5790	1958	Clemens,H.P. and K.E.Sneed
Latin Name	Sp Common Name	Trophic	Effect	Endpoint	Temp(C)	Hardness(mg/L)	pH	Conc(ug/L)	Year	Author
Ictalurus punctatus	Channel catfish	3, 5	MOR	LC50*	24	22	8.7	5790	1958	Clemens,H.P. and K.E.Sneed
Ictalurus punctatus	Channel catfish	3, 5	MOR	LC50	25			8300	1959	Clemens,H.P. and K.E.Sneed
Ictalurus punctatus	Channel catfish	3, 5	MOR	LC50	25			9100	1959	Clemens,H.P. and K.E.Sneed
Lamellidens marginalis	Mussel	2	MOR	LC50				10000	1989	Hameed,P.S. and A.I.M.Raj
Ictalurus punctatus	Channel catfish	3, 5	MOR	LC50*	16.5	22		10760	1958	Clemens,H.P. and K.E.Sneed
Ictalurus punctatus	Channel catfish	3, 5	MOR	LC50*	24	22	8.7	11860	1958	Clemens,H.P. and K.E.Sneed
Ictalurus punctatus	Channel catfish	3, 5	MOR	LC50*	24	22	8.7	11860	1958	Clemens,H.P. and K.E.Sneed
Ictalurus punctatus	Channel catfish	3, 5	MOR	LC50*	16.5	22		18250	1958	Clemens,H.P. and K.E.Sneed
Ictalurus punctatus	Channel catfish	3, 5	MOR	LC50*	10	22	8.7	21070	1958	Clemens,H.P. and K.E.Sneed
Ictalurus punctatus	Channel catfish	3, 5	MOR	LC50*	20	22	8.7	24000	1958	Clemens,H.P. and K.E.Sneed
Ictalurus punctatus	Channel catfish	3, 5	MOR	LC50	25			25000	1959	Clemens,H.P. and K.E.Sneed
Ictalurus punctatus	Channel catfish	3, 5	MOR	LC50	25			25000	1959	Clemens,H.P. and K.E.Sneed
Ictalurus punctatus	Channel catfish	3, 5	MOR	LC50	25			25000	1959	Clemens,H.P. and K.E.Sneed
Ictalurus punctatus	Channel catfish	3, 5	MOR	LC50*	24	22	8.7	34090	1958	Clemens,H.P. and K.E.Sneed
Ictalurus punctatus	Channel catfish	3, 5	MOR	LC50*	24	22	8.7	34090	1958	Clemens,H.P. and K.E.Sneed
Ictalurus punctatus	Channel catfish	3, 5	MOR	LC50	25			40000	1959	Clemens,H.P. and K.E.Sneed
Ictalurus punctatus	Channel catfish	3, 5	MOR	LC50*	10	22	8.7	50000	1958	Clemens,H.P. and K.E.Sneed
Ictalurus punctatus	Channel catfish	3, 5	MOR	LC50*	10	22	8.7	50000	1958	Clemens,H.P. and K.E.Sneed
Ictalurus punctatus	Channel catfish	3, 5	MOR	LC50*	10	22	8.7	50000	1958	Clemens,H.P. and K.E.Sneed
Ictalurus punctatus	Channel catfish	3, 5	MOR	LC50*	16.5	22		50000	1958	Clemens,H.P. and K.E.Sneed
Ictalurus punctatus	Channel catfish	3, 5	MOR	LC50*	16.5	22		50000	1958	Clemens,H.P. and K.E.Sneed
Ictalurus punctatus	Channel catfish	3, 5	MOR	LC50*	24	22	8.7	50000	1958	Clemens,H.P. and K.E.Sneed
Ictalurus punctatus	Channel catfish	3, 5	MOR	LC50*	24	22	8.7	50000	1958	Clemens,H.P. and K.E.Sneed

Appendix C3. Marine and Freshwater Spiked Sediment Toxicity Test Dataset for Arsenic (Source, ANZECC/ARMCANZ)

Sp Latin Name	Sp Common Name	trophic	Effect	Endpoint	Conc (ug/L)	Temper(C)	pH	pHrange	Year	Author
Tubifex tubifex	Tubificid worm	5	BMS	NR	2500			6.2 - 6.8	1992	Reuther,R.
Anodonta cygnea	Swan mussel	2	GRO	NR	2500- 25000			6.2 - 6.8	1992	Reuther,R.
Tubifex tubifex	Tubificid worm	5	IMM	EC50	8870				1991	Khangarot,B.S.
Tubifex tubifex	Tubificid worm	5	IMM	EC50	8870				1991	Khangarot,B.S.
Tubifex tubifex	Tubificid worm	5	IMM	EC50	13010				1991	Khangarot,B.S.
Tubifex tubifex	Tubificid worm	5	MOR	NR	25000			6.2 - 6.8	1992	Reuther,R.
Tubifex tubifex	Tubificid worm	5	MOR	LC50	127360	25	7.4		1994	Fargasova,A.
Tubifex tubifex	Tubificid worm	5	MOR	LC50	190540	25	7.4		1994	Fargasova,A.
Tubifex tubifex	Tubificid worm	5	MOR	LC50	398110	25	7.4		1994	Fargasova,A.

Appendix C4. Marine and Freshwater Spiked Sediment Toxicity Test Dataset for Cadmium (ANZECC/ARMCANZ)

Sp Latin Name	Sp Common Name	Trophic	Effect	Endpoint	Conc (ug/L)	Temp	Hardness Range	pH	Year|	Author
Macrobrachium rosenbergii	Giant freshwater prawn	4, 5	GRO	NR	1.0 - 8.0	27	242	7.9	1990	Liao,I.C. and
Macrobrachium rosenbergii	Giant freshwater prawn	4, 5	MOR	NR	1.0 - 2.0	27	242	7.9	1990	Liao,I.C. and C.S.Hsieh
Macrobrachium rosenbergii	Giant freshwater prawn	4, 5	TH MOR	NR-LE	4.0	27	242	7.9	1990	Liao,I.C. and C.S.Hsieh
Austropotamobius pallipes p	Crayfish	4, 5	MOR	LC50*	<10	16		7	1973	Boutet,C. and C.Chaisemartin
Orconectes limosus	Crayfish	4, 5	MOR	LC50*	<10	16		7	1973	Boutet,C. and C.Chaisemartin
Austropotamobius pallipes p	Crayfish	4, 5	MOR	LC50*	20	16		7	1973	Boutet,C. and C.Chaisemartin
Orconectes limosus	Crayfish	4, 5	MOR	LC50*	50	16		7	1973	Boutet,C. and C.Chaisemartin
Orconectes virilis	Crayfish	4, 5	MOR	LC50	60	20	24 - 28	6.9	1986	Mirenda,R.J.
Orconectes virilis	Crayfish	4, 5	MOR	LC50	700	20	24 - 28	6.9	1986	Mirenda,R.J.
Orconectes virilis	Crayfish	4, 5	MOR	LC50	1000	20	24 - 28	6.9	1986	Mirenda,R.J.
Procambarus sp	Crayfish	4, 5	MOR	LC50	1000	23	20		1978	Fennikoh,K.B., H.I.Hirshfield,
Orconectes virilis	Crayfish	4, 5	MOR	LC50	1800	20	24 - 28	6.9	1986	Mirenda,R.J.

Appendix C5. Marine and Freshwater Spiked Sediment Toxicity Test Dataset for Lead (ANZECC/ARMCANZ)

Sp Latin Name	Sp Common Name	Trophic	Effect	Endpoint	Conc (ug/L)	Temperature	Hardness Range	pH	Year|	Author
Navicula incerta	Diatom	1	PSR	EC50	43	19			1983	Rachlin,J.W.,
Ictalurus punctatus	Channel catfish	3, 5	MOR	NR	75	22	24.5 - 37.0		1976	Sauter,S., K.S.Buxton,
Dreissena polymorpha	Zebra mussel	2	GRO	NR	85	15	150	7.9	1994	Kraak,M.H.S.,
Ictalurus punctatus	Channel catfish	3, 5	MOR	NR	136	22	24.5 - 37.0		1976	Sauter,S., K.S.Buxton,
Dreissena polymorpha	Zebra mussel	2	GRO	NR	358	15	150	7.9	1994	Kraak,M.H.S.,
Dreissena polymorpha	Zebra mussel	2	MOR	LC50	497	15	150	7.9	1994	Kraak,M.H.S., Y.A.Wink,
Cyclotella meneghiniana	Diatom	1	PGR	EC50	1540	24			1989	Gowrinathan,K.P.
Lumbriculus variegatus	Oligochaete	5	MOR	LC50	1800	20	30		1980	Bailey,H.C. and D.H.W.Liu
Dreissena polymorpha	Zebra mussel	2	MOR	LC50	2330	15	150	7.9	1994	Kraak,M.H.S., Y.A.Wink,
Nitzschia obtusa	Diatom	1	PGR	EC50	2470	24			1989	Gowrinathan,K.P.
Cyclotella meneghiniana	Diatom	1	PGR	EC50	3250	24			1989	Gowrinathan,K.P.
Nitzschia palea	Diatom	1	PGR	EC50	3250	24			1989	Gowrinathan,K.P.
Lumbriculus variegatus	Oligochaete	5	MOR	LC50	3400	20	30		1980	Bailey,H.C. and D.H.W.Liu

Appendix C6. Trace metal concentrations in the Ankobra estuary

Locations	Lat	Lon	Cu (µ/g)	Cd (µ/g)	Zn (µ/g)	Pb (µ/g)	As (µ/g)	Hg (µ/g)
A1	4.900038	-2.2685	18.93	0.43	71.46	0.14	90.07	0.31
A2	4.900778	-2.26791	17.92	0.22	66.31	4.17	128.42	0.36
A3	4.900651	-2.26844	20.36	0.14	52.88	0.14	97.20	0.22
A4	4.90054	-2.26907	22.80	0.07	64.82	5.70	93.64	0.36
A5	4.900316	-2.26959	16.92	0.04	45.83	4.17	91.41	0.49
A6	4.901022	-2.2698	17.92	0.04	49.49	5.14	98.10	0.44
A7	4.901078	-2.26919	20.50	0.04	72.14	0.14	93.19	0.44
A8	4.901185	-2.26855	26.24	0.20	31.59	0.26	111.47	0.89
A9	4.901383	-2.26787	24.95	0.04	63.19	5.28	78.48	0.13
A10	4.901915	-2.26823	20.36	0.04	65.09	0.14	61.98	0.09
A11	4.901752	-2.2688	21.22	0.04	53.97	2.22	66.88	0.13
A12	4.901722	-2.26944	27.67	0.04	67.80	0.14	81.60	0.13
A13	4.901597	-2.26993	26.17	0.04	56.95	5.98	73.57	0.09
A14	4.902264	-2.26977	23.38	0.04	56.95	1.96	102.56	0.27
A15	4.902236	-2.26929	16.00	0.07	52.61	3.49	100.77	0.13
A16	4.902278	-2.26879	26.50	0.04	63.73	1.90	98.54	0.22
A17	4.902812	-2.26894	28.39	0.05	63.46	1.12	66.44	0.04
A18	4.902718	-2.2693	18.50	0.05	88.68	0.97	52.17	0.04
A19	4.902664	-2.26968	25.24	0.14	96.00	2.38	54.84	0.04
A20	4.9033	-2.26866	29.54	0.11	98.17	7.79	80.71	0.27
A21	4.903313	-2.26916	11.61	0.14	73.49	5.28	77.59	0.18
A22	4.903223	-2.2696	11.33	0.32	90.72	3.20	91.85	0.27
A23	4.903803	-2.26915	16.63	0.14	55.19	0.83	95.87	0.22
A24	4.903872	-2.26876	25.06	0.22	22.37	2.78	99.43	0.22
A25	4.903855	-2.26834	31.11	0.40	23.46	0.14	118.16	1.07
A26	4.904236	-2.26812	15.92	0.40	19.25	1.39	113.70	0.22
A27	4.904364	-2.2685	16.35	0.50	39.19	6.40	94.08	1.65
A28	4.904424	-2.26877	31.84	0.32	18.58	0.96	188.17	0.22
A29	4.904788	-2.26849	24.52	0.59	24.41	0.14	201.10	1.25
A30	4.904764	-2.26806	29.51	0.63	13.70	0.14	124.85	1.65

Appendix C7. Trace metal concentrations in the Sakumo II estuary

Locations	Lat	Lon	Cu	Cd	Zn	Pb	As	Hg
S1	5.615203	-0.032928	77.5	0.7	7.9	56.9	2.7	2.1
S2	5.616261	-0.032461	72.5	0.5	13.7	54.8	2.7	2.3
S3	5.616022	-0.032961	73.1	0.6	19.5	40.0	2.8	2.4
S4	5.615728	-0.034089	63.9	0.5	16.3	45.9	2.7	2.3
S5	5.616619	-0.034292	28.2	0.4	18.6	34.2	2.6	2.5
S6	5.616778	-0.033803	27.2	0.5	16.3	38.8	2.7	2.1
S7	5.616925	-0.033047	38.8	0.1	20.1	44.9	2.6	2.1
S8	5.617344	-0.032325	62.6	0.6	20.7	47.1	2.2	1.9
S9	5.617939	-0.032794	49.3	0.5	14.2	41.2	2.1	2.9
S10	5.617944	-0.033708	46.5	0.4	8.9	32.4	2.3	1.7
S11	5.617686	-0.034189	26.6	0.3	19.9	29.5	1.9	1.6
S12	5.617506	-0.034711	63.9	0.2	17.6	22.0	1.9	1.0
S13	5.618361	-0.034911	55.0	0.1	25.5	12.2	2.7	1.2
S14	5.618514	-0.034372	44.2	1.8	30.1	28.1	2.5	2.0
S15	5.618572	-0.033469	50.7	2.0	40.5	20.2	2.4	1.7
S16	5.619261	-0.034222	69.5	0.8	34.6	30.2	2.5	2.0
S17	5.619205	-0.035318	65.9	0.3	17.6	41.0	2.5	1.8
S18	5.619956	-0.035594	40.2	0.4	18.7	63.5	2.6	2.2
S19	5.619944	-0.035208	65.0	0.2	29.0	56.4	2.6	2.5
S20	5.620017	-0.034578	32.6	0.2	27.7	57.8	2.8	2.4
S21	5.620753	-0.035836	83.2	0.1	20.3	39.8	2.5	1.8
S22	5.620933	-0.034867	57.1	0.1	18.2	61.7	2.6	2.3

Appendix C8. Trace metal concentrations in the Volta estuary

Locations	Lat	Lon	Cu	Cd	Zn	Pb	As	Hg
V1	5.78118	0.67716	36.99	0.07	59.12	3.06	94.08	0.13
V2	5.77894	0.67178	34.41	0.09	63.73	2.78	95.87	0.31
V3	5.77757	0.66791	32.98	0.05	59.39	1.81	98.99	0.13
V4	5.77428	0.66324	2.29	0.09	89.49	4.87	91.85	0.18
V5	5.77653	0.65799	12.70	0.07	96.41	6.12	89.62	0.49
V6	5.78710	0.67642	12.73	0.02	99.53	5.00	80.71	0.27
V7	5.78576	0.67041	12.80	0.09	75.39	2.92	75.80	0.04
V8	5.78448	0.66402	17.21	0.07	77.16	5.42	38.35	0.04
V9	5.79428	0.67466	12.78	0.04	65.22	4.17	41.47	0.04
V10	5.79169	0.67052	14.91	0.05	26.17	1.67	57.97	0.18
V11	5.79097	0.66518	15.10	0.07	25.49	2.78	50.83	0.13
V12	5.79806	0.66985	23.08	0.09	20.61	3.06	50.65	0.13
V13	5.79590	0.66454	26.71	0.11	11.25	3.61	72.68	0.04
V14	5.80327	0.66423	25.39	0.04	7.46	5.14	61.09	0.04
V15	5.80118	0.65885	24.20	0.05	14.64	9.18	39.24	0.04
V16	0.65885	0.66053	25.97	0.07	14.78	7.92	49.05	0.04
V17	5.80538	0.65632	24.05	0.09	18.85	7.37	54.40	0.04
V18	5.81032	0.66340	25.81	0.02	20.34	9.73	48.16	0.18
V19	5.81340	0.66158	23.40	0.05	21.29	10.70	48.16	0.09
V20	5.81140	0.65673	25.52	0.05	14.64	11.54	50.39	0.04
V21	5.78819	0.65599	44.59	0.09	27.53	5.00	51.28	0.09
V22	5.79229	0.65201	48.03	0.11	30.92	5.42	40.13	0.04
V23	5.79651	0.65024	22.22	0.05	37.02	7.09	61.09	0.04
V24	5.79881	0.64728	22.80	0.07	18.85	10.70	62.87	0.09
V25	5.80456	0.64602	11.18	0.09	21.97	11.26	58.86	0.27
V26	5.77864	0.65382	65.53	0.04	20.07	10.29	89.62	0.09
V27	5.78059	0.64866	25.38	0.11	20.75	8.06	52.62	0.04
V28	5.78338	0.64402	23.37	0.09	20.34	5.84	56.63	0.18

V29	5.78538	0.64122	19.79	0.04	15.05	10.70	53.51	0.22
V30	5.78711	0.63675	27.96	0.05	15.19	10.29	60.20	0.18